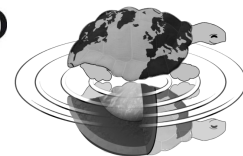




UNIVERSITÀ DEGLI STUDI DI MILANO
SCUOLA DI DOTTORATO
TERRA, AMBIENTE E BIODIVERSITÀ



Dottorato di Ricerca in Scienze della Terra
Ciclo XXV

**Deformation and metamorphism relationships in
acid and femic protoliths of the Austroalpine
continental crust subducted and exhumed in a
severely depressed thermal regime**

Ph.D. Thesis

Francesco Delleani
Matricola R08691

Tutore
Prof.ssa M. Iole Spalla

Anno Accademico
2011-2012

Coordinatore
Prof.ssa Elisabetta Erba

Co-Tutore
Prof.ssa Gisella Rebay

Ringrazio: i miei tutori Iole Spalla, Guido Gosso e Gisella Rebay per i loro insegnamenti sulla Scienza più bella di tutte; Michele Zucali e Davide Zanoni per i loro ottimi consigli ed insegnamenti; Curzio Malinverno per la preparazione delle splendide sezioni sottili ed Andrea Risplendente per la sua professionalità e capacità nello svolgimento delle analisi alla microsonda; la mia famiglia per il sostegno datomi in questi anni.

Index

I	Introduction	
1.	Geologic outline of the Western Alps	1
1.1.	Introduction to the Alps	1
1.2.	The Austroalpine domain	3
1.2.1.	Geologic outline	3
1.2.2.	The Dent Blanche Nappe	5
1.2.3.	The Sesia-Lanzo Zone	5
2.	Monte Mucrone mapping and mesoscale structural setting	9
2.1.	Introduction to the Monte Mucrone metagranitoids and country rocks	9
2.1.1.	P-T-d-t paths reconstruction in the Sesia-Lanzo Zone	9
2.1.2.	Prior works in the Mt. Mucrone sector	11
2.2.	Petro-structural map of the Monte Mucrone metagranitoids	11
2.2.1.	Field work for the petro-structural map of the Mt. Mucrone metagranitoids and country rocks	11
2.2.1.1.	Lithologic types distinction	11
2.2.1.2.	“Grey type” metagranitoid	12
2.2.1.3.	“Green type” metagranitoid	12
2.2.1.4.	Metaquartzdiorite	13
2.2.1.5.	Metaaplite and metapegmatoid	14
2.2.1.6.	Leucocratic metagranitoid	14
2.2.1.7.	Eclogite	14
2.2.1.8.	Paragneiss	15
2.2.1.9.	Micaschist	15
2.2.1.10.	Porphyric gneiss	16
2.2.1.11.	Glaucophanite	17
2.2.1.12.	Zoisite	17
2.2.1.13.	Qz-dominated vein	17
2.3.	Mesoscale structural analysis of the Monte Mucrone southern slope	18
3.	Microscale structural analysis and mineral chemistry evolution of the Monte Mucrone metagranitoids and country rocks	33
3.1.	Microstructure of Monte Mucrone metagranitoids and country rocks	34
4.	Ivozio mapping, multiscale analysis and mineral chemistry	99
4.1.	Previous works on the Ivozio metagabbroic Complex	99
4.2.	Petro-structural mapping of the Ivozio metagabbroic Complex and country rocks	103
4.2.1.	Field work for the petro-structural map of the Ivozio metagabbroic Complex	103
4.2.1.1.	Structural elements	104
4.2.1.2.	Lithologic types of the eclogitic micaschist complex	105

4.2.1.3.	Lithologic types of the Ivozio metagabbroic complex.....	106
4.2.1.3.1.	Amphibole-bearing eclogite.....	106
4.2.1.3.2.	Zoisite-bearing eclogite.....	108
4.2.1.3.3.	Amphibole-epidote-bearing eclogite.....	108
4.2.1.3.4.	Zoisite- and quartz-eclogite.....	109
4.2.1.3.5.	Ultramafic rocks.....	110
4.2.1.3.6.	Chlorite-amphibolite.....	111
4.3.	Mesoscale structural analysis of the Ivozio Complex and country rocks.....	111
4.3.1.	Pre-D1 mesostructural relics.....	112
4.3.2.	D1 deformation stage.....	113
4.3.3.	Grt-bearing veins.....	114
4.3.4.	D2 deformation stage.....	109
4.3.5.	Omp-bearing veins.....	115
4.3.6.	D3 deformation stage.....	116
4.3.7.	D4 deformation stage, Gln- and Zo-bearing veins.....	116
4.3.8.	D5 deformation stage.....	117
4.4.	Microscales structural analysis of the Ivozio Complex.....	118
4.4.1.	Pre-D1 microstructure and mineral association evolution of pre-D1 veins.....	119
4.4.2.	Amphibole-bearing eclogite microstructure.....	120
4.4.3.	Zoisite-bearing eclogite microstructure.....	122
4.4.4.	Amphibole-epidote-bearing eclogite microstructure.....	124
4.4.5.	Quartz-rich eclogite microstructure.....	124
4.4.6.	Ultramafic rocks microstructure.....	125
4.4.7.	Chlorite-amphibolite microstructure.....	126
4.4.8.	Grt-, Omp-, Gln- and Zo-bearing veins microstructure.....	127
4.5.	Fabric evolution vs reaction progress.....	128
4.6.	Mineral chemistry of the Ivozio Complex assemblages.....	128
4.6.1.	Samples selection and mineral chemistry analysis method.....	128
4.6.2.	Amphibole group.....	128
4.6.3.	Clinopyroxene group.....	131
4.6.4.	Garnet group.....	133
4.6.5.	White mica group.....	134
4.6.6.	Epidote group.....	136
4.6.7.	Chlorite group.....	136
4.6.8.	Serpentine, carbonate, phlogopite and talc group.....	137
4.6.9.	Lawsonite textural relicts.....	137
4.7.	Thermodynamic modeling.....	144
4.7.1.	Database, chemical systems selection and bulk composition.....	144
4.7.2.	Isochemical diagrams (pseudo-sections)	144
4.7.2.1.	Metapyroxenite.....	144
4.7.2.2.	Amphibole-bearing eclogite	146

4.7.2.3. Zoisite-bearing eclogite.....	146
5. Discussion and conclusions on the Ivazio tectono-metamorphic evolution.....	147
6. Conclusions.....	153
References.....	157

Introduction

The goal of this Ph.D. work is the comparison of the structural and metamorphic evolution of two portions of the same “Alpine nappe” in the case of Sesia-Lanzo Zone, recently interpreted, also in agreement with numerical modelling, as the result of accretion of different tectono-metamorphic units occurred in a hydrated mantle wedge during Alpine subduction (e.g. Spalla et al., 1996; Zucali et al., 2002 b; Meda et al., 2010; Roda et al., 2012). For this purpose two different associations of pre-Alpine igneous rocks have been selected within the Eclogitic Micaschists Complex: a) the Permian intrusive complex of Mt. Mucrone, comprising granites, granodiorites and quartz-diorites, emplaced in high grade gneisses (kinzigites), marbles and metabasics (Compagnoni & Maffeo, 1973; Hy, 1984; Oberhaensli et al., 1985); b) the Carboniferous gabbroic complex of Ivozio, deriving from a differentiated Ti-rich gabbro (Rubatto, 1998), surrounded by the metapelites of the Eclogitic Micaschists Complex. In this latter case pre-Alpine mineral and textural relicts have been totally obliterated by the pervasive re-equilibration under blueschist and greenschist facies conditions (Pognante et al., 1980; Zucali et al., 2004; Zucali & Spalla, 2011).

In a period in which accurate analyses of deformation-metamorphism relationships at the optical microscope, coupled with detailed structural mapping and careful mineral chemistry studies, are considered “a little out of date” (Vernon, 2004) the investigation to unravel the tectonic and metamorphic histories, in the two selected pre-Alpine magmatic complexes, has been approached with multiscale structural analysis associated with the detection of changes in chemical compositions of minerals supporting successive fabrics. Quality thermo-barometry and petrologic modelling in different bulk systems, with the support of isochemical PT diagrams (pseudo-sections), led to infer accurate Pressure-Temperature-deformation-time paths. The heterogeneity characterising deformation and associated metamorphic transformations, changing in space and time during poly-phase evolution, in polycyclic metamorphic terrains imposes a careful detection of distribution of deformation and mineral transformation gradients to avoid dangerous hiatuses in reconstructing structural and metamorphic rock-memory. Taking care of this aspect, maps of the degree of fabric evolution and metamorphic transformation have been derived by petro-structural maps, surveyed anew at different scales, both in the Mt. Mucrone and Ivozio areas. The southern slope of Mt. Mucrone has been mapped at 1:2,500 scale and the geology synthesised at the scale of 1:5,000; microstructural analysis involved the study of 96 thin sections, 15 of which have been analysed with the EMPA to unravel the metamorphic evolution. In the Ivozio complex, thank to the limited extent of the gabbroic body, field work has been performed at 1:10 - to 1:50 scale and synthesised in a petro-structural map at the scale of 1:1,000; here microstructural analysis has been executed on 108 thin sections, and EMPA investigations on variations in mineral compositions on 32 polished thin sections. In this latter case the PTdt evolution has been supported by three pseudosections for: metapyroxenite, amphibole-bearing eclogite and zoisite-bearing eclogite. The analytical method followed represented an effective tool to filter out the influence of heterogeneity in mechanical and chemical transformations that actually represent the most dangerous contamination of the comparison between the two inferred tectono-metamorphic evolutions.

Chapter 1

Geologic outline of the Western Alps

1.1 Introduction to the Alps

The European Alps are the most studied continental belt of the Earth together with the Scottish Caledonian orogen. The Alps belong to Alpine-Himalayan system, continuous over 18,000 km, from the Betic Cordillera of the Western Mediterranean to New Caledonia and New Zealand in the Southwest Pacific area. The Alps are a double-vergent orogen as evident in the cross sections of Argand, 1911 that developed since Cretaceous to Eocene age as the result of subduction of the Alpine Tethys and collision between Europe and Adria, which can be considered as a promontory of Africa or as an independent microplate (Stämpfli and Hochard 2009; Handy et al. 2010), with subduction of the oceanic plate under the Adria and continental collision in during late Eocene- early Oligocene age.

The crustal-scale portions of the Western Alps are divided into various structural domains on the basis of lithological associations, sedimentary covers, Alpine and metamorphic histories (e.g., Dal Piaz et al 2003). The subdivisions proposing since long time a correspondence of their present relative structural position, with a presumed paleogeography, were questioned on the base of a structural history more complex than a simple overthrust sequence to the NW (Polino et al. 1990; Spalla et al. 1996; Stöckhert and Gerya 2005).

Lithosphere-scale homogeneous structural domains (Polino et al. 1990; Fig. 1.1 of Spalla et al. 1996, and references therein) can however be objectively distinguished from the European foreland to the Adria basement: I) the domain of the European Foreland margin, nearly undeformed in Alpine time, only flexured and underthrust underneath the Helvetic-Dauphinois orogenic front during late convergence; II) the Helvetic-Dauphinois Domain, a thick-skinned thrust system of basement and cover slices or recumbent overthrust folds, dominantly retaining pre-Alpine tectono-metamorphic and lithostratigraphic signatures, often resulting from Tertiary tectonic inversion of the normal fault systems that had splitted up the European passive margin since the continental rifting of the Pangean breakup; III) the domain of the Pennine and Western Austroalpine composite nappe system, constituting the axial part of the belt: a highly heterogeneous group of plastically intermingled and metamorphosed continental and oceanic rocks since the late Cretaceous- to Tertiary early-Alpine subduction-exhumation event of oceanic consumption, later overprinted by continental collisional deformation and metamorphism, and by tectonic denudation; the Austroalpine exclusively displays continental material; IV) the N-vergent Central-Eastern Austroalpine system, almost continuously capping along strike the early-Alpine orogenic wedge, and locally affected by subduction imprints of Alpine age (Mortirolo e Koralpe), ; V) the Southalpine Domain, forming the hinterland of the early-Alpine belt, and evolving since Cretaceous as a S-East - vergent thick-skinned upper crustal thrust system of basement

and cover units, locally affected by very low- grade Alpine metamorphism (Polino et al. 1990; De Sitter L.U. and De Sitter-Koomans 1949, Diella V. et al. 1992, Doglioni and Bosellini, 1987; Gazzola D. et al. 2000).

Relict of the metamorphic and igneous imprints of the Variscan convergence and successive rifting processes exist in the crustal rocks of most of the five Alpine Domains, in the Alpine hinterland and foreland and even in volumes within the exhumed continental crust slivers of the axial belt; in spite of the sinking in the sub-lithospheric mantle of large amounts of continental crust and almost all oceanic lithosphere.

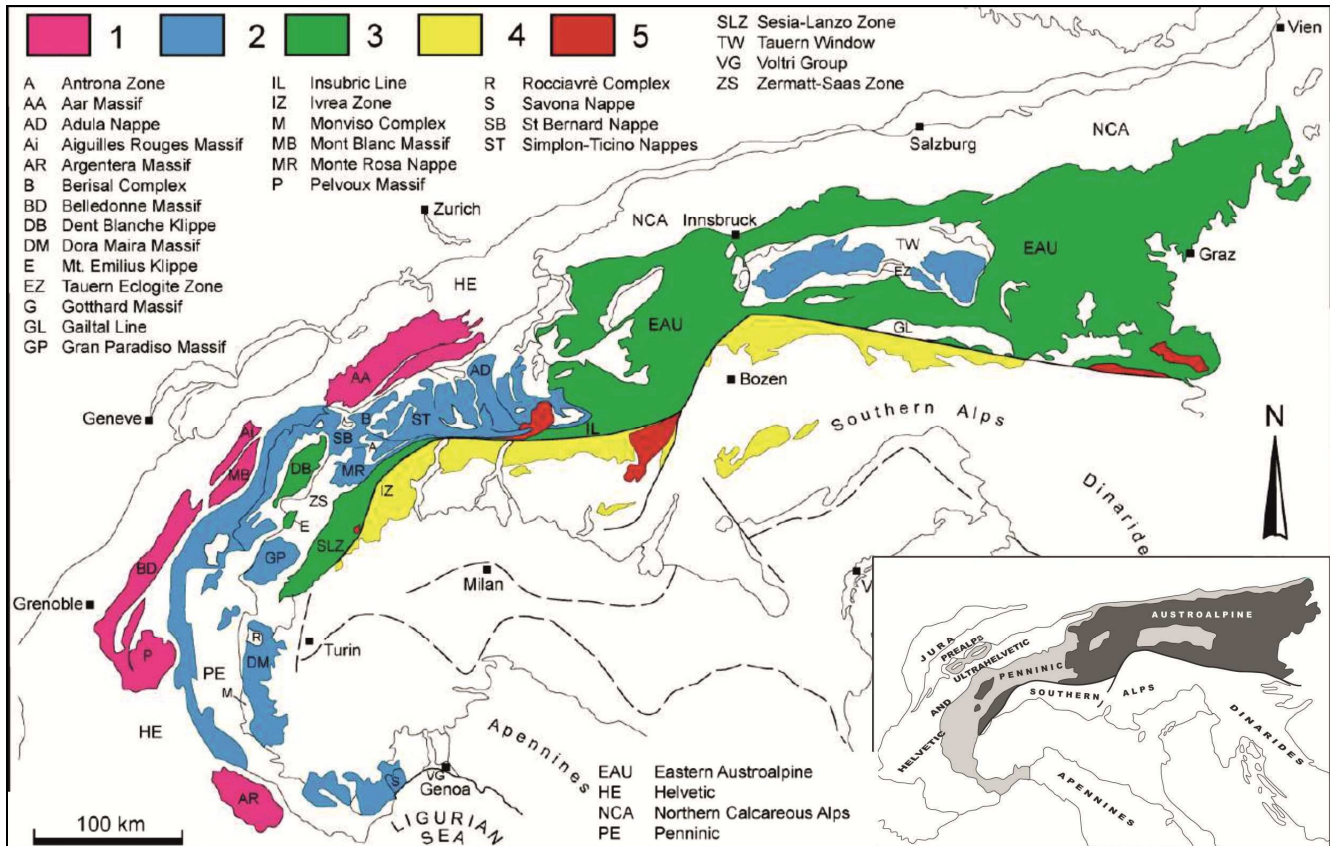


Fig.1.1 Tectonic sketch of the Alpine belt (redrawn after Spalla and Marotta, 2007) in the Alpine chain (inset). 1 = Helvetic Domain; 2 =Continental Crust of Penninic Domain; 3 = Austroalpine Domain; 4 = Southalpine Domain; 5 = Tertiary Intrusive Stocks. In the inset the location of the main tectonic domains.

Metamorphic and igneous markers of Permian and Triassic ages testifying a high thermal regime have been interpreted as the result of two possible geodynamic scenarios: the late-orogenic collapse of the Variscan belt enhanced by lithospheric unrooting (Schaltegger and Brack, 2007), or lithospheric thinning leading to continental rifting (Handy and Zingg, 1991; Lardeaux and Spalla 1991; Spalla and Marotta, 2007; Marotta et al. 2009). Even Permian volcanic activity and related basin formation have been linked to pull-apart basins formations (Muttoni et. al. 2003), or to lithospheric extension leading to the Pangea break-up (Staehele et al. 2001).

The seismic structure of the Alpine belt has been explored over the last 25 years by the deep seismic exploration traverses, Ecors-Crop, NFP20, and the TransAlp (Thouvenot et al. 1990; TransAlp Conference volume 2003; Cassinis 2006; Polino et al. 1990; Dal Piaz et al. 2001;) respectively fanning from the West to the East of the belt. Crustal scale structure was refined with the support of geophysical models (integrated seismics, gravimetry, and magnetism) of the collisional suture (axial belt), identifying two distinct Moho surfaces, the Adriatic and the deeper European Moho, both smoothly dipping from the forelands to the base

of the collisional wedge. In the axial part of the chain, well illuminated by seismic profiles is a Cretaceous-Paleogene rootless crustal prism comprised between the Penninic Front and Periadriatic Lineament bounding it towards the Helvetic and Southalpine domains.

Updated geometric representations of the tectonic implications of ocean and continental units of the Pennine units do not diverge substantially from the ones envisaged by Argand (1911) and Staub (1917). The crustal structure interpreted as recumbent fold stacks of continental basement and Mesozoic sediments and ophiolites (nappe architecture), is indeed impressive. These recumbent fold nappes, once believed to consist at their cores of thinned pre-Mesozoic continental crust occupying the ocean floor, had to be decolled from the mantle and wrapped by their Mesozoic sediments, including sporadic ophiolite associations, and were thought to have been generated by amplification of periodic ocean-crustal Europe-verging asymmetric anticlines. The surviving traditional regional nomenclature, from zero to VI, of the “Penninic nappes” introduced at the beginning of 1900s, indicates exclusively the reworked pre-Alpine continental sheets, multiply infolded during subduction-exhumation and collision with Mesozoic sediments and ocean floor slices.

The sequence of tectono-metamorphic imprints of the crustal fragments concordantly depicts the tectonic history of each of the five domains and homogeneously defines the main lithospheric frame of the belt: the Adriatic inner margin corresponding to the Southalpine Domain, made of shallow basement thrust sheets and detached cover units carrying greenschist to anchizonal mineral transformations (Zingg and Hunziker, 1990); the Austroalpine-Penninic units which forms now the axial zone of the Alps, is a fossil subduction complex and it is marked by ophiolitic units and displays polyphase metamorphism evolving from blueschist or eclogite-facies imprint due to the Alpine Tethys subduction to LP greenschist overprint, locally up to Barrovian (as in the Lepontine region) due to the slab break-off; the proximal European margin comprising European Foreland and Helvetic-Dauphinois Domain with transformations and deformations very similar to the Southalpine Domain.

The axial crustal prism comprises units recording high- to ultra-high-pressure metamorphism of Cretaceous to Late Eocene ages (Handy and Oberhänsli, 2004). This large time interval of eclogite formation in rocks of continental and oceanic origin suggests that they may have been generated during either continental collision or subduction of the oceanic lithosphere accompanied by tectonic erosion of the Adria active margin before the onset of continental collision (Spalla et al., 2010).

1.2 The Austroalpine Domain

1.2.1 Geologic outline

The Austroalpine Domain is the uppermost tectonic level of the Alpine belt. It is constituted by continental rocks overlying the Pennine stack of ocean and continent crustal slices, representing the ophiolitic suture, both comprised between the Penninic Front and the Periadriatic Lineament constituting the collisional wedge. It does not contain Mesozoic ophiolites, but is infolded within them and the related Mesozoic sediments.

In the Eastern Alps, the topmost Penninic unit underlying the Austroalpine is the Platta nappe, while in the Western Alps is the Piemonte ophiolite Zone. Its western termination in the Alps corresponds to the Ultramafic Lanzo Massif and the eastern one coincides with the eastern margin of the chain (Fig. 1.2). This Domain derives his name from the Austrian Alps in the eastern Alps where has a wider extension: showing a thick pile of continental cover and basement nappes which extends from the Swiss-Austrian border to the Pannonian basin, with minor Pennine outcrops in two tectonic windows (Tauern, Engadine and Reichnitz). In the western portion mostly outcrop rocks of the Pennine stack with minor Austroalpine isolated klippen

constituting the Austroalpine system in the Western Alps, which is composed by the Sesia-Lanzo Zone and numerous more external units grouped as Dent Blanche nappe. Austroalpine rocks from all around the chain recorded metamorphic condition indicating that they have been deeply involved in cold subduction processes (Thöni, 2006). The Dent Blanche nappe is subdivided by the Aosta-Ranzola fault, running along the middle Aosta valley, into northern (Dent Blanche, Mont Mary, Pilonnet, Etirol-Levaz and Grun) and southern klippen (Monte Emilius, Glacier-Rafray, Acque Rosse, Tour Ponton, Santanel and Chatillon). Its deformation history developed from Cretaceous to Lower Oligocene and was associated with different dominant imprints, from greenschist to eclogite-facies conditions. In the central Alps, east of the Ossola-Tessin window, the western Austroalpine has been correlated to the Margna nappe which is overlain by the Platta ophiolite. This means that the western Austroalpine and the Margna nappes are located at different structural levels, lower than that of the capping eastern Austroalpine, according to Dal Piaz (2001).

Part of the Austroalpine displays an eclogitic to Barrovian metamorphism, dated as early as Cretaceous (Thöni 2006). Metamorphic ages inferred for the eclogitic imprint are older in the eastern portion of the Austroalpine Domain than in the western portion (Handy and Oberhänsli 2004).

After the Alpine slab break off in the Oligocene several post orogenic intrusions occur within the Austroalpine Domain near the Periadriatic Lineament.

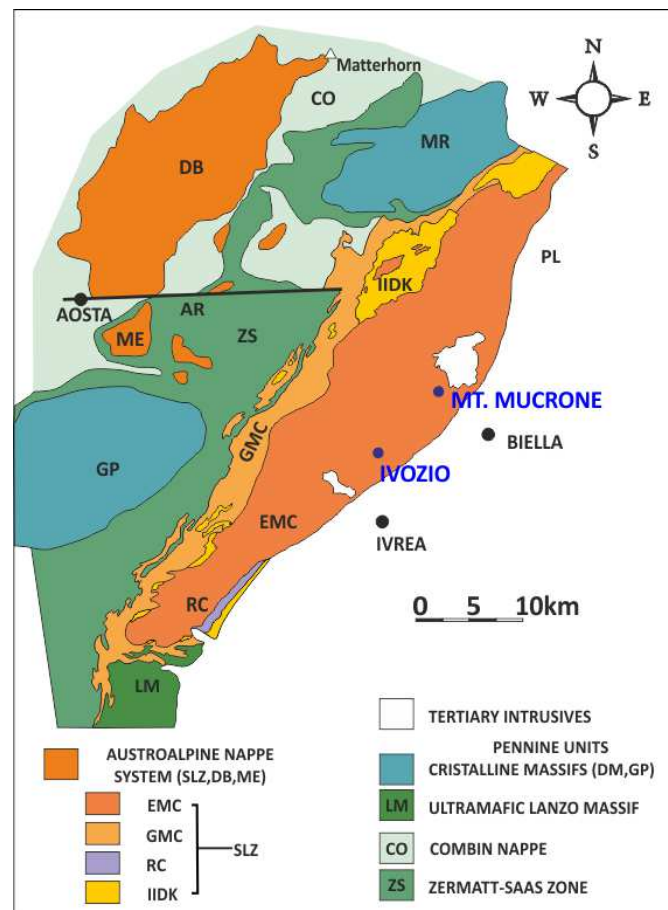


Fig. 1.2: Tectonic sketch of the internal Western Alps. Acronyms: Aosta-Ranzola Fault (AR); Combin Zone (CO); Dent Blanche Klippe (DB); Eclogitic Micaschist Complex (EMC); Gneiss Minuti Complex (GMC); Gran Paradiso Massif (GP); Monte Emilius Klippe (ME); Monte Rosa Massif (MR); Periadriatic Line (PL); Rocca Canavese Thrust Sheet (RC); Sesia-Lanzo Zone (SLZ); Il Zona Diorito-Kinzigitica (IIDK).

1.2.2 The Dent Blanche Nappe

The Dent Blanche nappe (DB) is characterized by a Paleozoic basement and lenses of Mesozoic metasedimentary cover. On the base of the Alpine tectono-metamorphic evolution it has been separated in two independent units (Ballevre and Kienast, 1987): I) an upper unit formed by Dent Blanche, Mont Mary and Pillonet klippe, characterized by a greenschist to blueschist dominant metamorphic imprint, displaying only a few relic mineral associations of relatively high pressure (aegirine, sodic amphiboles, garnet, and white mica with high Si contents) below a pervasive greenschist facies overprinting (Pennacchioni and Guermani, 1993; Roda and Zucali, 2007); II) a lower unit formed by Mont Emilius, Glacier-Rafray and Tour Ponton klippe and Etirol-Levaz slice characterized by an eclogitic Alpine dominant imprint.

The Klippen of the upper element are constituted by Valpelline and Arolla Series and some tectonic slices of Permian (Manzotti et al., 2012) and Mesozoic metasediments; only in the Pillonet klippe there are no representatives of the Valpelline Series. The Valpelline Series contains pre-Alpine high grade paragneisses with lenses and layers of basic granulites, garnet-clinopyroxene bearing amphibolites and marbles (Diehl et al., 1952). The Arolla Series is constituted by granites, diorites, gabbros and related orthogneisses, chlorite-white mica bearing gneisses and schists. Metric lenses of biotite bearing gneisses and amphibolites occur within the igneous rocks (Roda and Zucali, 2008). The metamorphic evolution of the Valpelline Series displays an early pre-Alpine re-equilibration under granulite-facies conditions, followed by an amphibolite-facies event, associated with the dominant foliation. The last pre-Alpine metamorphic imprint occurred under greenschist-facies conditions. The Valpelline Series shows a poor Alpine re-equilibration represented by static greenschist facies minerals, only locally related to Alpine foliations (Diehl et al. 1952), though kyanite-chloritoid associations have been described (Kienast and Nicot, 1971; Baletti, 2004). In the Arolla Series a penetrative Alpine foliation develops under greenschist-facies conditions, enclosing blueschist-facies relics as blue amphiboles and phengitic micas within metaintrusive rocks (Ballevre and Kienast, 1987; Canepa et al., 1990; Roda and Zucali, 2008).

Radiometric ages range around 290 My for the Arolla granites and two age clusters for the Valpelline Series, at 180-200 Ma related to the high-temperature pre-Alpine evolution, and at 130 Ma related to a successive pre-Alpine or early-Alpine metamorphic event. Ages ranging between 45 and 48 Ma have been interpreted in connection to the Alpine baric peak (Hunziker 1974; Roda and Zucali, 2008).

Klippen and slices of the lower element are characterized by paragneisses, marbles, metabasics and metagranitoids, locally preserving mineralogical pre-Alpine relics associated to an amphibolite-facies retrogradation probably coeval with the Variscan re-equilibration (Dal Piaz et al., 1983). The Alpine imprint is characterized by an eclogite-facies re-equilibration followed by blueschist and greenschist re-equilibration.

1.2.3 The Sesia-Lanzo Zone

The Sesia-Lanzo Zone (SLZ) represents the widest portion of continental crust of the Western Alps affected by eclogite-facies metamorphism. During the Alpine subduction, this portion of the Adria microplate was tectonically detached (ablative subduction) from the continental margin (Polino et al., 1990) and subducted to depths of at least 60 km. The SLZ overlies ophiolitic associations of the Alpine Tethys and is overlain by an hangingwall of lower crustal rocks of the Southalpine Domain (Ivrea Zone); it is separated from the latter by the Canavese fault, a portion of the Periadriatic Lineament. The Alpine thermobaric history of the SLZ

(Hunziker 1974; Castelli and Rubatto, 2002) consists of a low temperature eclogite imprint followed by blueschist re-equilibration (Castelli 1991; Pognante, 1991); it is coherent with an exhumation occurring when the subduction of the oceanic lithosphere was still active (Spalla et al., 1996; Zucali et al., 2004). This thermobaric evolution at a low - to very low T/P ratio, facilitated the preservation of pre-Alpine relics and of Alpine peak minerals and history in rocks that experienced several Alpine re-equilibration. After the Cretaceous pervasive eclogite-facies recrystallization a multistage exhumation emplaced the SLZ units into the uppermost part of the Tertiary nappe pile and induced partial greenschist-facies reequilibrations (Zucali et al., 2002).

The SLZ is traditionally separated in two elements (e.g. Compagnoni et al., 1977): an upper element or "II Zona Diorito-Kinzigitica" (IIDK), comprising metapelites, calc-silicate marbles and metabasics, with a dominant pre-Alpine metamorphic imprint under amphibolite-granulite facies conditions, and a lower element consisting of polymetamorphic metapelites, metagranitoids, metabasics and calc-silicate marbles with Permian igneous bodies (e.g. Monte Mucrone granitoids and Val Sermenza gabbro). The lower element is further divided in three metamorphic complexes: the "Gneiss Minuti Complex" (GMC), showing a dominant Alpine metamorphic imprint under greenschist facies conditions, the "Eclogitic Micaschists Complex" (EMC), showing a dominant Alpine imprint under eclogite-facies conditions and the "Rocca Canavese Thrust Sheet" (RC) in which a lawsonite blueschists-facies metamorphic imprint characterizes the retrograde exhumation path. Monometamorphic cover sequences of Mesozoic age and Piemonte Zone serpentinized peridotites were reported from the central SLZ (Castelli et al., 2007, and refs. therein). The EMC and GMC, both pervasively eclogitised, strongly differ in the volume percentage of the greenschist-facies reequilibration (Spalla et al., 1991). The EMC, which constitutes the innermost part of the SLZ, shows a greenschist-facies overprint confined to discrete shear zones. In the EMC pre-eclogitic fabrics are locally marked by P-T prograde blueschist-facies minerals (Pognante et al., 1980, Rebay and Messiga, 2007). Recently, different structural domains have been contoured in the GMC and EMC complexes of the central SLZ (Babist et al., 2006) and different P-T evolutions have been recognised between the two complexes in Valchiusella (Konrad-Scholke et al 2006), perfectly adherent with the tectonometamorphic outline inferred at the regional scale (Pognante, 1991). The RC consists of some kilometric lenses interposed between EMC and GMC that escaped the eclogitic re-equilibration and is characterized by widespread blueschist-facies conditions assemblages.

The pre-Alpine polyphase metamorphic evolution of the the SLZ is accomplished during pre-Alpine times under granulite to amphibolite- and then to greenschist-facies conditions (Lardeaux, 1981; Lardeaux and Spalla, 1991; Zucali, 2002; Zucali et al., 2002; Spalla et al., 2005) and during Alpine times under eclogite facies peak conditions, with a final retrogression under greenschist-facies conditions. Relics of this pre-Alpine history are preserved through the SLZ, GMC and IIDK.

The pre-Alpine evolution is recorded in different bulk rock compositions, such as marbles, metapelites, metagranitoids, metagabbros, granulites and amphibolites (Compagnoni, 1977; Lardeaux et al., 1982; Rebay and Spalla, 2001). Amphibolites with widely varying amphibole modal amount (up to hornblendites with amphibole > 90%) are the results of the earlier steps of the high temperature pre-Alpine re-equilibration.

Absolute age estimates and field relationships allowed attributing an age of 270 Ma to the granulite-facies stage, of 240 Ma to the amphibolite-facies and 170 Ma to the greenschist-facies event. During pre-Alpine deformations a penetrative foliation was imprinted within metapelites marked by Crd, Bt, Pl, Kfs, Sill, Grt and Ilm and by Pl, Amp, Bt and Ilm in basic granulites (mineral abbreviations as in Whitney and Evans, 2010, with Wm = white mica), the latter assemblage marking discrete shear zones, crosscutting massive granoblastic Opx-Grt-bearing assemblages (Lardeaux and Spalla, 1991). P-T estimates for the pre-Alpine evolution indicate that the early metamorphic imprint developed at $0.6 \leq P \leq 0.9$ GPa and $T = 700 - 900^\circ\text{C}$ under granulite-facies

conditions, followed by an amphibolite-facies re-equilibration stage ($P = 0.3 - 0.5$ GPa and $T = 570 - 670$ °C) and, finally, by a greenschist-facies retrogression ($P = 0.25 - 0.35$ and $T < 550$ °C; Lardeaux and Spalla, 1991).

Intrusions of felsic to mafic compositions are associated at the pre-Alpine granulite- and amphibolite-facies metamorphic events (Lardeaux and Spalla, 1991; Rebay and Spalla, 2001); field relationships and chronological estimates suggest a Permian age for these rocks. The Ivozio Complex is one of these mafic complexes (Pognante et al., 1980; Zucali et al., 2004). It is an association of metabasic rocks derived from pre-alpine gabbros accreted to the Austroalpine continental crust during the Variscan orogenic cycle. The basic protoliths of the Ivozio Complex have been dated by Rubatto (1998 and refs. therein) at 355 ± 9 Ma and have a Fe-gabbros genetically related to other MORB gabbroic intrusions (e.g. Cima di Bonze) suggesting an oceanic derivation of the protoliths.

The Ivozio Complex extensively records eclogite-facies assemblages with the occurrence of Lws-bearing rocks. Lws is the marker of very cold thermal state due to highly-depressed geothermal gradient reliable to a mature subduction zone. Lws-bearing assemblages also occur in other parts of the SLZ and were mainly interpreted as the product of retrograde re-equilibration (Compagnoni et al., 1977; Pognante et al., 1988; Zucali et al., 2004).

The Alpine evolution is characterized by polyphasic deformation under blueschist to eclogite-facies conditions followed by retrogression under blueschist to successive greenschist facies conditions (Castelli et al., 2007, and refs. therein). Mineral ages ranging between 60 and 70 Ma have been related to the Alpine eclogite-facies peak (Rubatto et al., 1999) although older ages (up to 90 Ma) have been recently discovered (Cenki-Tok et al., 2012).

The EMC is composed of a wide spectrum of continental crust lithotypes, which includes paraschists, metabasics, orthogneisses, marbles, metagranitoids, rare metadioritoids and metagabbros. The eclogitic mineral assemblages (e.g. Compagnoni, 1977; Droop et al., 1990; Zucali et al., 2004; Rebay and Messiga, 2007) for the most significant lithotypes are: micaschist: Qz, Ph, Na-Cpx (Jd to Omp), Grt, Rt \pm Pg \pm Zo \pm Gln \pm Cld \pm Ky; orthogneiss: Qz, Ph, Na-Cpx (Omp), Grt, Rt \pm Pg \pm Gln \pm Zo; leucocratic orthogneiss: Qz, Jd, Ph, Kfs, Al-Ttn \pm Grt \pm Zo; eclogite: Omp, Grt, Rt \pm Zo \pm Gln \pm Na-Ca-Amp \pm Cld \pm Ky \pm Qz \pm Ank \pm Ph \pm Pg \pm Po; impure marble: Cal, Qz, Ph \pm Na-Cpx (sodic Agt to Omp) \pm Zo \pm Dol \pm Grt \pm Ank \pm Pg \pm Ttn \pm Gr \pm Po; ultramafite: Atg, Fo, Mag.

Different P-T and P-T-d-t evolutions have been inferred on the ground of mineral phase equilibria, clinopyroxene-garnet geothermometry, thermodynamic analysis and stable isotope geothermometry (Castelli et al 2007 and references therein) in the whole complex, which experienced a quartz eclogite-facies imprint peaking at about 600 ± 50 °C and 2.1 GPa (Spalla et al., 1997; Tropper and Essene, 2002; Zucali et al., 2004).

During blueschist- to greenschist-facies retrogression km-scale folding of eclogitic foliation occurred, in places associated with a new penetrative foliation. Large-scale shear zones developed during final stages of greenschist-facies re-equilibration in central SLZ (Handy et al., 2005). Brittle-ductile faulting also occurred during the final stages of the Alpine evolution and postdates the Tertiary andesitic dykes and igneous stocks of Biella and Traversella (Zanoni, 2007). Both plutons are intruded in the innermost part of the Sesia Lanzo Zone (Eclogitic Micaschist Complex) close to the internal boundary of the Alpine metamorphic units (Periadriatic tectonic line).

Chapter 2

Monte Mucrone mapping and mesoscale structural setting

2.1 Introduction to the Monte Mucrone metagranitoids and country rocks

2.1.1 P-T-d-t paths reconstruction in the Sesia-Lanzo Zone

Different types of mineral assemblages marking structural elements formed during successive deformation stages, are the base for the reconstruction of a P-T path in the EMC of the SLZ; this procedure individuates at least two different tectonometamorphic units, that can be generated in single crustal slices following different trajectories during the subduction process (Stöckhert and Gerya, 2005; Agard et al., 2009; Meda et al., 2010; Roda et al., 2010) or from the evolution of the thermal gradients of the subduction dynamics (e.g. Cloos, 1982). In both cases, these fragments were mechanically independent until they were packed together, at $P \leq 0.6$ GPa and $T \leq 450^\circ\text{C}$ (Pognante, 1989; Zucali et al., 2004).

P-T evolution recorded in different portions of the SLZ reveal a depressed thermal regime characterizing the exhumation, and indicate an active oceanic subduction until the continental collision. Actually the 37-45 Ma age of the greenschist-facies re-equilibration in the SLZ ranges within the same time interval of the eclogitic peak recorded in the ophiolites of Zermatt-Saas (e.g. Lapen et al., 2003; Zanoni et al., 2008; Agard et al., 2009).

The field-analysis and microstructural correlation of strain states and the related micro- and meso-scale reacting volumes have been used as the basis of the reconstruction of deformation-metamorphism history in the multiscale analysis of the Mt. Mucrone and Ivozio rocks. Results of the field work are reported in the attachment A (petro-structural map of the Mt. Mucrone metagranitoids) and B (petro-structural map of the Ivozio metagabbroic Complex). In section 2.3 the comment to the new Mt. Mucrone structural map (Delleani et al., 2013) is reported.

2.1.2 Prior works in the Mt. Mucrone sector

The area of Mt. Mucrone has been the subject of numerous geological-petrological and geochronological studies over the past decades, due to the particularly well preserved eclogitic-peak mineral association and related structural elements occurring in different lithologic types and to the extended relicts of pre-Alpine age inferred by metamorphic and magmatic-tectonic evolution during Paleozoic times.

Main lithologic types (Droop et al., 1990, with refs. therein) are:

- Micaschists constituted by Qz, Ph, Jd ± Omp, Grt, Rt ± Gln ± Pg ± Zo ± Ctd ± Ky.
- Metagranitoids constituted by Qz, Ph, Jd ± Omp, Grt, Rt ± Kfs ± Gln ± Pg ± Zo ± Ctd.
- Eclogites constituted by Omp, Grt, Rt ± Gln ± Ph ± Pg ± Zo ± Ctd ± Ky ± Qz.
- Impure marbles constituted by Cal, Qz, Omp ± Agt, Ph ± Dol ± Pg ± Gr ± Grt ± Ank ± Ttn.

The EMC is part the Austroalpine continental crust that inherits the amphibolite- and granulite-facies mineral associations of the Variscan orogeny; it includes as protoliths the “kinzigitic” complex: rocks with gneissic texture, characterized by alternations of amphibolites and/or pyroxenites, basic granulites and quartz-rich layers; mainly composed by Qz, Pl, Hb, Di, Sil, Bt and Grt. Levels of ultramafites and marbles are interposed with these metasediments (Lardeaux and Spalla, 1991; Dal Piaz, 1999). This sequence is then intruded by granitoid and gabbroic rocks during Permian times.

The Mt. Mucrone metagranitoids show portions with perfectly preserved igneous texture, with partial to complete corona type replacement of igneous minerals by HP mineral assemblages. The igneous texture is erased only locally, within cm-thick shear zones (Compagnoni and Maffeo, 1973). In particular the growth of composite coronas around the igneous sites is observed: Bt is partially replaced by Ph, with formation of Grt along the contact with the igneous Pl; Pl is fully replaced by Zo, Jd, and Qz ± Kfs; igneous Kfs is partially substituted by Ph (Compagnoni, 1977; Rubbo et al., 1999).

The P and T metamorphic conditions of the eclogitic-peak have been evaluated by many authors: T=500-600°C e P=15-17 kbar (Compagnoni, 1977); 500-700°C e fino a 15 kbar (Ungaretti et al., 1983); 600°C e 14 kbar (Oberhänsli et al., 1985); 520-650°C e 16-21 kbar (Tropper and Essene, 2002). The highest pressure attained during subduction process (P of about 21 kbar with T of about 600 ° C, in Zucali et al., 2002) in the Eclogitic micaschists are recoded at the margins of the map.

In Mombarone-Mt. Mars-Mt. Mucrone area, located to the NW of the Mt. Mucrone southern slope, seven different groups of structures have been recognized (Zucali et al., 2002); they were related to the metamorphic Alpine (D1, D6) and a pre-Alpine (pre-D1) evolutions: the mineral associations and the characterization of meso- and micro-structures are reported in Fig. 2.1. The first three phases developed in eclogite-facies conditions; D4 forms m-thick shear zones marked by blueschist-facies mineral assemblages; D5 is represented by 10-m-scale closed folding associated to greenschist-facies, marked by corona type minerals formation; D6 is a 10-m-scale gentle bending and cm-thick shear zones associated greenschist-facies mineral assemblages.

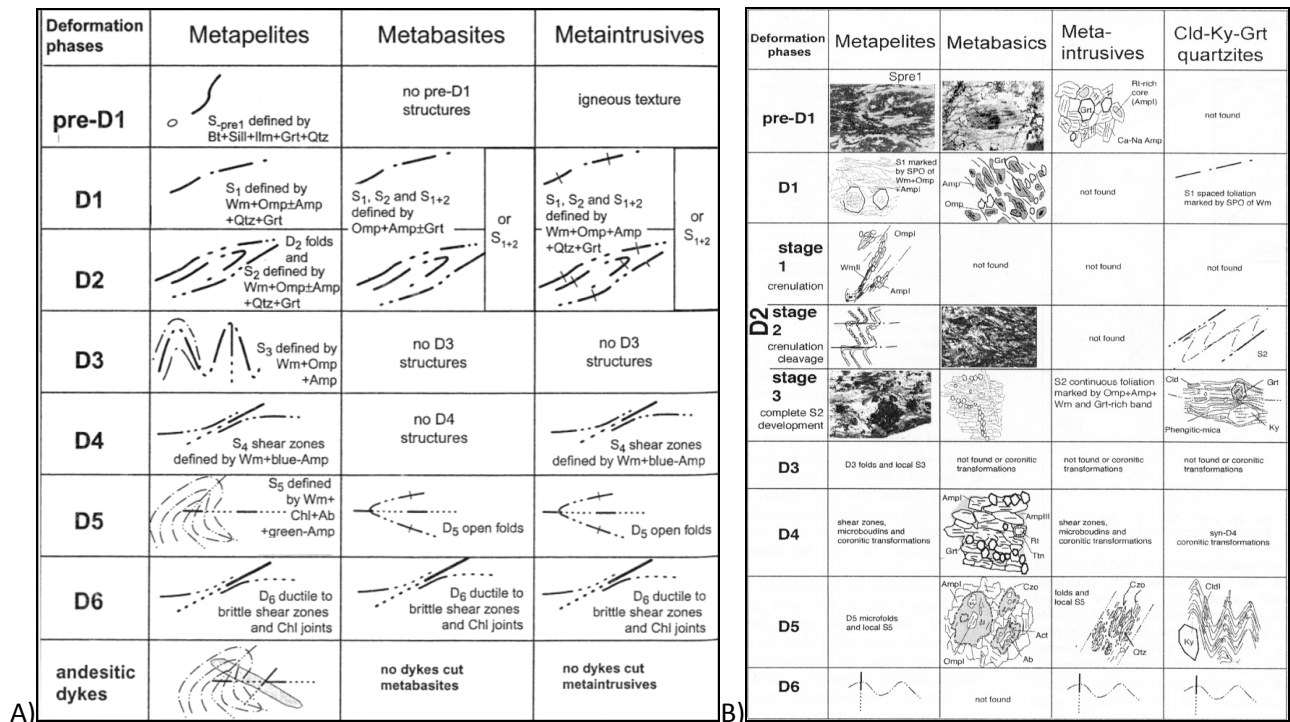


Fig. 2.1: Meso- (A) and micro-structural (B) histories, synthesised by Zucali et al. (2002) in the nearest surroundings of the area mapped during the present work.

2.2 Petro-structural map of the Monte Mucrone metagranitoids

2.2.1 Field work for the petro-structural map of the Mt. Mucrone metagranitoids and contry rocks

The results of original mapping at 1:2500 scale have been reported on a 1:5000 scale “drift and solid” map, in which rocks outcrops are separated by various types of drift cover; the geometric setting and its mineralogical support are reported in the “solid” map, which offers the interpretation of the full geology throughout the whole map area, including the unexposed parts. The full pattern of the superposed structures is shown in two sets of cross-sections that visualise the reconstructed 3D geometry.

2.2.1.1 Lithologic types distinction

The Mt. Mucrone southern slope is located about 4 Km northwest of the Canavese tectonic Line, the internal tectonic boundary of the SLZ, and 3 Km far from the western boundary of the Biella-Valle Cervo Tertiary intrusion, definitely outside of the metamorphic aureole margin.

Metagranitoids, paragneisses, micaschists and certain leucocratic metagranitoids are the main lithotypes of the map, with minor occurrences of porphyric gneisses, eclogites, glaucophanites and zoisitites.

Paragneisses and micaschists are the largest components of the country rocks in which metagranitoids of Permian age were intruded; the Mt. Mucrone metagranitoid complex includes: “grey-type” non-foliated metagranitoids; “green-type” foliated metagranitoids; metaquartzdiorites; metaaplitites and metapegmatoids. The latter are only in low- to medium-strained domains of the “grey-type” metagranitoid.

Locally, in paragneisses and micaschists, m-thick layers of porphyric gneisses, glaucophanites and zoisitites occur; eclogites and qz-rich veins may occur as m-thick layers within metagranitoids and paragneisses; moreover, a 100-m-wide body of leucocratic metagranitoids has been found within micaschists; this rock type has been separated from the other Mt. Mucrone metagranitoids because it is not geometrically connected and does not display pre-Alpine igneous relicts.

Glaucophanites, zoisitites and qz-rich veins location is individuated by colored diamonds on the “drift and solid” map since they occur as unmappable m-sized lenses on a 1:5000 scale map.

2.2.1.2 “Grey type” metagranitoid

Medium- to coarse-grained Jd, Grt, Zo and Ph “grey-type” metagranitoids presenting an almost perfectly preserved isotropic and hypidiomorphic igneous structure (Fig. 2.2A), with relicts of igneous fine-grained Bt and medium- to coarse-grained Kfs; this rock type is a non-foliated lower strain remnant of the “green-type” metagranitoid. The igneous texture was medium- to coarse-grained with lightly porphyric Ksp and color index of about 10%, due to Bt (the only recognizable femic igneous mineral); composition of the igneous protolith was about Qz (40%), Pl (40%, Ab > 90%), Kfs (20%), Bt (20%), Aln (acc.) and Zrn (acc.).

The average composition of the “grey type” metagranitoids is Qz (40%), Jd (25%), Wm (10%), Grt (10%), Bt (10%), Kfs (5%), Zo (acc.) and Aln (acc.): fine- to medium-sized Qz compose the igneous Qz domains; fine-grained Jd white aggregate occupy the igneous euhedral Pl sites (Fig. 2.2B); pale-grey fine-grained Wm, with a typical metallic sheen, overgrows on Kfs and Bt; rose fine-grained Grt rims Bt sites; Bt constitute up to cm-sized dark aggregates with bronze shining; pale pink to beige Kfs euhedral crystals is medium-grained, only locally cm-sized crystals occur; rare yellowish medium- to coarse-grained Aln can be detected also at the mesoscale analysis.

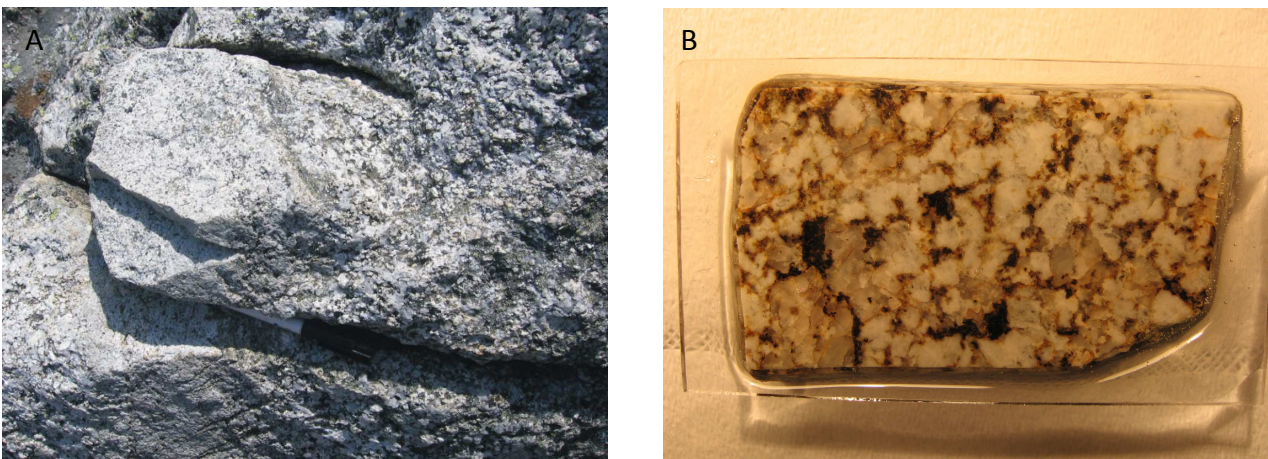


Fig. 2.2: (A) contact between a 10-cm-thick aplitic dike with a “grey type” metagranitoid; (B) hypidiomorphic texture of the “grey type” metagranitoid with square-shaped whitish aggregates of Jd and black tabular-shaped aggregates of Bt.

2.2.1.3 “Green type” metagranitoid

Fine- to medium-grained Jd (or Omp), Grt, Ph, Gln “green-type” metagranitoids constituted by syn-metamorphic Alpine deformed Mt. Mucrone metagranitoids, which are about the 80% of the whole metagranitic complex. It has white-green coloration due to prominent Na-Cpx greenish crystals and whitish Qz aggregates (Fig. 2.3A and 2.3B). Within this lithologic type the distinction of igneous contacts, texture and

compositional variation is no more possible and it includes the foliated products of the low deformed portions (coronitic texture) here only partially recognizable. The “green type” metagranitoid always shows 10-cm- to cm-spaced discontinuous foliation marked by lens- or tabular-shaped mineral aggregates of Na-Cpx and Qz and by Wm SPO, only locally evolving into a mm-spaced continuous mylonitic foliation.

The average composition of the “green type” metagranitoids is Qz (40%), Jd/Omp (25%), Wm (20%), Grt (10%), Zo (5%) and Gln (acc.): fine- to medium-sized Qz compose the lens- or tabular-shaped domains; medium-grained greenish Na-Cpx is mainly Omp with rare paler- to colorless Jd; medium-grained Wm is pale-grey with the typical metallic sheen; pink to pale-red fine-grained Grt are in trails parallel to the main foliation; Zo is white and very fine-grained; locally dark-blue or violet Gln occur in quantities appreciable at the mesoscale.

The boundary with other metagranitoids is a gradual transition taking place in a m- to 5m-thick range from coronitic textures to foliated ones, with the progressive complete diminution of Bt and Kfs, by replacement of larger Wm and formation of larger euhedral green Na-Cpx instead of whitish fine-grained Jd aggregates.

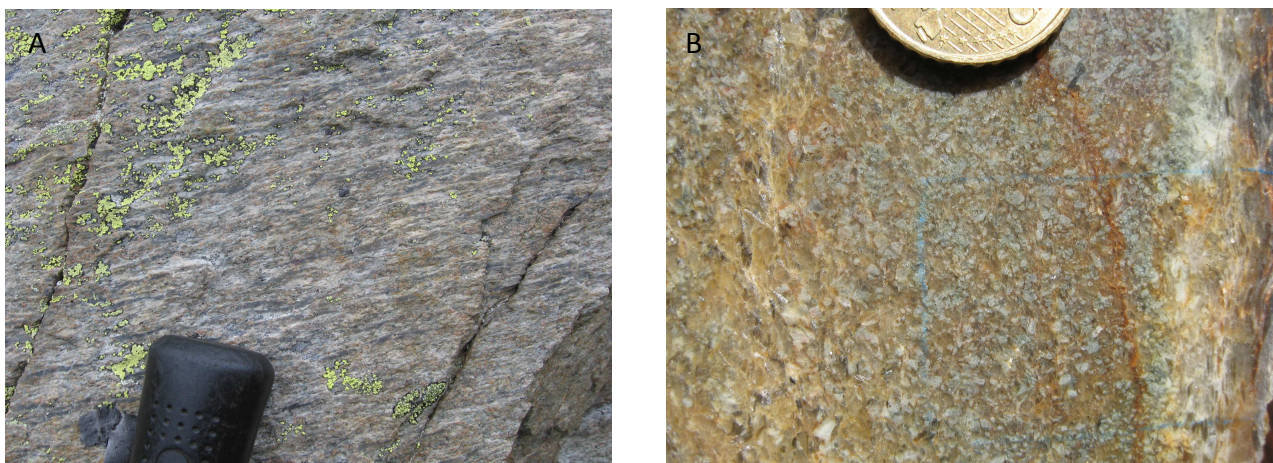


Fig. 2.3: Mylonitic (A) and poorly developed (B) foliation in “green type” metagranitoids marked by green Na-Cpx, Wm SPO and lens-shaped Qz domains.

2.2.1.4 Metaquartzdiorite

Medium- to coarse-grained Omp, Grt, Ph and Gln poorly to non-foliated metaquartzdiorites. This rock type constitute m-thick layers comprised within “grey type” metagranitoids: a 100m-sized body outcrops near to the main “green type” metagranitoid-paragneiss, within paragneiss and rimmed by syn-D3 shear zones (Fig. 2.4A).

The average composition of metaquartzdiorites is Omp (30%), Qz (25%), Grt (25%), Gln (10%) and Wm (10%): coarse-grained green Omp crystals may reach a length of 1cm; fine-grained aggregates of Qz form irregular Qz domains; Grt is red and medium-grained; blue, violet or dark-green Amp is fine grained and occupy intergranular spaces between larger Omp, Grt and Qz domains; fine-grained Wm is pale-grey with metal sheen.

The igneous texture is less recognizable than in other poorly deformed metagranitoids, due to the formation of Omp coarse-grained partially obliterating it. However the igneous composition can be estimated as follows: Pl (30%, with high An content), Qz (25%), Kfs (5%) and femic minerals (40%). The occurrence and quantities of the femic components, which could be Bt, Amp or Cpx cannot be discriminated; nevertheless the higher content in Gln and lesser Wm suggest a higher K/Na ratio probably due to a larger quantity of igneous Amp than of Bt.

This different composition, with respect to “grey type” metagranitoids, reflects on the formation of metamorphic minerals: Cpx is only emerald green Omp; Amp is always one of the major components; more Grt develops; lesser content of igneous Kfs infer lesser metamorphic Wm.

Metaquartzdiorites mainly show an isotropic texture with randomly oriented Omp, Ph and Amp, but between the boudaries of the main bodies a 10-cm to mm-spaced discontinuous foliation appears and is marked by fine-grained Wm and Amp, involving Grt and Omp porphyroclasts.

2.2.1.5 Metaaplite and metapegmatoid

Fine-grained aphyric Jd metaaplitites and coarse-grained Jd, Wm and Grt metapegmatoids (Fig. 2.4B). Both lithologic types occur in low- to medium-strain domains of the “grey-type” metagranitoid and retain primary intrusive contacts with the host rock.

The average composition of metaaplitites is Jd (45%), Qz (45%), Wm (10%), Grt (acc.) and Zo (acc.); metapegmatoids are composed as follows Qz (40%), Jd/Omp (30%), Wm (25%), Grt (5%) and Zo (acc.).

Except for grain size variations and modal amount of minerals they do not show mesoscale differences with the “grey type” metagranitoids.

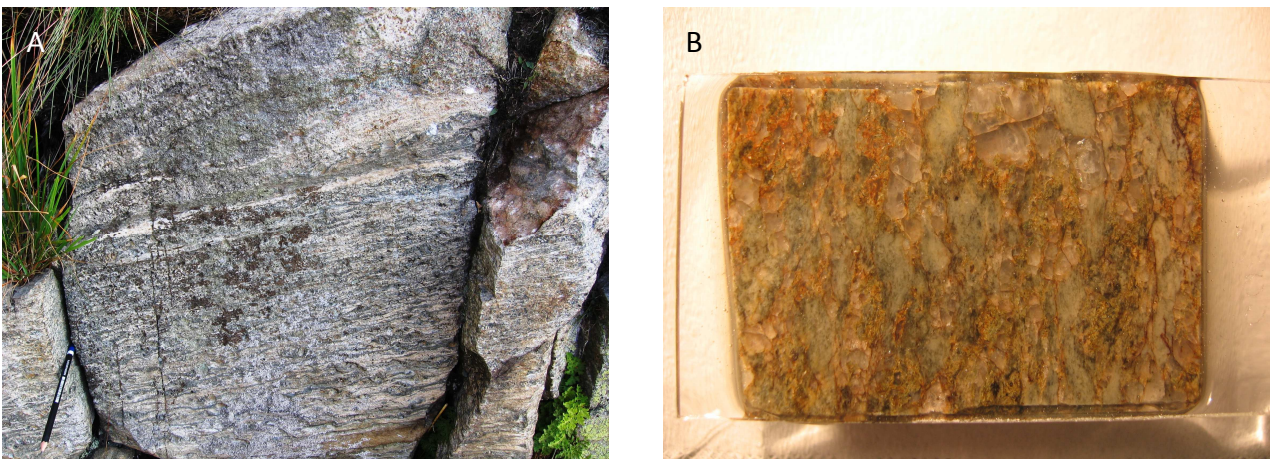


Fig. 2.4: (A) mylonitic foliation in metaquartzdiorite, rimming a large, 100m-sized, body; (B) metapegmatoids still recognizable within “green type” metagranitoids with foliation marked by the elongation of lens-shaped Qz and Na-Cpx domains.

2.2.1.6 Leucocratic metagranitoid

Medium- to fine-grained non-porphyric leucocratic Ab, Ph and Gln foliated metagranitoids (Fig. 2.5A). A single 100m-sized body of these metagranitoids occurs in the SW of the map area, with an average composition of Qz (40%), Ab (40%), Wm (20%), Gln (acc.), Cb (acc.) and Ep (acc.); fine-grained Qz constitutes mm- to 5mm-length lens-shaped domains; fine-grained white Ab in aggregates forms round-shaped domains; Wm is generally medium-grained and surrounded by Ab aggregates; locally coarse-grained Wm crystals occur. The large amount of Ab is obliterated Na-Cpx crystals; it may also have substituted Grt, anyhow the very poor amount of Fe/Mg minerals suggests a very low color index of the protolith.

Leucocratic metagranitoids always have cm- to mm-spaced continuous foliation marked by Wm SPO and lens- or tabular-shaped Qz domains.

2.2.1.7 Eclogite

Fine-grained Gln, Ph and Zo eclogites occur as meter- to 10-m-sized lenses within metagranitoids and micaschists (Fig. 2.5B), its average composition is Omp (40%), Grt (30%), Gln (20%), Wm (10%), Qz (acc.) and Zo (acc.): Omp is mainly medium-grained and emerald green; Grt is deep red and fine-grained; fine-grained Wm is grey with metallic sheen. Only one mappable body has been found just S of the top of Mt. Mucrone.

Core parts of the eclogite bodies have isotropic texture with random orientation of crystals, while along boundaries of layers mm- to cm-spaced discontinuous foliation develops, marked by fine-grained Omp, Gln, Wm SPO and by Grt trails; mm-thick intergranular shear planes are marked by growth of green-Amp and Chl.

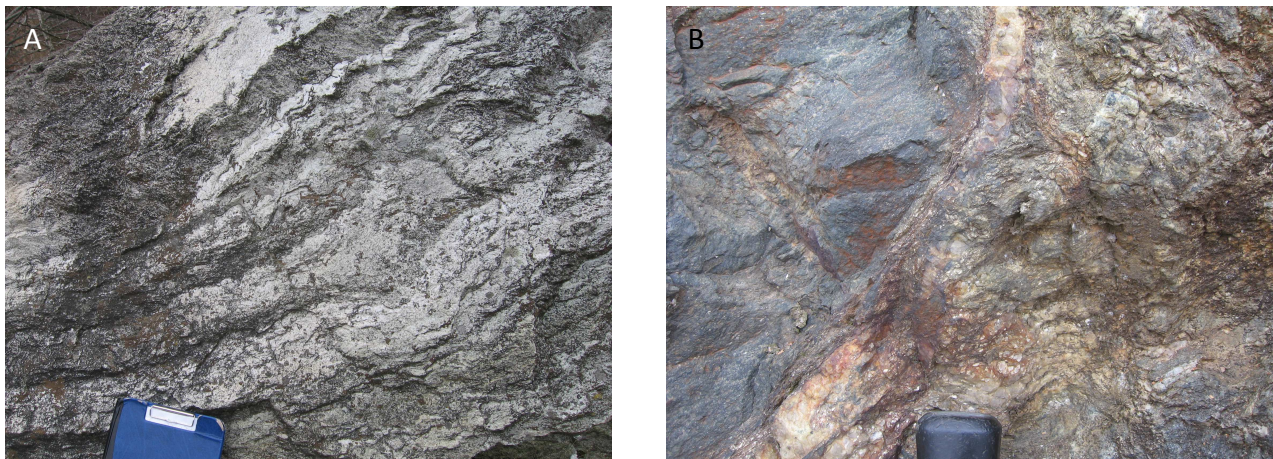


Fig. 2.5: (A) mm-spaced foliation in leucocratic metagranitoids; (B) boudinaged eclogite layer embodied within micaschists.

2.2.1.8 Paragneiss

Medium- to coarse-grained Grt and Wm paragneisses constituted by alternating whitish Qz and Grt layers and bluish Gln, Omp and Grt layers (Fig. 2.6A); the thickness of layers is generally comprised between 5 and 20cm, but locally some m-thick Gln, Omp and Grt layers occur.

Qz and Grt layers are mainly composed by Qz (65%), Grt (15%), Wm (15%), Gln (acc.) and Omp (acc.): Qz is an aggregate of fine- to medium-grained crystals; Grt is medium- to coarse-grained and is pink and locally larger crystals have reddish cores; Wm is fine-grained and pale-grey with metallic sheen.

Gln, Omp and Grt layers are mainly composed of Gln (50%), Omp (25%), Grt (15%), Qz (acc.), Wm (acc.) and Zo: fine-grained Gln constitutes the matrix of the level on which medium- to coarse-grained euhedral emerald green Omp and red Grt crystals stand out.

Within the layers a mm-spaced irregular foliation generally occur; it is parallel to the alternations and is marked by Wm in Qz and Grt layers and by Gln in Gln, Omp and Grt Layers.

Layering is more preserved on the western side of the slope, while on the eastern side it obliterated by the development of mm-spaced continuous foliation (Fig. 2.6B); only some tabular-shaped Qz layers, with length up to 50cm, occur as relict remembering the prior alternations. The foliation is marked by fine- to medium-grained Qz, Wm, Gln, Omp SPO and Grt trails; the average composition of these volumes is Qz (35%), Wm (30%), Jd/Omp (15%), Gln (10%), Grt (10%) and Zo (acc.): Qz is fine- to medium-grained and constitute lens-shaped domains; Wm is generally medium-grained and pale grey colored with the typical metallic sheen; Na-Cpx occurring is green Omp or colorless Jd, both medium-grained; Gln crystals are generally medium-grained, locally coarse-grained crystals mark a lineation; Grt has pink-reddish color and is fine-grained.

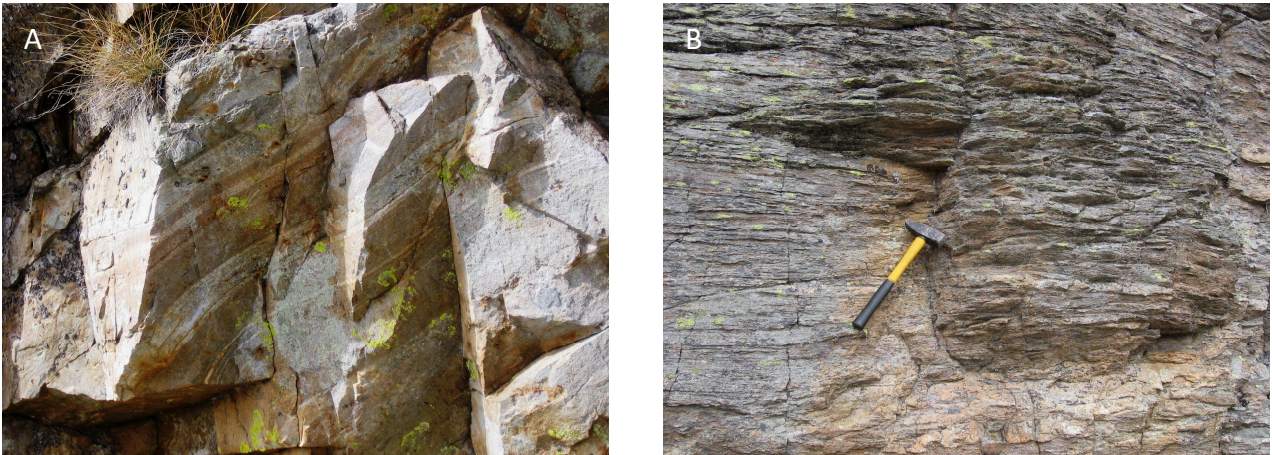


Fig. 2.6: (A) 10-cm-thick alternations in paragneisses; (B) gradual transition to mm-spaced foliated paragneisses.

2.2.1.9 Micaschist

Fine-grained Wm, Grt, Gln and Jd/Omp micaschists and/or Qz-rich micaschists; the average composition is Qz (30%), Wm (25%), Ab (25%), Gln (10%), Grt (10%), Jd/Omp (5%) and Zo (acc.): Qz is fine- to medium-grained and forms lens-shaped domains; Wm is fine- to medium-grained and grey colored with metallic sheen; Ab constitute round- or tabular-shaped aggregates of fine- to medium-grained crystals; Grt has a pink color and is fine-grained; Gln crystals are generally medium-grained, locally coarse-grained crystals mark a lineation; Na-Cpx is a green Omp, or a colorless Jd, both fine-grained.

Compositional differences mainly consist of modal variations of Gln (5 to 25%), Qz (15 to 50%) and Wm (15 to 40%). Locally micaschists show a diffuse formation of fine-grained white Ab, greenish Chl and yellowish Ep on the previous mineral assemblage, especially substituting Wm and Cpx.

Micaschists always show a mm-spaced continuous foliation marked by Wm, Gln, Omp SPO and Qz lens-shaped domains transposing a previous mm spaced foliation marked by Wm, Gln, Omp SPO and lens-shaped Qz domains (Fig. 2.7A). The boundary with the paragneisses is not sharp because the mm-spaced foliation makes the latter very similar to micaschists.

2.2.1.10 Porphyric gneiss

This lithologic type occurs as m- to 10-m-thick layers within paragneisses; they are medium- to coarse-grained Ab, Wm, Gln and Kfs porphyric gneisses, with the average composition of Qz (35%), Ab (25%), Wm (20%), Kfs (20%) and Gln (5%); medium-grained Qz constitute cm-scale lens-shaped domains; fine- to medium-grained white aggregates of Ab form round-shaped domains; Wm is generally medium- to coarse-grained and has pale-grey color; Kfs is coarse-grained (up to 1cm-length) and has pale-pink to white color; Gln crystals are generally medium-grained, locally coarse-grained crystals mark a lineation.

Porphyric gneisses always have a cm-spaced discontinuous foliation, marked by Wm, Gln SPO, Kfs and Qz elongated domains. The foliation wraps around Kfs porphyroclasts.

2.2.1.11 Glaucophanite

Fine-grained Omp, Grt and Wm glaucophanites occur as m-thick layers at the contact between metagranitoids and micaschists. The average composition is Gln (50%), Omp (20%), Grt (20%), Wm (10%) and Qz (acc.): fine-grained Gln constitute the matrix of the level on which medium- to coarse-grained euhedral emerald-green Omp and red Grt crystals stand out; Wm is fine-grained and has grey-metal shine.

In the matrix Gln and Wm have SPO marking mm-spaced continuous foliation overprinted by coarse-grained Omp and Grt with no preferred orientation. Locally mm-spaced continuous foliation marked by Gln and Wm SPO wraps around Omp and Grt porphyroclasts (Fig. 2.7B).

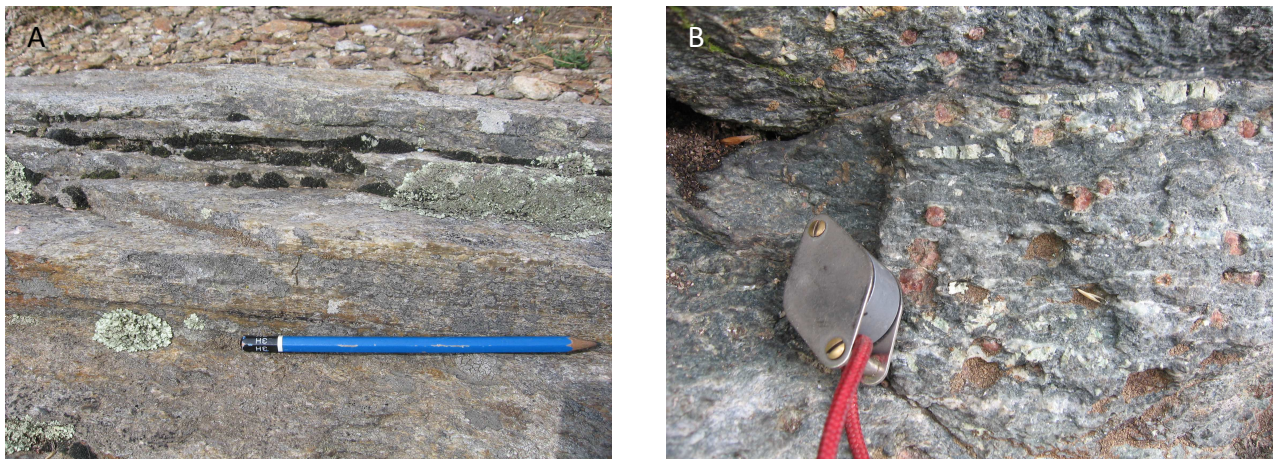


Fig. 2.7: (A) mm-spaced continuous foliation in micaschists; (B) Grt and Omp porphyroclasts involved by Amp-rich foliation in glaucophanite.

2.2.1.12 Zoisitite

Fine-grained Qz, Wm and Gln zoisitites, with Grt megablasts, up to 15 cm in size, occur within “green type” metagranitoids in m-thick layers. The average composition of zoisitites is Zo (35%), Grt (30%), Qz (15%), Wm (10%), Omp (10%) and Gln (acc.): Zo is fine-grained with pale yellowish color; Grt is red and generally constitutes 3-4cm sized poikiloblasts with widespread inclusions of Qz and Zo; Qz is fine-grained and comprised within lens-shaped domains; Wm is fine-grained and has a grey color with metallic sheen; Omp has a pale green color and is fine-grained.

Zoisitites always have mm-spaced continuous foliation marked by Zo, Wm SPO and Qz lens-shaped domains. This foliation is overgrown by Grt megablasts (Fig. 2.8A), which locally are wrapped by a new foliation marked by Zo, Wm, Omp SPO and Qz lens-shaped domains.

Locally large patches of Chl totally replace the Grt megablasts.

2.2.1.13 Qz-dominated vein

All the lithologic types, with the exception of glaucophanites, contain cm- to m-thick Wm, Grt, Zo and Gln bearing Qz veins, mostly constituted by Qz (95%), Wm (acc.), Grt (acc.), Gln (Acc.) and Zo (acc.): Qz is medium- to coarse-grained, while all the accessories are very fine-grained.

Qz-dominated veins always have a 10-cm-spaced foliation marked by Wm SPO (Fig. 2.8B).

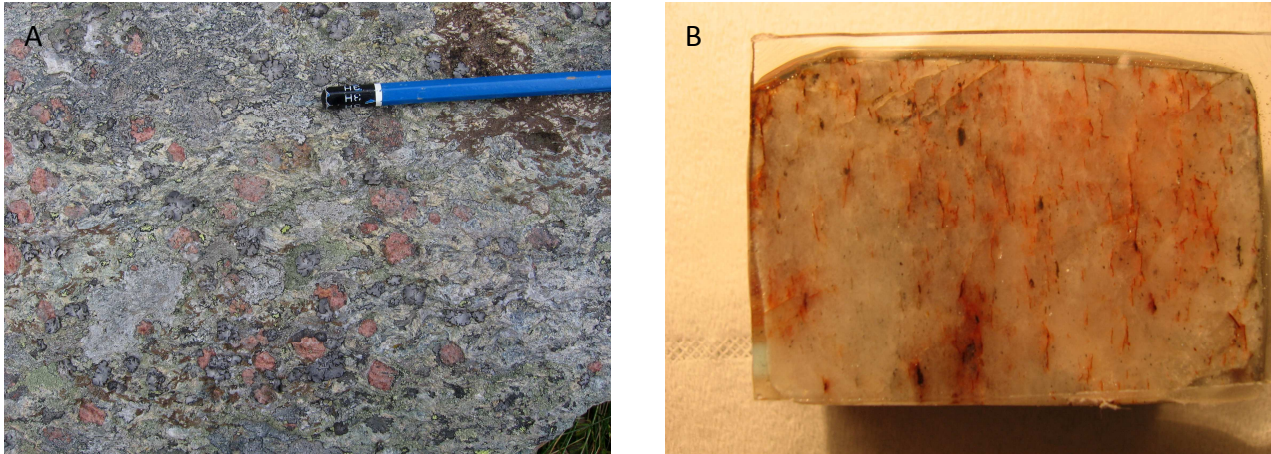


Fig. 2.8: (A) cm-sized megablasts of red Grt in zoisite; (B) Qz-dominated veins constituted by medium-grained Qz with foliation marked by Wm.

2.3 Mesoscale structural analysis of the Monte Mucrone southern slope

The following section contains the revised manuscript accompanying the petrostructural map executed on the Southeastern slope of Monte Mucrone, submitted to the Journal of Maps (Fig. 2.9).

Journal of maps
www.journalofmaps.com

Visual Hierarchical organization

Scouring by comparison: The map is incredibly fragmented, and the mapped areas are deemphasized. The pictures dominate, but are so large and tightly packed together that it is hard to focus on them. The caption boxes seem to be randomly interspersed among the picture groups, making it difficult to keep track of what goes with which pictures. The legend is very cramped. The title is small and kind of hanging on its own with nothing around it. The three maps have differently shaped neelines, even though they are mapping the same areas.

- Suggestors are as follows: all three of the main maps need to have rectangular neelines and should all have the same headline.
- The pictures need to be deemphasized and arranged around the three maps. The three maps should be near one another/adjacent. The legend needs more space. The inset maps should not be so near the top of the map. The caption boxes should be made less wordy and deemphasized, perhaps by making the text 80% gray. The box outlines around the pictures and caption boxes should perhaps be replaced by colored fills without outlines (e.g., 30% gray fill behind a group of pictures and its caption, adjacent to another group of pictures with a white background behind them and their caption).
- The maps need to be emphasized more by grouping them out in the visual hierarchy.
- The title needs to be redone as a map title, not a poster title. Author names and affiliations should be deemphasized and put near the bottom of the map.
- I recommend getting rid of the empty space near the top of the map.
- I also recommend getting rid of the borderlines/outlines around the differently shaded areas on the map. These should probably have no borderlines fill or the same fill color as the fill itself. If they are going to have outlines, they should have white outlines. Right now there are a lot of lines on these maps competing with colors and text. Getting rid of the outlines will make it much easier to read.

Map Review Sheet
The Map Review Sheet is used to provide authors with feedback on a map submitted to the Journal of Maps. In conjunction with the referees' reports, it is indicative of items that require correction or further comment. Detailed observations have been made by a professional cartographer that reflect the extent to which the map meets acceptable standards of map design. Maps will only be accepted when they are deemed by the editors to have reached a standard suitable for publication.

Author:	Delleani, Francesco; Spalla, Telle; Castellani, Daniela; Gosso, Guido
Map Title:	Petrostructural map of Monte Mucrone Metagranitoids (Sesia-Lanzo Zone, Western Alps)
Reviewer:	Ian Muehlenhaus, University of Wisconsin – La Crosse, United States

Cartographic Generalisation

Design Element	Comments
Classification of map data	– Ordinal scale based on grains. Fine.
Exaggeration/feature enhancement	– The star symbols are tiny and only visible if you really zoom in. Enhancement may help greatly.
Data elimination/smoothing	– Some smoothing and agglomeration may be helpful when small pockets of fine grained things run into one another. The amount of detail is a little overwhelming in some places, and I am not sure it helps the map reader much. At the same time, I appreciate this accuracy is probably important to these map makers. It is a dilemma.
Location & design of symbols	– The star symbols should be changed. They do not look good, do not have solid fills, and are hard to see. A geometric shape is appropriate, but stars for certain rocks just don't make intuitive sense to me. Unless this is a geological symbolization norm I am unaware of, perhaps a square, triangle, or other shape is more fitting. Also need to be larger. – the color schemes used for the ordinal, grain-based ranked data is unintuitive and inappropriate. Instead of color hues (yellow, green, purple, blue), I recommend using color values (shades of purple, shades of green, etc.). Ordinal data represented with hue is misleading and makes the map difficult to read. – The fold axes attitudes (do they mean attitudes?) numbers are color-coded, which is nice, but almost impossible to read on the map itself. These numbers might be made larger or given halos/drop-shadows so that one can clearly and easily read them.

Typographic design (style, form)

Design Element	Comments
Type size	<ul style="list-style-type: none"> • Altitude fonts are too small. The caption sizes seem cramped and too crowded as well. Perhaps a title more leading between the lines of text would help. • CK type color on the maps, but type is simply illegible on the photos. Cannot read it very clearly at all. Needs major work. It is also not consistent – on one picture it will be white, on the next black, and it will be difficult to read on both. • Naming conventions are fine.
Type Position	
Naming conventions	

Visual Balance of Map Elements

Design Element	Comments
Map orientation & position	
Visual balance of map elements	<ul style="list-style-type: none"> • The layout of this map is the most problematic thing about it and will require by far the most work to fix. The map is bottom heavy and not very well balanced. The maps themselves have decent contrast, with the exception of the Schmidt Equal Area Diagrams, which look
Visual contrast of map elements	

Map Inclusions

Design Element	Comments
Statement of scale	Scale is same on all three maps.
Suitability of co-ordinate system	Coordinate system does not seem to be noted anywhere that I could find, which means even if it is, it probably isn't prominent enough. I believe it is UTM, but I have no idea the zone, etc.
Statement of map orientation	Map orientation is stated on each map.
JoM Copyright Statement	I don't see a JoM copyright statement, but I may have missed it.
Appropriateness of text	Textboxes are cramped, small, and probably too ubiquitous.
Author name/contact details	Author names and contact details should be moved away from the title in my opinion.
Suitability of legend	The legend has everything and is very detailed. However, it isn't centered and looks cramped with the outline box around it. Give it a little more space. It is also very wordy.
Suitability of map frames & insets	The map frames are out of place and need to be completely redone using rectangles and consistency between the maps. The inset maps are okay, but cramped into weird places and almost take precedent over the mapped areas. They should be deemphasized by moving them away from the top.

Overall, Synopsis:
Overall, I am sure this data has a lot of scientific merit and it took a lot of time and effort to compile this data. The presentation, though, is wanting and needs to be touched up. The data and idea are good; however, consulting cartographic texts and revising the end visualization quite dramatically is necessary before publication.

PDF Output
PDF file with vector data?

Please note: our technical policy is to ensure the highest possible print quality whilst minimising map file sizes. All vector linework must be included as vector data within the PDF. Fully rasterized maps will not be accepted.

Decision on Publication of Map

<input type="checkbox"/> Accept	<input type="checkbox"/> Accept with revisions	<input checked="" type="checkbox"/> X	<input type="checkbox"/> Reject
---------------------------------	--	---------------------------------------	---------------------------------

Editor-in-Chief: Dr Mike J Smith
School of Geography, Geology and the Environment, Kingston University, Penrhyn Rd, Kingston upon Thames, Surrey, KT1 2EE

2

Fig. 2.9: Response letter of Journal of Maps, with reviewer's comments, by Nov. 2012.



A new petrostructural map of Monte Mucrone metagranitoids (Sesia-Lanzo Zone, Western Alps).

Journal:	<i>Journal of Maps</i>
Manuscript ID:	TJOM-2012-0077.R1
Manuscript Type:	Original Article
Date Submitted by the Author:	31-Dec-2012
Complete List of Authors:	Delleani, Francesco; Università degli Studi di Milano, Scienze della Terra; Spalla, Iole; Università degli Studi di Milano, Castelli, Daniele; Università degli Studi di Torino, Gosso, Guido; Università degli Studi di Milano,
Keywords:	structural mapping, petrological mapping, multiscale analysis, deformation evolution, metamorphic evolution, Sesia-Lanzo Zone

A new petro-structural map of the Monte Mucrone metagranitoids (Sesia-Lanzo Zone, Western Alps)

Francesco Delleani^{*1}, M. Iole Spalla^{*1,2}, Daniele Castelli^{*3} and Guido Gosso^{*1,2}

^{*1}Dipartimento di Scienza della Terra "A. Desio", Università di Milano, Via Mangiagalli 34, 20133, Milano, Italy

^{*2}C.N.R.-I.D.P.A., Sezione di Milano, Via Mangiagalli 34, 20133, Milano, Italy

^{*3}Dipartimento di Scienze della Terra, Università di Torino, Via Valperga Caluso 35, 10125, Torino, Italy

ABSTRACT

The Mt. Mucrone metagranitoid area is an extensively investigated intrusive Permian body, located in the Eclogitic Micaschists Complex of the Sesia-Lanzo Zone, within the high-pressure metamorphic belt of the Western Alps formed during the Alpine plate convergence. The structure of the northwestern sector of Mt. Mucrone, including both the metagranitoids and country rocks, has been mapped, although an integrated structural and petrological analysis is still lacking in its southwestern sector, a topic investigated in this contribution. During the field structural analysis, six groups of ductile structures were recognized as having evolved as follows: the D1 and D2 fabrics took place under eclogite-facies, D3 under blueschist-facies and D4 to D6 under greenschist-facies conditions, respectively. Foliation trajectories revealing the chronology of the superposed structures are represented in the analytical (drift and solid) and interpretative (solid) maps, both at a 1:5000 scale, and a panel of structural cross-sections allows the 3D representation of the poly-deformed lithostratigraphy. The related metamorphism indicates the changes within the subduction-collision tectonic frame.

INTRODUCTION

The petrology and geochemistry of the Mt. Mucrone metagranitoids have been widely investigated (e.g., Compagnoni, 1977; Oberhänsli et al., 1985; Rubbo et al., 1999; Cenki-Tok et al., 2011; with refs.), but an integrated structural and petrological analysis of the southern slope of Mt. Mucrone was needed to reconstruct the superposed grid of foliation trajectories by taking into account the degree of fabric evolution and the associated mineral assemblages. The purpose of this work is to infer the deformation history of this area and correlate it with the structural and metamorphic history deduced in the nearby Mombarone-Mt. Mars-Mt. Mucrone sector to the NW (Zucali et al., 2002). The results are summarized for these new objectives using interpretative structural maps constructed at a 1:5000 scale (original analysis at a 1:2500 scale) and two sets of cross-sections that assist in visualizing the reconstructed 3D structure. Details of the metamorphic evolution are also summarized in the legend, and symbols are used to highlight the metamorphic environment of the successive steps of the fabric development.

GEOLOGIC OUTLINE

The Sesia-Lanzo Zone (SLZ) represents the largest portion (~90 x 20 km) of the western Austroalpine region, the topmost sheet of the continental crust overriding the Alpine oceanic suture and eclogitized during the Alpine subduction (Fig. 1). This portion is elongated parallel to its eastern tectonic boundary (Periadriatic Lineament), which separates the SLZ from the Southalpine domain. Two structural elements are traditionally described (e.g., Dal Piaz et al., 1972): an upper element or the "II Zona Diorito-Kinzigitica" (IIDK), and a lower structural element divided in two main metamorphic complexes, i.e., the Eclogitic Micaschists Complex (EMC) and the Gneiss Minuti Complex (GMC). More

1
2
3 recently, another tectonic unit has been identified in the southern SLZ: the Rocca Canavese Thrust Sheet (RC of
4 Pognante 1989a and 1989b). A redefinition of these metamorphic complexes has been proposed by Babist et al., 2006.

5
6 The IIDK was not re-equilibrated under eclogite-facies conditions during the Alpine convergence and widely
7 preserves the pre-Alpine high temperature-low pressure (HT-LP) metamorphic imprints. The IIDK is principally
8 composed of metapelites and metabasites characterized by a dominant pre-Alpine metamorphic imprint under
9 amphibolite/granulite-facies conditions (the so-called kinzigitic complex, e.g., Compagnoni et al., 1977) with minor
10 metagranitoids and a few slices of mantle peridotite (Beccaluva et al., 1978). The Alpine metamorphic evolution is
11 polyphase and displays a pervasive re-equilibration under greenschist-facies conditions that partly obliterates the
12 blueschist-facies mineral assemblages.
13
14

15 The EMC and the GMC complexes have been eclogitized during Alpine times, but only the first preserves the
16 eclogitic imprint as dominant, whereas the second shows a pervasive Alpine retrogression under greenschist-facies
17 conditions (Spalla et al., 1983). The EMC and GMC rocks include metapelites, paragneisses, metagranitoids,
18 metabasites and impure marble with an Alpine polyphasic deformation under eclogite-facies conditions, followed by
19 retrogression under blueschist- to greenschist-facies conditions (e.g., Compagnoni et al., 1977; Pognante et al., 1980;
20 Lardeaux et al., 1982; Castelli, 1991; Pognante, 1991; Zucali and Spalla, 2011).
21
22
23

24 High-pressure (HP) assemblages in the metapelites consist of Ky, Gln, Grt, Ph, Zoand Cld, yielding temperature
25 estimates that do not exceed 650°C (e.g., Dal Piaz et al., 1971; Compagnoni et al., 1977; Gosso, 1977; Lardeaux et al.,
26 1982; Vuichard, 1987; Zucali and Spalla 2011; Roda et al., 2012).
27

28 The pre-Alpine evolution of the SLZ is characterized by a granulite facies imprint followed by successive re-
29 equilibrations under amphibolite and greenschist-facies conditions (e.g., Lardeaux and Spalla, 1991). The pre-Alpine
30 ages of 280 and 240 Ma (e.g., Hunziker et al., 1992) have been interpreted as dating the granulite- and amphibolite-
31 facies imprints, respectively (Lardeaux and Spalla, 1991) whereas the early Alpine metamorphism has been dated to 60-
32 70 Ma or older (e.g., Rubatto et al. 1999; Cenki-Tok et al., 2011). The exhumation of this portion of SLZ to shallow
33 structural levels (low-pressure, greenschist-facies conditions) was accomplished before the emplacement of the Tertiary
34 intrusive bodies of Biella and Traversella, as evidenced by the development of HT-LP contact mineral assemblages that
35 overprint the greenschist-facies and late-Alpine parageneses (e.g., Zanoni et al., 2010).
36
37
38

39 Permian metaintrusives, of felsic to mafic bulk chemical compositions, variably re-equilibrated under HP
40 conditions during the Alpine convergence (i.e., the Mt. Mucrone metagranitoids or the Sermenza and Corio and
41 Monastero metagabbros) are embodied in the metasediments of the SLZ (e.g., Bertolani, 1971; Compagnoni and
42 Maffeo, 1973; Compagnoni et al., 1977; Koons, 1982; Oberhänsli et al., 1985; Castelli et al., 1994; Bussy et al., 1998;
43 Rebay and Spalla, 2001; Zucali et al., 2002).
44
45
46

47 MAPPING TECHNIQUE

48 The present work describes the correlation of the structural fabric and metamorphic assemblages in the subducted-
49 exhumed polyphased tectonites and a consequent effort to distinguish the pre-Alpine protoliths, of both the meta-
50 intrusives and of their country rocks, on a more convincing base.
51
52

53 The mapped structural elements include the lithologic boundaries, differentiated mineral layerings (foliations) and
54 lineations or fold systems with the related axial plane traces distinguished based on the overprinting relationships. The
55 mineralogical support of the new grain-scale planar and linear fabrics is the primary reference to select mineral
56 compatibilities marking each successive foliation (Turner and Weiss, 1963; Hobbs et al., 1976; Williams, 1985; Spalla
57 et al., 2000; Passchier and Trouw, 2005; Spalla et al., 2005). The inferred lithostratigraphic configuration has been
58
59
60

1
2
3 represented on the “drift and solid” map (in which surfacing rocks are separated by drift cover), and the full pattern of
4 the superposed structures has been reported on the “solid” map and on the cross-section grid. The terms “solid” and
5 “drift and solid” conceptually refer to the mapping and representation techniques in use at the Geological Survey of
6 Great Britain, which concisely convey to readers the extent of lithostratigraphic and structural interpretation inherent to
7 the map document (e.g., Sheet 62W Loch Quoich, 1:50,000 scale solid edition) by means of displaying either the extent
8 of the Quaternary cover (incoherent deposits = drift) or an indication of the fully interpreted lithostratigraphic
9 configuration below it (solid map) or a synthetic combination of both representations (drift and solid). Such objectivity
10 in displaying mapping results has also been attempted in the German (bedekte-covered and unbedekte-uncovered maps)
11 and Italian (carta oggettiva-covered and interpretativa-uncovered maps) geological mapping literature (Rau and
12 Tongiorgi, 1972a, b; Spalla et al., 1983; Spalla et al., 2002). Note that the meta-sediments and meta-granitoids, which
13 are distinguished as different varieties in the “drift and solid” map, are undistinguished in the lithologic legend of the
14 sub-outcropping map. The results of the 1:2500 scale survey of the outcrop contours and structural elements have been
15 drawn using Adobe Illustrator CS6 at a 1:5000 scale. The curves and polylines have been exported in a GIS system as
16 polyline geo-referencing locations using common landmarks between the topography and the reproduced elements.
17

18
19 The orientation of structural elements, such as axial plane foliations, axial surface traces and fold axes, are
20 reported on the outcrop map together with their relative chronology. The orientation data have been elaborated with the
21 StereoWin 1.2 software to generate equal area Schmidt diagrams grouped according to their relative chronology. On the
22 interpretative form surface map, the traces of the foliation trajectories are grouped based on relative age, and the
23 metamorphic minerals marking successive fabrics are specified. This representation technique conveys an evolutionary
24 visualization in a complex structural framework together with an immediate perception of the paleo-thermal regimes
25 that characterize the deformation history.
26
27

28 **FIELD DATA**

29
30 Metagranitoids, paragneisses, micaschists and certain leucocratic metagranitoids are the main lithotypes in the
31 mapped area, with minor occurrences of eclogites, glaucophanites and zoisitites.
32

33
34 In all of these rocks, the Alpine eclogitization obliterated most of the previous metamorphic mineral assemblages.
35 The HP metamorphic imprint is dominant and is pervasively replaced only locally by the subsequent blueschist and
36 greenschist-facies re-equilibrations. Structural relics dominate on mineralogical relics of pre-Alpine age with the
37 exception of certain low strain domains of metagranitoids in which more than 40% in volume of the igneous minerals is
38 preserved.
39

40
41 The lithologic types are as follows: 1) metagranitoids of Mt. Mucrone subdivided into a) “grey-type”
42 metagranitoids comprising medium- to coarse-grained rocks showing a well-preserved isotropic and hypidiomorphic
43 igneous structure with igneous relics Bt, Aln, and Kfs only partially replaced by Alpine Jd, Grt, Zo and Ph (photo A in
44 the “lithologic types” of the map plate; mineral abbreviations after Whitney and Evans 2010 plus Wm for white mica);
45 metaquartzdiorite; metaaplite; metapegmatoid; b) “green-type” metagranitoids consisting of fine- to medium-grained
46 rocks showing a deformed igneous texture with a dominant foliation marked by Jd (or Omp), Grt, Wm, Gln and Czo
47 (photo B in “lithologic types” of the map plate); 2) leucocratic metagranitoids; 3) eclogites; 4) micaschists; 5)
48 paragneisses; 6) porphyric gneisses; 7) zoisitites; and 8) glaucophanites. All of these lithotypes contain Qz-dominated
49 high-pressure veins (HP veins). The last two rock types and the HP veins are marked on the map using colored
50 diamonds because they occur as unmappable meter-sized lenses. The mineral associations and dominant textures of
51 these lithotypes are detailed in table 1.
52
53
54
55
56
57
58
59
60

Metaintrusives:

The intrusive protoliths consist principally of granitoids that occur as 10-m to km-sized bodies, including minor meter-sized granodioritic lenses. The first metagranitic complex (“grey-type” metagranitoids and “green-type” metagranitoids) represents the upper part of Mt. Mucrone and derives from Permian intrusive rocks (287-293 Ma) in primary contact with metasedimentary country rocks (Oberhänsli et al., 1985; Bussy et al., 1998; Cenki-Tok et al., 2011) that preserve the HT-LP pre-Alpine metamorphic imprint. The second 100-m metagranitoid (leucocratic metagranitoid) occurs in the lower part of the southeastern ridge of Mt. Mucrone and is embodied in the eclogitized micaschists.

In the first metagranitic complex, the partitioning of Alpine syn-metamorphic deformation is responsible for the differentiation of the two main types: part of the metagranitoids underwent only Alpine metamorphism and preserve the igneous texture, i.e., the “grey-type” metagranitoids and part of the metagranitoids also display an intense Alpine deformation locally associated with the development of a mylonitic fabric (the “green-type” metagranitoids). The “grey-type” metagranitoid is of a smaller volume (approximately one tenth) than the entire metagranitic complex.

Both portions are poorly affected by the metamorphic re-equilibrations under blueschist or greenschist-facies conditions, which are mainly concentrated along centimeter- to meter-thick mylonitic shear zones.

Metasediments:

The metasediments consist mostly of paragneisses and micaschists with minor gneisses, glaucophanites and zoisitites. The paragneisses are structured as Qz- and Grt-bearing mineral layers alternating with mafic layers primarily consisting of Omp, Grt and Gln with interstitial Qz and Wm; this alternance marks the gneissic S1 foliation. Meter-thick layers of porphyric gneiss and coarse-grained Ksp crystals occur in the paragneisses. In agreement with the observations of adjacent areas (Zucali, 2002), these materials are interpreted as derived from pre-Alpine partial melting of the kinzigites (high grade Bt, Sil-bearing gneisses). The micaschists are fine-grained rocks with a pervasive foliation with millimeter-scale spacing marked by alternating Qz- and Wm-rich layers. The boundary with the paragneisses is not sharp because the paragneisses are Wm-rich and shade into the micaschists in the high strain domains. Minor bodies of glaucophanites (1 m to 10 m in size) and HP Qz-dominated veins occur within the micaschists. The glaucophanites display a spaced foliation marked by a Gln-shape preferred orientation (SPO) and are overgrown by randomly oriented Omp crystals. The zoisitites occur as enclaves with a thickness of 10 m in the “green-type” metagranitoid; these rocks are characterized by Grt blasts 10 cm in size.

STRUCTURAL ANALYSIS

The mesoscale structural analysis is aimed at recognition of strain gradients that aid in individuating the protoliths and revealing the superposition of tectonic structures. Six groups of superposed structures (D1 to D6) are defined, mainly consisting of fold systems, foliations and shear zones (cross-sections and solid map of the map plate) developed during the Alpine subduction-exhumation cycle. As detailed in Table 2, the relationships between the superposed fabrics and successive mineral assemblages lead us to infer the following metamorphic and structural evolution:

- D1 folding, with the formation of a S1 eclogite-facies foliation;
- D2 folding, with the formation of a S2 eclogite-facies foliation;
- D3 shear zones, with the formation of a S3 blueschist-facies foliation;
- D4 folding, associated with a greenschist-facies partial re-equilibration but not accompanied by a new mesoscopic foliation;
- D5 shear zones occurring under greenschist-facies conditions;

- D6 gentle folding, without a new foliation development and occurring under greenschist- to sub-greenschist-facies conditions.

The orientation of the structural elements is shown on the map plate. The D1 is the main pervasive deformation, which, together with the development of contemporary eclogite-facies mineral assemblages, extensively obliterates all of the previous textures, structures and mineralogical associations.

Structural and mineralogical pre-Alpine relics: Selected portions of the metagranitoids and metasediments of Mt. Mucrone escaped the granular scale deformation during D1, maintaining the igneous contacts and internal structures between “grey-type” metagranitoids and pre-Alpine lithological layering of the metasediments. Rare mineralogical relics escaped replacement by Alpine minerals, particularly in the metagranitoids, and retain igneous Bt and Aln crystals. Certain magmatic Kfs occur in the metagranitoids and in porphyric gneisses, and reddish Grt cores represent the pre-Alpine relics preserved in the micaschists and paragneisses.

D1: A geometrically coherent fold system with its related pervasive axial plane foliation, S1, overprints the lithologic boundaries and is attributed to the D1 deformation event. The S1 is defined by Qz, Ph, Pg, Na-Cpx, Grt, Gln, Zo and Rt in the metasediments and metagranitoids. In addition, the same assemblage also occurs for the foliated eclogites, though in different component proportions. In the “green-type” metagranitoid, the S1 is mainly marked by Wm, Amp, Omp and Qz lenticular domains (photo B in the “syn-D1 microstructure” of the map plate).

During D1, only coronitic and/or pseudomorphic replacements occur in the poorly-strained portions of the metagranitoids, paragneisses and eclogites:

- In the metagranitoids, the igneous Pl is replaced by fine-grained aggregates of whitish Jd, Zo and Qz, and Bt is partially overgrown by fine-grained Ph and rimmed by Grt; fine-grained Ph replaces igneous Kfs (photo A in the “syn-D1 microstructure” of the map plate);
- In the paragneisses and eclogites, randomly oriented Omp develops.

D2: Several shapes of the D2 folds (1-10 m in size) develop with wavelengths of 5-10 meters. An axial plane S2 foliation occurs only in the micaschists and is marked by Qz, Gln, Ph, Pg, Grt, Czo and Rt with SPO of the Wm, prismatic minerals, and lenticular or tabular Qz domains. In all lithologic types, Gln commonly displays the prismatic elongation parallel to the D2 fold axes. Locally, in the “green-type” and leucocratic metagranitoids, S1 is partially reactivated and is oriented parallel to the D2 axial plane; it grades laterally into a continuous foliation associated with grain-size reduction (composite S1+S2 fabric). In places where S2 is lacking, the microstructure displays the corona-type of syn-D2 minerals (Gln, Omp, Ph, Grt and Czo) growing over the previous mineral assemblages.

D3: These structures are a group of shear zones (1-cm to 1-m thick) marked by Qz, Ph, Pg, Grt, Mg-Chl, Czo and Ttn; they are generally located at a low angle to the pre-existing S1 and S2 that are therefore reactivated as slip planes giving rise to S1+S3 and S2+S3 composite fabrics, especially near the main lithologic boundaries. The S3 foliated zones display a 1-m to 10-m spacing, and in the metagranitoids and paragneisses, the deformation is localized in bands with a thickness of 1-2 cm whereas in the other lithologic types, the S3 is less localized and affects much larger volumes of the rock. Almost everywhere, the S3 foliations wrap around eclogite and metaquartzdiorite boudins with a size of 10 m. The syn-D3 minerals are coarse-grained where they are concentrated along discrete layerings, especially those consisting of Ph and Pg.

D4: These fold structures are not accompanied by a new foliation. Tight (30°) to open (120°) symmetric folds with 10-m wavelengths are spaced (20 m) in the metagranitoids and paragneisses and also spaced (5 m) in the micaschists and leucocratic metagranitoids. The syn-D4 fold systems and the related granular scale fabric are associated with the growth of fine-grained Ab, Wm, Chl, Act, Ttn, Ksp (Adl), Ep and Bt, partially replacing the coarser-grained eclogite-

1
2
3 and blueschist-facies mineral assemblages as coronitic aggregates. A penetrative crenulation develops locally in the
4 micaschists, associated with the almost complete passive replacement of Cpx by Ab and Wm and Act aggregates.

5 **D5:** Mylonitic shear zone systems with a thickness of 0.5-1 cm formed during this deformation episode; the new
6 grain-scale fabric is marked by Ab, Chl, Qz, Ep, Act and green Bt, with a 10-m spacing in the northern portion of the
7 map and a narrower spacing in the southern portion, and increasing dynamic re-crystallization in the Qz grains of the
8 micaschists. The shear zones are a few centimeters wide in all lithologic types, and the new mineral growth generated a
9 grain-size reduction.

10 **D6:** The gentle folding of D6 imposes weak undulations of the previous structures. A centimeter-scale kinking of
11 the mineral layering is associated with these folds. The major undulations display a 100-m wavelength responsible for
12 the bimodal distribution of the previous fabric elements. The formation of a disjunctive cleavage is associated to the D6
13 axial planes with formation of Ab, Wm, Adl, dark Amp and Fe-oxides.

14 15 16 17 18 19 20 CONCLUSIONS

21 The petro-structural mapping and representation technique used in this work offers a powerful tool for modeling of
22 the superposed grid of foliated textures and the deformation history in space together with the related succession of
23 mineral assemblages shown in a time sequence. Both maps provide better insights into the sequence of metamorphic
24 conditions under which different groups of structures were imprinted; they additionally provide a consistent
25 visualization of the vertical displacements experienced during the tectonic evolution based on the pressure and thermal
26 variations recorded by this portion of the Austroalpine basement during Alpine orogeny. Field data supported by
27 microstructural results are therefore a coherent base from which to infer the tectonics steps of Alpine geodynamics.

28 In detail, the metamorphic and structural evolution indicates that: 1) the D1 and D2 stages are synchronous with
29 mineral assemblages that widely testify to the persistence of HP metamorphic conditions under a low thermal regime
30 and are compatible with active subduction, and 2) the metamorphic assemblages syn-kinematic with D3 to D6 suggest
31 that these deformations took place during cooling and decompression, indicating tectonic exhumation to shallower
32 structural levels. The latter occurred prior to 30 Ma, as indicated by the relationships with the Biella and Traversella
33 intrusive body (e.g., Zaroni et al., 2010, with refs.). The structural and metamorphic outline is coherent with that
34 inferred by Zucali, 2002a, and Zucali et al., 2002b, in the northernmost sector, from Mombarone to Mt. Mars. The
35 detailed multi-scale structural investigation demonstrates that the “green- and “grey-type” metagranitoids differ mainly
36 in the degree of fabric evolution (highly deformed vs. poorly- to undeformed, respectively) accomplished during the
37 eclogite-facies re-equilibration. This result supports the interpretation proposed for the metagranitoids of the eastern
38 wall of Mt. Mucrone (Castelli et al., 1994).

39 40 41 42 43 44 45 46 47 Acknowledgements:

48 Critical readings by P. Manzotti, I. Muehlenhaus, B. Stoeckhert and C. Valeriano greatly improved the text and the
49 graphical presentation of maps and cross-sections. The field work was carried out by F.D., and M. Zucali is thanked for
50 stimulating discussions. Funding is acknowledged from PRIN 2008 “Tectonic trajectories of subducted lithosphere in
51 the Alpine collisional orogen from structure, metamorphism and lithostratigraphy”.

52 53 54 55 REFERENCES

- 1
2
3 BABIST, J., HANDY, M. R., KONRAD-SCHMOLKE, M. and HAMMERSCHMIDT, K. (2006) Precollisional,
4 multistage exhumation of subducted continental crust: The Sesia Zone, western Alps, *Tectonics*, 25, TC6008, doi:
5 6010.1029/2005TC001927.
6
7 BECCALUVA, L., DAL PIAZ G. V., MACCIOTTA, G. and ZEDA, O. (1978) The austroalpine harzburgite body of
8 the Artona valley (Italian Western Alps), *Mem. Sc. Geol. Padova*, 33, 173-181.
9
10 BERTOLANI, M. (1971) La petrografia della cosiddetta Seconda Zona Kinzigitica nelle alte Valli del Mastallone e del
11 Sermenza (Val Sesia), *Rend. Soc. It. Miner. Petrol.*, 27(1), 367-391.
12
13 BUSSY, F., VENTURINI, C., HUNZIKER, J. and MARTINOTTI, G. (1998) U-Pb ages of magmatic rocks of the
14 Western Austroalpine Dent Blanche-Sesia Unit, *Schweiz. Mineral. Petrogr. Mitt.*, 78, 163-168.
15
16 CASTELLI, D. (1991) Eclogitic metamorphism in carbonate rocks: the example of impure marbles from the Sesia -
17 Lanzo Zone, Italian Western Alps, *J. metamorphic Geol.*, 9, 61-77.
18
19 CASTELLI, D., COMPAGNONI, R. and NIETO, J.M. (1994) High pressure metamorphism in the continental crust:
20 eclogites and eclogitized metagranitoids and paraschists of the Monte Mucrone area, Sesia Zone, In: COMPAGNONI
21 R., MESSIGA B. AND CASTELLI D. (Eds.): High pressure metamorphism in the Western Alps. Guide-book to the B1
22 "field excursion of the 16th Gen." IMA Meeting, Pisa, 4-9 settembre 1994, 107-116.
23
24 CASTELLI, D., GOSSO, G., ROSSETTI, P.G., SPALLA, M.I., ZANONI, D. and ZUCALI, M. (2007) Guide-book to
25 the DRT 2007 Workshop "Field Excursion on the subducted continental crust of the Sesia-Lanzo Zone (Monte Camino-
26 Monte Mucrone; Oropa-Biella, Western Italian Alps)", *Quad. di Geodin. Alp. e Quat.*, 9, 35-70.
27
28 CENKI-TOK, B., OLIOT, E., RUBATTO, D., BERGER, A., ENGI, M., JANOTS, E., THOMSEN, T.B., MANZOTTI,
29 P., REGIS, D., SPANDLER, C., ROBYR, M. and GONCALVES, P. (2011) Preservation of Permian allanite within an
30 Alpine eclogite facies shear zone at Mt Mucrone, Italy: Mechanical and chemical behavior of allanite during
31 mylonitization, *Lithos*, 125, 40-50, doi:10.1016/j.lithos.2011.01.005.
32
33 COMPAGNONI, R. (1977) The Sesia-Lanzo zone: high-pressure low-temperature metamorphism in the Austroalpine
34 continental margin, *Rend. Soc. It. Mineral. Petrol.*, 33, 335-374.
35
36 COMPAGNONI, R. (2003) HP metamorphic belt of the Western Alps, *Episodes*, 26/3, 200-204.
37
38 COMPAGNONI, R. and MAFFEO, B. (1973) Jadeite-Bearing Metagranites I. s. and Related Rocks in the Mount
39 Mucrone Area (Sesia-Lanzo Zone, Western Italian Alps), *Schweiz. Mineral. Petrogr. Mitt.*, 53, 355-378.
40
41 COMPAGNONI, R., DAL PIAZ, G.V., HUNZIKER, J.C., GOSSO, G., LOMBARDO, B. and WILLIAMS, P.F.
42 (1977) The Sesia-Lanzo Zone, a slice of continental crust with Alpine HP-LT assemblages in the Western Alps, *Rend.*
43 *Soc. It. Mineral. Petrol.*, 33, 281-334.
44
45 DAL PIAZ, G. V., GOSSO, G. and MARTINOTTI, G. (1971) La II Zona Dioritico-kinzigitica tra la Val Sesia e la
46 Valle d'Ayas (Alpi Occidentali), *Mem. Soc. Geol. It.*, 10, 257-276.
47
48 GOSSO, G. (1977) Metamorphic evolution and fold history in the eclogite micaschists of the upper Gressoney valley
49 (Sesia-Lanzo zone, Western Alps), *Rend. Soc. It. Mineral. Petrol.* 33, 389-407.
50
51 HOBBS, B. E., MEANS, W. D. and WILLIAMS, P. F. (1976) An outline of structural geology, Wiley, New York, 571
52 pp.
53
54 HUNZIKER, J. C., DESMONS, J. and HURFORD, A. J. (1992) Thirty-two years of geochronological work in the
55 Central and Western Alps: a review on seven maps, *Mém. Géol. Lausanne*, 13, 1-59.
56
57 KOONS, P.O. (1982) An investigation of experimental and natural HP assemblages from the Sesia Zone, Western Alps,
58 Italy, PhD Thesis, ETH Zürich, 260 pp.
59
60

- 1
2
3 KROGH RAVNA, E.J. and TERRY, M.P. (2004) Geothermobarometry of UHP and HP eclogites and schists; an
4 evaluation of equilibria among garnet-clinopyroxene-kyanite-phengite-coesite/quartz, *Journal Metam. Petrol.*, 22, 579-
5 592.
6
7 LARDEAUX, J. M., GOSSO, G., KEINAST, J.R. and LOMBARDO, B. (1982) Relations entre le métamorphisme et la
8 déformation dans la zone Sésia-Lanzo (Alpes Occidentales) et le problème de l'éclogitisation de la croûte continentale,
9 *Bull. Soc. géol. Fr.*, 24, 793-800.
10
11 OBERHÄNSLI, R., HUNZIKER, J.C., MARTINOTTI, G. and STERN, W.B. (1985) Geochemistry, geochronology
12 and petrology of Monte Mucrone: an example of Eo-Alpine eclogitization of Permian granitoids in the Sesia-Lanzo
13 Zone, Western Alps, Italy, *Chemical Geology*, 52, 165-184.
14
15 PASSCHIER, C. W. and TROUW, R. A. J. (2005) *Microtectonics*, Springer, Verlag Berlin Heidelberg, 366 pp.
16
17 PASSCHIER, C. W., URAI, J. L., VAN LOON, J. and WILLIAMS, P. F. (1981) Structural geology of the central Sesia
18 Lanzo Zone, *Geologie en Mijnbouw*, 60, 497-507.
19
20 POGNANTE, U. (1989a) Lawsonite, blueschist and eclogite formation in the southern Sesia Zone (Western Alps,
21 Italy), *Eur. J. Mineral.*, 1, 89-104.
22
23 POGNANTE, U. (1989b) Tectonic implications of lawsonite formation in the Sesia Zone (Western Alps).
24 *Tectonophysics*, 162, 219-227.
25
26 POGNANTE, U. (1991) Petrological constraints on the eclogite- and blueschist-facies metamorphism and P-T-t paths
27 in the Western Alps, *J. metamorphic Geol.*, 9, 5-17.
28
29 POGNANTE, U., COMPAGNONI, R. and GOSSO, G. (1978) Micro-mesostructural relationships in the continental
30 eclogitic rocks of the Sesia-Lanzo Zone (italian Western Alps): a record of a subduction cycle, *Red. Soc. It. Min.*
31 *Petrol.*, 36, 169-186.
32
33 RAMSAY, J.G. (1967) *Folding and fracturing of rocks*, Mc Graw-Hill, 568 pp, New York.
34
35 RAU, A. and TONGIORGI, M. (1972a) Carta Geologica dei Monti Pisani a Sud-Est della Valle del Guappero (I) - scala
36 1:25.000. Centro di Minerogenesi, Petrogenesi e Tettogenesi dell'Appennino Settentrionale del C. N. R., Pisa (ed.),
37 L.A.C., Firenze.
38
39 RAU, A. and TONGIORGI, M. (1972b). Carta geologica interpretativa dei Monti Pisani a Sud-Est della Valle del
40 Guappero (II) - scala 1:25.000. Centro di Minerogenesi, Petrogenesi e Tettogenesi dell'Appennino Settentrionale del C.
41 N. R., Pisa (ed.), L.A.C., Firenze.
42
43 RODA, M., SPALLA, M. I. and MAROTTA, A. M. (in press) Integration of natural data within a numerical model of
44 ablative subduction: A possible interpretation for the Alpine dynamics of the Austroalpine crust, *J. Metam. Geol.*,
45 (2012).
46
47 RUBATTO, D., GEBAUER, D. and COMPAGNONI, R. (1999) Dating of eclogite-facies zircons: the age of Alpine
48 metamorphism in the Sesia-Lanzo Zone (Western Alps), *Earth Planet. Sci. Lett.*, 167, 141-158.
49
50 RUBBO, M., BORGHI, A. and COMPAGNONI, R. (1999) Thermodynamic analysis of garnet growth zoning in
51 eclogite facies granodiorite from M. Mucrone, Sesia Zone, western Italian Alps, *Contrib. Mineral. Petrol.*, 137(4), 289-
52 303.
53
54 SPALLA, M. I., DE MARIA, L., GOSSO, G., MILETTO, M. and POGNANTE, U. (1983) Deformazione e
55 metamorfismo della Zona Sesia - Lanzo meridionale al contatto con la falda piemontese e con il massiccio di Lanzo,
56 Alpi occidentali, *Mem. Soc. Geol. Ital.*, 26, 499-514.
57
58
59
60

- 1
2
3 SPALLA, M. I., SILETTO, G. B., DI PAOLA, S. and GOSSO, G. (2000) The role of structural and metamorphic
4 memory in the distinction of tectono-metamorphic units: the basement of the Como Lake in the Southern Alps, *J.*
5 *Geodynamics*, 30, 191-204.
6
7 SPALLA, M. I., DI PAOLA, S., GOSSO, G., SILETTO, G. B. and BISTACCHI, A. (2002) Mapping tectono-
8 metamorphic histories in the Lake Como Basement (Southern Alps, Italy). *Mem. Sci. Geol. Padova*, 54, 1-25.
9
10 SPALLA, M. I., ZUCALI, M., DI PAOLA, S. and GOSSO, G. (2005) A critical assessment of the tectono-thermal
11 memory of rocks and definition of tectono-metamorphic units: evidence from fabric and degree of metamorphic
12 transformations, *Geological Society Special Publications*, 243, 227-247.
13
14 SPALLA, M.I. and ZULBATI, F. (2003) Structural and petrographic map of the southern Sesia-Lanzo Zone (Monte
15 Soglio-Rocca Canavese, Western Alps, Italy), *Mem. Sci. Geol.*, 55, 119-127.
16
17 TURNER, F. J. and WEISS, L. E. (1963) *Structural analysis of metamorphic tectonites*, MacGraw-Hill, New York, 545
18 pp.
19
20 VUICHARD, J. P. (1987) Conditions P-T du métamorphisme antéalpin dans la "seconde zone diorito-kinzigitique"
21 (Zone Sesia-Lanzo, Alpes occidentales), *Schweiz. Miner. Petr. Mitt.*, 67, 257-271.
22
23 WILLIAMS, P. F. (1985) Multiply deformed terrains - problems of correlation, *J. Struct. Geol.*, 7(3/4), 269-280.
24
25 ZUCALI, M. and SPALLA, M. I. (2011) Prograde lawsonite during the flow of continental crust in the Alpine
26 subduction: Strain vs. metamorphism partitioning, a field-analysis approach to infer tectonometamorphic evolutions
27 (Sesia-Lanzo Zone, Western Italian Alps), *J. Struc. Geol.*, 33, 381-398, doi:10.1016/j.jsg.2010.12.006.
28
29 ZUCALI, M., SPALLA, M.I. and GOSSO, G. (2002) Strain partitioning and fabric evolution as a correlation tool: the
30 example of the eclogitic micaschists complex in the Sesia-Lanzo Zone (Monte Mucrone – Monte Mars, Western Alps
31 Italy), *Schweiz. Mineral. Petrogr. Mitt.*, 82, 429-454.
32
33 WHITNEY, D.L. and EVANS, B.W. (2010) Abbreviations for names of rock-forming minerals, *Am. Mineral.*, 95, 185-
34 187, doi: 10.2138/am.2010.3371.
35
36
37
38
39
40
41
42
43
44
45
46
47
48
49
50
51
52
53
54
55
56
57
58
59
60

1
2
3
4
5
6
7
8
9
10
11
12
13
14
15
16
17
18
19
20
21
22
23
24
25
26
27
28
29
30
31
32
33
34
35
36
37
38
39
40
41
42
43
44
45
46
47
48
49
50
51
52
53
54
55
56
57
58
59
60

A new petrostructural map of the Monte Mucrone metagranitoids (Sesia-Lanzo Zone, Western Alps)

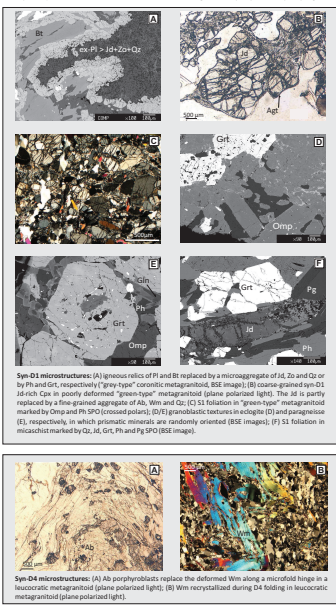
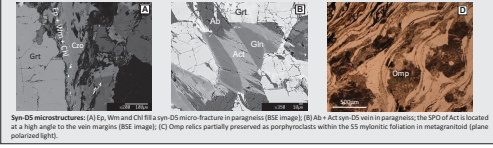
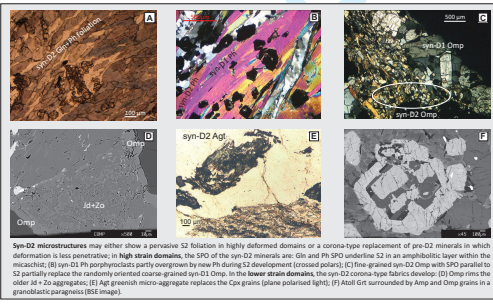
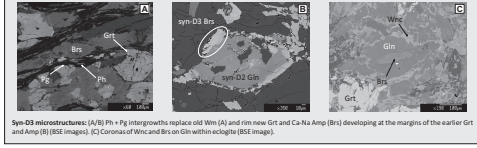
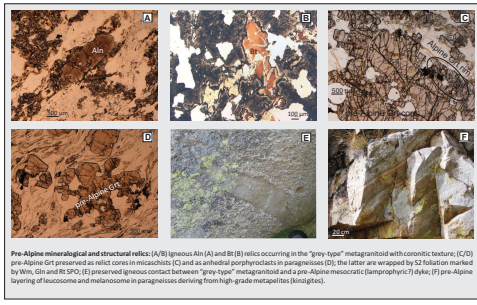
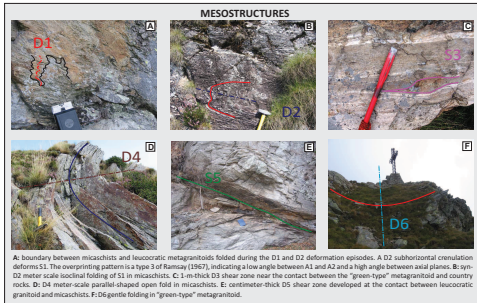
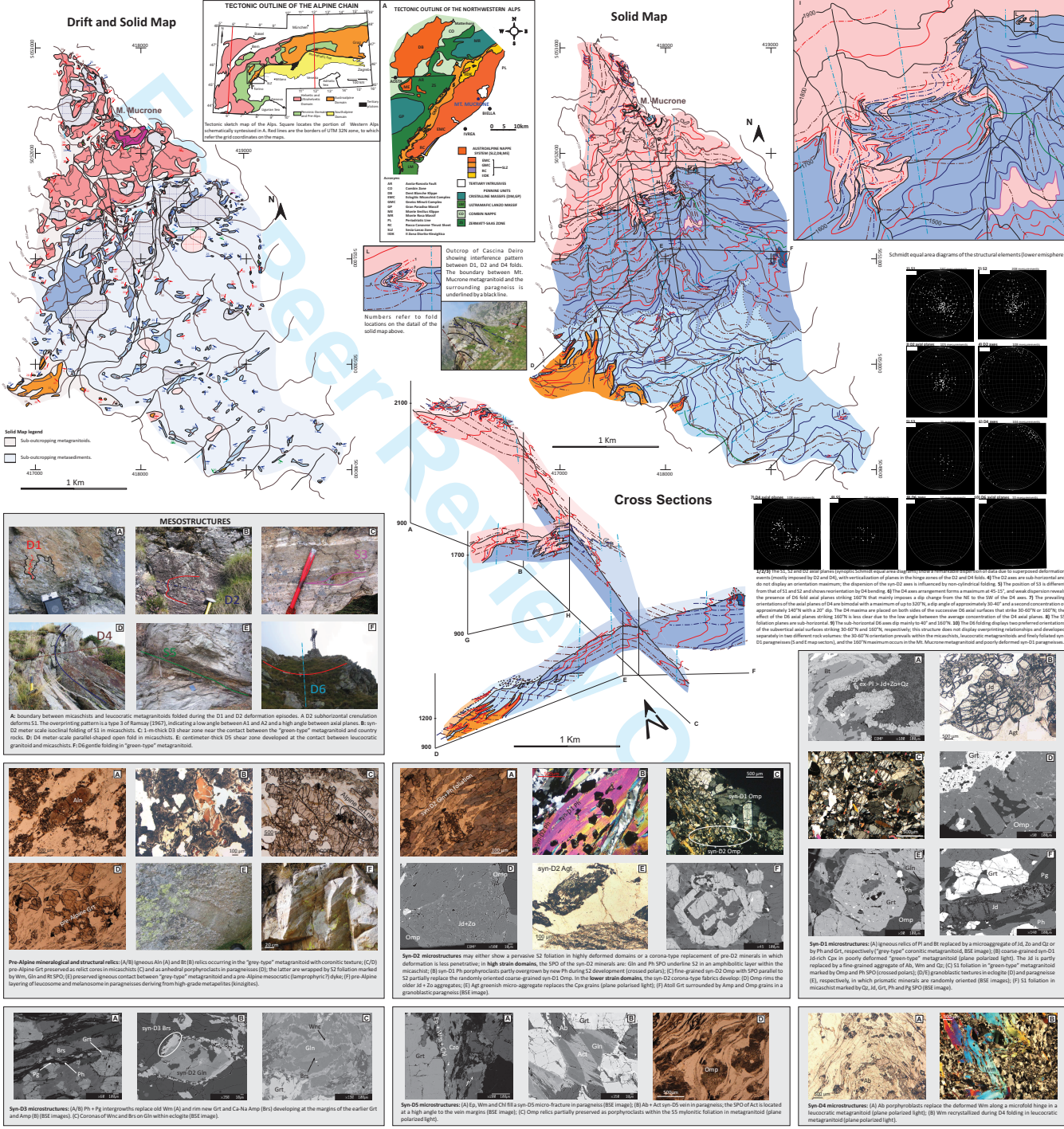
Francesco Delleani*, M. Iole Spalla*, Daniele Castellani* and Guido Gosso*^{1,2}

*¹Dipartimento di Scienze della Terra A. D. Università di Milano * ²C.N.R.-I.D.P.A. - Sezione di Milano *Dipartimento di Scienze della Terra - Università di Torino

© Journal of Maps, 2013

LEGEND FOR DRIFT AND SOLID AND SOLID

- 14 deposits
- 15 to 26 Mesozoic
- 27 to 32 Mesozoic foliations and axial plane trajectories
- 33 LITHOLOGIC TYPES



1
2
3
4
5
6
7
8
9
10
11
12
13
14
15
16
17
18
19
20
21
22
23
24
25
26
27
28
29
30
31
32
33
34
35
36
37
38
39
40
41
42
43
44
45
46
47
48
49
50
51
52
53
54
55
56
57
58
59
60

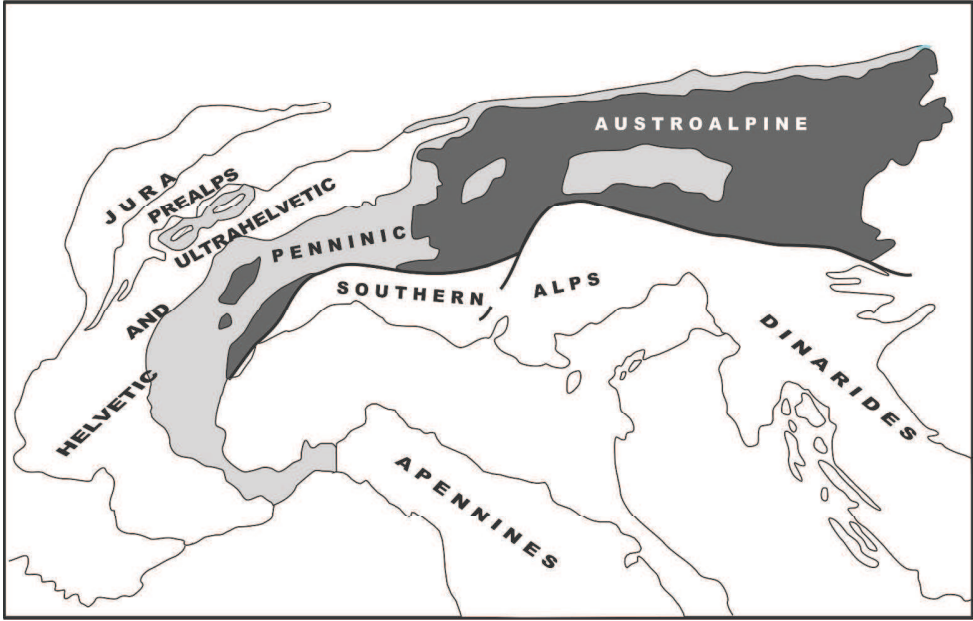


Fig. 1. Tectonic sketch of the Sesia-Lanzo Zone (redrawn after Passchier et al., 1981; Spalla and Zulbati, 2003) and location of the SLZ in the Alpine chain (inset).
281x179mm (300 x 300 DPI)

Review Only

Table 1. Mineral associations and dominant textures in metagranitoids and surrounding rocks of Monte Mucrone southern slope.

	Rock-type	Modal composition	Coronitic texture	Tectonitic texture	Mylonitic texture	
Metaintrusives	Green-type metagranitoid: Jd or Omp, Grt, Wm and Gln fine to medium grained bearing metagranitoid	Qz 30-50%, Cpx (Jd/Omp) 20-30%, Wm 15-20%, Grt 15-20%, Zo 5% and Gln 5%		green coloured rock medium grained with gneissic spaced foliation evidenced by Wm and Cpx SPO	fine grained mm spaced foliation evidenced by Wm and Cpx SPO	
	Grey-type metagranitoid: Jd, Grt and Wm bearing medium to coarse grained metagranitoid with relics of igneous of Bt, Ksp and Aln	Qz 50%, Jd 25%, Wm 15%, Grt 5% and Zo 5%. Estimated igneous composition: Qz 40%, plagioclase 40%, Ksp 20% and bt 10%	grey coloured rock with preserved ipidiomorphic igneous texture, with withish aggregates of Jd + Qz and Grt rimming Bt microsites		localized mm thick shear zones marked by Act, Wm and Ep SPO	
	Metaquartzdiorite: Omp, Grt, Wm and Gln medium to coarse grained bearing metaquartzdiorite	Omp 30%, Grt 25%, Qz 20%, Wm 10% and Gln 10%. Igneous composition: Pl 30%, Qz 20%, Ksp 10% and mafic minerals 40%	medium to coarse grained rock with randomly oriented Omp, Ph and Gln	tectonitic to mylonitic textures occur at the boundaries of metaquartzdiorite lenses with foliation marked by Gln, Grt and Ph SPO		
	Metaaplite-metapegmatoid: Jd-bearing fine grained aphyric bearing metaaplite and Jd, Wm and Grt bearing coarse grained metapegmatoid	Qz 50%, Jd 25%, Wm 15%, Grt 5% and Zo 5%	same of grey-type metagranitoid s.s.	gneissic texture with foliation marked by Ph and elongated Qz-rich domains		
	Leucocratic metagranitoid: Ab, Wm and Gln medium to fine grained leucocratic metagranitoid	Qz 40%, Ab 40% and Wm 20%		spaced continuous foliation tactionitic to mylonitic foliation, medium to fine grained, marked by Ph SPO and elongated Qz domains		
	Eclogite: Gln, Wm and Zo bearing fine grained eclogite	Omp 35%, Grt 25%, Gln 20%, Wm 10% and Zo 10%	massive to very poorly foliated rock with S2 foliation marked by Gln		localized mm thick shear zones marked by Act, Wm and Ep SPO	
Paraderivates	Micaschist: Wm, Grt, Gln, Cpx (Jd/Omp) and Zo bearing fine grained micaschist	Wm (15-40%), Qz (15-50%), Gln (5-25%), Grt 15%, Cpx 10% and Zo 5%		micaschist always have a tectonitic to mylonitic pervasive texture, with mm spaced continuous foliation marked by Qz, Cpx, Gln, Wm and Zo. Foliation could be reactivated as slip plane by successive deformation stages		
	Paragneiss: alternances of Qz and Grt bearing layers and mafic layers	Qz and Grt bearing layers: Qz 65%, Grt 15%, Wm 15% and Gln 5%. mafic layers: Gln 50%, Omp 25%, Grt 15%, Qz 5% and Wm 5%	gneissic texture inherited by pre-Alpine metasediments is marked by alternating layers	in less developed tectonitic texture the tectonitic fabrics are concentrated in Qz and Grt layers marked by Wm SPO. In more developed tectonite and in mylonitic texture a mm spaced foliation occur in all layers marked by Qz, Wm, Cpx and Gln SPO		
	Porphyric gneiss: Qz, Ab, Wm and Ksp fine to medium grained porphyric gneiss with coarse grained Ksp cristals	Qz 35%, Ab 25%, Wm 20% and Ksp 20%		gneissic texture with foliation marked by Wm SPO and by elongation of Qz and Ksp-rich domains		
	Zoisitite: Qz, Wm and Gln bearing fine grained Zoisite with Grt megAblast	matrix (70% volume) composed of Zo 35%, Qz 15%, Wm 10%, Gln 5% and Omp 5%, with ten cm sized Grt blast 30%	unfoliated granoblastic texture		mylonitic foliation marked by Zo, Wm and Gln enveloping Grt blast	
	Glaucophanite: Omp, Grt and Wm bearing porphiric fine grained glaucophanite	Gln 50%, Omp 20%, Grt 20% and Wm 10%. Locally Qz occurs		foliation maked by Gln and Wm SPO with randomly oriented Omp and Grt		

Table 2. Relationships between superposed fabrics and successive mineral assemblages in metaintrusives and paraderivates of Monte Mucrone so

	Rock-type	pre-D1	D1	D2	D3	D4
Metaintrusives	Green-type metagranitoid	Ap, Aln and Zrn	S1 gneissic massive foliation marked by Qz, Omp/Jd, Ph, Grt, Zo and Rt	coronitic growth of Cpx, Ph, Czo and Qz mainly associated to crenulation	dm-thick shear zones oroducing Qz and Wm, mica fish texture on Ph and Jd. Brs formation on bounied Omp	ten m scale open parallel folds. Ab, Act, Ep and Wm replacement on Cpx , Gln, Zo and Ph
	Grey-type metagranitoid	igneous texture preserved with Bt, Aln, Ap and Zrn relics	coronitic substitution of Pl by Qz+Jd+Zo aggregates, Bt and Ksp partially replaced by Ph. Grt rims igneous Bt	ten m scale isoclinal parallel folds, coronitic growth of Omp on Cpx. Ph recrystallization of older Wm	cm-thick shear zones. S3 marked by Ph, Brs, Czo and Ttn	ten m scale open parallel folds. Ab, Act, Ep and Wm replacement on Cpx , Gln, Zo and Ph
	Metaquartzdiorite	igneous texture preserved with Bt, Aln, Ap and Zrn relics	granoblastic texture of Omp and Grt with interstitial Qz, Gln and Ph	ten m scale parallel isoclinal folds, corotitic reaction forming Qz, Omp, Gln, Ph, Grt, Czo and Rt	m-thick shear zones on boundaries of bodies. S3 marked by Qz, Ph, Brs, Grt, Czo, Mg-Chl and Ttn	ten m scale open parallel folds. Ab, Act, Ep and Wm replacement on Cpx , Gln, Zo and Ph
	Metaaplite and metapegmatoid	igneous texture preserved with Bt, Aln, Ap and Zrn relics	coronitic substitution of Pl by Qz+Jd+Zo aggregates, Bt and Ksp partially replaced by Ph. Grt rims igneous Bt	ten m scale isoclinal parallel folds, coronitic growth of Omp on Cpx. Ph recrystallization of older Wm	cm-thick shear zones. S3 marked by Ph, Brs, Czo and Ttn	ten m scale open parallel folds. Ab, Act, Ep and Wm replacement on Cpx , Gln, Zo and Ph
	Leucocratic metagranitoid	/	S1 cm spaced continuous foliation marked by Ph and elongated Qz domains	ten m scale isoclinal similar folds. Partial dynamic recrystallization of Ph and growth of Gln parallel to the	/	open to close parallel folds, crenulation of hinge zones and dynamic ricrystallization of Qz, Ab, Act, Wm and Ep
	Eclogite	/	granoblastic texture of Omp, Gln. Grt and Ph	coronitic growth of Omp, Gln, Grt and Ph	cm-thick shear zones. S3 marked by Ph, Brs, Czo and Ttn	ten m scale open parallel folds. Ab, Act, Ep and Wm replacement on Cpx , Gln, Zo and Ph
Paraderivates	Micaschist	pre-Alpine Grt cores, Ap, Aln and Zrn	isoclinal stretched similar folds. S1 marked by Qz, Cpx (Jd/Omp), Ph, Gln, Zo and Rt	m scale isoclinal similar folds, with associated S2 obliterating S1 marked by Qz, Omp, Ph, Gln, Grt, Czo and Rt	deformation distributed in all the volume with Qz, Ph and Brs grain size reduction	open to close folds with intense crenulation. Widespread growth of Ab, Wm, Qz, Act, Chl, Ep and Ttn
	Paragneiss	pre-Alpine layer alternation of metasediments and Grt cores, Ap, Aln and Zrn	coronitic texture growth of Omp, Grt, Gln, Ph, Zo and Rt. S1 marked by Qz, Cpx (Jd/Omp), Ph, Gln, Zo and Rt	m scale isoclinal parallel folds. Coronitic growth of Qz, Omp, Ph, Gln, Czo and Rt	cm-thick shear zones. S3 marked by Ph, Brs, Czo and Ttn	ten m scale open parallel folds. Coronitic growth of Qz, Ab, Act, Chl, Ep and Wm
	Porphyric gneiss	Ksp relics	isoclinal stretched similar folds. S1 marked by Qz, Ksp, Ph, Gln, Zo and Rt	m scale isoclinal parallel folds. Coronitic growth of Qz, Omp, Ph, Gln, Czo and Rt	cm-thick shear zones. S3 marked by Ph, Brs, Czo and Ttn	ten m scale open parallel folds. Coronitic growth of Qz, Ab, Act, Chl, Ep and Wm
	Zoisite	Aln	S1 cm spaced discontinuous foliation marked by Ph, Zo, Gln and Qz	m scale isoclinal similar folds, with associated S2 marked by rotation of Ph and Gln	cm-thick shear zones. S3 marked by Ph, Brs, Czo and Ttn	open to close folds with crenulation among hinge zones. Abundant formation of Ep, Act, Wm, Qz, Chl and Ttn
	Glaucophanite	/	S1 mm spaced discontinuous foliation marked by Gln with granoblastic texture of Omp and Grt	/	cm-thick shear zones. S3 marked by Ph, Brs, Czo and Ttn	/
	HP quartz vein	/	S1 cm spaced discontinuous foliation marked by Ph, Zo, Gln and Grt trails	m scale isoclinal similar folds, S2 marked by Ph, Gln and Czo SPO	deformation distributed in all the vein volume with large deformation of Qz crystals	/

3.1 Microstructure of Monte Mucrone metagranitoids and country rocks

A selection of photomicrographs showing examples of successive synmetamorphic microstructures that represent a complement to the “Microstructure” paragraph of the paper by Delleani et al., submitted to Journal of Virtual Explorer, follows hereafter.

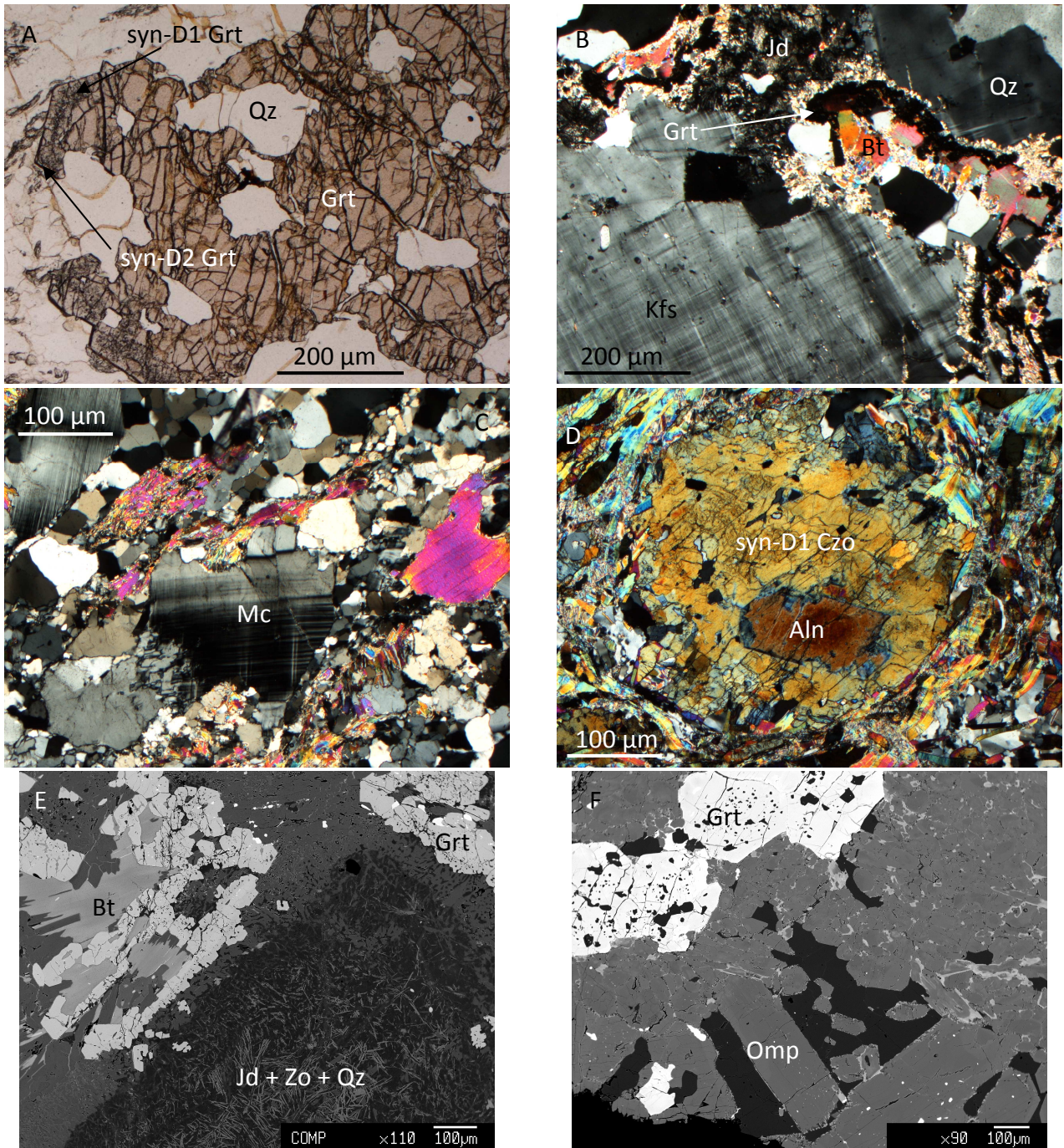


Fig. 3.1: (A) pinkish pre-Alpine Grt core rimmed by syn-D1 and syn-D2 lighter Grt in Qz- and Grt-bearing layers of the paragneisse (plane polarized light); (B) igneous red-brownish Bt and Kfs preserved in “grey type” metagranite (crossed polars); (C) Mc porphyroclasts involved by S1 in porphyric gneiss (crossed polars); (D) Aln relic rimmed by syn-D1 Czo porphyroclasts involved by S2 foliation in zoisitites (crossed polars); (E) coronitic and pseudomorphic reactions in grey-type metagranite with Grt rimming igneous Bt (partly replaced by Ph), and fine-grained Jd + Zo + Qz replacing igneous Pl (BSE image); (F) randomly oriented Omp and peciloblastic Grt developed during D1 in eclogite (BSE image).

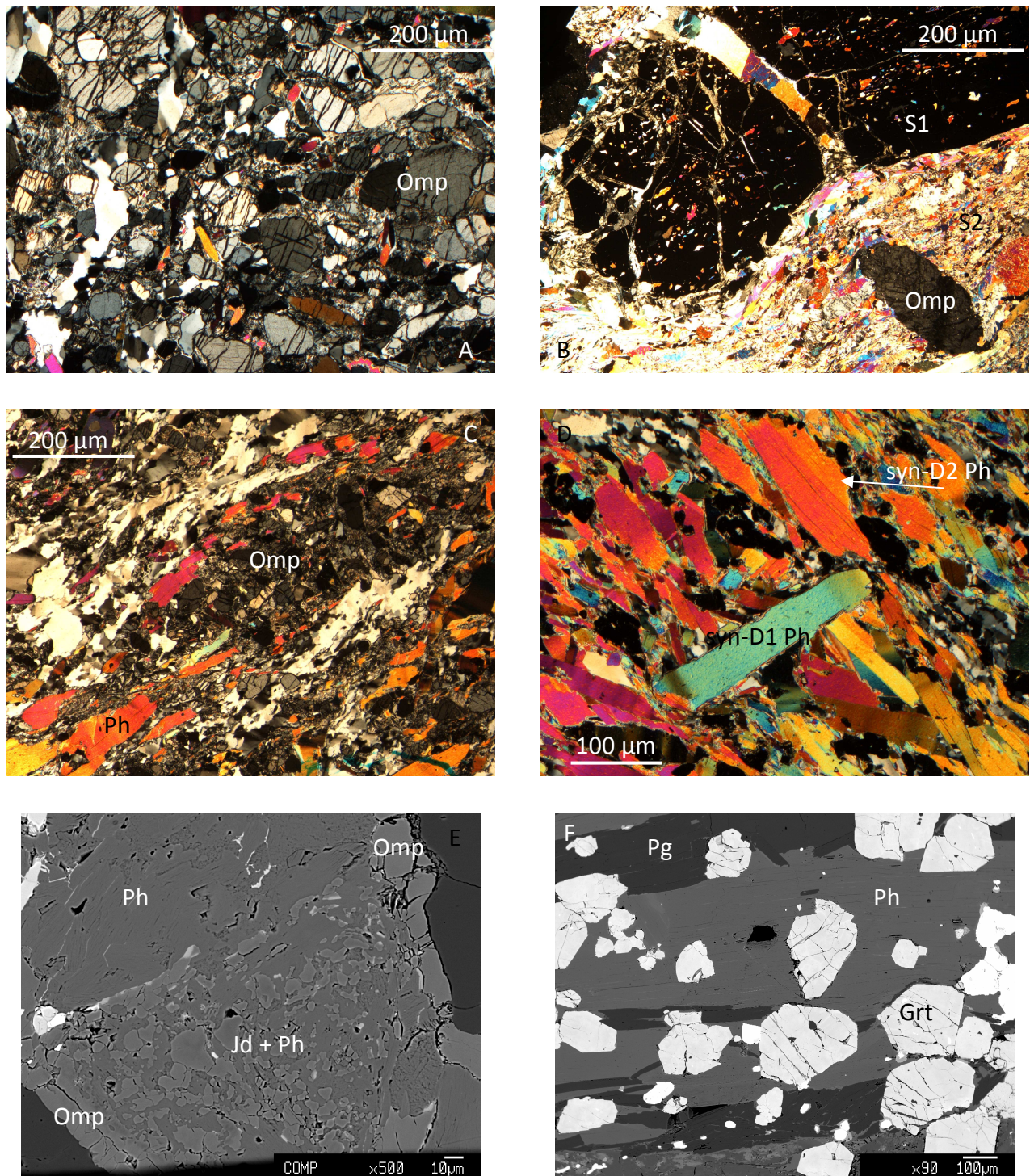


Fig. 3.2: (A) weakly-oriented, euhedral Omp and Ph crystals parallel to the S1 foliation in "green type" metagranite (crossed polars); (B) S1 foliation preserved within Grt in glaucophanite (crossed polars); (C) S1 foliation in "green type" metagranite reutilized as slip plane during S2 forming S1+ S2 texture (crossed polars); (D) large syn-D1 Ph porphyroclasts involved by S2 and rimmed by syn-D2 Ph crystals in micaschist (crossed polars); (E) Omp rims on Jd and Qz aggregate in "grey type" metagranite (BES image); (F) syn-D2 Ph and Pg marking S2 foliation in micaschist (BSE image).

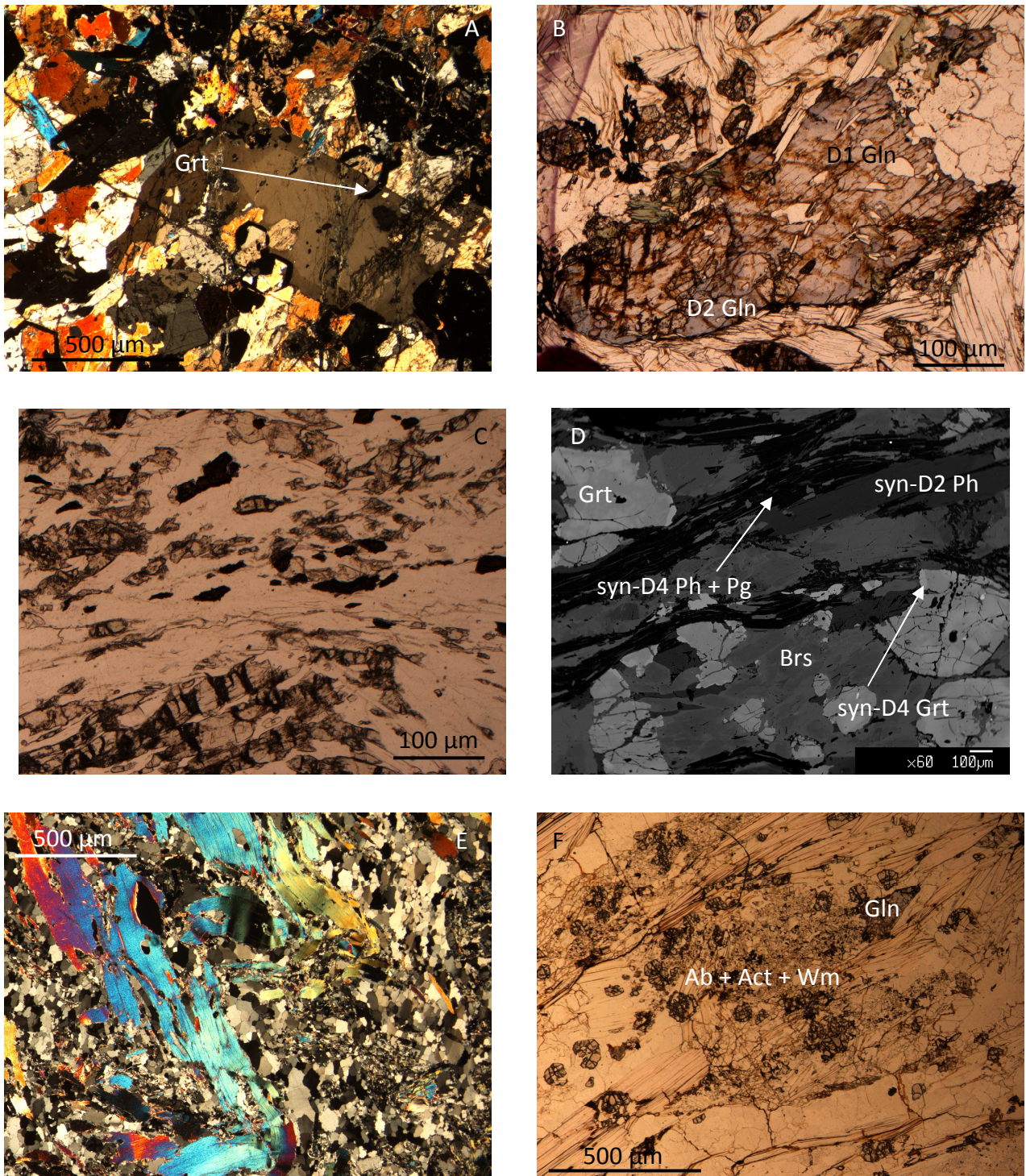


Fig. 3.3: (A) atoll-shaped Grt developed in syn-D2 Gln within eclogite (crossed polars); (B) syn-D2 deeper violet colored Gln rimming lighter colored syn-D1 Gln in micaschist (plane polarized light); (C) S2 foliation cut by S4 shear planes in "gren- type" metagranites (plane polarized light); (D) S4 foliation marked by Ph and Ph aggregates substituting syn-D2 Ph, Brs replacing the prior Amp and thin lighter syn-D4 Grt rimming previous Grt crystals (BSE image); (E) D4 crenulation of syn-D1 large Ph crystals in leucocratic metagranitoid (crossed polars); (F) medium-grained Ab with fine-grained Wm, Act forming aggregate replacing previous Gln in micaschist (plane polarized light).

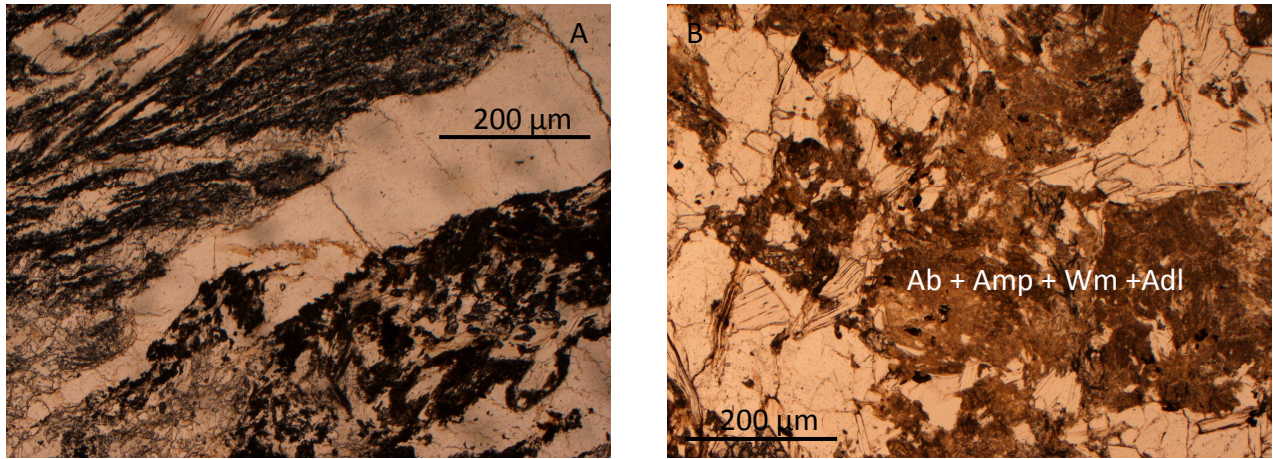


Fig. 3.4: (A) D5 shear planes obliterating shape and minerals of the $Jd + Qz + Zo$ by large formation of Ab and Wm in "green type" metagranite (plane polarized light); (B) syn-D6 replacing of $Na-Cpx$ in "grey type" metagranite forming Ab , brown- Amp , Wn and Adl aggregates (plane polarized light) .

Multiscale structural analysis in the Subducted Continental Crust of the internal Sesia-Lanzo Zone (Monte Mucrone, Western Alps).

Francesco Delleani¹, M. Iole Spalla^{1,2}, Daniele Castelli³ and Guido Gosso^{1,2}

¹Dipartimento di Scienze della Terra “A. Desio”, Università degli Studi di Milano, Via Mangiagalli 34, 20133, Milano, Italy

²C.N.R.-I.D.P.A., Sezione di Milano, Via Mangiagalli 34, 20133, Milano, Italy

³Dipartimento di Scienze della Terra, Università degli Studi di Torino, Via Valperga Caluso 35, 10125, Torino, Italy

Abstract:

Intrusives of Permian age and their high grade country rocks, subducted-exhumed in Alpine time, has been studied with petro-structural methods, applied after previous quality mapping; in this subduction environment of the Sesia-Lanzo Zone of the internal the Western Alps, focus was oriented on mechanisms of interaction, between deformation and progress of metamorphic transformations in an area offering a mosaic of different tectonometamorphic evolutionary steps. Such apparently incoherent distribution of structural imprints, representing various discrete states of the tectonic sequence heterogeneously frozen in adjacent space, has been previously recomposed into a coherent progression of deformation events by means of foliation trajectory mapping; such work guaranteed a petrographic analysis of the mineralogical support of sequentially ordered planar fabrics. Six deformation episodes (D1 to D6) were recognised, as superposed fold, foliations and ductile shear zones systems, evidently related to the Alpine tectonic history; petrologic estimates on time-related microstructures well manifest that eclogite facies metamorphic conditions assisted D1 and D2 deformation stages, blueschist facies reequilibration was contemporaneous with D3 and greenschist facies with D4. Recognition of numerous assemblages and textures of pre-Alpine protoliths supported validity of the individuation of the earliest, more cryptic tectonic environment of the widespread eclogitisation predating D2. The coherent correlation between structural and metamorphic mineral growth histories on a wide study area served as a base for further refinement and revealed that full granular scale diffusion of newly forming parageneses is generally related to attainment of a threshold of intensity in the development of the new planar fabrics, as similarly established in another subducted-exhumed metamorphic complex of the internal Central Alps.

Introduction

Multi-scale structural and petrographic analysis allowed the reconstruction of the tectonic evolution in crustal rocks of orogenic belts giving insights on the development of deformation events and the

evolution of thermal history through time (e.g. Spalla *et al.*, 2000; Spalla *et al.*, 2011; Spalla *et al.*, 2005). The reconstruction of structural and metamorphic evolutions in polycyclic metamorphic terrains is performed since long time through a multidisciplinary approach based on detailed correlation of superposed fabric elements, microstructural analysis and recognition of fabric gradients (Hobbs *et al.*, 1976; Johnson & Vernon, 1995; Park, 1969; Passchier *et al.*, 1990; Salvi *et al.*, 2010; Spalla, 1993; Spalla *et al.*, 2000; Turner & Weiss, 1963; Williams, 1985; Zucali, 2002). Rocks belonging to a single tectono-metamorphic unit generally record heterogeneously the succession of tectonic imprints and the related metamorphic re-equilibrations: in many cases this has been interpreted as due to the catalyzing effect of deformation on metamorphic reaction progress (see Hobbs *et al.*, 2010 and refs therein). At the end of the deformation history the result is a patchy distribution of different fabrics and their supporting mineral assemblages and an estimate of the final distribution of differently re-equilibrated volumes has given fundamental insights into the accomplishment of structural and/or metamorphic re-equilibrations at different structural levels along active plate margins (e.g.: Salvi *et al.*, 2010; Spalla *et al.*, 2005). Such kind of evaluation can highlight, for example, the influence of different deformation mechanisms, phase transitions and, consequently, density and viscosity variations influencing the mechanical behaviour of the lithosphere in subduction zones: all these parameters play a fundamental role in quantitative geodynamic modelling. The Sesia-Lanzo Zone, which in Alpine time was deformed at high pressure under a very low thermal regime, represents an interesting subject to infer the deformation-metamorphism interactions in the continental crust during subduction (Roda *et al.*, 2012; Zucali & Spalla, 2011). In this paper, we will infer the deformation-metamorphism relationship in the Mt. Mucrone area, where Permian intrusives are exposed with their country rocks, both belonging to the Eclogitic Micaschists Complex, to evaluate the degree of fabric evolution during successive deformation stages together with the progress of syn-kinematic metamorphic reactions. At this purpose, maps reporting in detail the heterogeneous distribution of textural and metamorphic transformations were performed, taking into account the degree of mechanical and mineral-chemical transformation of different rocks at micro- to km-scale. In these maps low- and high-strain domains are represented, for each deformation phase, and supported by the information on the volumes occupied by newly formed, or relict, mineral assemblages: the result consists in maps of deformation partitioning and metamorphic imprints. These maps may facilitate the perception of the influence that the heterogeneous distribution of deformation and metamorphism can play on the lithostratigraphy variations during a polyphase tectonic evolution.

In the following, mineral abbreviations are used according to Whitney & Evans (2010).

Geological setting

The Sesia-Lanzo Zone (SLZ) represents the widest portion of continental crust in the Western Alps that underwent high pressure (HP) metamorphism during Alpine subduction (e.g. Babist *et al.*, 2006; Compagnoni *et al.*, 1977; Dal Piaz *et al.*, 1972; Meda *et al.*, 2010; Pognante, 1991; Roda *et al.*, 2012), preceding the collision between European and Adria continental plates.

The Alpine metamorphic history of the SLZ comprises the record of an eclogite facies imprint followed by blueschist and greenschist facies re-equilibration (e.g. Castelli & Rubatto, 2002; Compagnoni, 1977; Gosso, 1977; Lardeaux *et al.*, 1982; Pognante, 1989a; Rebay & Messiga, 2007; Spalla *et al.*, 1983; Zucali & Spalla, 2011). The very low T/P ratio characterising this evolution assists the preservation of many pre-Alpine igneous and metamorphic relics in rocks with an Alpine polyphasic recrystallization. P-T conditions for the early-Alpine HP imprints range between 500–625 °C and 1.3–2.5 GPa (see Roda *et al.*, 2012 for a review of available PT estimates). The SLZ (Fig. 1) external margin is bounded by eclogitized ophiolitic relics of the Liguria-Piemont Ocean, the Piemontese Zone, and its internal margin is a thick mylonitic belt (the Canavese Line), separating SLZ from lower crustal rocks of the Southalpine Ivrea Zone, which escaped the Alpine HP evolution (Bigi *et al.*, 1990).

A pre-Alpine polyphase metamorphic evolution, from granulite to amphibolite-facies conditions, is still preserved in marbles, metapelites, metagranitoids and metabasics (Castelli, 1991; Compagnoni *et al.*, 1977; Lardeaux *et al.*, 1982; Lardeaux & Spalla, 1991; Rebay & Spalla, 2001): the pre-Alpine T-climax has been constrained at T=730–830 °C for P of 0.7-0.9 GPa (Lardeaux & Spalla, 1991). Granulite and amphibolite-facies imprints have been interpreted as the result of an extension-related uplift of a portion of the Variscan crust, occurred in Permian–Triassic times during the lithospheric thinning leading to Tethys opening (Marotta & Spalla, 2007; Marotta *et al.*, 2009).

This pre-Alpine tectono-metamorphic evolution is preserved in the metamorphic complexes forming the SLZ: the Eclogitic Micaschist Complex (EMC), the Gneiss Minuti Complex (GMC), the II Dioritic–Kinzigitic Zone (IIDK) and the Rocca Canavese Thrust Sheets (RCT) (e.g.: Compagnoni *et al.*, 1977; Pognante, 1989a; Pognante, 1989b). The IIDK consists of kilometeric lenses, lying between EMC and GMC, in which Alpine eclogitic assemblages are not described, even if in the Vogna Valley the tectonic contact underlying the margin between IIDK and EMC is marked by eclogite facies mylonites (Lardeaux, 1981; Lardeaux *et al.*, 1982). Eclogitic parageneses are widely described both in EMC and GMC with a strong difference in the volume affected by greenschist retrogradation: the GMC, which lies along the tectonic boundary with the Piemontese Zone, is diffusely re-equilibrated under greenschist facies conditions; the EMC, constituting the

internal part of the SLZ, records the greenschist re-equilibration mainly along discrete shear zones and shows a dominant metamorphic imprint under eclogite-facies conditions (e.g. Spalla, 1983; Spalla *et al.*, 1991).

The EMC protoliths are high-grade paragneisses, granulites, amphibolites and minor marbles and quartzites, which are the country rocks of Permian granitoids and gabbros (Bussy *et al.*, 1998; Callegari *et al.*, 1976; Castelli, 1987; Cenki-Tok *et al.*, 2011; Compagnoni *et al.*, 1977; Oberhaensli *et al.*, 1985) and from which the Mt. Mucrone body is the most renown. The deformation history of EMC, in this area, comprises four generations of Alpine folds, two of which are associated with the high-pressure (HP) mineral assemblages, and two generations of shear zones synchronous with the blue- and greenschist-facies re-equilibrations, respectively (Hy, 1984; Zucali *et al.*, 2002b). According to the literature D1 and D2 deformation are responsible for the development of isoclinal folding synchronous with the eclogitic imprint, generally associated with axial plane foliations marked by Ph, \pm Pg, Na-Cpx, Grt, Rt and Zo. D3 is accompanied by a widespread re-equilibration under blueschist-facies, confined along metric mylonitic shear zones, which locally developed at the boundary between metagranitoids and country rocks. D4 Mega-scale folds, D5 centimetre-thick mylonitic shear zones and D6 gentle folding overprinting blueschist mylonites and the eclogitic foliations, are synchronous with formation of a typical greenschist-facies mineral association of Qz, Ab, Wm, Ep, Ttn and green-Amp.

Lithostratigraphy

In this region the EMC consists of metagranitoids, mainly derived from Permian intrusives, and metasediments (mainly paragneisses and micaschists), descending from high-grade paragneisses, that represent the country rocks of Permian intrusives, with minor metabasics.

The top of Mt. Mucrone, in the north-western sector of the studied area, mainly consists of Permian metagranitoids in primary contact with the hosts rocks (Maffeo, 1970; Oberhaensli *et al.*, 1985). Part of metagranitoids suffered only the Alpine metamorphism, preserving the igneous structure (*grey-type metagranitoids*), whereas the others recorded also an intense Alpine deformation (*green-type metagranitoids*). The grey-type metagranites represent a small volume of the whole igneous Permian complex.

In the *grey-type metagranitoids* hypidiomorphic-granular primary textures are still recognizable, as well as compositional and grain size heterogeneities inherited from the igneous protoliths, consisting of: granites, minor quartzdiorites, pegmatites and aplites. In poorly-deformed volumes igneous contact are generally preserved. Grey-type metagranites had a primary igneous composition consisting of: Qz (40%), Pl (40%), Kfs (20%) and Bt (10%). Only Bt, Kfs and rare Aln are partially

preserved, while Pl micro-site is totally replaced by Qz, Jd and Zo; Ph and Grt developed in coronas between Bt, Pl and Kfs. The grain size is medium and the texture is weakly porphyritic and the Bt content is $\leq 10\%$. Metaquartzdiorites generally occur in meter-thick boudins inside the grey-type metagranites; the main outcrop, a hundred meters wide, is located near the contact with the paragneisses. This rock type is medium- to coarse-grained, with isotropic texture; the igneous structure is poorly preserved due to the diffused replacement of igneous phases by Alpine minerals: Omp (30%), Grt (25%), Qz (20%), white mica (10%) and Gln (10%). The inferred igneous modal composition with Pl (30%), Qz (20%), Kfs (10%) and mafic minerals (40%) is very close to that of a quartzdiorite-quartztonalite. Metaaplitites and metapegmatites are fine-grained and coarse-grained rocks, respectively, with Jd, Grt and white mica and occur in layers of centimetre to metre thickness. *Green-type metagranitoids* are fine- to medium-grained rocks with gneissic texture and a pervasive foliation underlined by white mica and clinopyroxene shape preferred orientations (SPO). These green coloured metagranitoids constituting about 80% of the Mt. Mucrone intrusives contain: Jd or Omp, Grt, white mica and Gln. This lithotype does not show the same original textural and compositional heterogeneities displayed by the grey-type metagranitoids, due to the strong textural and metamorphic reworking. For these characters they have been interpreted as a more deformed and mineralogically re-equilibrated under eclogite facies conditions, equivalent of the “grey-type” (Castelli *et al.*, 1994). The most representative mineral association of the green-type metagranitoids is: Qz (30-50%), Na-Cpx (20-30%), white mica (15-20%), Grt (15-20%), Zo (5%) and Gln (5%). Leucocratic metagranitoids are exposed at the south-western margin of the mapped area and they do not show primary or deformed contact with the other metagranitoids. Generally they have a gneissic texture, without significant textural and compositional variations, and are medium- to fine-grained with a penetrative foliation marked by white mica SPO and Qz-ribbons. The mineralogical composition is: Qz (40%), Ab (40%) and white mica (20%).

The metasediments consists of paragneisses and micaschists with interlayered minor metapegmatites, glaucophanites and zoisitites. Paragneisses are medium-grained and show a mineralogical foliation marked by alternating Qz and Grt-, with Omp-Grt- and Gl- layers, parallelised to S1. Metapegmatites (porphyric gneisses in the legend of Fig. 2) occur in meter-thick layers, with coarse-grained Kfs porphyroclasts (20%), Qz (35%), Ab (25%) and white mica (20%) within paragneisses and, as already suggested in adjacent areas, they are interpreted as deformed and eclogitised leucosomes (Zucali, 2002; Zucali *et al.*, 2002b), deriving from pre-Alpine partial melting of the high grade gneisses (kinzigites). The dominant foliation is defined by white mica SPO and elongation of quartz- feldspar-bearing domains. Micaschists are fine-grained rocks containing white mica, Qz, Grt, Gln and Jd or Omp. The dominant foliation (S1 in paragneiss and

S2 in micaschists) is marked by alternating quartz- and mica-rich layers and has millimetre scale spacing. The boundary with the paragneisses is transitional, due to the large amount of mica in the highly deformed paragneisses, which graduate into the micaschists. Metre to ten-metre thick glaucophanites occur in lenses or layers at the boundaries between micaschists and metagranitoids. they contain a spaced foliation, marked by Gln SPO and cut by randomly oriented Omp porphyroblasts. Zoisitites occur as ten-meter thick enclaves in the green-type metagranitoids and at the margin of the green-type metagranitoids; they contain ten centimetres-sized garnets, locally showing compositional zoning.

Mineral composition of zoisitites is: Zo (35%), Qz (15%), white mica (10%), Omp (10%) and Grt porphyroblasts (30%). Ten-centimetre to metre-thick Qz-rich veins occur within metagranitoids and their country-rocks and contain minor amounts of white mica, Grt, Gln and Zo. Metabasics are of medium- to fine-grained eclogites, locally showing a S2 discontinuous foliation, marked by Amp SPO. They are cut by millimetre- to centimetre-thick shear zone, rich in blue or green Amp. The mineral association is: Omp (35%), Grt (25%), Gln (20%) Zo (10%), white mica and minor Qz.

Mesostructure

In the investigated area six groups of superposed ductile structures, named in the following D1 to D6, have been recognized during field mapping that was performed at 1:5.000 scale, with small portions mapped in more detail (Delleani *et al.*, submitted). They are all syn-metamorphic and Alpine in age (Delleani *et al.*, 2010). Scattered pre-Alpine mineral and fabric relics (pre-D1) are preserved in domains in which the early Alpine deformation is poor or absent, mainly in meta-intrusive rocks.

The interpretative map of Fig. 2 synthesises the structural framework, reconstructed following to various extent criteria of, fold style of similar rock multilayers, kinematic compatibilities of fold systems, interference patterns, symmetry of minor folds, orientation of structures and different assemblages marking foliations (e.g. Connors & Lister, 1995; Hobbs *et al.*, 1976; Johnson & Vernon, 1995; Passchier *et al.*, 1990; Passchier & Trouw, 2005; Spalla, 1993; Turner & Weiss, 1963; Williams, 1985). The geological boundaries have been traced on the interpretative map according to two classes of confidence: objective, indicated with solid lines, and interpretative with dashed lines, on the base of exposure and amount of structural data occurring on the objective map (Delleani *et al.*, submitted). The map synthesizes the objective structural characters as foliation and fold axial surface trajectories, the sense of asymmetry of folds described by mineralogical or lithologic layerings, and interference patterns between superposed folds.

Degree of fabric evolution and peculiar structures developed during the successive metamorphic stages in metagranitoids and metasediments are shown in Figures 3 and 4, respectively.

Pre-Alpine relics (pre-D1) - Metaintrusive and metasedimentary rocks preserve some mineralogical pre-Alpine relics, such as Bt, Ksp, Aln, Ap and Zrn pre-Alpine relics within metagranitoids of Mt. Mucrone (Fig. 3) and pinkish Grt cores and Aln occur within micaschists and paragneisses (Fig. 4). In low deformed domains metagranitoids and paragneisses preserve pre-Alpine structural relics such as inequigranular igneous texture. Primary igneous contacts between meter-thick aplitic and mesocratic dykes and metagranitoids are preserved.

Alpine deformations (D1-D6) - The first group of structures (D1) comprises isoclinal stretched similar folds and a pervasive axial plane foliation: S1, which is defined by SPO of Ph, Omp or Jd, Gln and Zo and by Grt-rich bands. S1 is a well-differentiated crenulation, showing a spaced to continuous character and is the most pervasive planar structure at the map scale in micaschists, paragneisses or metagranitoids. In metasediments the degree of D1 fabric evolution ranges from stage 3 to stage 5 of the six stages decrenulation model of Bell and Rubenach (1983), whereas in metagranitoids it varies between stage 3 and 4 (Fig. 5) of the foliation development model of an originally isotropic rock, as described by Salvi *et al.* (2010).

D2 structures consist of isoclinal similar folds, metre to ten-metre in size, transposing the S1 foliation. An associated penetrative S2 foliation developed only in micaschists and paragneisses and is marked by SPO of Omp, Zo, Gln, Ph and Pg. The same mineral assemblage supports the axial planar continuous fabric where folding did not occur along with a differentiation of a new mineral layering. In metasediments and metagranitoids the degree of D2 fabric evolution is similar to that of D1 stage, but the volume recording the more evolved stage of fabric development is sensibly smaller, as testified by the development of a penetrative foliation only in metasediments. During deformation stages synchronous with the development eclogite-facies assemblages in poorly strained domains 10 centimetre-thick shear zones developed, locally associated with Grt-bearing veins.

D3 structures principally consist of thick (up to 3 m) shear zones usually located at the main boundaries between different rocks. The associated S3 mylonitic foliation, occurring in these shear zones, is marked by Qz, Ph, \pm Pg, Amp, \pm Grt, \pm Chl, Czo and Ttn. Thicker shear zones locally occur along the boundaries between metagranitoids and country rocks, while in the inner portion of metagranitoids, eclogites and porphyric gneisses deformation and transformation are concentrated in cm-thick bands. During this stage deformation is extremely localised and the degree of fabric

evolution corresponds to stage 5-6, according to Bell & Rubenach (1983) and Salvi *et al.* (2010), in correspondence of D3 shear zone but never exceed stage 2 in the rest of the area.

D4 structures comprise tight to open folds, associated with an intense crenulation, which is mainly located in the hinge zone. These up to ten metre scale parallel folds represent the most recurrent fold system. Where the fabric evolution exceeds stage 2 the HP-minerals underlying the earlier fabric elements are replaced, to various extent (from 10 to 70%), by Ab, green Amp, Chl, Ep and new white mica.

D5 folds range from meter to hundred meters in size with a weakly SW dipping axial plane. No new foliation develops during D4 folding: this deformation stage is associated, as it is the case for D3, with the growth of greenschist facies minerals. In the localised D5 centimetre-thick shear zones S5 foliation is defined by Qz, Ab, Chl, green Amp, new white mica and Fe-Ep.

Large-scale D6 structures are gentle folds that appear as undulations of earlier structures at the hundred meter-scale; they are chronologically grouped with brittle-ductile small fractures and joint systems filled by Chl, Ab and Kfs. D6 axial planes are marked by growth of very fine-grained dark Amp, white mica, Ab, Chl and Kfs (adularia).

The orientations of the fabric elements, plotted on Schmidt diagrams of Table 1, suggest that the superposed fold systems (D2-D1, D4-D2 and D6-D4) have perpendicular axial surfaces, and fold axes intersecting at a low angle. These geometric relationships between the four fold groups are indicated by consistent interference pattern of type 3 (Ramsay, 1967), at the outcrop and map scale (Figs. 2, 3 and 4).

Microstructure

The interpretation of the Alpine structural and metamorphic evolution was grounded on the overprinting relationships indicated by the mesostructural study, linked with the petrographic evidences on the evolutionary sequence of parageneses supporting microfabric changes. Deformation-metamorphism relationships have been inferred on the basis of the microstructural analysis of 93 thin sections, distributed over an area of $\approx 10 \text{ Km}^2$ (Fig. 2). Careful analysis of the effects of heterogeneous deformation during successive structural and mineralogical re-equilibration stages made clear the contemporaneous development in adjacent rock volumes of equivalent mineral assemblages, although manifested as different textures, corresponding respectively with a low (LD = where the granular scale strain is extremely poor and is associated to metamorphic mineral growth localised at the rims of previous grains), medium (MD) and high degree (HD) of fabric evolution, as shown in Fig. 5.

Examples of microfabrics characteristic of LD, MD and HD domains generated during successive deformation stages in metaintrusives and metasediments are shown in Figures 6 and 7, respectively.

Pre-Alpine relics (pre-D1) - Relics of the pre-Alpine mineral associations are widespread both in Mt. Mucrone metagranitoids and their country rocks (surrounding metasediments). In metagranitoids numerous igneous mineral relics have been preserved in LD and MD domains. They consist of: i) medium- to fine-grained brownish Bt, constituting up to the 20% of the modal composition of “grey-type” metagranitoids; ii) medium-grained Aln and Kfs (< 5% in volume) and rare very fine-grained Ap and Zrn. Skeletal-shaped reddish Grt cores are pre-Alpine mineral relics in metagranitoid country rocks, well preserved in low D1 strain domains of paragneisses, and occasionally occurring in HD D1 domains. These Grt have numerous inclusions of fine-grained Qz, Ap and Rt. Medium-grained pale violet Aln relicts occur also in paragneisses and zoisitites as in metagranitoids, whereas coarse-grained pinkish Mc occur in porphyric layers of the paragneisses. As already pointed out, in poorly deformed domains pre-Alpine igneous relics are preserved in metagranitoids, however, most of these rock volumes are replaced by Alpine high pressure minerals. Poorly deformed metagranitoids consist of “grey-type” metagranitoids, metaaplites and metapegmatoids, in which the eclogite-facies minerals Jd, Ph, Grt and Zo replace more than 70% of the igneous assemblage. Pl is replaced by a fine-grained Jd-Qz-Zo aggregate, where colourless, randomly oriented and anhedral Jd, up to 3mm-sized encloses bubbly Qz and randomly oriented acicular Zo; rare fine-grained Ph occurs within the thin symplectitic sites of plagioclase. Kfs is replaced by fine-grained and randomly oriented Ph crystals, and brownish Bt is only partially overgrown by fine- to medium-grained Ph. Coronas formed by trails of fine- to medium-grained Grt mark the margins between igneous Bt and Pl.

Alpine microstructures (D1-D6) - Tectonic to mylonitic syn-D1 foliations develop in both metaintrusive and metasedimentary rocks. In “green type” metagranitoids, metaaplites and metapegmatoids cm- to 10-cm-spaced discontinuous S1 foliation is marked by syn-D1 Omp/Jd, Ph, Gln, Zo SPO and lensoidal Qz-rich domains. The Omp/Jd forms euhedral coarse-grained: in “green type” metagranitoids and metapegmatoids Cpx is mostly pale green Omp, or more rarely Jd; in metaaplites only colorless Jd occurs. Medium- to coarse-grained Ph crystals enclose Qz and Rt with rational grain boundaries. Ph and Cpx grain size is coarser in metapegmatoids and “green type” metagranitoids. Grt trails are aligned parallel to the S1 foliation, and are formed by colourless or pale pink crystals with very fine-grained inclusions of Ap, Qz, Ph and Rt. Syn-D1 Grt are mainly fine-grained and may reach porphyroblastic dimensions in highly strained domains (up to 5mm in

diameter). Greater-sizes (up to 5cm) occur in Grt near the boundary between “green type” metagranitoids and zoisitites. In metaquartzdiorite the 10- to 20cm-spaced discontinuous S1 foliation is only locally preserved after D2 and D3 reworking: Omp, Ph, Zo SPO, elongated lenticular Qz domains and Grt trails mark S1. Omp has an internal foliation (Si) parallel and continuous with S1 and marked by SPO of fine-grained Ph and Zo and by small size Grt and Rt rows. In leucocratic metagranitoids and porphyric gneisses scarce syn-D1 minerals are locally preserved within MD syn-D2 domains: coarse-grained Ph and rare fine-grained crystals of violet Gln and Zo with SPO parallel to S1. In porphyric gneisses S1 is mainly underlined by coarse-grained Ph, Gln and Zo SPO, as in leucocratic metagranitoid, and wraps around Mc porphyroclasts showing recrystallized rims.

In syn-D1 HD domains the S1 foliation is generally continuous and has almost the same characteristics and mineralogical support in both micaschists and paragneisses, but in micaschists is only preserved within S2 microlithons. S1 is marked by SPO of medium-grained Ph, Gln Omp/Jd, Zo, by Grt strings and by mm- to cm-thick Qz lenses. Cpx generally is Omp, and Jd appeared only once. Ph is medium- to coarse-grained with inclusions of round-shaped Qz and euhedral Grt and Rt. Locally paragneisses are massive, with randomly oriented Omp, Gln, Zo and Ph occurring together with Grt and Qz in different modal amount within alternating layers. In glaucophanites S1 foliation is mainly preserved as Si in coarse-grained Omp and Grt and is marked by the alignment of Gln, Ph, Zo and accessory Rt. Omp and Grt porphyroblasts are interpreted as syn-tectonic with late D1, as suggested by gentle bending of their Si, and as pre-tectonic with respect to D2, as suggested by the relationships with S2, wrapping these porphyroclasts. In zoisitites the S1 foliation is mainly preserved as Si within Grt megablasts (up to 12cm in diameter) and rare relicts occur in the S2 microlithons within the matrix. S1 spaced foliation is marked by elongated lenticular Qz-domains and by SPO of fine-grained Czo, Ph, Gln and Omp.

During D2 normal foliations textures (S2) were imprinted as the dominant fabric exclusively in leucocratic metagranitoids, micaschists, eclogites, zoisitites and glaucophanites. Where D2 axial-planes intersect at a low angle, the S1 foliation acted as a microshear plane during D2, developing an S1-S2 composite fabric (of S-C type), accompanied by the growth of new fine-grained Ph crystals aligned in the foliations. In leucocratic metagranitoids relict S2 is marked by SPO of fine- to medium-grained Ph and Gln; Gln also defines L2. In micaschist the continuous S2 foliation is marked by SPO of Ph, Pg, Gln, Omp/Jd and Zo/Czo, by Grt trails and by Qz elongated lenses. Euhedral fine-grained Ph and Pg form new-grains from syn-D1 Ph or grew independently with long margins parallel to S2; light rose Grt rims syn-D1 Grt in microlithons, or define S2 with trails of euhedral fine-grained new grains. Fine-grained violet Gln elongated parallel to S2 may preserve

pre-D2 pale cores, and up to 1 cm long grains mark D2 axes. Omp/Jd and Zo/Czo can occur in rims of mm-thickness on the earlier Cpx and Zo grains.

S2 in eclogite is confined to 20cm-thick rims at the margins of boudinaged layers and is defined by SPO of fine- to medium-grained Omp and Ph, Pg and Grt rows. In D2 LD domains coarse-grained pale-green pre-D2 Omp grains with Grt, Ph and Rt inclusions have random orientations and colourless Grt occur also as medium grains with Rt and Ph inclusions. Oriented syn-D2 Omp developed from the re-crystallization of pre-D2 grains; thin coronas of rose Grt rims pre-D2 Grt. In zoisitites up to the 50% of the rock volume is replaced by new minerals during D2. Czo, Ph and Gln define S2, together with lens-shaped Qz-aggregates. In glaucophanites up to the 70% of the rock volume is replaced by syn-D2 minerals and few Omp and Grt coarse-grained porphyroclasts occur. S2 foliation is supported by the alignment of Gln, Ph and Czo: fine-grained new grains of Gln replace pre-D2 crystals. Qz shows deformation bands, subgrains and polygonal new grains indicating syn-D2 dynamic recrystallization in LD domains of successive deformation stages in all rocks.

In D2 LD domains coronas of Omp, Grt, Gln, Ph and Czo rimming syn-D1 minerals developed never exceed 30% of the whole rock volume. Syn-D2 rims are mainly of < 1mm-thickness, regardless of the presence of an early oriented fabric. Within these rims inclusions are very rare, only locally very-fine grained Qz, Rt and Ap occurs. In “grey type” metagranitoids and metapegmatoids fine-grained green-yellowish Acm corona develops around Bt and Pl sites at the contact with Qz and locally colourless Jd is partially replaced and rimmed by greenish Omp, randomly oriented and as very fine-grained acicular crystals or very thin rims.

In cm- to m-thick D3 shear zones mylonitic texture developed in all rocks and are accompanied by the growth of new minerals replacing up to 50% of the previous mineral assemblages. In paragneisses poorly deformed during D1 the D3 deformation is localised in Qz- and Grt-bearing layers, thinned during this stage. In micaschists, zoisitites, glaucophanites and paragneisses, with a penetrative S1, D3 deformation is diffused, with no signs of concentration in shear zones, with a minor modal amount (<20%) of syn-D3 minerals. S3 is accompanied by grain size reduction and is marked by fine- to very fine-grained Qz elongated grains, SPO of Ph, Brs, Czo and by Ttn strings. In metaquartzdiorite fine-grained oriented Mg-Chl develops parallel to S3 or in pressure shadows of Omp porphyroclasts, very thin rims of Aug and Grt develops on pre-D3 Omp and Grt crystals and Ph + Pg aggregates replacing the earlier white mica grains are individuated at the electron microscope.

Generally during D4 poor new minerals growth is observed and do not exceed the 20% of the whole rock volume in all lithologic types, with the exception of Ph-rich micaschists and leucocratic

metagranitoids in which syn-tectonic mineral transformations could replace up to the 60% of the previous assemblages. Diffused fine-grained granoblastic Qz aggregates are associated with this deformation stage. Mineral transformation are mainly characterised by the formation of fine- to medium-grained aggregates of Ab, new white mica, Ep and Act replacing older Amp, Na-Cpx and Ph; in porphyric gneisses and micaschists in these aggregates also Adl occur. Ttn rims, Rt and Fe-Chl partially replaces Grt along boundaries and micro-fractures; green Bt partially overgrowing Ph and Grt may occur in paragneisses and micaschists.

During D5 mm- to cm-thick shear zones develop in all lithotypes and the new fabric (S5) is marked by fine- to very fine-grained Qz, Ab, Wm, Act, green Bt, Ep, Ttn and Fe-oxides grain alignments. The same mineral association may occur in < 0,5mm-thick veins with syntaxial filling. Transformations associated with D5 are localized along shear planes and never exceed 5% of the whole rock volume.

Mineral transformations are poor or absent within microstructures related to D6; they are a faint, variably spaced disjunctive axial plane foliation (fracture cleavage-type). Partial replacement of pre-D3 Jd aggregates by very fine-grained Ab, Wm, brown-Amp and Adl occurs locally in metagranitoids along these microfracture sets.

Fabric evolution vs reaction progress

The study of the inter-relationships between degree of planar fabric evolution and of metamorphic changes was respectively supported by structural maps of foliation trajectories, imaging the history of superposed granular deformation imprints (Fig. 2), and by maps of the metamorphic transformation domains and (Fig. 8 and 9); the deformation history was derived from the structural study of the Mt. Mucrone Metagranitoid (Delleani *et al.*, submitted), in which the chronology of superposed foliations (S1 to S5) and fold systems (D1 to D6) was inferred on the basis of overprinting criteria, aided by cross-controls of corresponding metamorphic assemblages.

Individuation of homogeneous fabric domains was facilitated by integration of meso-structural information with microstructural analysis, to estimate the degree of fabric evolution and metamorphic transformation in terms of volume percentage; for this purpose 93 thin sections have been analysed, from samples selected in accord with the deformation sequence. The degree of fabric evolution, in term of volume percentage of new planar fabric, has been inferred together with the associated degree of syn-tectonic metamorphic transformations, in term of modal amount of mineral assemblages expressed in percentage.

As already experienced by Salvi *et al.* (2010) the degree of grain-scale reorganization of the

dominant fabric has been used as a guide to estimate the fabric evolution referring to the successive stages of crenulation cleavage development as proposed by Bell & Rubenach (1983): from crenulation up to a complete transposition; see also Passchier & Trouw (2005). The scheme proposed by Salvi *et al.* (2010), elaborated starting from originally foliated or isotropic igneous fabric, has been adopted as a reference to discriminate between low-, medium- and high-deformation degree (Fig. 5). This reference perfectly fits with the examined case of Mt. Mucrone, where, during Permian times, granitoids emplaced in polydeformed metapelites with which shared the polyphase structural and metamorphic Alpine evolution.

Microstructural analysis showed that the discriminating intervals well fit with those proposed by Salvi *et al.* (2010) in which, precisely, the low degree (LD) of deformation corresponds to the early development stage of the new fabric (volume of newly oriented fabric ranges from 0 to 20%) and includes an incipient crenulation or the appearance of a weak, non-persistent new foliation in country metapelites, and of no strain or a weak foliation in meta-intrusives, respectively; in other words this corresponds to the fabrics referred to above as coronitic.

The medium degree of deformation (MD) corresponds to a successive evolution up to the differentiation of a new foliation, which can reach the stage of a differentiated crenulation cleavage or a pervasive foliation (volume of newly differentiated fabric ranging from 20 to 60%), in originally foliated or isotropic rocks, respectively; this corresponds to the fabrics described above as tectonic. The high degree of deformation (HD) coincides with the progressive obliteration of relics of the earlier fabric in metapelites and meta-intrusives and to development of a new continuous foliation of mylonitic type (volume of newly oriented fabric can rise up to 100%), thus corresponding to fabrics above described as so.

The estimate of volume percentage occupied by Alpine mineral assemblages syn-tectonic with successive deformation stages varies from 5 to 100%. Generally the higher is the degree of fabric evolution, the more pervasive is the mineral growth of the related syn-tectonic assemblages. The assemblages developed during D1, under eclogite facies conditions, represent an exception: they can occupy a volume $\geq 90\%$ in the mapped area.

Disregarding D1 stage, LD is generally characterised by a volume of synkinematic metamorphic products ranging from 0 to 20% in metasediments (= originally foliated rocks). In meta-intrusives (the only originally isotropic rocks) the relationships between degree of fabric evolution and metamorphic transformation is similar with a special case occurring during D4 in the leucocratic metagranitoids, outcropping at the south-western margin of the map (Fig. 9), where the volume occupied by the Ph and Na-Cpx breakdown products rises up to 70%. MD domains show a volume of syn-tectonic metamorphic products varying from 20 to 70% both in originally foliated and in

isotropic rocks. Finally, always with the anomaly of syn-D1 assemblages, in HD domains the mineral– chemical re-equilibration can reach up to 80% of the volume during D2 and never exceed 50% during D3: this latter represents the maximal degree of syn-D3 mineral replacement, which is generally < 10% in LD and MD syn-D3 domains.

Rock composition seems to exert an additional control on reaction progress, as can be inferred from Fig.8 and 9, where the different modal amount of white mica and Na-Cpx influences the development of syn-D2 and syn-D4 metamorphic assemblages, more pervasive in micaschists and leucocratic metagranitoids, respectively. In addition to original mineral rock composition and fabric evolution, the thermal regime can significantly influence the degree of metamorphic transformation where the fabric evolution remains below the HD stage: for the same degree of fabric evolution, the metamorphic reaction progress is more evolved during D2 (eclogite facies) than during D3 (blueschist facies).

The microstructural analysis results highlight that the two processes do not necessarily develop at the same rate, but above the transition to the HD the mechanical and mineral–chemical transformations of the rocks increase proportionally, in agreement with the observations of Salvi *et al.* (2010), Spalla *et al.* (2005) and Zucali *et al.* (2002b).

Mineral Chemistry

Mineral compositions have been determined selecting micro-structural sites, chosen for their potential to reveal the transformation pathways accompanying fabric evolution, and to support estimates of PT conditions during successive foliation-forming episodes and related mineral equilibrations.

Compositional variations in minerals have been determined using a Jeol, JXA-8200 electron microprobe (WDS, accelerating voltage of 15 kV, beam current of 15 nA) operating at the Earth Sciences Department “A. Desio” of Milano University. Natural silicates have been used as standards and the results were processed for matrix effects using a conventional ZAF procedure. Proportional formulae have been calculated on the basis of: 23 oxygens for Amp, 6 oxygens for Cpx, 12 oxygens for Grt and Ep, 11 oxygens for micas, 28 oxygens for Chl, 8 oxygens for Fsp and 10 for Ttn. Fe³⁺ was determined for Amp, Grt and Cpx; cations are in atoms per formula unit (a.p.f.u.). Variations, synthesised below, are detailed in Table 2 and in diagrams of Figures 10, 11, 12, 13, 14, which show the compositional trends for mineral phases such as Amp, Cpx, Grt and white micas that are significant for thermobarometric estimates.

Amphiboles are scattered in composition over the edenite-hornblende, glaucophane, and actinolite fields. Most of them have edenite-hornblende compositions, and only a few data cluster around the

glaucophane end-member, as shown in Figures 10a and 10c, where the compositional gap described by Ungaretti *et al.* (1983) between Ca- and Na-amphiboles, is evident only in metagranitoids and eclogites. Glaucophane is the most common composition for syn-D1 and syn-D2 amphiboles and only a few cases in grey-type metagranitoids and paragneisses show an edenitic composition. Syn-D3 compositions range from edenitic to pargasitic, whereas in syn-D5 the edenite content decreases up to actinolite composition. A decrease in Al^{VI} associated with an increase in Al^{IV} mark the transition from syn-D2 to syn-D3 amphiboles, whereas a strong decrease in Al^{tot} characterises amphibole re-equilibration during D5 (Figs. 10b and 10d). Ti content generally ranges between 0.01 and 0.039 a.p.f.u. and Na(B) in NaCa-amphibole varies from 1.48 to 0.06 a.p.f.u. from syn-D3 to syn-D5, respectively.

Clinopyroxenes varies in composition from Jd to Di, in a range from Jd 98, to Jd 15 (Fig. 11). The highest acmitic values occur in Cpx from some “grey type” metagranitoids. The Jd-content in metagranitoids, both grey and green-types, is also controlled by the bulk chemistry as shown by the two clusters of pre-D3 and syn-D1 and D2 grains in Figure 11. In green-type metagranitoids and in eclogites a weak increase in Jd and a decrease in Acn tenors characterise the transition from syn-D1 to syn-D2 Cpx. Similarly a Jd increment characterises the transition from syn-D1 to syn-D2 compositions in paragneisses and micaschists. A higher Di content distinguishes post-D3 Cpx, both in eclogites and paragneisses. XMg varies from 0.01 to 0.62 with higher values in syn-D3 grains.

Garnets, as inferred microstructurally, grew during both Alpine and pre-Alpine metamorphic evolutions, and pre-Alpine relics have been recognized in paragneisses (open circles in Fig. 12 and zoning profile in Fig. 13). The transition from pre-Alpine to Alpine syn D1-D2 garnets is characterised by an Alm, Sps and Adr decrease and a Grs and Prp increase. The transition from syn-D1 to syn-D2 Grt in paragneisses is marked by a Sps decrease associated with a Grs increase, while Grt occurring in micaschists (Fig. 12) show an homogeneous composition with Alm 65-70, Prp 10-20 and Grs 15-25; also syn-D1 Grt megablasts of zoisitites (Fig. 13) show a quite uniform compositional profile. The strong heterogeneous composition of pre-D3 Grt in grey-type metagranitoids is controlled by their microstructural position. As already described these Grt develop in coronas at the boundary between Pl and Bt sites and, as already described by Koons *et al.* (1987), the highest Grs values distinguish Grt growing on the Pl site from those replacing Bt, that are characterised by higher Alm+Prp contents (Figs. 12 and 13). Grt filling the veins at high angle with mylonitic foliation in D1 shear zones are characterised by very low amounts of Prp and Sps (<5%). In green-type metagranitoids and metaquartzdiorite the Alm+Prp tenor decrease, and Grs increase, characterise the transition from syn-D1 to syn-D2 compositions. In eclogites Alm ranges from 60 and 65%, Prp from 10 and 20%, Grs from 20 to 30 % and Sps is <5%.

White micas consist of paragonite and phengite (Fig. 14) with Ca never exceeding 0.03 a.p.f.u. and K content in paragonite rising up to 0.09 a.p.f.u., whereas Pg is ≤ 0.13 a.p.f.u. in phengite. Eclogites contain phengitic micas that show the highest Si^{4+} content (3.35–3.55 a.p.f.u.), with the highest values characterising syn-D2 grains. In metagranitoids Si^{4+} varies from 3.2 to 3.5 a.p.f.u. from syn-D5 to syn-D1/D2 grains. In metasediments the compositional variations in Ph are lower than those of metaintrusives ($3.35 < \text{Si}^{4+} < 3.45$ a.p.f.u.). Mg values are 0.25–0.4 a.p.f.u. in Ph from metasediments and more scattered (0.2–0.8 a.p.f.u.) in those from metaintrusives, where a higher variation in Fe^{3+} tenor is suggested by the deviation from the Ph-Lc trend in the diagram (Fig. 14) of Massonne & Schreyer (1987). Ti content does not exceed the value of 0.24 a.p.f.u.: in grey-type metagranitoids $0.10 < \text{Ti} < 0.24$ a.p.f.u. where Ph replaces igneous Bt and is ≤ 0.10 a.p.f.u. in all the other micro-sites.

Chlorite has XMg values between 0.73 and 0.48 and Si ranges from 2.78 to 2.98 a.p.f.u.; Mg-richer Chl occurs in metaquartzdiorites. *Epidotes* shows Fe_2O_3 up to 15.93 wt.% and Mn_2O_3 is lower than 0.21 wt.%; generally syn-D3 Ep are Czo and pre-D3 Zo, whereas greenschist facies epidote are Fe-Ep. Alpine *plagioclase* has An < 0.05 and Or < 0.01 and *titanite* has Al_2O_3 ranging from 2.03 to 2.11 wt. %.

P-T estimates and metamorphic evolution

Micro-structural analysis indicates that the Mt. Mucrone rocks preserve evidence of superposed metamorphic and structural re-equilibrations, even in volumes as small as that of a thin section, and allows definition of assemblage sequences in metapelites and metagranitoids, syn-tectonic with successive deformation stages. To infer PT conditions active during each metamorphic re-equilibration, the favourable sites where microstructures suggest attainment of grain-scale equilibrium have been identified. For this purpose, samples dominated by a single structural and metamorphic imprint at thin section scale have been selected, to obtain internally coherent PT estimates, using independent thermo-barometers. Even so, metamorphic conditions inferred using critical minerals such as Grt, for which the compositional zoning suggests a heterogeneous re-equilibration with the matrix assemblage, have been calculated selecting mineral pairs with textural relationships indicating equilibrium. We also considered that mica, Cpx and Amp grains associated with different fabric elements in the same rock, may have different chemical compositions, reflecting different intra- and inter-crystalline deformation mechanisms, as it has been demonstrated under various metamorphic conditions (e.g. Buatier & Lardeaux, 1987; Cimmino & Messiga, 1979; di Paola & Spalla, 2000; Gazzola *et al.*, 2000; Lardeaux *et al.*, 1983; Spalla, 1993; Spalla & Zucali, 2004). This makes these minerals proper to estimate of physical conditions during the development

of successive fabrics. PT conditions of each re-equilibration stage have been inferred using: a) the comparison of natural assemblages with experimental univariant equilibria; b) calculation of average PT using THERMOCALC (Holland & Powell, 1998; Powell & Holland, 1994) based on specific mineral compositions; c) the application of well calibrated independent thermometers and barometers: calibrations have been applied, taking into account the best fit between the compositional range of mineral pairs in different samples.

Mineral assemblages marking successive groups of structures (Tab. 3) indicate that D1 and D2 occurred under eclogite facies conditions, D3 under blueschist-facies conditions and D4 to D6 under greenschist facies conditions. In *metagranitoids* the integrated use of AX and average PT of THERMOCALC gives $P = 1.9 \pm 0.3$ GPa and $T = 479^\circ \pm 50^\circ$ C for syn-D1 assemblage Gln-Omp-Grt-Ph-Zo (with Qz in excess), $P = 2.6 \pm 0.3$ GPa and $T = 522^\circ \pm 45^\circ$ C for syn-D2 assemblage Gln-Omp-Grt-Ph-Pg-Zo (with Qz in excess), $P = 1.4 \pm 0.4$ GPa and $T = 515^\circ \pm 45^\circ$ C for syn-D3 assemblage Brs-Grt-Czo-MgChl-Ph-Di-rich Cpx (with Qz in excess). Temperatures have also been estimated using the Fe-Mg exchange between garnet and white mica (Wu *et al.*, 2002) stable during D2 at $586^\circ \pm 49^\circ$ C. Si⁴⁺ content in pre-D3 Ph ranges from 3.4 and 3.5 a.p.f.u., covering the same composition interval obtained in Ph synthesized under HP condition in metatonic systems at $P \geq 2.0$ GPa (Schmidt, 1993). In *eclogites* average PT calculations on the assemblage Omp-Gln-Grt-Ph-Zo-Qz, stable during D1, gives $P = 1.9 \pm 0.5$ and $T = 504^\circ \pm 150^\circ$ C. Temperatures have been evaluated using the Fe-Mg exchange between garnet and clinopyroxene marking D1 fabric at $T = 488^\circ \pm 25^\circ$ C for $P = 1.4 - 2.3$ GPa (Krogh Ravn, 2000). Variation in garnet compositions from syn-D1 to syn-D2 grains if compared with experimental results at high pressure on metabasalts (Poli, 1993) indicates P ranging from 2.0 to 2.2 GPa, in agreement with D1-D2 P -interval estimated with average PT also in metagranitoids. In *micaschists* and *paragneisses* the garnet - white mica thermometer applied to syn-D2 mineral pairs gives $T = 554^\circ \pm 49^\circ$ C and $T = 597^\circ \pm 44^\circ$ C, respectively. The coexistence of actinolitic amphibole ($Al^{tot} = 0.2 - 0.9$ a.p.f.u.) with albite ($An \leq 0.5$) during D5 in paragneisses allows the evaluation of $P \leq 0.4$ GPa and $T \leq 400^\circ$ C (Plyusnina, 1982). The inferred PT values for the different syn-tectonic assemblages perfectly justify the variations of mineral chemical compositions, such as: i) CaNa-amphiboles, in which the evolution from syn-D1/D2 to syn-D3 grains is marked by a decrease in Al^{tot} and Na; ii) the increase of Jd-content in Cpx grains from D1 to D2; iii) the decrease of Si⁴⁺ tenor in Ph, from syn-D1 to syn-D5; iv) Grt zoning. These results on the chemistry of single minerals, constituents of the progressive fabrics, are compatible with the sequence of syn-tectonic assemblages and are synthesized in the Pressure-Temperature-deformation-time (PTdt) path diagram of Fig. 15 that shows that the structural evolution from D1 to D2 occurred during a P-prograde path, characterised by a slight T-

increase. D2 deformation assisted the P-T climax conditions and was followed by decompression at quite constant T, characterising D3 conditions. The first occurrence of greenschist facies mineral assemblages during D4, and the syn-D5 PT estimates, indicate that the last deformation stages developed during a more significant T-decrease, associated with decompression.

Conclusive remarks

The multiscale structural analysis here performed in a portion of the subducted-exhumed Alpine continental crust evidenced that the accomplishment of syn-tectonic polyphase metamorphic transformations has been controlled not only by bulk and mineral compositions, but was also variably influenced by fabric evolution, as shown by the maps of degree of fabric evolution and metamorphic transformation. This result agrees with the conclusions obtained in other portions of the Alpine continental crust, variably reworked in the Mesozoic-Tertiary subduction (Roda & Zucali, 2011; Salvi *et al.*, 2010; Spalla *et al.*, 2000; Spalla *et al.*, 2005; Zucali *et al.*, 2002b). Heterogeneity of Alpine deformation assisted the preservation of volumes dominated by relict igneous textures, even where magmatic minerals were widely replaced by Alpine eclogitic assemblages. The detailed structural and petrographic mapping allowed the reconstruction of the tectonic and metamorphic evolutionary steps of the Mt. Mucrone southern slope, back to the nearly undeformed igneous textural relics of the Permian granitoids.

The correlation between degree of fabric evolution and reaction progress in different lithotypes has shown that the differences of mineral assemblages and textures of the protoliths influenced reaction accomplishment when the degree of fabric evolution remains lower than HD, as discussed in the paragraph “*Fabric evolution vs reaction progress*”. Maps of volumetric estimates of mineral transformation, confronted with those reporting the diffusion of granular scale deformation throughout the rock indicate, as already proposed by Salvi *et al.* (2010), that the HD stage represents a threshold after which deformation and metamorphism effects proportionally increase until total replacement of pre-existing minerals where new fabrics evolved up to the stage of a continuous foliation. These observations call attention on the role of strain energy in catalysing metamorphic reactions (Hobbs *et al.*, 2010).

In addition the evaluation of metamorphic reaction progress for the same degree of fabric evolution, during successive deformation stages, suggests that also the metamorphic environment has an influence as indicated by the more diffused development of eclogite facies assemblages (syn-D2) with respect to the blueschist facies (syn-D3) or greenschist facies ones (syn-D4).

Finally strain gradients may induce variations in lithostratigraphy as in the case of transformation of

grey type into green-type metagranitoids, as a consequence of deformation and mineral replacement intensity during syn-eclogitic stages, or of the transformation of paragneisses into micaschists localized along syn-D1 HD domains. As a consequence caution is suggested in the use of lithostratigraphy as an independent key to contour tectonic units in polydeformed and polymetamorphic terrains, without the support of the multiscale structural and petrographic analysis.

Structural and metamorphic evolution point to the development of D1 and D2 stages under PT conditions of the Qtz-eclogite facies at the boundary with Coe stability field, of D3 stage under blueschist-facies conditions, and of D4-D6 stages under greenschist-facies conditions (Fig. 15).

Peak conditions reached in the course of D2 ($T = 480^{\circ}$ - 580° C and $P = 2.3 - 2.7$ GPa) are accomplished after a P and T prograde path during which Mt. Mucrone metagranitoids and their country rocks recorded D1 deformation at $T = 430^{\circ} - 530^{\circ}$ and $P = 1.9 \pm 0.3$ GPa. The retrograde path is marked by a transition to $T = 470^{\circ} - 560^{\circ}$ C and $P = 1.4 \pm 0.4$ GPa during D3, and successively re-equilibrated under greenschist facies conditions up to $P \leq 0.4$ GPa and $T \leq 400^{\circ}$ C (syn-D5 re-equilibration). This structural and metamorphic history predates the emplacement of Oligocene dykes, indicating that these rocks have been exhumed to greenschist facies conditions before Tertiary magmatic activity, in agreement with the exhumation time suggested for adjacent areas of SLZ, also on the basis of the structural relationships with Biella and Traversella intrusive stocks (Zanoni, 2010; Zanoni *et al.*, 2008; Zanoni *et al.*, 2010; Zucali, 2002; Zucali *et al.*, 2002a). The age of deformation history recorded under eclogite-facies conditions can be estimated between 90 and 65 Ma according to U/Pb determinations on Aln and Zrn (Cenki-Tok *et al.*, 2011; Rubatto *et al.*, 1999). The inferred PTdt evolution is in good agreement with that deduced by Zucali *et al.* (2002) for the Mt. Mucrone-Mt. Mars area (Fig. 15) but minimal P for climax conditions attain higher values of 2.3 GPa and are constrained at maximum values of 2.7 GPa by the Coe stability field.

To conclude, D1 and D2 stages are characterised by a P–T ratio lower than that of cold subduction zones (Cloos, 1993), whereas D3 falls in this thermal state of about 6° C/Km, indicating that this part of the structural and metamorphic history has been recorded in a scenario of active subduction of a cold and old oceanic plate. Post-D3 exhumation took place under a thermal state comprised between those corresponding to warm subduction zones and plate interior (Cloos, 1993), therefore compatible with continental collision.

Acknowledgements: M. Zucali and G. Rebay are thanked for stimulating discussions and helpful suggestions. Funding by PRIN 2008 ‘*Tectonic trajectories of subducted lithosphere in the Alpine*

collisional orogen from structure, metamorphism and lithostratigraphy'. A. Risplendente provided the technical support at the Dipartimento di Scienze della Terra "A. Desio", where the analytical work with the EPMA has been performed.

REFERENCES

- Babist, J., Handy, M.R., Konrad-Scmolke, M. and Hammerschmidt, K. (2006). *Precollisional, multistage exhumation of subducted continental crust: the Sesia Zone, Western Alps*. *Tectonics*, **25**: doi: 10.1029/2005TC001927.
- Bell, T.H. and Rubenach, M.J. (1983). *Sequential porphyroblast growth and crenulation cleavage development during progressive deformation*. *Tectonophysics*, **92**: 171-194.
- Bigi, G., Castellarin, A., Coli, M., Dal Piaz, G.V., Sartori, R., Scandone, P. and Vai, G.B. (1990). *Structural Model of Italy, sheets 1-2*. In: Progetto Finalizzato Geodinamica del C.N.R.. S.E.L.C.A., Florence.
- Buatier, M. and Lardeaux, J.M. (1987). *Intracrystalline deformation of omphacite and garnet under high-pressure and low-temperature conditions - example from the Sesia-Lanzo Zone (Western Alps)*. *Comptes Rendus Academie des Sciences (Series II)*, **305(9)**: 797-800.
- Bussy, F., Venturini, C., Hunziker, J. and Martinotti, G. (1998). *U-Pb ages of magmatic rocks of the Western Austroalpine Dent Blanche-Sesia Unit*. *Schweizerische Mineralogische und Petrographische Mitteilungen*, **78**: 163-168.
- Callegari, E., Compagnoni, R., Dal Piaz, G.V., Frisatto, V., Gosso, G. and Lombardo, B. (1976). *Nuovi affioramenti di metagranitoidi nella zona Sesia-Lanzo*. *Rendiconti della Società Italiana di Mineralogia e Petrologia*, **32**: 97-111.
- Castelli, D. (1987). *Il metamorfismo alpino delle rocce carbonatiche della Zona Sesia-Lanzo (Alpi occidentali)*. PhD Thesis, Università di Torino, 141 pp.
- Castelli, D. (1991). *Eclogitic metamorphism in carbonate rocks: the example of impure marbles from the Sesia - Lanzo Zone, Italian Western Alps*. *Journal of Metamorphic Geology*, **9**: 61-77.
- Castelli, D., Compagnoni, R. and Nieto, J.M. (1994). *High pressure metamorphism in the continental crust: eclogites and eclogitized metagranitoids and paraschists of the Monte Mucoen area, Sesia Zone*. In: High pressure metamorphism in the Western Alps. Guidebook to the B1 field excursion of the 16th Gen. IMA Meeting, Pisa, 4-9 settembre 1994, 107-116.
- Castelli, D. and Rubatto, D. (2002). *Stability of Al and F-rich titanite in metacarbonate: petrologic and isotopic constraints from a polymetamorphic eclogitic marble of the internal Sesia Zone (Western Alps)*. *Contributions to Mineralogy and Petrology*, **142**: 627-639.
- Cenki-Tok, B., Oliot, E., Rubatto, D., Berger, A., Engi, M., Janots, E., Thomsen, T.B., Manzotti, P., Regis, D., Spandler, C., Robyr, M. and Goncalves, P. (2011). *Preservation of Permian*

- allanite within an Alpine eclogite facies shear zone at Mt Mucrone, Italy: Mechanical and chemical behavior of allanite during mylonitization. Lithos, 125: 40-50.*
- Cimmino, F. and Messiga, B. (1979). *I calcescisti del Gruppo di Voltri (Liguria occidentale): le variazioni composizionali delle miche bianche in rapporto all'evoluzione tettonico-metamorfica alpina. Ofioliti, 4(3): 269-294.*
- Cloos, M. (1993). *Lithospheric buoyancy and collisional orogenesis: subduction of oceanic plateaus, continental margins, island arcs, spreading ridges and seamounts. Geological Society of America Bulletin, 105: 715-737.*
- Compagnoni, R. (1977). *The Sesia-Lanzo zone: high-pressure low-temperature metamorphism in the Austroalpine continental margin. Rendiconti della Società Italiana di Mineralogia e Petrologia, 33: 335-374.*
- Compagnoni, R., Dal Piaz, G.V., Hunziker, J.C., Gosso, G., Lombardo, B. and Williams, P., 1977. *The Sesia-Lanzo Zone: a slice of continental crust, with alpine HP-LT assemblages in the Western Italian Alps. Rendiconti della Società Italiana di Mineralogia e Petrologia, 33: 281-334.*
- Connors, K.A. and Lister, G.S. (1995). *Polyphase deformation in the western Mount Isa Inlier, Australia; episodic or continuous deformation? Journal of Structural Geology, 17(3): 305-328.*
- Dal Piaz, G.V. (1999). *The Austroalpine-Piedmont nappe stack and the puzzle of Alpine Tethys. Memorie di Scienze Geologiche, Padova, 51: 155-176.*
- Dal Piaz, G.V., Hunziker, J.C. and Martinotti, G. (1972). *La Zona Sesia - Lanzo e l'evoluzione tettonico-metamorfica delle Alpi Nordoccidentali interne. Memorie della Società Geologica Italiana, 11: 433-460.*
- Delleani, F., Castelli, D., Spalla, M.I. and Gosso, G. (2010). *The record of subduction-related deformation in the Mt. Mucrone metagranitoids (Sesia-Lanzo Zone, Western Alps). Rendiconti online Società Geologica Italiana, 10: 46-49.*
- Delleani, F., Spalla, M.I., Castelli, D. and Gosso, G. (submitted). *A new petrostructural map of Monte Mucrone metagranitoids (Sesia-Lanzo Zone, Western Alps). J. of Maps.*
- Di Paola, S. and Spalla, M.I. (2000). *Contrasting tectonic records in pre-Alpine metabasites of the Southern Alps (Lake Como, Italy). Journal of Geodynamics, 30: 167-189.*
- Ernst, W.G. (1979). *Coexisting sodic and calcic amphiboles from high pressure metamorphic belts and the stability of barroisitic amphibole. Mineralogical Magazine, 43: 269-278.*
- Ernst, W.G. and Liou, J.G. (2008). *High- and ultrahigh-pressure metamorphism: Past results and future prospects. American Mineralogist, 93: 1771-1786.*

- Gazzola, D., Gosso, G., Pulcrano, E. and Spalla, M.I. (2000). *Eo-Alpine HP metamorphism in the Permian intrusives from the steep belt of the central Alps (Languard-Campo nappe and Tonale Series)*. *Geodinamica Acta*, **13**: 149-167.
- Gosso, G. (1977). *Metamorphic evolution and fold history in the eclogite micaschists of the upper Gressoney valley (Sesia-Lanzo zone, Western Alps)*. *Rendiconti della Società Italiana di Mineralogia e Petrologia*, **33**: 389-407.
- Hobbs, B.E., Means, W.D. and Williams, P.F. (1976). *An outline of structural geology*. Wiley, New York, 571 pp.
- Hobbs, B.E., Ord, A., Spalla, M.I., Gosso, G. and Zucali, M. (2010). *The interaction of deformation and metamorphic reactions*. *Geological Society of London Special Publication*, **332**: 189-222.
- Holland, T.J.B. and Powell, R. (1998). *An internally-consistent thermodynamic data set for phases of petrological interest*. *Journal of Metamorphic Geology*, **16**: 309-343.
- Hy, C. (1984). *Métamorphisme polyphasé et évolution tectonique dans la croûte continentale éclogitisée: les séries granitiques et pélitiques du Monte Mucrone (zone Sesia-Lanzo, Alpes italiennes)*. PhD Thesis, Université Paris VI, 198 pp.
- Johnson, S.E. and Vernon, R.H. (1995). *Inferring the timing of porphyroblast growth in the absence of continuity between inclusion trails and matrix foliations: can it reliably be done?* *Journal of Structural Geology*, **17(8)**: 1203-1206.
- Koons, P.O., Rubie, D.C. and Frueh-Green, G. (1987). *The effects of disequilibrium and deformation on the mineralogical evolution of quartz-diorite during metamorphism in the eclogite facies*. *Journal of Petrology*, **28**: 679-700.
- Krogh Ravna, E. (2000). *The garnet-clinopyroxene Fe^{2+} -Mg geothermometer: an updated calibration*. *Journal of Metamorphic Geology*, **18(2)**: 211-219.
- Laird, J. and Albee, A.L. (1981). *Pressure, temperature and time indicators in mafic schists: their application to reconstructing the polymetamorphic history of Vermont*. *American Journal of Science*, **281**: 127-175.
- Lardeaux, J.M., 1981. *Evolution tectono-metamorphique de la zone nord du Massif de Sesia-Lanzo (Alpes occidentales): un exemple d'éclogitisation de croûte continentale*. PhD Thesis, Université Paris VI, 226 pp.
- Lardeaux, J.M., Gosso, G., Kienast, J.R. and Lombardo, B. (1982). *Relations entre le métamorphisme et la déformation dans la zone Sesia-Lanzo (Alpes Occidentales) et le problème de l'éclogitisation de la croûte continentale*. *Bulletin de la société géologique de France*, **24**: 793-800.

- Lardeaux, J.M., Gosso, G., Kienast, J.R. and Lombardo, B. (1983). *Chemical variations in phengitic micas of successive foliations within the Eclogitic Micaschists complex, Sesia-Lanzo zone (Italy, Western Alps)*. Bulletin de Minéralogie, **106**: 673-689.
- Lardeaux, J.M. and Spalla, M.I. (1991). *From granulites to eclogites in the Sesia zone (Italian Western Alps): a record of the opening and closure of the Piedmont ocean*. Journal of Metamorphic Geology, **9**: 35-59.
- Liu, J., Bohlen, S.R. and Ernst, W.G. (1996). *Stability of hydrous phases in subducting oceanic crust*. Earth and Planetary Science Letters, **143**: 161-171.
- Maffeo, B., 1970. Studio petrografico dell'ammasso granitico del Monte Mucrone e dei suoi rapporti con i «micascisti eclogitici». Unpublished Tesi di Laurea, Università di Torino, 117 pp.
- Marotta, A.M. and Spalla, M.I. (2007). *Permian-Triassic high thermal regime in the Alps: result of Late Variscan collapse or continental rifting? Validation by numerical modeling*. Tectonics, **26**: TC4016, doi:10.1029/2006TC002047
- Marotta, A.M., Spalla, M.I. and Gosso, G. (2009). *Upper and lower crustal evolution during lithospheric extension: numerical modelling and natural footprints from the European Alps*. Geological Society of London Special Publication, **321**: 33-72.
- Massonne, H.J. and Schreyer, W. (1987). *Phengite geobarometry based on the limiting assemblage with k-feldspar, phlogopite and quartz*. Contributions to Mineralogy and Petrology, **96**: 212-224.
- Meda, M., Marotta, A.M. and Spalla, M.I. (2010). *The role of mantle hydration into continental crust recycling in the wedge region*. Geological Society of London Special Publication, **332**: 149-172.
- Moody, J.B., Meyer, D. and Jenkins, J.E. (1983). *Experimental characterization of the greenschist-amphibolite boundary in mafic system*. American Journal of Science, **283**: 48-92.
- Morimoto, N. (1988). *Nomenclature of pyroxenes*. Mineralogical Magazine, **52**: 535-550.
- Oberhaensli, R., Hunziker, J.C., Martinotti, G. and Stern, W.B. (1985). *Geochemistry, gheochronology and Petrology of Monte Mucrone: an example of Eo-Alpine eclogitisation of Permian granitoids in the Sesia-Lanzo Zone, Western Alps, Italy*. Chemical Geology, **52**: 165-184.
- Park, R.G. (1969). *Structural correlations in metamorphic belts*. Tectonophysics, **7(4)**: 323-338.
- Passchier, C.W., Myers, J.S. and Kröner, A. (1990). *Field geology of high-grade gneiss terrains*. Springer Verlag, Berlin, 150 pp.
- Passchier, C.W. and Trouw, R.A.J. (2005). *Microtectonics*, Second Edition. Springer, 366 pp.

- Plyusnina, L.P. (1982). *Geothermometry and geobarometry of plagioclase-hornblende bearing assemblages*. Contributions to Mineralogy and Petrology, **80**: 140-146.
- Pognante, U. (1989a). *Lawsonite, blueschist and eclogite formation in the southern Sesia Zone (Western Alps, Italy)*. European Journal of Mineralogy, **1**: 89-104.
- Pognante, U. (1989b). *Tectonic implications of lawsonite formation in the Sesia zone (Western Alps)*. Tectonophysics, **162**: 219-227.
- Pognante, U. (1991). *Petrological constraints on the eclogite- and blueschist-facies metamorphism and P-T-t paths in the Western Alps*. Journal of Metamorphic Geology, **9**: 5-17.
- Poli, S. (1993). *The amphibolite-eclogite transformation: an experimental study on basalt*. American Journal of Science, **293**: 1061-1107.
- Poli, S. and Schmidt, M.W. (1995). *H₂O transport and release in subduction zones: experimental constraints on basaltic and andesitic system*. Journal of Geophysical Research, **100(B11)**: 22299 - 22314.
- Powell, R. and Holland, T.J.B. (1994). *Optimal geothermometry and geobarometry*. American Mineralogist, **79**: 120-133.
- Ramsay, J.G., 1967. *Folding and Fracturing of Rocks*. McGraw-Hill, New York, 568 pp.
- Rebay, G. and Messiga, B. (2007). *Prograde metamorphic evolution and development of chloritoid-bearing eclogitic assemblages in subcontinental metagabbro (Sesia-Lanzo Zone, Italy)*. Lithos, **98**: 275-291.
- Rebay, G. and Spalla, M.I. (2001). *Emplacement at granulite facies conditions of the Sesia-Lanzo metagabbros: an early record of Permian rifting?* Lithos, **58**: 85-104.
- Roda, M., Spalla, M.I. and Marotta, A.M. (2012). *Integration of natural data within a numerical model of ablative subduction: a possible interpretation for the Alpine dynamics of the Austroalpine crust*. Journal of Metamorphic Geology, **30**: 973-996.
- Roda, M. and Zucali, M. (2011). *Tectono-metamorphic map of the Mont Morion Permian metaintrusives (Mont Morion - Mount Collon - Matterhorn Complex, Dent Blanche Unit), Valpelline -Western Italian Alps*. Journal of Maps, **2011**: 519-535.
- Rubatto, D., Gebauer, D. and Compagnoni, R. (1999). *Dating of eclogite-facies zircons; the age of Alpine metamorphism in Sesia-Lanzo Zone (Western Alps)*. Earth and Planetary Science Letters, **167**: 141-158.
- Salvi, F., Spalla, M.I., Zucali, M. and Gosso, G. (2010). *Three-dimensional evaluation of fabric evolution and metamorphic reaction progress in polycyclic and polymetamorphic terrains: a case from the Central Italian Alps*. Geological Society of London Special Publication, **332**: 173-187.

- Schmidt, M.W. (1993). *Phase relations and compositions in tonalite as a function of pressure: an experimental study at 650°C*. American Journal of Science, **293**: 1011-1060.
- Spalla, M.I. (1983). *Struttura e petrografia delle successioni del margine esterno della zona Sesia-Lanzo al contatto con la Falda Piemontese tra il lago di Monastero e il Ponte Cusard (Valli di Lanzo)*. Unpublished Tesi di Laurea, Università di Torino, 181 pp.
- Spalla, M.I. (1993). *Microstructural control on the P-T path construction in the metapelites from the Austroalpine crust (Texel Gruppe, Eastern Alps)*. Schweizerische Mineralogische und Petrographische Mitteilungen, **73**: 259-275.
- Spalla, M.I., De Maria, L., Gosso, G., Miletto, M. and Pognante, U. (1983). *Deformazione e metamorfismo della Zona Sesia - Lanzo meridionale al contatto con la falda piemontese e con il massiccio di Lanzo, Alpi occidentali*. Memorie della Società Geologica Italiana, **26**: 499-514.
- Spalla, M.I., Lardeaux, J.M., Dal Piaz, G.V. and Gosso, G. (1991). *Metamorphisme et tectonique a la marge externe de la zone Sesia-Lanzo (Alpes occidentales)*. Memorie di Scienze Geologiche, Padova, **43**: 361-369.
- Spalla, M.I., Siletto, G.B., di Paola, S. and Gosso, G. (2000). *The role of structural and metamorphic memory in the distinction of tectono-metamorphic units: the basement of the Como Lake in the Southern Alps*. Journal of Geodynamics, **30**: 191-204.
- Spalla, M.I., Zanoni, D., Williams, P. and Gosso, G. (2011). *Deciphering cryptic P-T-d-t histories in the western Thor-Odin dome, Monashee Mountains, Canadian Cordillera: A key to unravelling pre-Cordilleran tectonic signatures*. Journal of Structural Geology, **33**: 399-421.
- Spalla, M.I. and Zucali, M. (2004). *Deformation vs. metamorphic re-equilibration heterogeneities in polymetamorphic rocks: a key to infer quality P-T-d-t path*. Periodico di Mineralogia, **73(2)**: 249-257.
- Spalla, M.I., Zucali, M., di Paola, S. and Gosso, G. (2005). *A critical assessment of the tectono-thermal memory of rocks and definition of tectono-metamorphic units: evidence from fabric and degree of metamorphic transformations*. Geological Society of London Special Publication, **243**: 227-247 pp.
- Turner, F.J. and Weiss, L.E. (1963). *Structural analysis of metamorphic tectonites*. MacGraw-Hill, New York, 545 pp.
- Ungaretti, L., Lombardo, B., Domeneghetti, C. and Rossi, G. (1983). *Crystal-chemical evolution of amphiboles from eclogitized rocks of the Sesia-Lanzo Zone, Italian western Alps*. Bulletin de Minéralogie, **106**: 645-672.

- Whitney, D.L. and Evans, B.W. (2010). *Abbreviations for names of rock-forming minerals*. American Mineralogist, **95**: 185-187.
- Williams, P.F. (1985). *Multiply deformed terrains - problems of correlation*. Journal of Structural Geology, **7(3/4)**: 269-280.
- Wu, C.M., Wang, X.S., Yang, C.H., Geng, Y.S. and Liu, F.L. (2002). *Empirical garnet-muscovite geothermometry in metapelites*. Lithos, **62**: 1-13.
- Zanoni, D. (2010). *Structural and petrographic analysis at the north-eastern margin of the Oligocene Traversella pluton (Internal Western Alps, Italy)*. Italian Journal of Geosciences, **129(1)**: 51-68.
- Zanoni, D., Bado, L. and Spalla, M.I. (2008). *Structural analysis of the Northeastern margin of the Tertiary intrusive stock of Biella (Western Alps, Italy)*. Bollettino della Società Geologica Italiana, **127(1)**: 125-140.
- Zanoni, D., Spalla, M.I. and Gosso, G. (2010). *Structure and PT estimates across late-collisional plutons: constraints on the exhumation of Western Alpine continental HP units*. International Geology Review, **52**: 1244-1267.
- Zucali, M. (2002). *Foliation map of the "Eclogitic Micaschists Complex" (M. Mucrone-M.Mars-Mombarone, Sesia-Lanzo Zone, Italy)*. Memorie di Scienze Geologiche, Padova, **54**: 87-100.
- Zucali, M., Chateigner, D., Dugnani, M., Lutterotti, L. and Ouladdiaf, B. (2002a). *Quantitative texture analysis of naturally deformed hornblendite under eclogite facies conditions (Sesia-Lanzo Zone, Western Alps): comparison between x-ray and neutron diffraction analysis*. Geological Society of London Special Publication, **200**: 239-253.
- Zucali, M. and Spalla, M.I. (2011). *Prograde lawsonite during the flow of continental crust in the Alpine subduction: Strain vs. metamorphism partitioning, a field-analysis approach to infer tectonometamorphic evolutions (Sesia-Lanzo Zone, Western Italian Alps)*. Journal of Structural Geology, **33**: 381-398.
- Zucali, M., Spalla, M.I. and Gosso, G. (2002b). *Fabric evolution and reaction rate as correlation tool: the example of the Eclogitic Micaschists complex in the Sesia-Lanzo Zone (Monte Mucrone – Monte Mars, Western Alps Italy)*. Schweizerische Mineralogische und Petrographische Mitteilungen, **82**: 429-454.

Figure Captions:

Fig. 1: Tectonic sketch of Western Alps (modified after Dal Piaz, 1999) showing the location of the Sesia-Lanzo Zone (SL); red diamond locates the mapped area of Fig. 2. In the two bottom insets the location of the tectonic sketch in the frame of the European Alps. Legend: 1) Penninic continental nappes: MR = Monte Rosa, AB = Arcesa-Brusson, GP = Gran Paradiso, SB = Grand St. Bernard; 2a) Austroalpine nappes: DB = Dent Blanche (Vp = Valpelline lower crust, Ar = Arolla series), MM - P = Mt. Mary-Pillonet thrust system, AR = Acque Rosse, CH = Chatillon-St. Vincent, E = Etirol-Levaz, G = Grun, EM = Mt. Emilius, GR = Glacier-rafay, S = Santanel, TP = Tour Ponton, SL = Sesia-Lanzo Zone (Dk = Dioritic-kinzigitic upper element, Gm = Gneiss Minuti complex with (2) or without (1) eclogitic relics, Emc = Eclogitic Micaschists complex, Rct = Rocca Canavese Thrust Sheets); 2b) Mesozoic metasedimentary covers in Austroalpine Domain: R = Roisan Zone, Sc = Scalero unit; 3) Ophiolitic Piedmont Zone: CO = Combin Zone, PCB = Pancherot-Cime Bianche, FC = Faisceau de Cogne, ZS = Zermatt-Saas Zone, MA = Mt. Avic, A = Antrona ophiolite, LM = Lanzo Massif; 4) Southalpine Domain: CA = Canavese Zone; 5) Oligocene Plutons: B = Biella, M = Miagliano, T = Traversella; 6) Lineaments: CL = Canavese Line, SF = Simplon Fault, AR = Aosta-Ranzola fault system.

Fig. 2: Structural map of the southern slope of Mt. Mucrone with foliation trajectories traced on standard lithological information. Relative chronology of superposed foliations (S1, S2, S3, etc.) is graphically represented by progressive number of dots in dashed lines. The inferred metamorphic conditions, under which successive foliations, folds and shear zones developed, can be inferred by the supporting mineral assemblages listed in the legend.

Fig. 3: Representative structures characterising low, medium and high degree (LD, MD and HD, respectively) of fabric evolution during the successive deformation stages in the two main types of metagranitoids. “Grey type” metagranitoids: a) poorly deformed igneous texture in D1 LD; b) localized progressive foliation developed close to a cm-thick syn-D1 mylonitic shear zone; c) poorly deformed Qz igneous domains in D2 LD; d) D2 crenulation in hinge zone type” metagranitoids: i) 10-cm-spaced discontinuous S1 foliation associated with D1 fold, emphasized by the contact with micaschists; l) mm-spaced S1 foliation and D1 fold, underlined by Qz-rich vein; m) syn-D2 parallel shape folding of S1; n) S1 + S2 composite fabric in D2 MD; o) mm-spaced S3 mylonitic foliation wrapping around 10-cm-thick eclogite boudin; p) gentle D4 folding with parallel shape; q) localized mm-thick shear zones in D5 HD; r) syn-D6 gentle folding.

Fig. 4: Representative structures characterising low, medium and high degree (LD, MD and HD, respectively) of fabric evolution during the successive deformation stages in the two main types of country rocks. Paragneisses: a) pre-Alpine compositional layering totally replaced by Amp-, Omp- and Grt-assemblages in poorly deformed D1 domains; b) tight D1 folding of pre-Alpine alternating layers; c) mylonitic S1 foliation obliterating the pre-Alpine layering of paragneisses; d) parallel shape D2 folding; e) nearly isoclinal D2 folds with similar profile; f) cm-thick shear zone in D3 HD; g/h) open (g, LD) and tight (h, MD) D4 folds; i) cm-thick D5 shear zone in a Qz-rich layer of the paragneisses. Micaschists: l) rare preservation case of continuous S1 foliation re-oriented by D2 crenulation; m) transposition of S1 foliation during the development of the new S2 axial plane foliation; n) S2 foliation crosscut by S3 in D3 HD; o) D4 gentle folding; p) D4 crenulation in a micaschist re-equilibrated under greenschist facies conditions; q) numerous D5 mm-thick shear zones marked by whitish Ab and reddish Fe-oxides; r) D6 kink fold associated with the 10-m-wavelength D6 gentle bending.

Fig. 5: Scheme of qualitative estimate of the degree of fabric evolution during foliation development, starting from originally foliated or initially isotropic rocks, as proposed by Salvi *et al.* (2010); the volume occupied by newly oriented fabric elements, including the newly differentiated mineral layering, is used to define the degree of fabric evolution, and to establish conventionally a low, medium or high degree of granular scale deformation (LD, MD and HD, respectively).

Fig 6: Representative microstructures of low, medium and high degree (LD, MD and HD, respectively) of fabric evolution during the successive deformation stages in the two main types of metagranitoids. “Grey type” metagranitoids: a) coronitic replacement of igneous Bt and Pl by eclogite-facies mineral as Cpx, Grt, Ph; b) syn-D2 Omp rimming pre-D3 coronitic Jd – white mica aggregate; c) S1+ S2 composite fabric wrapping Aln porphyroclast, associated with syn-D2 Grt and Ph partial re-crystallization; d) fine-grained white mica growing after Jd aggregates in a poorly deformed domain close to D3 shear zone; e) syn-D1 localized mylonitic shear zone, reactivated during D3 with consequent flattening of Jd aggregates, partially replaced by fine-grained white mica; f) replacement of syn-D4 Ab and Wm on the previous Jd, Qz and Zo aggregate, along old grain boundaries and microfractures; g) very fine-grained re-crystallization of Ph along D5 shear plane; h) dark-Amp, Wm, Adl and Ab after Jd, Qz and Zo aggregates close to a D6 fold hinge. “Green type” metagranitoids: i/l) incipient (i) and well developed (l) S1 foliation marked by SPO of Na-Cpx grains; m) syn-D2 coronitic Acm rimming igneous Pl sites; n) S1+S2 composite fabric

associated with recrystallization of Ph, Na-Cpx and Qz; o) syn-D3 Brs rimming compositionally zoned Gln; p) S3 foliation marked by Ph and Pg aggregates partially replacing older and coarser Ph and Brs; q) Act and Wm filling of D4 fracture across syn-D2 Gln; r) Na-Cpx stretched in a syn-D5 shear zone; Qz ribbon, new white mica and Chl overgrowing Cpx mark the mylonitic foliation.

Fig 7: Representative microstructures characterising low, medium and high degree (LD, MD and HD, respectively) of fabric evolution during the successive deformation stages in the two main types of country rocks. Paragneisses: a) randomly oriented growth of Omp and Grt in an Amp-Omp-Grt-rich layer; b) mm-spaced S1 foliation mainly marked by Ph SPO wrapping pre-Alpine Grt porphyroclasts; c) atoll Grt in D2 LD domains, enclosing Ph, Pg and Gln; d) D2 folding of S1 with bending of Grt- and white mica-rich layers; the latter is only partially re-crystallized; e) Brs partially replacing syn-D2 Gln in Amp-Omp-Grt-rich layer along mm-thick syn-D3 shear zone; f) D4 microfolding of syn-D1 Ph with partial re-crystallization of Ph in new white mica and Ttn recrystallisation; g) Chl overgrew Grt and Gln in a Md domain close to D5 shear zone; h) Ab and new white mica aggregates developed along syn-D5 shear plane. Micaschists: i) S1 foliation marked by Jd and Ph, whereas the timing of Pg growth is ambiguous and may postdate S1; l) coronitic growth of syn-D2 Gln enclosing a large amount of fine-grained Grt, Ph and Qz marking S1; m) S2 foliation marked by Ph and Omp SPO and by elongated Qz-domains with polygonal structure; n) S3 shear plane marked by Ph, with the formation of Ttn rims on Rt; o) syn-D4 coronitic replacement of Gln by Ab, Wm, Ep and Act aggregates; p) D4 folding of syn-D1 Ph; q) very fine-grained aggregate of Ab and Wm developed on Na-Cpx during D5; r) Chl, Wm and Fe-oxides formation along D5 shear plane.

Fig. 8: Maps of the degree of fabric evolution and metamorphic transformation (M) for D1 and D2 stages. Syn-D1 mineral assemblages always constitute more than 70% of the rock volume. For this reason the map of the degree of metamorphic transformation is show only for D2 stage. D1 HD domains are mainly localised in micaschists, leucocratic metagranitoids and in the eastern portion of the paragneisses, while in metagranitoids syn-D1 HD domains mainly occur close to the boundaries with paragneisses (eastern portion of Mt. Mucrone southern slope) and micaschists (north of Mt. Mucrone).

Fig. 9: Maps of the degree of fabric evolution and metamorphic transformation (M) for D3 and D4 stages. D3 mineral assemblages always constitute less than 10% of the rock volume in LD domains

and no more than 60% in HD. For this reason the map of the degree of metamorphic transformation is show only for D4 stage.

Fig. 10: Compositional range of amphiboles from metaintrusives (a, b) and metasediments (c, d). Stars locate end-member composition (Act = actinolite; Brs = barroisite; Ed = edenite; Gln = glaucophane; Ktp = katophorite; Prg = pargasite; Ts = tschermakite; Win = winchite). Straight lines define high-pressure and intermediate pressure amphibole trends from Vermont (Laird & Albee, 1981). Amphibole composition trends during Alpine evolution is shown by the grey arrows on the Al(VI) vs Al(IV) diagrams (b, d). Different colors identify rock types and simbols deformation stages: grey-type metagranitoids in red; green-type metagranitoids in orange; eclogites in green; metaquartzdiorites in violet; micaschists in light-blue; paragneisses in brown; D1 = full triangle; D2 = open triangle; D3 = full box; D4 = open box; D5 = open diamond. In eclogites full triangle identifies pre-D3 grains.

Fig. 11: Pyroxene compositions according to Morimoto (1988) for Cpx in metaintrusives and metasediments. Different colors identify rock types and simbols deformation stages: grey-type metagranitoids in red; green-type metagranitoids in orange; eclogites in green; metaquartzdiorites in violet; micaschists in light-blue; paragneisses in brown; D1 = full triangle; D2 = open triangle; D3 = full box; D4 = open box; D5 = open diamond. In grey-type metagranitois full triangle identifies pre-D3 grains. See discussion in the text.

Fig. 12: Garnet compositional variations in metasediments and metaintrusive rocks. Different colors identify rock types and simbols deformation stages: grey-type metagranitoids in red; green-type metagranitoids in orange; eclogites in green; metaquartzdiorites in violet; micaschists in light-blue; paragneisses in brown; D1 = full triangle; D2 = open triangle; syn-D1 veins = yellow cross; D3 = full box; D4 = open box; D5 = open diamond. In grey-type metagranitois full triangle identifies pre-D3 grains. See discussion in the text.

Fig. 13: Examples of compositional zoning in Grt from pargneisses, zoisitites and grey-type metagranitoids. Paragneisses: zoning from pre-Alpine core (a: pre-D1) to Alpine rim (b: syn-D1-D2). Zoisitites: Rim-to-rim (a to b) compositional profile across a syn-D1 megablast. Grey-type metagranitoids: variations in composition across a Grt corona developed between the Pl (a) and Bt (b) site.

Fig. 14: Phengite compositions in metasediments and intrusive rocks displayed in the ternary diagram of Massonne & Schreyer (1987) and in the Si/Mg (in a.p.f.u.) plot. Stars locate end-member composition (Ph = phengite; Lc = leucite). Different colors identify the rock types and symbols the deformation stages: grey-type metagranitoids in red; green-type metagranitoids in orange; eclogites in green; metaquartzdiorites in violet; micaschists in light-blue; paragneisses in brown; D1 = full triangle; D2 = open triangle; D3 = full box; D4 = open box; D5 = open diamond. In grey-type metagranitoids full triangle identifies pre-D3 grains. In metagranitoids a higher content in Fe^{3+} is suggested by the deviation from the Ph-Lc tie-line.

Fig. 15: PT paths inferred for the Mt. Mucrone rocks; boxes represents the average PT estimates performed with AX and average PT using THERMOCALC in metagranitoids (colored boxes) and eclogites (dashed box). Red dashed lines represents T-intervals estimated with the Grt-Amp thermometer in eclogites. Blue dashed lines represents T-intervals estimated with the Grt-white mica thermometer in micaschists and paragneisses. Green open triangle locates the evaluation of syn-D5 conditions in paragneisses. Metamorphic facies (Ernst & Liou, 2008): GS = greenschist; EA = epidote-amphibolite; BS = blueschist; AM = amphibolite; Amp-EC = amphibole-bearing eclogite; HGR = high pressure granulite; GR = granulite. Brs/Act transition (Ernst, 1979); Act/Hbl transition (Moody *et al.*, 1983); Omp-in and Amp-out (Poli & Schmidt, 1995); Pl-out and Grt-in (Liu *et al.*, 1996). In the inset the inferred PTdt path (orange) is compared with that of Zucali *et al.* (2002), shown in blue. Light-green lines are geotherms: 1) “cold” subduction zones, 2) “warm” subduction zones, 3) normal gradient of old plate interior, 4) near spreading ridge or volcanic arc (Cloos, 1993).

Tab. 1: Schmidt equal area diagrams of the structural elements (lower hemisphere): 1/2/3) The S1, S2 and D2 axial planes (synoptic Schmidt equal area diagrams) show a remarkable dispersion of data, due to superposition of deformation events (mostly by D2 and D4), with verticalization of surfaces in the hinge zones of the D2 and D4 folds; red crosses in the S1 diagram are poles to D1 fold axes. 4) D2 axes are sub-horizontal and do not display an orientation maximum; the dispersion of the D2 axes is influenced by non-cylindrical folding. 5) The distribution of S3 differs from that of S1 and S2 and admits reorientation by bending imposed during D4. 6) The D4 axes population forms a maximum at about 45-15°, and its weak dispersion reveals the effect of D6 fold axial surfaces striking 160°N, that mainly imposes to the D4 axes a dip change from the NE to the SW. 7) The prevailing orientations of the axial planes of D4 are bimodal, with a maximum of up to 320°N, and dip about 30-40°; the second maximum is about 140°N, and dip about 20°. The D4

surfaces maxima are located on both sides of the successive D6 axial surfaces, that strike 30-60°N or 160°N; the effect of the D6 axial planes striking 160°N is less clearly envisaged, due to the low angle between the average concentration of the D4 axial planes. 8) The S5 foliation planes are sub-horizontal. 9) The sub-horizontal D6 axes dip mainly to 40° and 160°N. 10) D6 folds display two preferred orientations of the subvertical axial surfaces striking 30-60°N and 160°N, respectively; these structures do not offer overprinting relationships and affect two separate rock volumes: the 30-60°N orientation prevails within the micaschists, leucocratic metagranitoids and finely foliated syn-D1 paragneisses (S and E map sectors), and the 160°N maximum occurs in the Mt. Mucrone metagranitoid and poorly deformed syn-D1 paragneisses.

Tab. 2: Representative compositions of Amp, Cpx, Grt and Wm in micaschists (= Micas.), paragneisses (= Parag.), eclogites (= Eclog.), zoisitites (Zoisit.), metaquartzdiorite (= Qzdior.), grey type metagranitoids (“grey” Gran.) and green type metagranitoids (= “green” Gran.).

Tab. 3: Mineral assemblages marking successive fabrics in the different lithotypes of Mt. Mucrone lithostratigraphy.

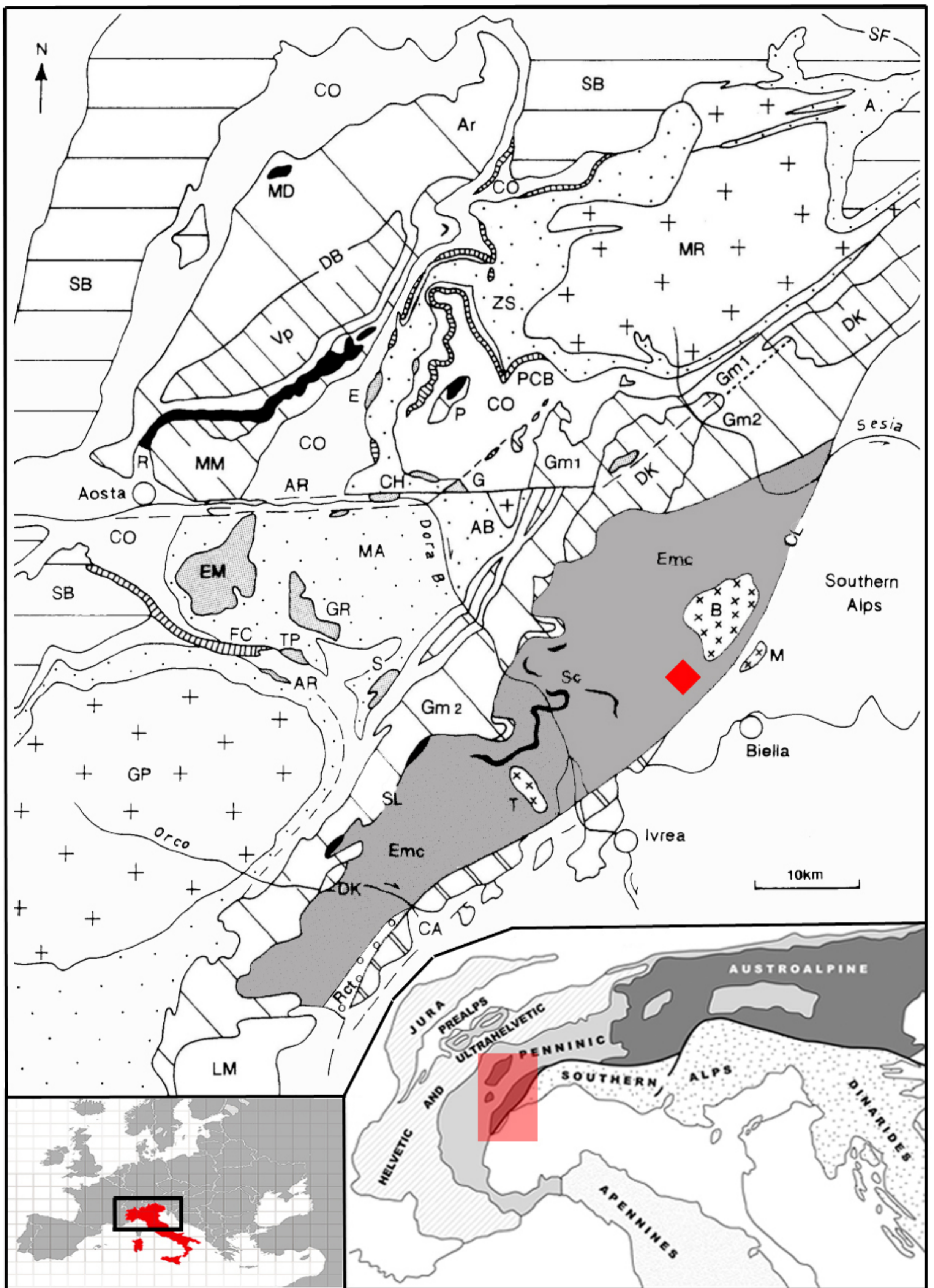


Fig. 1

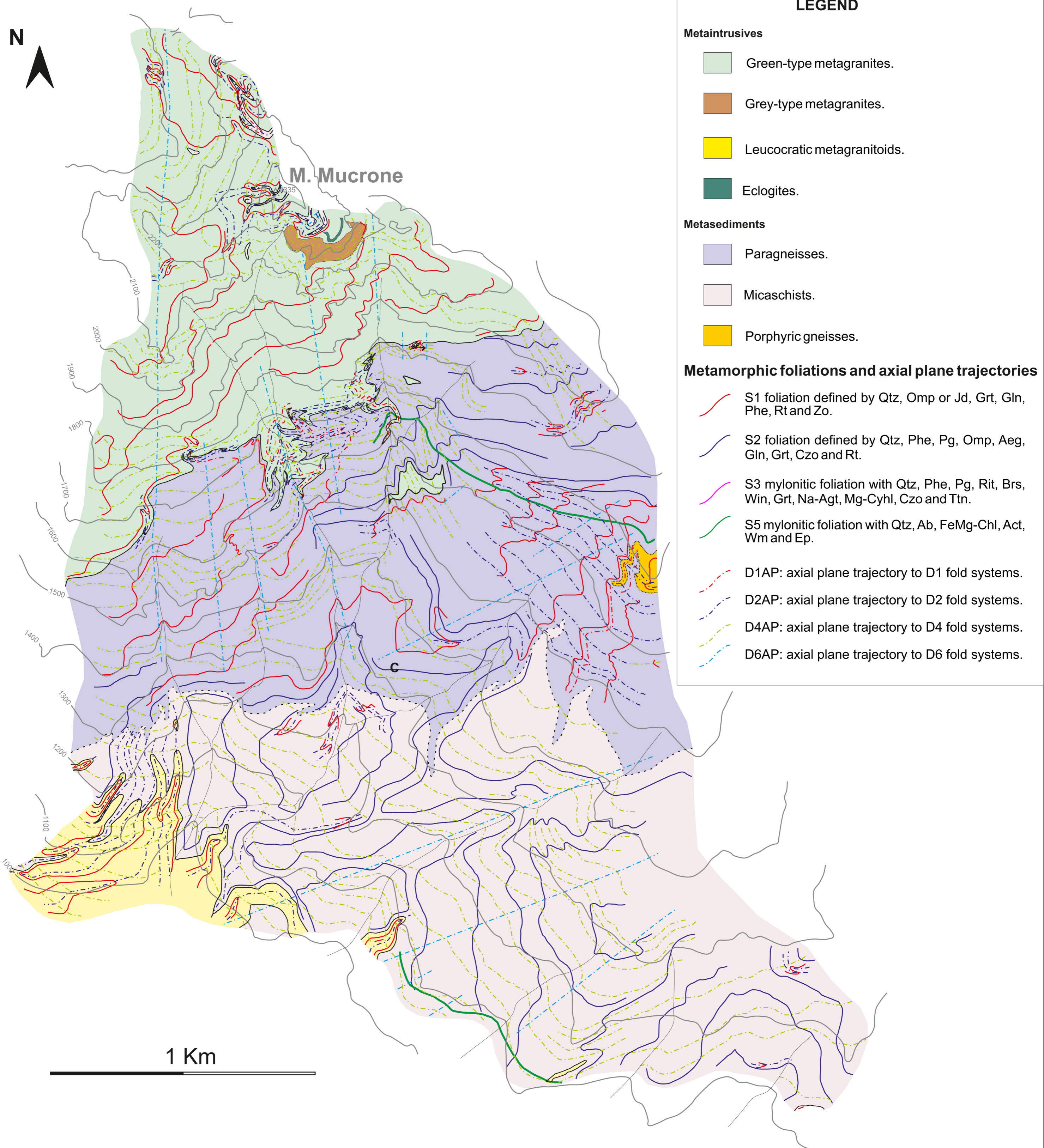


Fig. 2


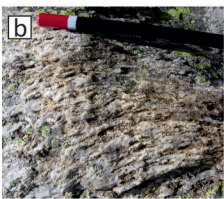
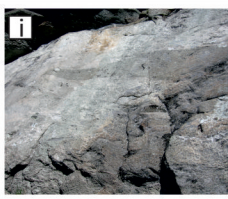




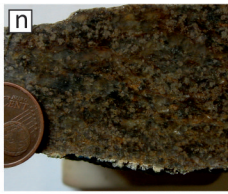


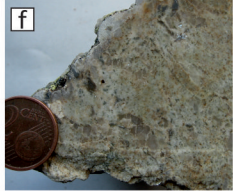


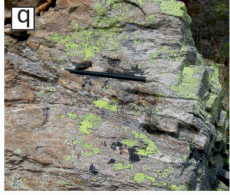


	“grey type” metagranitoids			“green type” metagranitoids		
	Ld	Md	Hd	Ld	Md	Hd
D1						
D2						
D3						
D4						
D5						
D6						

Fig. 3


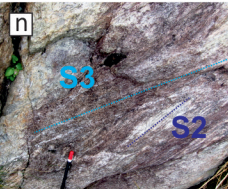





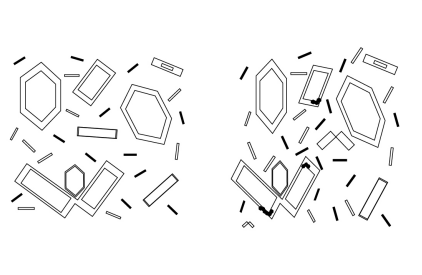
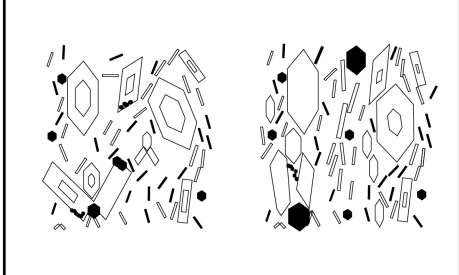
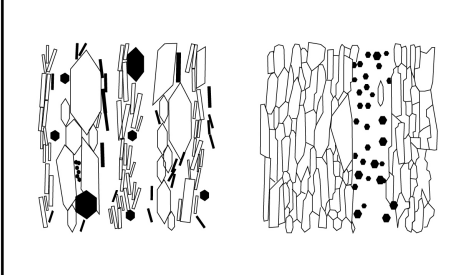
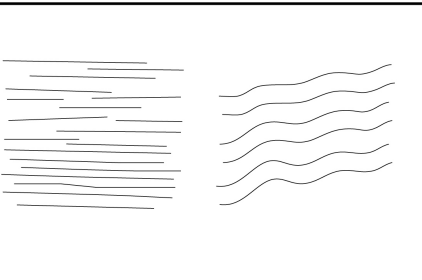
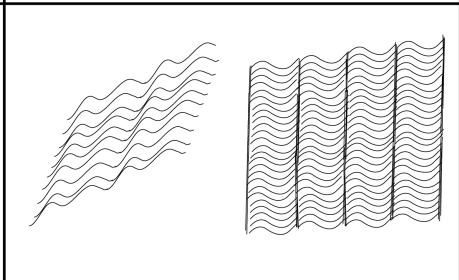
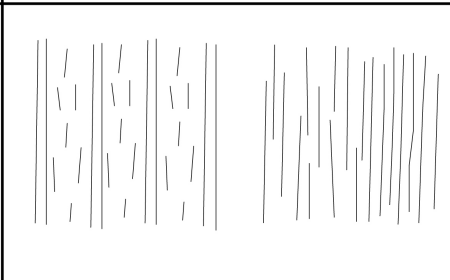
	paragneisses			micaschists		
	Ld	Md	Hd	Ld	Md	Hd
D1						
D2						
D3						
D4						
D5						
D6						

Fig. 4

Fig. 5

	Low deformation degree	Medium deformation degree	High deformation degree
Originally isotropic			
Originally foliated			
Fabric evolution degree	0-20%	20-40% 40-60%	60-80% 80-100%

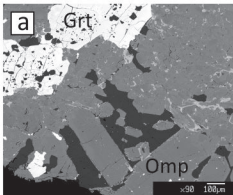
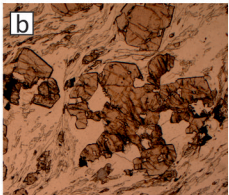
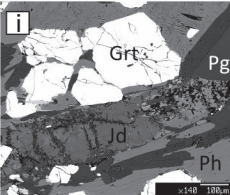
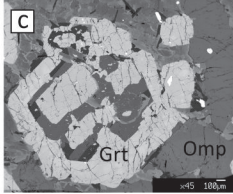
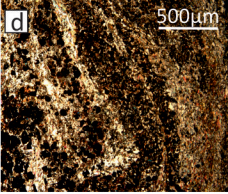
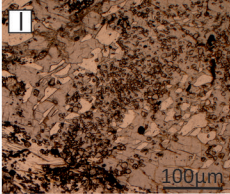
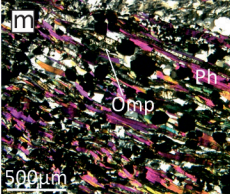
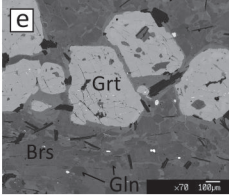
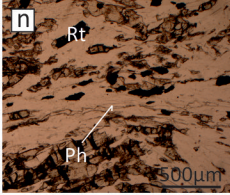
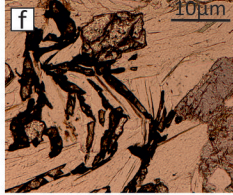
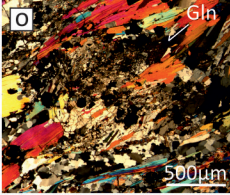
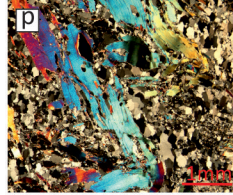
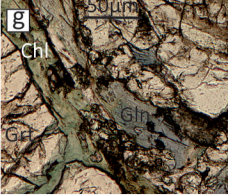
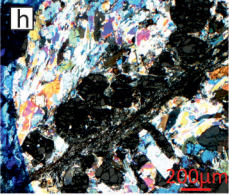
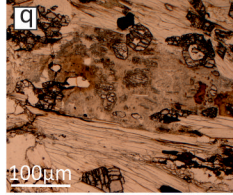
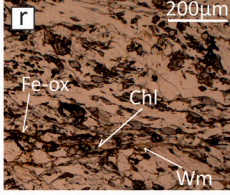
	paragneisses			micaschists		
	Ld	Md	Hd	Ld	Md	Hd
D1						
D2						
D3						
D4						
D5						
D6						

Fig. 6

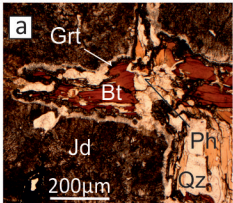
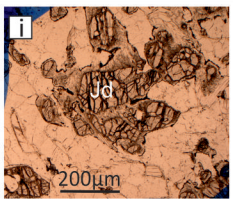
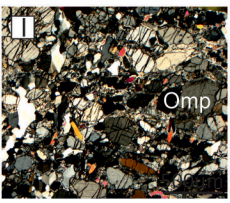
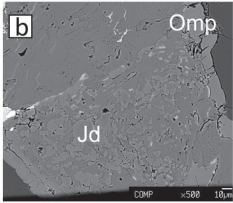
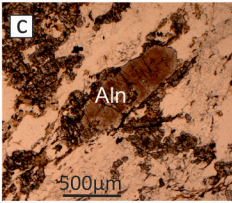
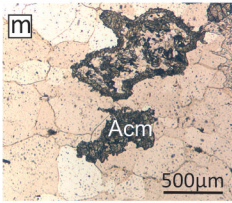
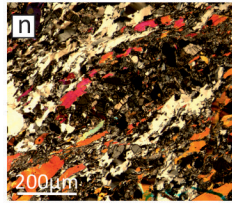
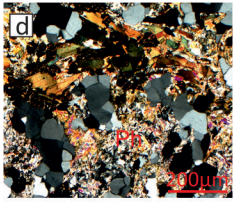
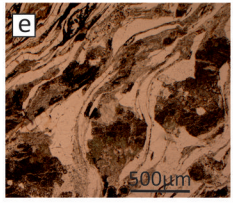
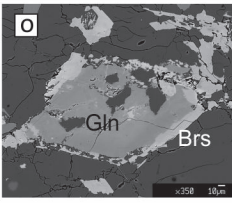
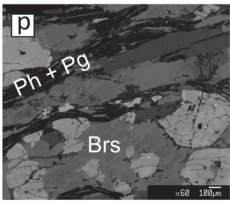
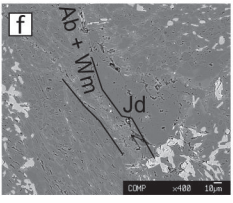
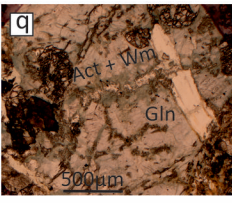
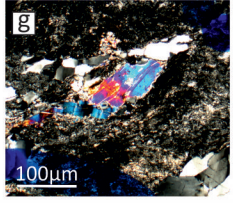
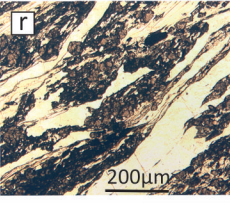
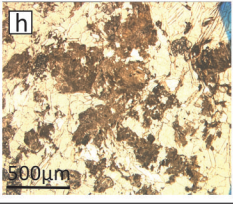
	"grey type" metagranitoids			"green type" metagranitoids		
	Ld	Md	Hd	Ld	Md	Hd
D1						
D2						
D3						
D4						
D5						
D6						

Fig. 7

Fig. 8

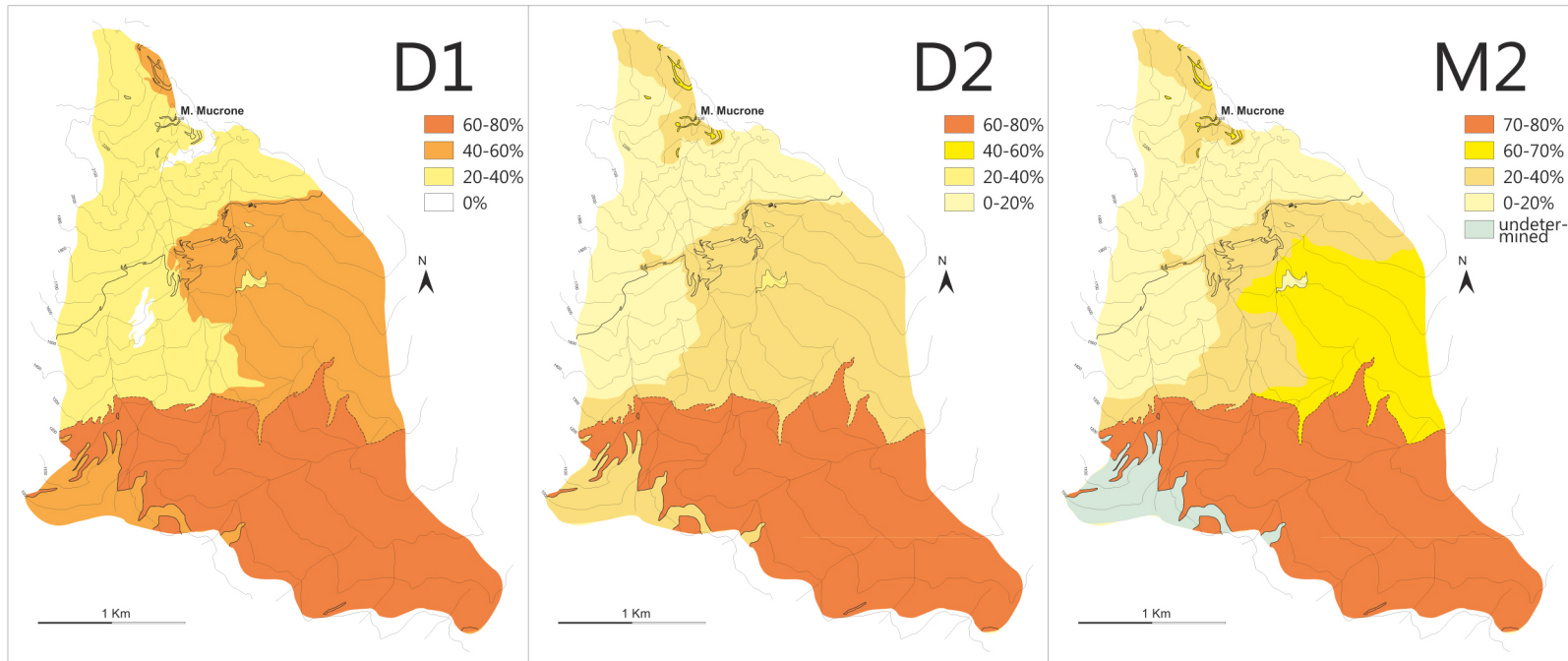
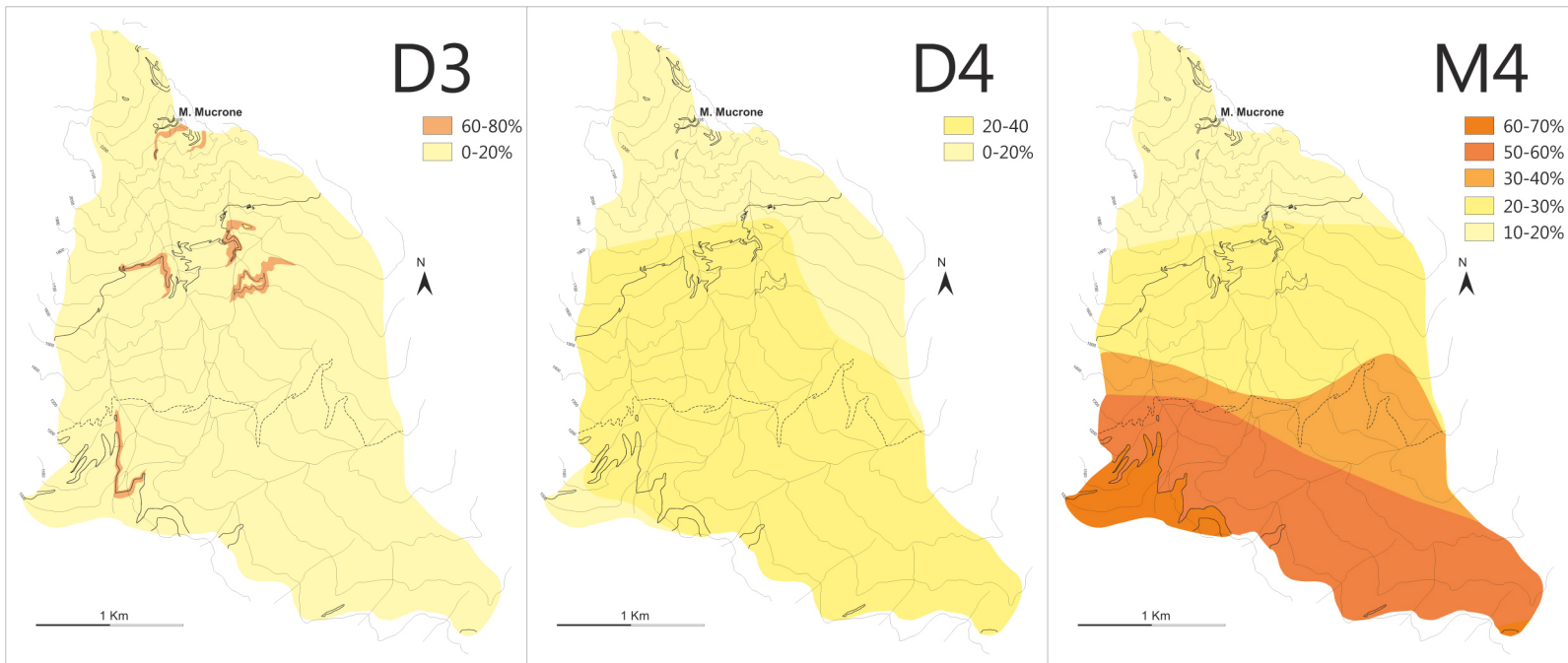


Fig. 9



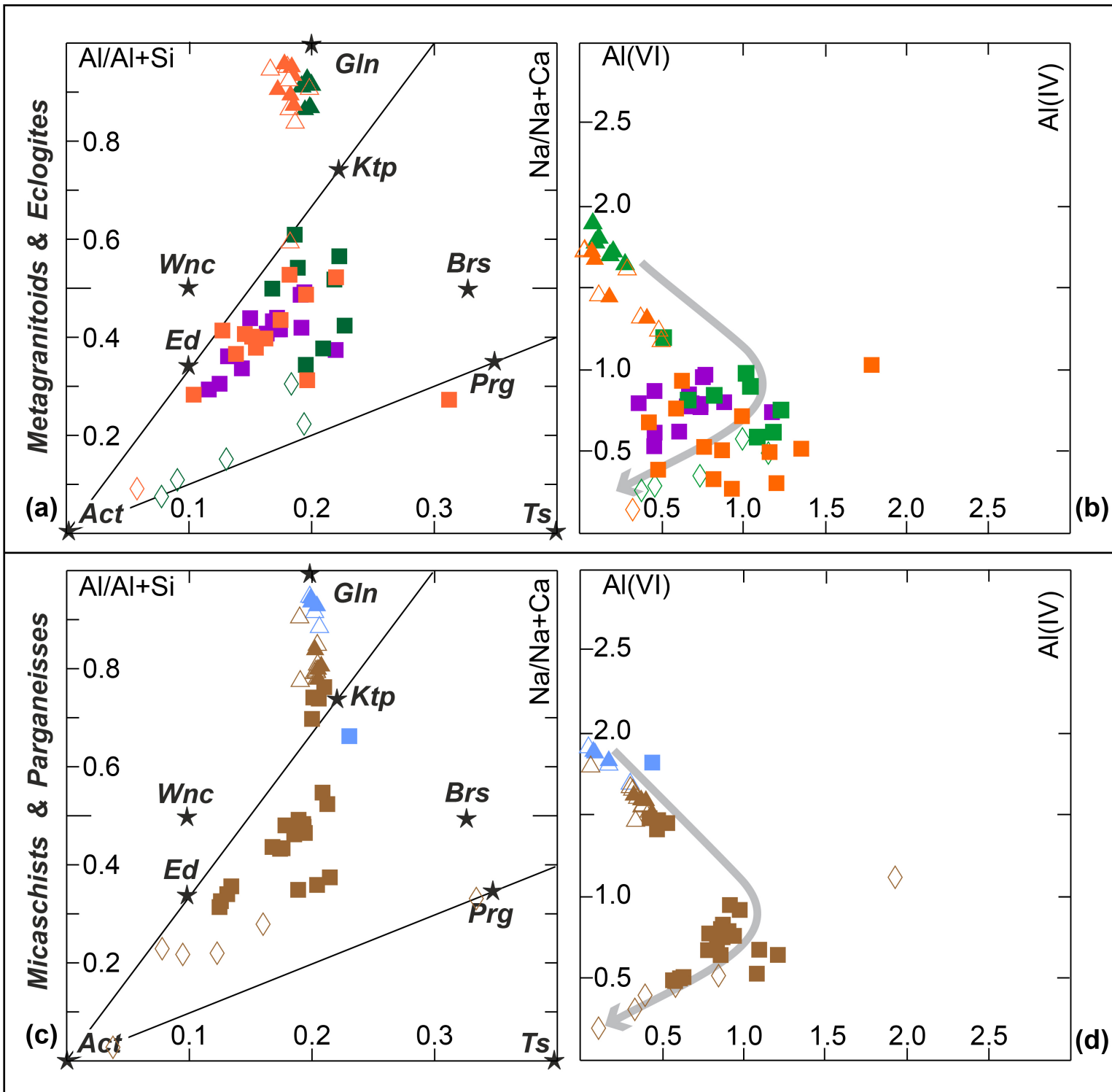


Fig. 10

Metagranitoids & Eclogites

Acm20%



Micaschists & Paragneisses

Acm20%

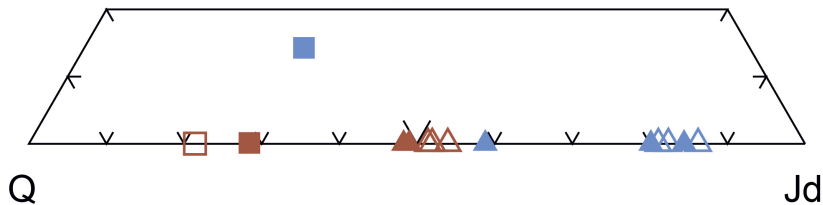


Fig. 11

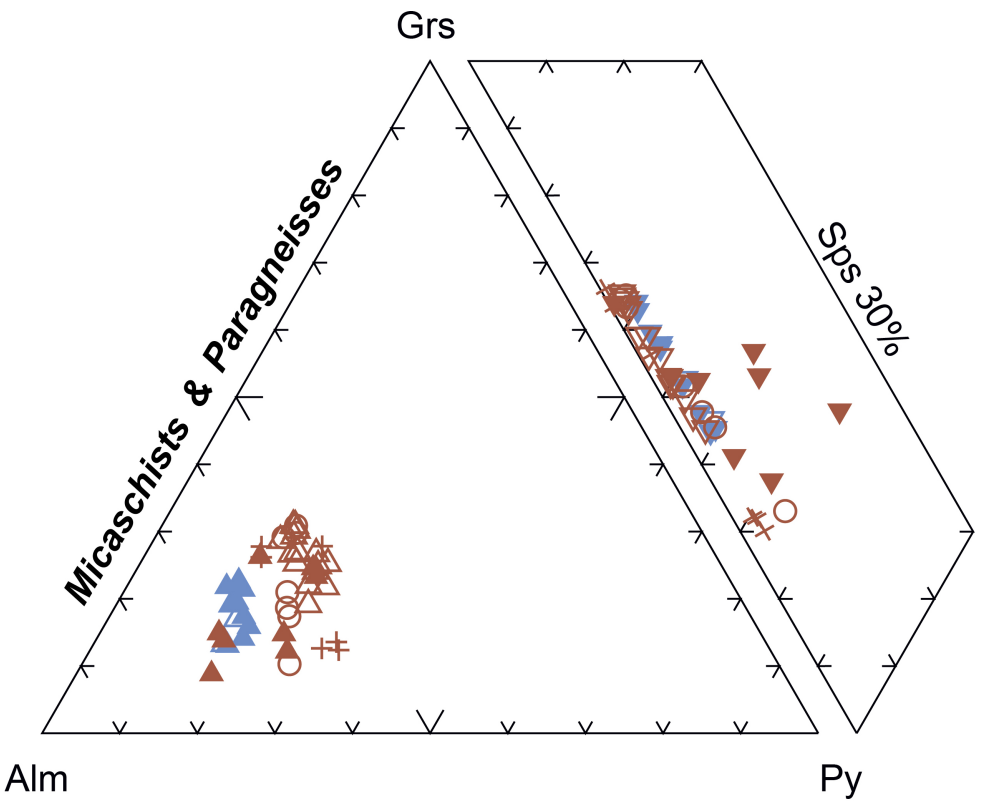
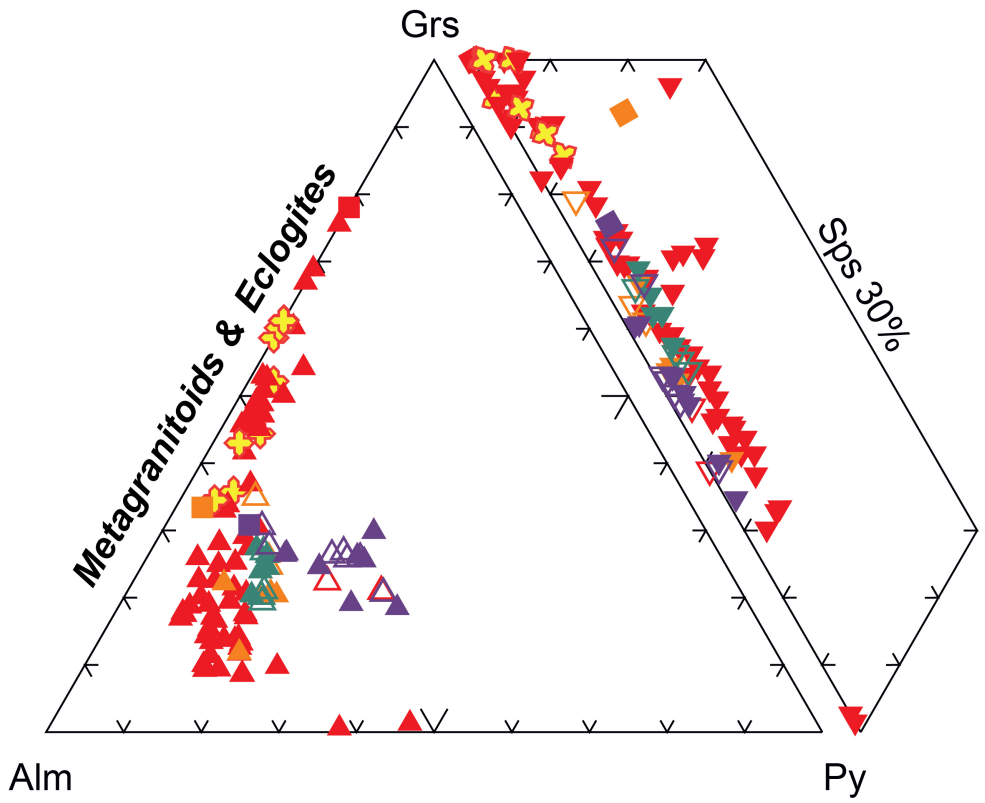
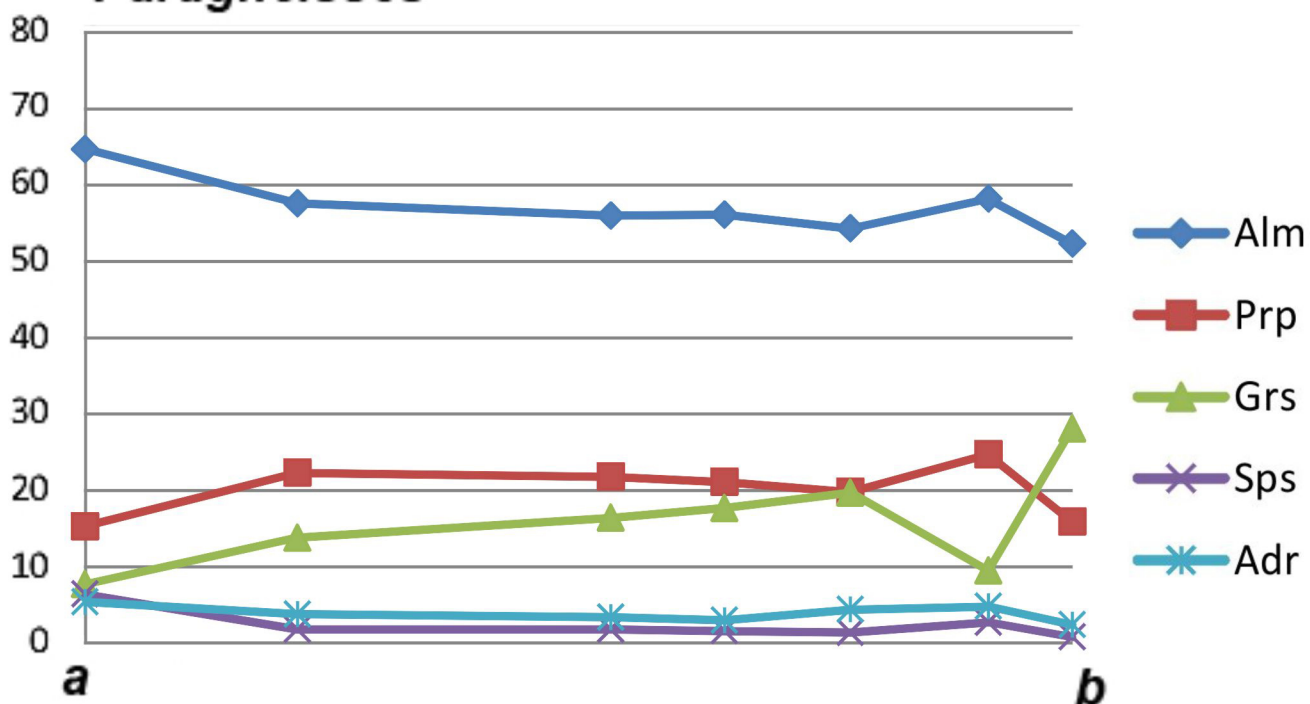
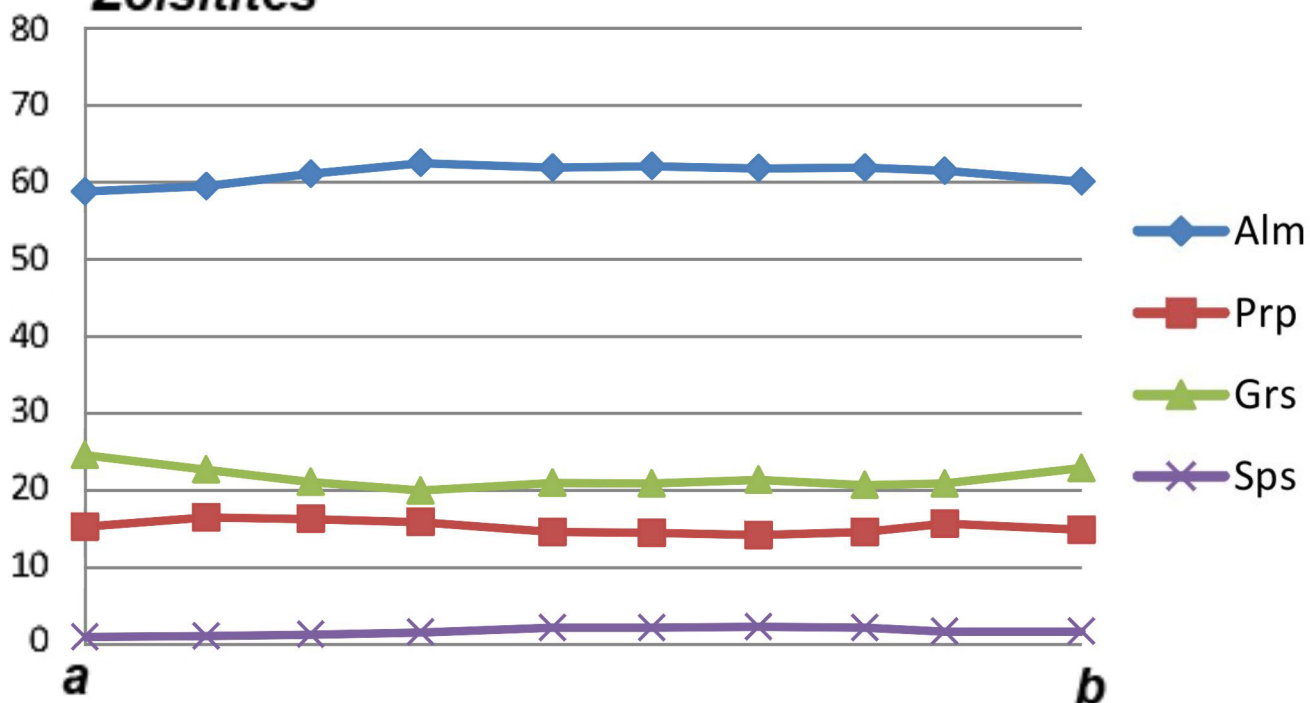


Fig. 12

Paragneisses



Zoisitites



Grey-type metagranitoids

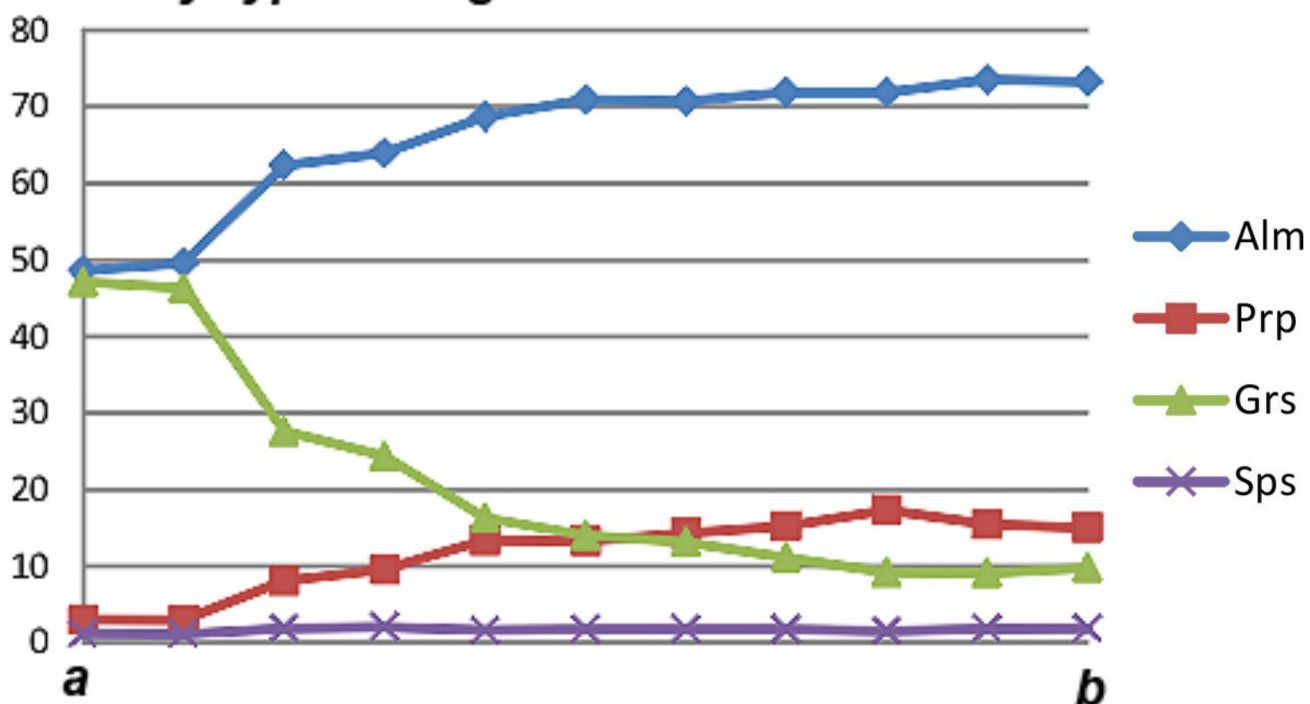


Fig. 13

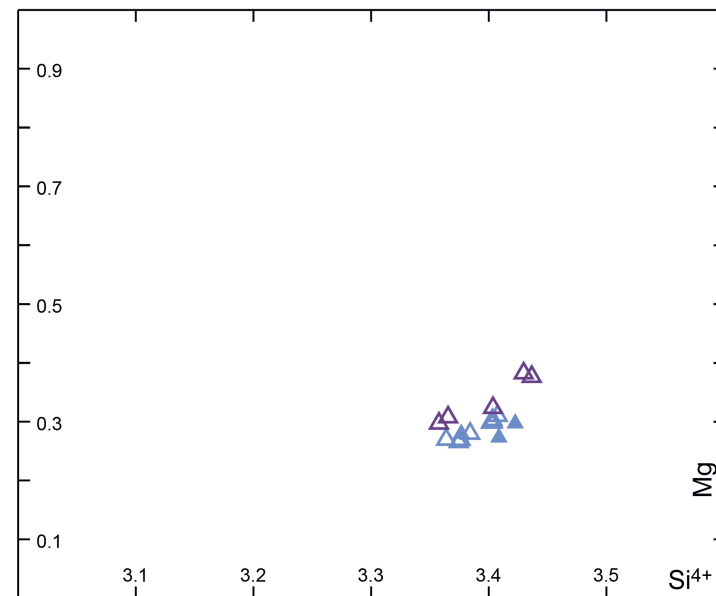
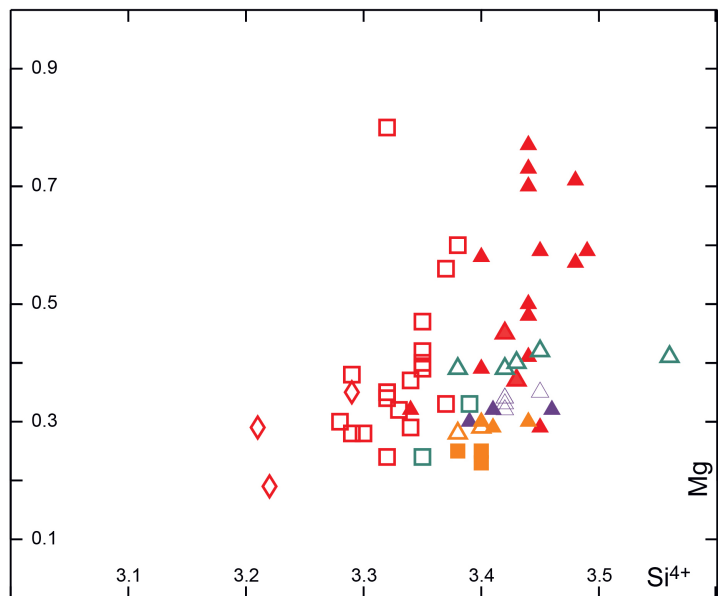
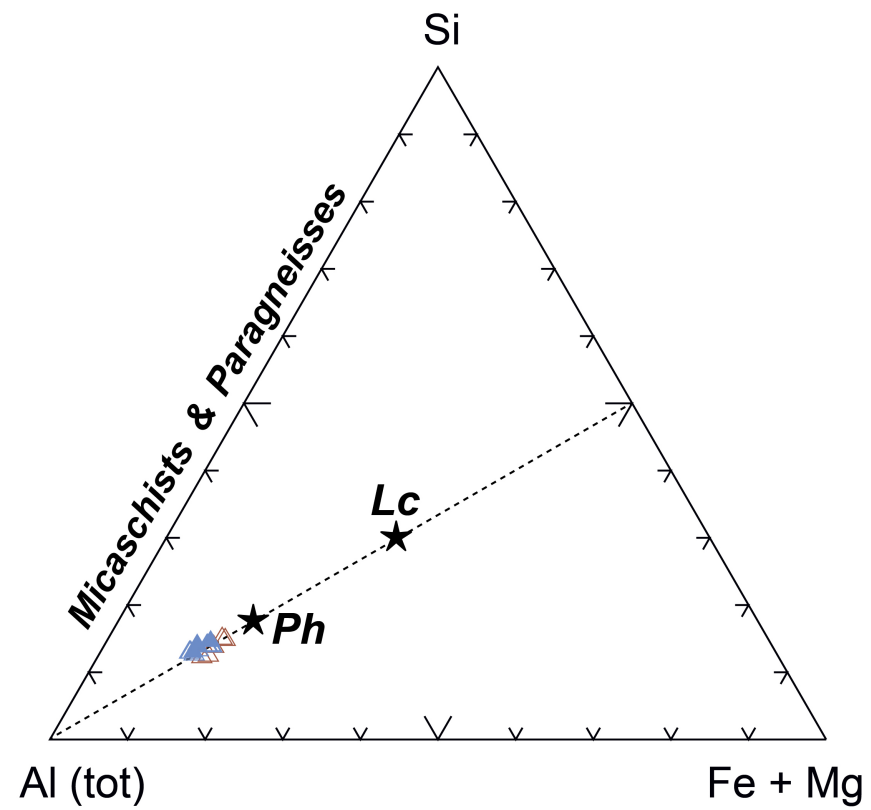
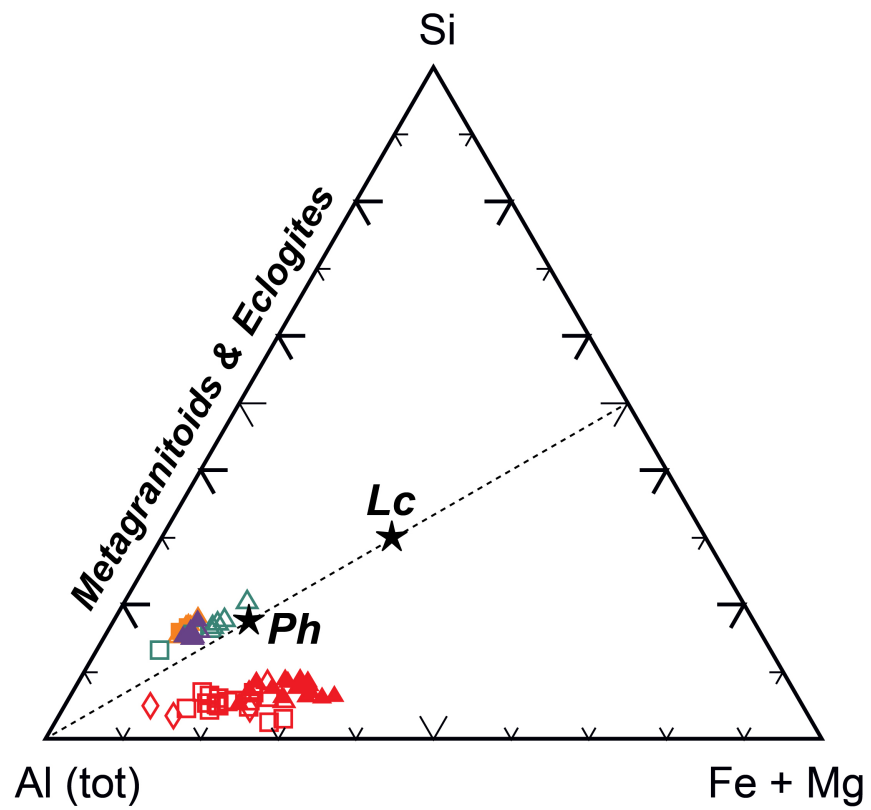


Fig. 14

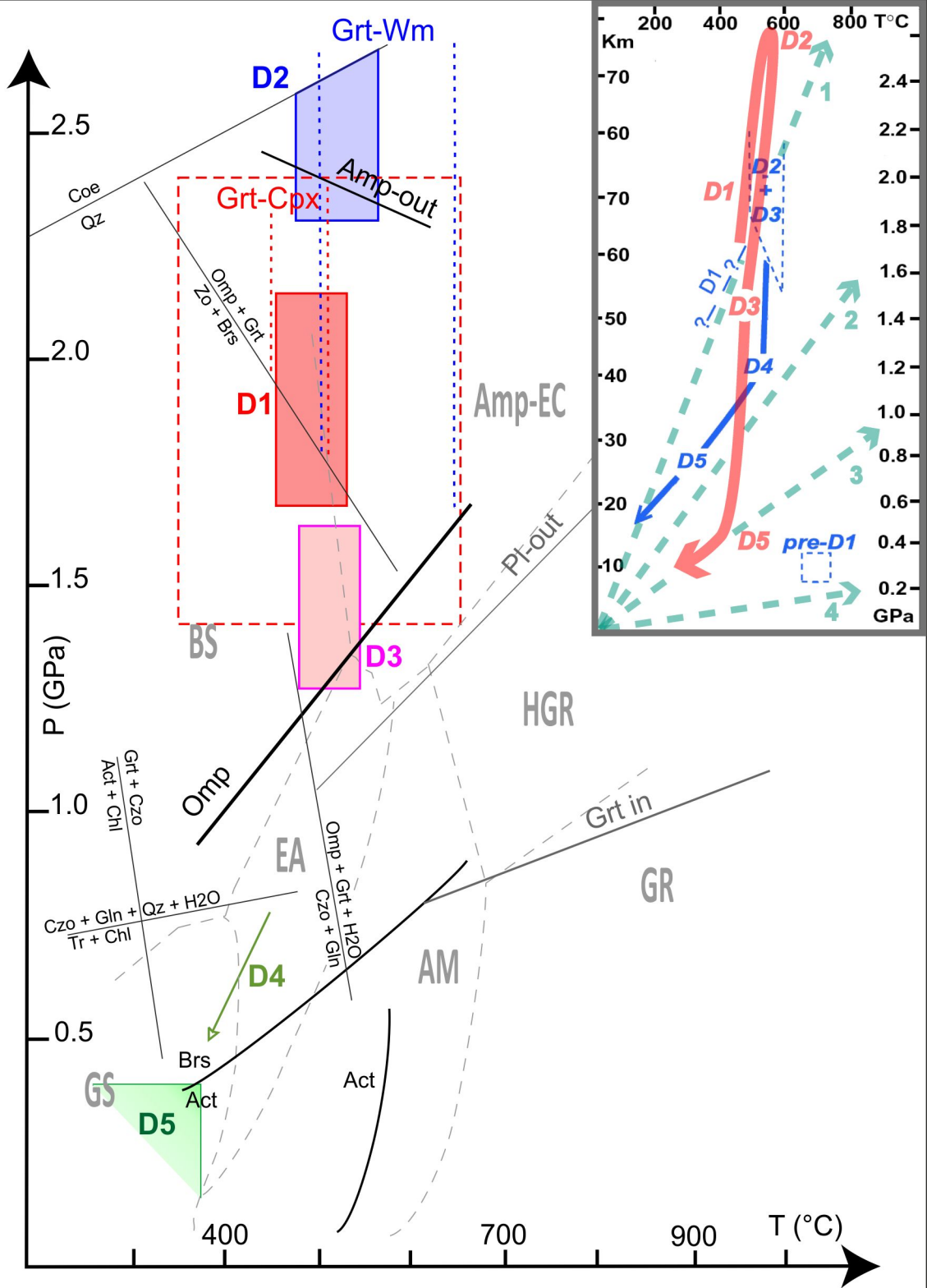


Fig. 15

Table 1

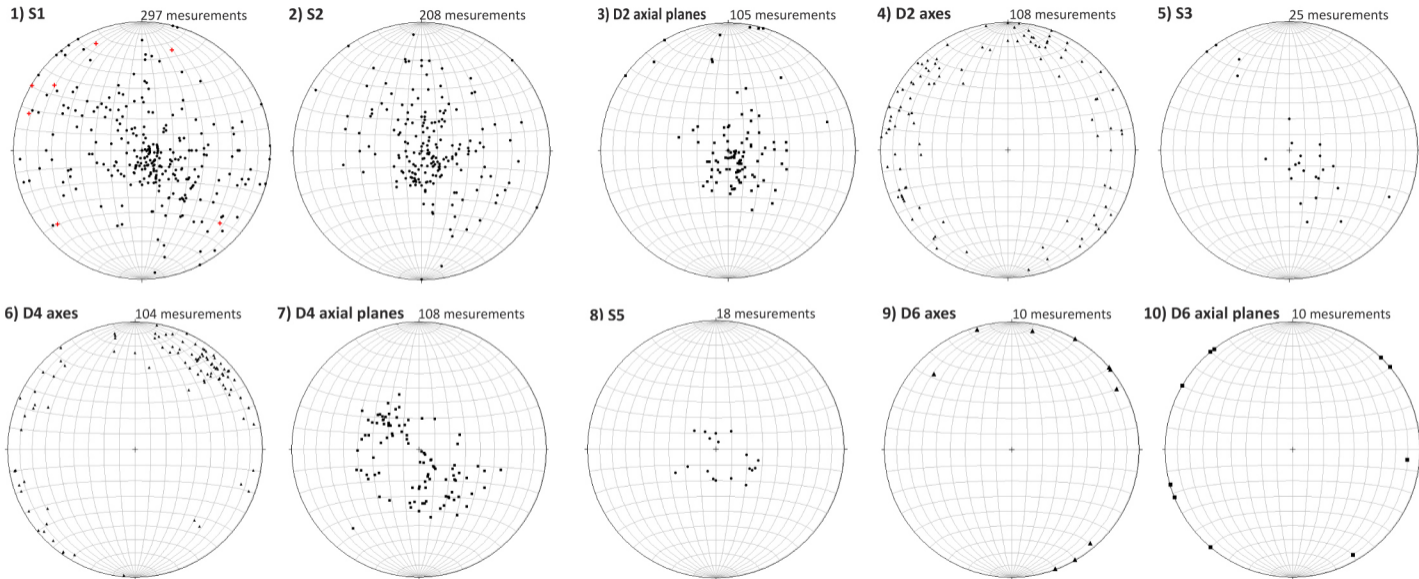


Table 2

Mineral Lithologic type	Amp						Ph					Na-Cpx					Grt								
	Micas.	Micas.	Qzdior.	Parag.	Eclog.	Eclog.	"green" Gran.	"green" Gran.	Qzdior.	"grey" Gran.	"grey" Gran.	Stage	"grey" Gran.	"green" Gran.	Eclog.	Parag.	Parag.	Parag.	Zoisit.	Mica.	Parag.	Mica.	Qzdior.		
	D1	D2	D3	D3	D4	D4	D1	D2	D3	D4	D5		D1 MD- HD	D1 LD	D2 MD- HD	D3 HD	D4	pre- Alp.	progr. D1	D1 MD- HD	D1 LD	D2	D3		
SiO2	58.13	56.65	54.52	53.00	54.14	50.65	SiO2	52.63	54.93	52.97	52.66	50.78	SiO2	57.25	58.66	57.29	48.06	50.85	SiO2	38.70	39.45	36.74	38.57	39.29	38.75
TiO2	0.01	0.00	0.11	0.08	0.08	0.09	TiO	1.06	0.44	0.28	0.72	0.67	TiO2	0.00	0.01	0.11	0.10	0.03	TiO	0.02	0.08	2.83	0.27	0.06	0.00
Al2O3	11.11	10.57	10.59	5.91	3.87	6.45	Cr2O3	0.08	0.04	0.00	0.05	0.07	Cr2O3	0.00	0.00	0.01	0.04	0.01	Cr2O3	0.00	0.00	0.00	0.05	0.00	0.07
Cr2O3	0.00	0.00	0.02	0.01	0.05	0.03	Al2O3	31.71	28.09	28.32	30.50	34.51	Al2O3	23.42	23.03	13.45	10.37	7.21	Al2O3	22.49	21.94	20.86	21.19	21.45	26.58
FeO	11.36	12.91	13.21	9.68	12.06	17.23	FeO	2.11	2.11	3.47	4.47	1.37	FeO	1.58	3.43	4.19	17.62	16.71	FeO	28.42	19.50	31.71	20.05	21.71	8.55
MnO	0.07	0.07	0.10	0.07	0.10	0.15	MnO	0.02	0.00	0.00	0.07	0.05	MnO	0.01	0.01	0.02	0.10	0.17	MnO	0.38	0.55	0.74	1.48	0.30	0.06
MgO	9.14	8.36	10.58	14.98	15.44	11.42	MgO	1.83	4.15	2.62	1.55	1.00	MgO	0.20	0.04	6.34	9.44	11.11	MgO	6.42	6.96	3.28	1.42	6.30	0.03
CaO	0.65	0.65	5.57	9.81	12.58	11.64	CaO	0.02	0.00	0.00	0.01	0.04	CaO	0.81	1.20	10.82	10.25	10.60	CaO	5.20	10.66	6.02	17.65	9.46	23.73
Na2O	6.96	6.95	4.79	2.25	0.56	1.15	K2O	10.81	0.42	0.67	10.76	10.69	Na2O	14.29	14.32	8.64	2.59	2.02	Na2O	0.00	0.02	0.02	0.08	0.01	0.01
K2O	0.04	0.02	0.15	0.14	0.18	0.54	Na2O	0.12	10.15	9.60	0.09	0.17	K2O	0.00	0.01	0.05	0.54	0.20	K2O	0.00	0.00	0.01	0.01	0.00	0.15
Si	8.03	7.97	7.49	7.54	7.62	7.26	Si	3.32	3.42	3.40	3.34	3.22	Si	1.99	1.99	2.00	3.63	3.86	Si	2.96	3.03	2.94	3.00	3.05	2.95
Ti	0.00	0.00	0.01	0.01	0.01	0.01	Ti	0.10	0.02	0.01	0.07	0.06	Ti	0.00	0.00	0.00	0.01	0.00	Ti	0.00	0.00	0.00	0.00	0.00	0.00
Al	1.81	1.75	1.71	0.99	0.64	1.09	Al	2.36	2.06	2.14	2.28	2.58	Al	0.95	0.91	0.55	0.69	0.48	Al	2.03	1.99	1.97	1.94	1.96	2.39
Cr	0.00	0.00	0.00	0.00	0.01	0.00	Cr	0.01	0.00	0.00	0.01	0.01	Cr	0.00	0.00	0.00	0.00	0.00	Cr	0.00	0.00	0.00	0.00	0.00	0.01
Fe3+	0.00	0.20	0.54	0.50	0.22	0.58	Fe3+	0.00	0.00	0.00	0.00	0.00	Fe3+	0.02	0.04	0.03	0.12	0.00	Fe3+	0.00	0.00	0.00	0.00	0.00	0.00
Fe2+	1.31	1.32	0.98	0.65	1.21	1.48	Fe2	0.22	0.00	0.04	0.47	0.15	Fe	0.02	0.06	0.09	0.56	0.53	Fe2	1.82	1.25	2.12	1.30	1.41	0.55
Mn	0.01	0.01	0.01	0.01	0.01	0.02	Mn	0.00	0.00	0.00	0.01	0.01	Mn	0.00	0.00	0.00	0.00	0.00	Mn	0.02	0.04	0.05	0.10	0.02	0.01
Mg	1.88	1.75	2.17	3.18	3.24	2.44	Mg	0.34	0.39	0.25	0.29	0.19	Mg	0.01	0.00	0.33	0.53	0.63	Mg	0.73	0.80	0.39	0.16	0.73	0.01
Ca	0.10	0.10	0.82	1.50	1.90	1.79	Ca	0.00	0.00	0.00	0.00	0.01	Ca	0.03	0.04	0.40	0.41	0.43	Ca	0.43	0.88	0.52	1.47	0.79	1.94
Na	1.86	1.90	1.28	0.62	0.15	0.32	Na	0.03	0.05	0.08	0.02	0.04	Na	0.96	0.94	0.58	0.09	0.07	Na	0.00	0.00	0.00	0.01	0.00	0.00
K	0.01	0.00	0.03	0.03	0.03	0.10	K.	0.87	0.81	0.79	0.87	0.87	K	0.00	0.00	0.00	0.01	0.00	K	0.00	0.00	0.00	0.00	0.00	0.01
Al(VI)	0.00	0.03	0.52	0.46	0.38	0.74	Al(VI)	1.37	1.48	1.55	1.32	1.56	Q	3.19	5.28	41.42	78.52	84.44	Alm	58.36	42.27	68.91	42.95	47.85	78.55
Al(IV)	1.81	1.72	1.20	0.53	0.26	0.35							Jd	94.53	90.94	55.67	15.12	17.18	Prp	23.50	26.90	12.71	5.41	24.76	21.88
Na(M4)	1.86	1.90	1.18	0.50	0.10	0.21							Ae	2.27	3.77	2.86	6.37	0.00	Grs	13.68	29.61	16.76	48.44	26.71	0.13
																			Sps	0.78	1.21	1.63	3.21	0.68	7.78
																			Adr	3.68	0.00	0.00	0.00	0.00	0.14

Table 3

Lithologic type	pre-Alpine	D1	D2	D3	D4	D5	D6
Grey-type metagranite	Bt+Aln+Zrn+Ap+Qz	Jd+Qz+Ph+Grt+ Zo+Rt	Omp+Acn+Qz+Ph+Pg+Grt+Gln+Czo+Rt	Qz+Ph+Pg+Brs+ Czo+Ttn	Qz+Ab+Wm+Act+ Ttn+Bt+Ep	Qz+Ab+Wm+Act+ Ttn+Bt+Ep+Fe-Ox	Ab+brown-Amp+ Wm+Adl
Metaquartz-diorite	Aln+Qz	Omp+Gln+Qz+Ph+Grt+Zo+Rt	Omp+Acn+Qz+Ph+Pg+Grt+Gln+Czo+Rt	Qz+Ph+Pg+Brs+Aug+ Mg-Chl+Czo+Ttn	Qz+Ab+Wm+Act+ Ttn+Bt+Ep	Qz+Ab+Wm+Act+ Ttn+Bt+Ep+Fe-Ox	-
Metaaplite	Bt+Aln+Zrn+Ap+Qz	Jd+Qz+Ph+Grt+ Zo+Rt	Omp+Acn+Qz+Ph+Pg+Grt+Gln+Czo+Rt	Qz+Ph+Pg+Brs+ Czo+Ttn	Qz+Ab+Wm+Act+ Ttn+Bt+Ep	Qz+Ab+Wm+Act+ Ttn+Bt+Ep+Fe-Ox	Ab+brown-Amp+ Wm+Adl
Metapegmatoid	Bt+Aln+Zrn+Ap+Qz	Jd±Omp+Qz+Ph+Grt+ Zo+Rt	Omp+Acn+Qz+Ph+Pg+Grt+Gln+Czo+Rt	Qz+Ph+Pg+Brs+ Czo+Ttn	Qz+Ab+Wm+Act+ Ttn+Bt+Ep	Qz+Ab+Wm+Act+ Ttn+Bt+Ep+Fe-Ox	Ab+brown-Amp+ Wm+Adl
Green-type metagranitoid	Zrn+Aln	Omp±Jd+Qz+Ph+Grt+ Gln+Zo+Rt	Omp+Acn+Qz+Ph+Pg+Grt+Gln+Czo+Rt	Qz+Ph+Pg+Brs+ Czo+Ttn	Qz+Ab+Wm+Act+ Ttn+Bt+Ep	Qz+Ab+Wm+Act+ Ttn+Bt+Ep+Fe-Ox	-
Leucocratic metagranitoid	-	Ph+Gln+Zo+Rt	Ph+Gln	Qz+Ph+Pg+Brs+ Czo+Ttn	Qz+Ab+Wm+Act+ Ttn+Bt+Ep	Qz+Ab+Wm+Act+ Ttn+Bt+Ep+Fe-Ox	-
Eclogite	-	Omp+Grt+Gln+Ph+ Zo+Rt	Omp+Grt+Ph+Pg+ Rt+Zo	Qz+Ph+Pg+Brs+ Czo+Ttn+Aug	Qz+Ab+Wm+Act+ Ttn+Bt+Ep+Di-Cpx	Qz+Ab+Wm+Act+ Ttn+Bt+Ep+Fe-Ox	-
Paragneiss	Grt+Qz+Rt+Aln+Ap	Omp+Ph+Grt+Qz+ Gln+Zo+Rt	Omp+Ph+Pg+Grt+ Qz+Gln+Czo+Rt	Qz+Ph+Pg+Brs+ Czo+Ttn	Qz+Ab+Wm+Act+ Ttn+Bt+Ep+Di-Cpx	Qz+Ab+Wm+Act+ Ttn+Bt+Ep+Fe-Ox	-
Micaschist	Grt+Qz+Rt+Ap	Omp±Jd+Qz+Ph+Grt+ Gln+Zo+Rt	Qz+Ph+Pg+Omp±Jd+ Grt+Gln+Zo±Czo	Qz+Ph+Pg+Brs+ Czo+Ttn	Qz+Ab+Wm+Act+ Ttn+Bt+Ep+Adl	Qz+Ab+Wm+Act+ Ttn+Bt+Ep+Fe-Ox	-
Porphyric gneiss	Mc	Qz+Ph+Mc+Gln+ Zo+Rt	Qz+Ph+Gln+Czo+Rt	Qz+Ph+Pg+Brs+ Czo+Ttn	Qz+Ab+Wm+Act+ Ttn+Bt+Ep+Adl	Qz+Ab+Wm+Act+ Ttn+Bt+Ep+Fe-Ox	-
Glaucophanite	-	Gln+Ph+Zo+Rt	Omp+Grt+Ph+ Czo+Qz+Rt	Qz+Ph+Pg+Brs+ Czo+Ttn	Qz+Ab+Wm+Act+ Ttn+Bt+Ep	Qz+Ab+Wm+Act+ Ttn+Bt+Ep+Fe-Ox	-
Zoisitite	Aln	Grt+Zo+Ph+Omp+ Gln+Rt	Qz+Czo+Ph+Gln+Rt	Qz+Ph+Pg+Brs+ Czo+Ttn	Qz+Ab+Wm+Act+ Ttn+Bt+Ep	Qz+Ab+Wm+Act+ Ttn+Bt+Ep+Fe-Ox	-
Qz-bearing vein	-	Ph+Omp+Qz+Grt+ Gln+Zo+Rt	Qz+Grt+Omp+Ph+ Gln+Czo+Rt	Qz+Ph+Pg+Brs+ Czo+Ttn	Qz+Ab+Wm+Act+ Ttn+Bt+Ep	Qz+Ab+Wm+Act+ Ttn+Bt+Ep+Fe-Ox	-

Chapter 4

Structural mapping of the Ivazio complex, multiscale analysis and mineral chemistry

4.1 Previous works on the Ivazio metagabbroic Complex

The Ivazio metagabbroic Complex is primarily known for the presence of Lws-bearing mineral assemblages occurring in some volumes. Lws-bearing rocks are the most acknowledged markers of a severely depressed thermal regime due to a very cold subduction zone dynamics (Cloos, 1982) as generally occurs during oceanic subduction: Lws generally characterises rocks of subducted oceanic lithosphere (Tsuji-mori et al., 2006; Cetinkaplan et al., 2008; Ghent et al., 2009) and it is rarely reported in the continental crust (Sesia-Lanzo Zone - Italy: Compagnoni et al., 1977; Pognante, 1989b; Zucali et al., 2004; Dabie - China: Li et al., 2004; Calabria - Southern Italy: Piccarreta, 1981; Turkey: Okay, 2002; Okay and Whitney, 2010). Therefore, discrimination between prograde and retrograde Lws crystallization is crucial to individuate highly depressed geothermal gradients and their extent during the subduction process. Analysis of deformation-metamorphism relationships of lithospheric portions that underwent Alpine subduction is therefore a powerful tool to infer paleo-thermal gradients characterizing burial and exhumation stages during Alpine subduction.

Lws occurrence in the southern portion of the SLZ is known since Caron and Saliot (1969) and was interpreted as retrograde to the HP climax minerals in all the units composing the SLZ (in the EMC: Caron and Saliot, 1969; Compagnoni et al., 1977; Pognante et al., 1980, 1988, 1989; Spalla and Zulbati, 2003; Zucali et al., 2004; in the IIDK: Pognante et al., 1988; in the GMC: Pognante et al., 1987). In the EMC it has been described in metabasics (Pognante et al., 1980; Pognante et al., 1987; Spalla and Zulbati, 2003; Zucali et al., 2004; Zucali and Spalla, 2011) and in marbles (Castelli, 1987). Pseudomorphosed Lws also occurs in some micaschists of the GMC and in mylonites of the IIDK (Pognante et al., 1987 and 1988).

The Ivazio Complex includes various types of Amp-bearing eclogites, Lws-bearing eclogites and scarce ultramafics that consist of layers of metapyroxenites and Atg-serpentinites; primary magmatic layering has also been recognized (Pognante et al., 1980; Zucali et al., 2004; Zucali and Spalla, 2011). The rock-types of the Ivazio Complex are comprised within micaschist and metagranitoids belonging to the EMC and have been deformed together during eclogite- to greenschist-facies deformation stages. The Alpine metamorphic imprint is penetrative, whereas the pre-Alpine assemblages are scarce. The metagabbro protoliths have been dated by Rubatto (1998) at 355 ± 9 Ma and the Alpine eclogitic imprint in the surrounding EMC of the lower Aosta Valley have been dated by Rubatto (1999) at 65 ± 3 Ma.

Pognante et al. (1980) related the formation of porphyroblastic Lws in the Ivazio Complex to decreasing T, infiltration of H₂O-rich fluids, conductive-cooling during coupling-decoupling with other units in depth during

the Alpine exhumation geodynamic process (Pognante et al., 1989); he also individuated a prograde (heating) path prior to the Alpine climax in scattered relicts of Gln-bearing foliation within the Grt.

Zucali et al. (2004) and Zuacli & Spalla (2011) recognized three deformation phases associated to the Alpine history and firstly related the Lws formation to the prograde path in the SLZ, individuating: 1) in the country rocks an older S1 foliation is preserved within as mm-thick relicts in rootless D2 folds, with an S2 axial plane foliation, parallel to the margin of the complex at the Km-scale; both foliations are marked by eclogite-facies minerals, mainly represented by Ph, Amp and Omp SPO with associated growth of Grt; finally a local sub-vertical gentle D3 fold system overprinting S1 and S2 formed. 2) In the metagabbros, the earliest foliation (S1) is parallel to a cm- to m-scale compositional layering, of igneous origin, now corresponding to alternate eclogite types with ultramafic and amphibole-bearing schists and by SPO of Amp, Wm-rich and Zo-rich layers. D2 folds of m- to 10m- size, successively develop; they have S2 axial plane foliations marked by the growth of Amp, Ep, Omp, Wm, Srp and Chl SPO and Grt, while randomly oriented cm-sized Omp and Grt grew in syn-D2 poorly deformed volumes; a last sub-vertical gentle D3 fold system is not associated with the development of a new planar fabric. Widespread fracturing occurs cutting across the S1 foliation in metabasics with different sealing minerals, as Omp and Grt. Gln and Ep veins cut across the S1 and S2 foliations. The metamorphic-deformation history may be zoomed into more detail in some volumes of the eclogitised gabbros (Fig. 4.1): S1 foliation imprint has been subdivided microstructurally into stages S1a, b and c) and S2 into two stages (S2a and S2b). Assemblages' development related to these stages is as follows: Lws grew after stage S1c (growth event post-D1a), and was replaced by Ky and Zo before foliation stage S2a (retrograde growth stage post-D1b). Estimated thermo-baric conditions are: P of 0.5-1.3 GPa and T of 300-500 °C for S1a; P of 1.15-1.8 GPa and T of 470-550 °C for S1b-c; P of 1.8 GPa and T of 520-600°C for post-D1a; P >1.5 GPa and T > 580°C for post-D1b; P < 1.8 GPa and T of 500-600°C for S2a; P of 0.5-1.3 GPa and T 300-500°C for S2b.

This PTtd path of the Ivozio Complex is clearly of clockwise type, documenting a heating between the P-peak conditions and the end of the retrogradation, whereas in the southern SLZ, the retrograde evolution, conversely to the northern SLZ, indicates a counterclockwise path (e.g. Pognante, 1989).

In most of the Lws occurrences in other localities of the SLZ the relationships between metamorphic mineral growth and structures are poorly known, suggesting that its retrograde or prograde nature may only be revealed through a detailed petro-structural field-mapping able to manifest the deformation vs. mineral-growths, partitioned in time and space.

Therefore the reconstruction of PTdt, supported by detailed field mapping, involving Lws-bearing metabasic rocks may help in the definition of a coherent metamorphic evolution during a time interval (i.e. the tectonometamorphic units, Spalla et al., 2005) and confronting results from different location within the EMC should provide data on different evolution and dimension of elements composing the SLZ, which most probably derives from multiple mixing of tectonic elements within the subduction wedge before collisional stacking, in accord with results of numerical simulation (Roda et al., 2010; 2012).

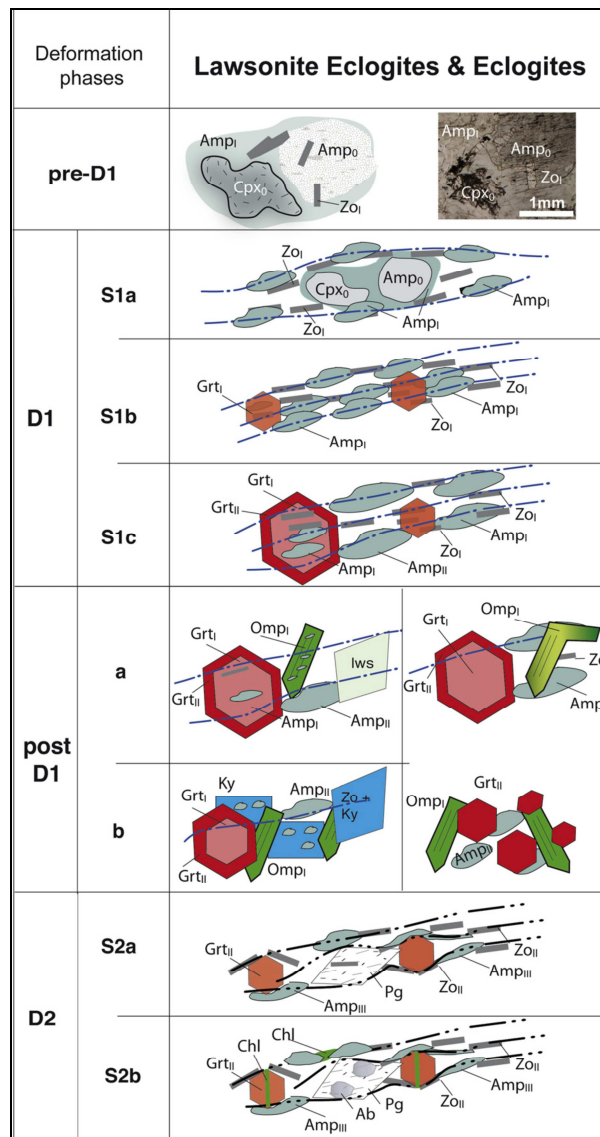


Fig. 4.1: Schematic view of the microstructural relationships inferred from microstructural analysis for lawsonite-bearing eclogites and eclogites from Zucali and Spalla (2011).

4.2 Petro-structural mapping of the Ivazio metagabbroic Complex and country rocks

4.2.1 Field work for the petro-structural map of the Ivazio metagabbroic Complex

The results of the 1:20 to 1:100 scale survey of the outcrop contours and structural elements have been represented on the petro-structural map at the 1:1.000 scale and on enlargements at scale 1:20, 1:50, 1:100 and 1:200 of the most significant points of the structure. A petro-structural map is a graphical representation describing the correlation of the structural fabric and metamorphic assemblages in the subducted-exhumed polyphased tectonites and as a consequence, an effort to distinguish the pre-Alpine protoliths of the metabasites, on a more convincing base. The lithostratigraphic configuration of the Ivazio metagabbroics is therefore deduced and the main contact with their country rocks has been represented on a drift and solid

map (in which outcropping rocks are separated by drift cover). The full pattern of the superposed structures has been reported on the cross-section.

4.2.1.1 Structural elements

Mesoscale observation allows to recognize numerous structural elements, such as foliations, axes, axial planes, shear zones and veins with the related time scale distinguished on the basis of their overprinting relationships and of the metamorphic minerals marking successive fabrics, as specified. The mineralogical support of the new grain-scale fabrics is the primary reference to select mineral compatibilities marking each successive stage (Turner and Weiss, 1963; Hobbs et al., 1976; Williams, 1985; Spalla et al., 2000; Passchier and Trouw, 2005; Spalla et al., 2005). This representation technique conveys an evolutionary visualization in a complex structural framework together with an immediate perception of the paleo-thermal regimes that characterize the deformation history.

The orientation data have been elaborated to generate equal area Schmidt diagrams grouped according to their relative chronology. Structural elements are:

- Grt, Omp, Gln and Ep veins
- S1 foliation, D1 axial planes
- S2 foliation, D2 axes and axial planes
- D3 axes and axial planes
- S4 foliation
- D5 axes and axial planes, shear zones and fibrous veins

Rocks constituting the two main lithologic types, amphibole- and zoisite-bearing eclogite, are characterized by the presence of numerous vein types:

- Grt-bearing veins are defined by the alignment of pinkish, poikiloblastic, fine- to coarse-grained (up to 2cm wide) Grt, developed within the embedding rocks. They have a lateral continuity of maximum 2m;
- Omp-bearing veins are fractures, up to 10cm wide, filled by coarse-grained Omp, Ph, Gln and Qtz. They have a lateral continuity of maximum 10m;
- Gln-bearing veins have a lateral continuity of 10 to 20m and are mainly zones defined by the substitution of fine-grained Gln in the salbande of the embedding rocks. Nonetheless they may also have a syntactical filling of medium- to fine-grained Gln, Wm and Zo of the fracture generating the vein;
- Zo-bearing veins are up to 1cm wide fractures filled by fine-grained Zo or Czo, and have a lateral continuity of maximum 2m.

The S1 foliation is marked by blue-Amp, Wm, Zo/Ep and Grt trails and is parallel to the up to 10-cm-thick compositional layering. It is the main foliation observed within the Ivazio Complex and it is developed in all the lithologic types, even though it was possible to measure only a handful of data, on 10-cm wide folds, in the field; most of the D1 100-m wide folds have been reconstructed drawing the lithologic boundaries between the different metabasic rocks of the Ivazio Complex.

Isoclinal similar-shaped D2 folds with 10m wavelength are widespread in all the lithologic types and a localized S2 mm- to cm-thick foliation marked by blue-Amp, Omp, Wm, Zo/Ep and Grt is also present.

D3 gentle folds with 10 to 20m wavelength occur in all the Ivozio Complex; no new mineral assemblages develop during this deformation stage, but only corona type recrystallization of blue-green Amp, Wm and Zo is observed related to these structures.

During the D4 deformation stage m-thick shear zones occur with the development of a new S4 mm-thick foliation marked by Gln, Ep and Wm.

D5 fold system consists of gentle to close folds with 10m wavelength occurring in all the Ivozio Complex; no new mineral assemblages develop associated to this deformation stage, but only corona type replacement, such as Ab on Cpx or Chl on Grt, occurs.

M-thick shear zones related to the last deformation stage (D5) occur with the development of a new S5 mm-thick foliation marked by Chl, Act, Ab, Wm and Ep.

4.2.1.2 Lithologic types of the eclogitic micaschist complex

The NW-SE section of the Valle d'Aosta comprised between Pont Saint Martin and Ivrea cuts at right angle the Sesia-Lanzo Zone and its tectonic boundaries, the NE-SW oriented Austroalpine Front and the Canavese Line. Ivozio is about halfway between Pont Saint Martin and Ivrea on the right side of the Valle d'Aosta within the EMC of the SLZ.

In the area surrounding the metabasics of the Ivozio Complex, the EMC mainly occur as micaschists with minor metagranitoids in the form of ten-meter thick layers (Fig. 4.2).

Micaschists are fine-grained rocks composed of Wm (30%), Qz (30%), blue-Amp (10%), Omp/Jd (10%), Grt (15%) and Zo (5%). White mica is gray with the typical metallic sheen and may have a grain-size up to 5mm; Quartz is up to 1mm and constitutes lens-shaped domains of 2-10mm length; Amphiboles are fine-grained and vary from dark-blue typical of Ca-Na Amp to pale violet typical of Gln; Clinopyroxenes are fine-grained and have color variations from pale- to dark-green (Omp or Jd); Garnets are pinkish and very fine-grained, < 1mm in diameter; Zoisite is very fine-grained. The modal composition of the EMC is heterogeneous: Qz varies from 15% to 40%, Wm from 20% to 40%, and blue-Amp from 5% to 20%. Locally, micaschists present a diffuse crystallization of fine-grained white Ab, greenish Chl and yellowish Ep on the previous mineral assemblage, substituting mostly Wm and Cpx. Rt, Ttn, Ksp and Ap may occur as accessories.

Micaschists always present mm-thick continuous foliation marked by Wm, blue-Amp, Omp/Jd and Zo SPO and lens-shaped Qz-rich domains. Often, relict microlithons in the foliation show a previous foliation, mainly evidenced by Wm orientation transposed along the newer foliation.

Metagranitoids are 1- to 10-m-thick layers comprised within micaschists. They are medium to coarse-grained porphyric rocks composed by Qz (40%), Wm (30%) and Jd (30%): Qz has a grain-size up to 1cm and constitutes lens- and tabular-shaped domains up to 3cm wide; Wm is pale-gray with the typical metallic sheen and has a grain-size up to 2cm; Jd is pale-green or whitish and may have a very large-size, up to 8cm, with numerous Qz and Wm inclusions. Locally, fine-grained white Ab and yellowish Ep develops in metagranitoids substituting Jd. Gln, Grt, Rt, Ttn and Chl may occur as accessories.

Metagranitoids always present a discontinuous foliation marked by Wm and Jd SPO and by the disposition of Qz domains in poor deformed domains, whereas in deformed domains, near the boundaries with micaschists and in thin layers, the foliation has 1cm spacing and wraps around Jd and lens-shaped Qz domains.



Fig. 4.2: micaschists interlayered with 5m-thick metagranitoids and the S2 mineral-scale foliation, which is more prominent in micaschists.

4.2.1.3 Lithologic types of the Ivozio metagabbroic complex

Rocks constituting the Ivozio Complex are derived from a gabbroic complex presenting numerous primary igneous compositional internal variations. These variations influence the evolution of mineral associations forming in layers of different composition, but some variations in the mineral associations are due to differentiation during the metamorphic evolution and the intrusive layering is not always preserved. Therefore the distinction and grouping of lithologic types in the metabasics of the Ivozio Complex is of fundamental importance for a plausible reconstruction of the primary igneous assessment.

On this ground, field distinctions within metabasics of the Ivozio Complex have been assessed on the basis of the abundance of only some of the mineral components: blue-green Amp, dark-green Amp, Di, Atg, Zo, Ep, Grt, Chl and Qz. This is because in low deformed portions of metabasics the modal abundance of these minerals is clearly related to the primary compositional variation between and within different layers. Omphacite and white mica, although being major mineral components in the metabasics and presenting significant modal variations, have been excluded from the mineral components considered for the distinction between lithologic types as their presence is already implied in the name “eclogite” regardless their modal abundance and considered only for distinctions within each individual lithologic type.

Six lithologic types have been distinguished within the Ivozio metagabbroic Complex:

1. Amphibole-bearing eclogite
2. Zoisite-bearing eclogite
3. Amphibole-epidote-bearing eclogite
4. Quarz-rich eclogite
5. Ultramafic rocks
6. Chlorite-amphibolite

4.2.1.3.1 Amphibole-bearing eclogite

The Amphibole-bearing eclogite lithologic type comprises all the rocks constituted by at least 30% in volume of blue-green Amp. They are medium- to fine-grained blue-green Amp and Grt eclogites, constituted by blue-green Amp (40%), Grt (30%), Omp (20%), Wm (5%) and Zo (5%). Chl, Ep, Rt, Ttn, Qz and Ab may occur as accessories. Rare relict tabular-shaped domains, now substituted by Zo + Pg aggregates, occur within Amphibole-bearing eclogite and are interpreted as former lawsonite.

In the Amphibole-bearing eclogite three different layers are recognized (Fig. 3A and Fig. 3B):

- a) amphibole rich layer;
- b) garnet rich layer;
- c) omphacite rich layer.

Interlayered bands of 3- to 20-cm-thick Amp and Grt layers are recognizable in almost all the Amphibole-bearing eclogite volume. This layering has been transposed parallel to D1 axial planes and has been mapped as S1 within Amphibole-bearing eclogite. The boundary between two layers can be transitional or sharp (Fig. 3B); locally the boundary is marked by mm-thick Ep-rich layers. As pointed out by the presence of gradual transition between two layers of different composition, Amp and Grt interlayered bands are interpretable as reflecting an igneous layering.

Where the layering is clearly visible Grt can form trails parallel to the boundaries of the layer. At the meso-scale, Amp and Grt layers do not have any appreciable internal fabric orientation, with randomly oriented Omp and Amp crystals scattered through each layer.

- a) Amphibole rich layers are composed by medium- to fine-grained blue/blue-green Amp (50-70%), Grt (15-30%) and Omp (10-30%). Amphibole has blue rims around blue-green colored cores and is fine-grained; locally some crystals are 5mm-sized. Garnet is pinkish, and fine-grained with rare poikiloblastic crystals up to 1-cm in length. Green colored Omphacite is mainly found as medium-grained crystals, up to 1cm length, and as fine-grained, 1 to 3mm long hollow acicular crystals.
- b) Garnet rich layers are composed by medium- to fine-grained Grt (60-80%), blue-green Amp (40-20%) and Omp (5%). Garnet is pinkish, medium-grained, and with some poikiloblastic crystals up to 1-cm wide. Amphibole is blue-green colored and fine-grained; rare fine-grained Omp, 1-3mm long hollow acicular crystal occur here as well.
- c) Omphacite rich layers are locally interposed between amphibole and garnet layers. However the scarcity of well-exposed omphacite layers does not allow interpret them as representing primary igneous features (Fig. 3A).

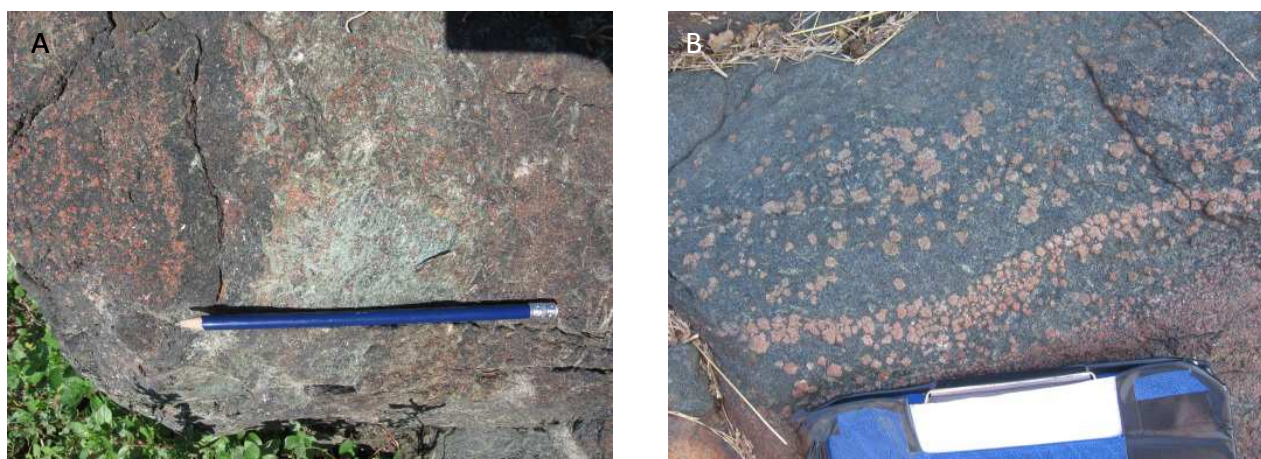


Fig. 4.3: (A) Amp, Grt and Omp alternating layers in Amphibole-bearing eclogite with cm-thickness; (B) gradual transition between Amp and Grt layers in Amphibole-bearing eclogite, evidenced by progressive impoverishment of fine-to medium grained Grt trails.

These layers are composed of medium- to coarse-grained omphacite (40-60%), amphibole (20-30%), phengite (15-25%) and garnet (5%). Omphacite is coarse-grained, up to 1cm, and has emerald green color. Amphibole has blue-green color, is fine-grained and fills the interstices between omphacite and phengite. Phengite is

medium- to coarse-grained, with grain-size up to 1cm, and is pale-gray with the typical metallic sheen. Rare pinkish, fine-grained, < 2mm garnet crystals occur in these layers. Omphacite layers do not present an appreciable internal fabric orientation at the meso-scale, with randomly oriented Omphacite and Phengite crystals.

4.2.1.3.2 Zoisite-bearing eclogite

The Zoisite-bearing eclogite lithologic type comprises all the rocks constituted by at least 30% in volume of white Zo. They are medium- to coarse-grained Zo and blue Amp eclogites, constituted by Zo (30-60%), blue Amp (15-35%), Wm (15-25%), Grt (10-20%), Omp (10-20%) and Qz (5-15%). Zoisite is medium- to coarse-grained, with up to 1cm, tabular-shaped, white crystals. Blue amphibole is fine- to medium-grained. White mica is medium-grained pale-gray phengite and silver white paragonite. Garnet is reddish and medium- to coarse-grained, with grain size up to 2cm. Omphacite is coarse grained emerald green crystals, locally up to 5cm in length. Quartz is fine-grained and occurs within mm- to cm-thick lens-shaped domains. Rare portions of Zoisite-bearing eclogite present large blast of Grt, with dimension up to 10 cm, and a large amount of white mica, up to 35% in volume. Chlorite, epidote, rutile, titanite and albite may occur as accessories.

Zoisite-bearing eclogite always presents textural relicts of Lawsonite, as tabular-shaped coarse-grained domains, up to 3 cm length consisting of whitish aggregates of Zo + Pg. At times rare bluish crystals of Ky, testifying the previous substitution of Ky on Lws, are found in the core of these domains.

Zoisite-bearing eclogite have cm-spaced discontinuous S1 foliation marked by medium- to coarse-grained Zo, Wm and blue-Amp shape preferred orientation (SPO, Fig. 4.4A). Also lawsonite pseudomorphs are oriented parallel to the S1. Minor volumes of Zoisite-bearing eclogite have mm-spaced discontinuous to continuous S2 foliation marked by fine-grained Omp, Wm and Zo wrapping around lawsonite (Fig. 4.4B) tabular-shaped pseudomorphed porphyroblasts and around large-size (3-10cm) omphacite and garnet porphyroblasts.

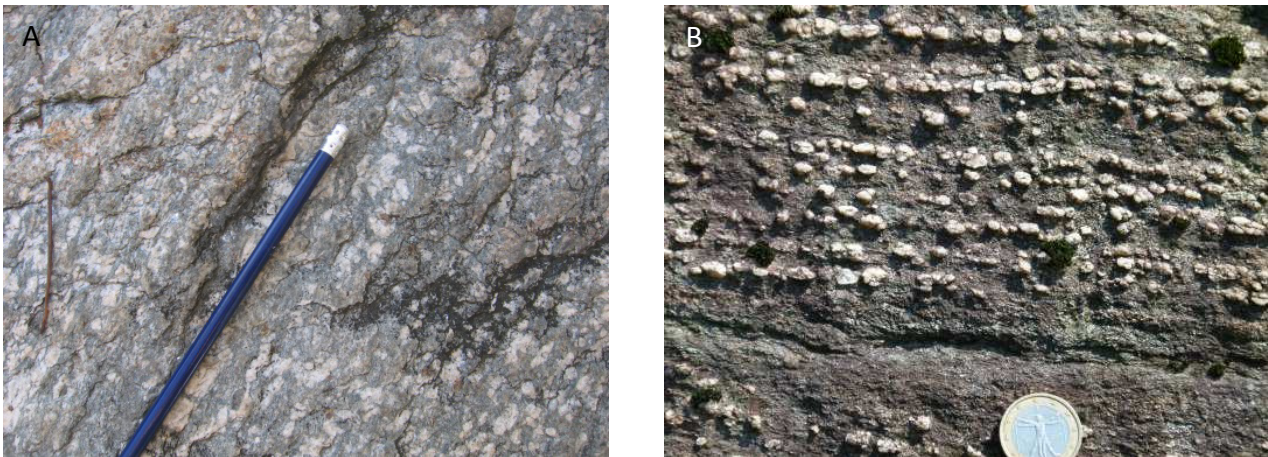


Fig. 4.4: (A) cm-spaced S1 foliation marked by medium-grained Zo, white mica and blue-Amp SPO within Zoisite-bearing eclogite; (B) Lws medium-grained textural relicts comprised in Zoisite-bearing eclogite affected by S2 mm-thick foliation.

4.2.1.3.3 Amphibole-epidote-bearing eclogite

The amphibole and epidote-eclogite lithologic type comprises rock volumes constituted by 5- to 15-cm-thick alternations of dark-green Amp and Ep layers (Fig. 4.5A). This layering has been transposed parallel to D1 axial plane and has been mapped as S1, as in Amphibole-bearing eclogite.

Dark-green Amp layers are composed by medium- to fine-grained dark-green Amp (70-90%), Grt (10-20%) and Omp (5-15%): dark-green amphibole is medium- to fine-grained, with up to 5mm crystals; garnet is pinkish and

medium- to coarse-grained, up to 2cm in diameter; omphacite is green and medium-grained. Wm, Chl, Ep, Rt, Ttn, Qz and Ab may occur as accessories.

Epidote - amphibole layers are composed of fine-grained Ep (60-70%), dark-green Amp (20-30%) and Chl (5-10%). Epidote is yellow-green and fine grained; dark-green amphibole is fine-grained; chlorite is greenish and very fine-grained. Omp, Grt, Wm, Rt, Ttn, Qz and Ab may occur as accessories.

Where layering is clearly visible, minor mm-thick layers of dark-green Amphibole are visible within Epidote layers and vice versa. Omphacite has the same randomly oriented texture as in the other lithologic types. Dark-green Amp, Omp and Grt trails mark S2 foliation in D2 high strain domains (Fig. 4.5B).

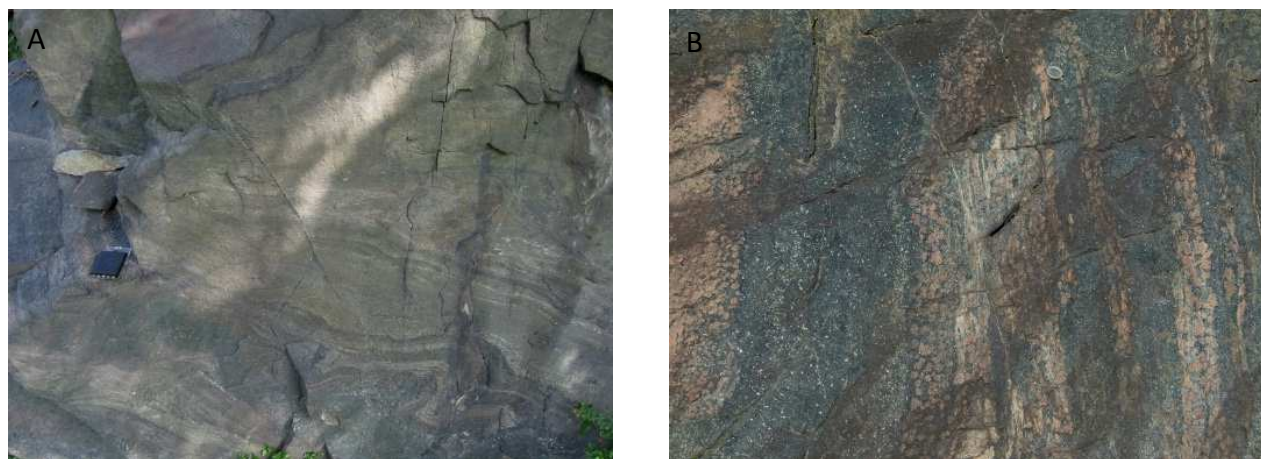


Fig. 4.5: (A) Amp and Ep 10-cm-thick layers of the amphibole-epidote-bearing eclogite parallel to S1 foliation bended by D2 folds; (B) cm-thick S2 foliation within amphibole-epidote-bearing eclogite underlined by Grt trails, composed of Grt-bearing veins and syn-D2 Grt crystals.

4.2.1.3.4 Zoisite- and quartz-eclogite

The Zoisite- and quartz-eclogite lithologic type comprises all the rocks constituted by at least 30% in volume of both Zo and Qz (Fig. 4.6A); they are coarse-grained Zo and Qz eclogites constituted by Zo (30-50%), Qz (30-50%), Omp (20-40%) and Wm (5-15%). Zoisite is coarse-grained, with tabular-shaped, up to 3cm, white crystals; quartz is medium- to fine-grained and occurs within cm-thick lens-shaped domains; Omp is emerald green and coarse-grained, locally up to 5cm in length; Wm is pale-gray. Blue Amp, Grt, Chl, Ep, Rt, Ttn and Ab may occur as accessories.

Zoisite- and quartz-eclogite mainly shows a 5-cm-spaced discontinuous S1 foliation marked by coarse-grained Zo and Wm SPO, and by lens-shaped Qz domains. Minor volumes have cm-spaced discontinuous S2 foliation marked by medium- to fine-grained Zo and Wm wrapping around large omphacite (3-5cm) porphyroblasts and around quartz lens-shaped domains (Fig. 4.6B).

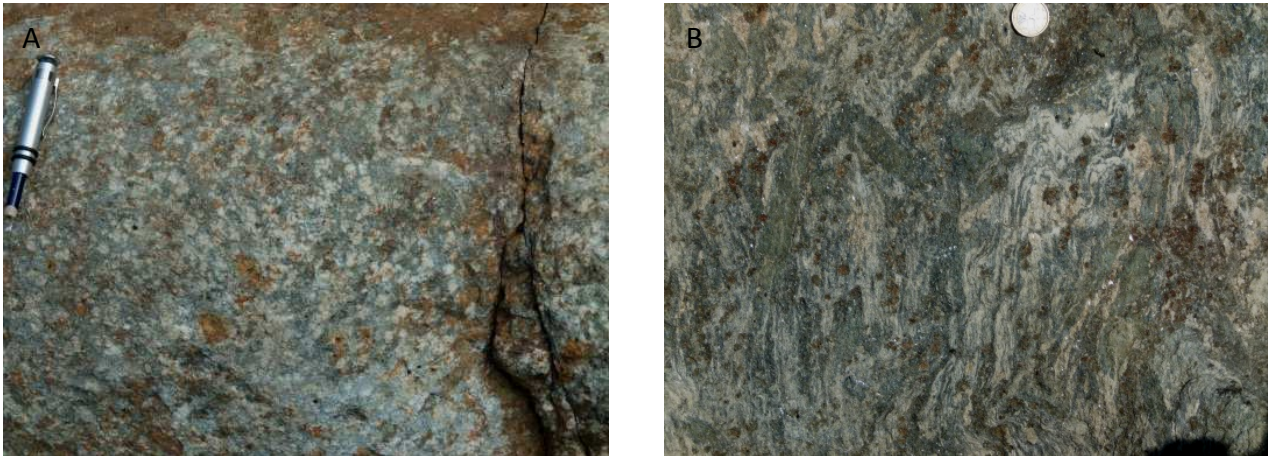


Fig. 4.6: Poorly deformed syn-D1 and syn-D2 volume of zoisite- and quartz-eclogite; (B) S2 mm-thick foliation in zoisite- and quartz-eclogite marked by fine-grained Zo, Wm and Omp, with large cm-thick syn/post-D2 Omp crystals crenulated during D3 deformation event.

4.2.1.3.5 Ultramafic rocks

The ultramafic rocks lithologic types comprise:

- Atg-serpentinites
- Metapyroxenites

Constituting 1 to 5 m-thick layers within the eclogites (Fig. 4.7A). These rocks do not contain garnet.

Atg-serpentinites (Fig. 4.7B) are rocks constituted by fine-grained Atg (60-70%), Ctl (10-20%), Cb (10-20%) and Mt (5-10%): Atg is dark-green and fine-grained; white fibrous Ctl fills fracture of the Atg-serpentinites; Cb is red and fine-grained constituting cm-sized domains; Mt is very fine grained, crystal size < 1mm, and dispersed in the Atg-serpentinite volume. Tr, Mg-Chl and Di may occur as accessories. Atg-serpentinites always show mm-thick foliation marked by medium-grained Atg, Chl and Tr SPO. This foliation cannot be geometrically related to previously described structures for lack of significant outcrops.

Metapyroxenites are rocks constituted by fine- to medium-grained Di (40-60%), Tr (20-30%), Omp (10-20%) and Mg-Chl (10-20%). Di and Tr have a similar bottle green color, with Di lightly yellowish than Tr and Tr lightly paler than Di. They form medium- to coarse-grained, up to 5mm wide, porphyroclasts rimmed by fine-grained, < 2mm, Di + Tr aggregates. Omphacite is emerald green and medium-grained, up to 5mm in length. Mg-Chl is colorless and fine-grained. Wm, Phl and Zo may occur as accessories.

Metapyroxenites show a 10-cm-spaced S2 foliation marked by fine-grained Mg-Chl, Tr and Di SPO, wrapping around old Tr and Di medium-grained prophyroblasts. Medium-grained omphacite develops with the same typical randomly oriented texture as in the other lithologic types.

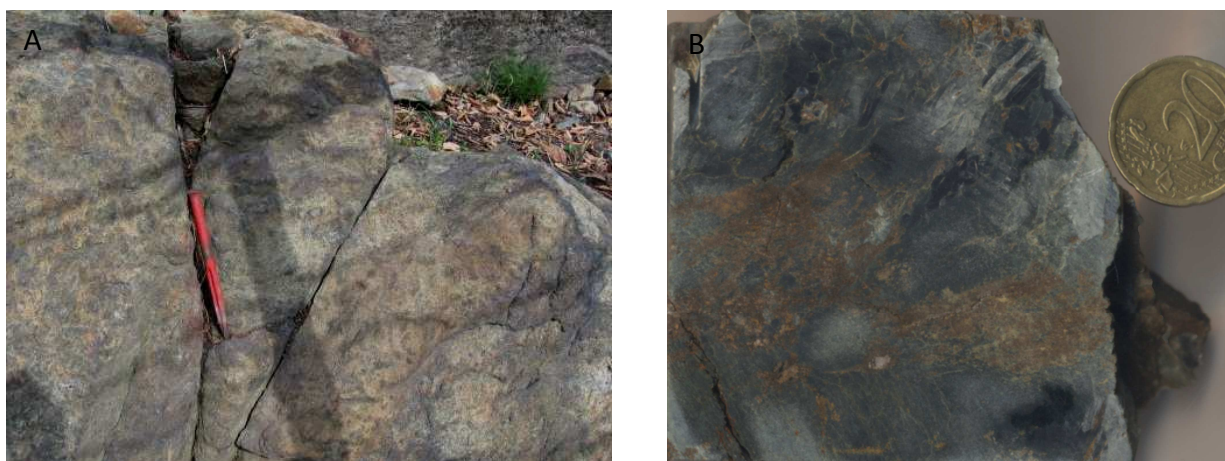


Fig. 4.7: (A) M-thick layer of clinopyroxenite with cm-spaced S2 foliation; (B) Atg-serpentinite with mm-thick foliation enveloping Ank aggregates, both crosscut by mm- to cm-thick fractures filled by fibrous Ctl.

4.2.1.3.6 Chlorite-amphibolite

The chlorite-amphibolite (Fig. 4.8A and 4.8B) lithologic type comprises all the rocks with Amp ($\geq 50\%$) and Chl ($\geq 15\%$). They are medium- to fine-grained amphibolites constituted by Amp (50-70%), Chl (20-30%), Ep (10-20%), Wm (5-10%) and Omp (5-10%). Amphibole forms medium-grained, up to 5mm wide, crystals; chlorite is pale-green and is fine grained; epidote has green yellowish color and is medium- to fine-grained; omphacite has emerald green color and is medium- to coarse-grained, with crystals up to 1cm. Ksp, Qtz and Ab may occur as accessories. Chlorite-amphibolite mainly shows cm-spaced S2 foliation marked by Act, Omp, Chl, Ep and Wm SPO.



Fig. 4.8: (A) M-thick layer of chlorite-amphibolite crosscut by syn-D5 fractures, filled by medium-grained Ab crystals; (B) Chlorite-amphibolite with poorly developed S2 foliation crosscut by mm-thick Ab filled fractures.

4.3 Mesoscale structural analysis of the Ivozio Complex and country rocks

Rocks of the Ivozio Complex have been folded during Alpine deformation, to which 0.5m- to 100m- scale folding and localized growth of new minerals are associated. The pre-Alpine structure and mineral relics are very scarce and almost totally erased by the early Alpine metamorphic imprint. The mesoscale structural

analysis is aimed at the characterization of mineral support of fabrics and of their strain gradients in order to define the primary lithologic types and reveal the superposition of tectonic structures.

Five groups of superposed structures (grouped in D1 to D5) are defined. They consist of fold systems, foliations and shear zones developed during the Alpine subduction-exhumation cycle, with the metamorphic mineral assemblages related to the deformation stages indicating an eclogite- to greenschist-facies conditions evolution. Four vein types developed in the eclogite- and blueschist-facies conditions with clear geometric relationships with the fold systems and foliations. Relationships between the superposed fabrics and successive mineral assemblages (detailed in Table 4.1) lead us to infer the following metamorphic and structural evolution:

- pre-D1 mesostructural relicts
- D1 deformation stage
- Grt-bearing veins
- D2 deformation stage
- Omp-bearing veins
- D3 deformation stage
- D4 deformation stage, Gln-bearing veins and Zo-bearing veins
- D5 deformation stage

The positioning of veins in the deformation stages time scale is not completely unambiguous, because of their limited spatial extent.

4.3.1 Pre-D1 mesostructural relicts

Some transitional contacts between layers defined by varying modal composition related to the pre-Alpine igneous layering are still preserved in some portions of the amphibole - eclogites and amphibole – epidote - bearing eclogites. These bands are observed in poorly deformed D1, D2, D4 and D5 domains and are still very visible, represented by Amp and Grt layers in amphibole-eclogites and by Amp and Ep layers in amphibole-epidote-bearing eclogites, respectively.

Other structural elements recognizable as pre-D1 are a group of veins, crosscutting the pre-Alpine igneous banding, transposed parallel to the S1 foliation and overgrown by Alpine mineral assemblages. These veins are:

1. Qz-bearing, 1 to 5cm-thick-veins that occur in all lithologic types (Fig. 4.9A);
2. Amp- and Wm-bearing (Fig. 4.9B), up to 15cm thick veins, occurring in all lithologic types, and composed of coarse grained, up to 7cm, dark-green Amp (90%) and fine-grained Tlc (10%);
3. Ep-bearing 1- to 5cm- veins (Fig. 4.9C), observed within amphibole-epidote-bearing eclogite, and composed of fine-grained yellowish-green Ep (80%), coarse-grained, up to 4cm wide, ruby red Grt (10%), and minor Chl (10%).

Moreover, in correspondence of a zoisite- and amphibole-eclogite boundary, a fold system older than D1 is transposed by a D1 fold (enlargement F of the map and Fig. 4.9D), testifying the length and complexity of the tectonic and metamorphic evolution and suggesting it may be even more complex than the one here inferred.

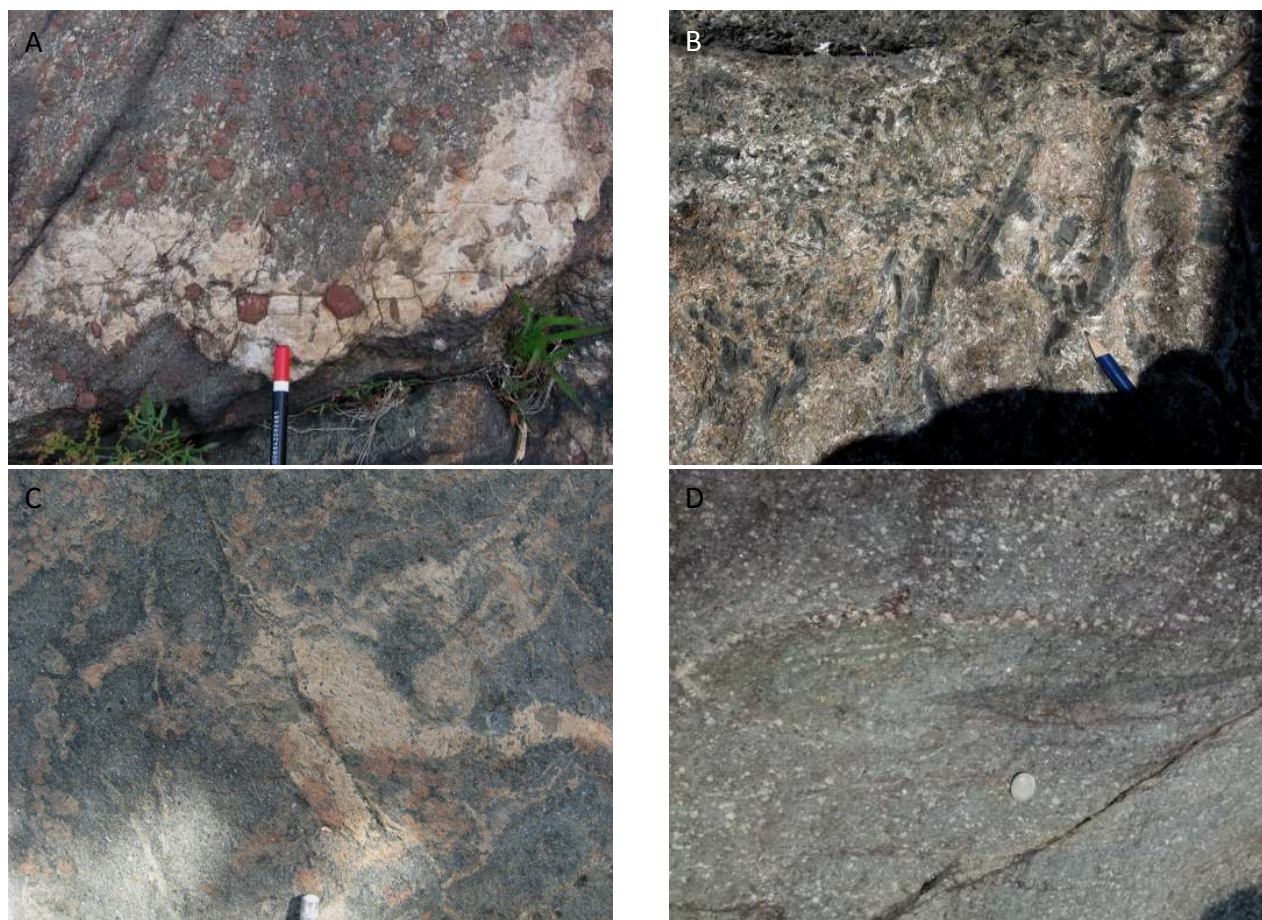


Fig. 4.9: (A) 5cm-thick Qz-bearing vein comprised in zoisite-eclogites, with growth of coarse-grained syn-D2 Grt and Omp; (B) 10-cm-thick Amp- and Wm-bearing vein with very coarse-grained, up to 5cm length, dark-green Amp crystals and fine-grained Wm; (C) 2cm-thick Ep-bearing vein deformed by D2 folds, comprised within amphibole-epidote-bearing eclogite; (D) D1 hinges folding a cm-thick Amp-rich layer within zoisite-eclogite, successively parallelized to a syn-D1 axial plane.

4.3.2 D1 deformation stage

D1 is a geometrically coherent fold system evidenced by 0.1 m to 1m wide folds, with shape similar to those of class 3 of Ramsay (1983). In zoisite-eclogite and zoisite-quartz-eclogite lithologic types, S1 foliation is marked by blue-amphibole, white mica and zoisite SPO developed parallel to the D1 axial planes. In amphibole-eclogite, in chlorite-amphibolite and in amphibole-epidote-bearing eclogite the presence of an internal fabric developed parallel to the D1 axial planes is no longer detectable, due to the scarceness of tabular sin-D1 minerals (such as Wm, Chl, Ep and Zo) and to the fact that syn-D1 Amp is only preserved as relic within sin-D2 blue amphibole. Locally in amphibole- and in amphibole-epidote-bearing eclogite the S1 orientation is preserved in Grt trails parallel to the banding. In metapyroxenite pre-D2 minerals are Tr and Di and do not define any preferred orientation of the fabric. In Atg-serpentinite the main mm-thick foliation marked by medium-grained Atg, Mg-Chl and Tr could be synchronous with D1 or D2 on the basis of its orientation and geometric relationships with what observed in other rock types.

D1 folds are very rare in the field, as shown by the scarcity of D1 axes and axial planes, whereas the S1 foliation is the main mappable structural element (Fig. 4.10). Schmidt equal area diagrams of S1 orientation principally evidence the dispersion of data due to D5 folding, even though axes, are dipping approximately to 80°N.

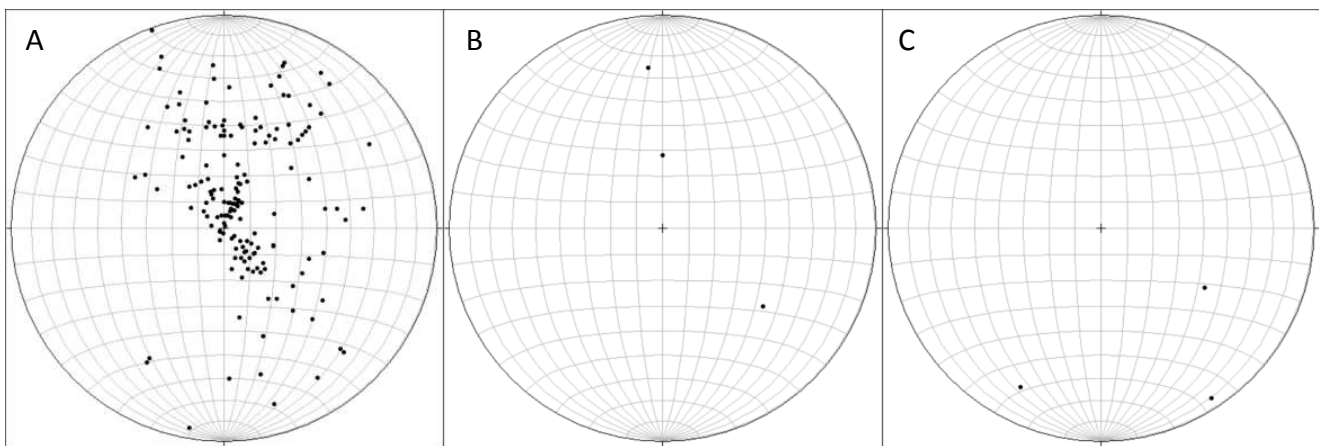


Fig. 4.10: Synoptic Schmidt equal area diagrams: (A) The S1 foliation shows a remarkable dispersion mainly due to D5, with verticalization of planes in the hinge zones of the D5 folds; only three data on the disposition of syn-D1 poles of axial planes (B) and their axes (C), have been collected.

4.3.3 Grt-bearing veins

Grt-bearing veins are common in all lithologic types excluding zoisite-, quartz-eclogite, chlorite-amphibolite and ultramafic rocks. They are composed of pinkish poikiloblast medium-grained Grt trails, growing within the embedding rocks (Fig. 4.11A).

Garnet veins are frequent in amphibole-eclogite, where they are localized in amphibole layers, in the form of 10 - to 30 - cm long garnet trails oriented at about 90° from each other (Fig. 4.11B). This could suggest that these veins formed under a deformation regime dominated by pure flattening strain or during a stage of high fluid pressure (e.g.: Vannucchi, 2001; Zulauf et al., 2011). Grt-bearing veins always crosscut the S1 banding and are always transposed parallel to S2, in syn-D2 high strain domains.

In amphibole-epidote-bearing eclogite Grt-bearing veins have the same characters than those in amphibole-eclogite, the only difference being their scarcity.

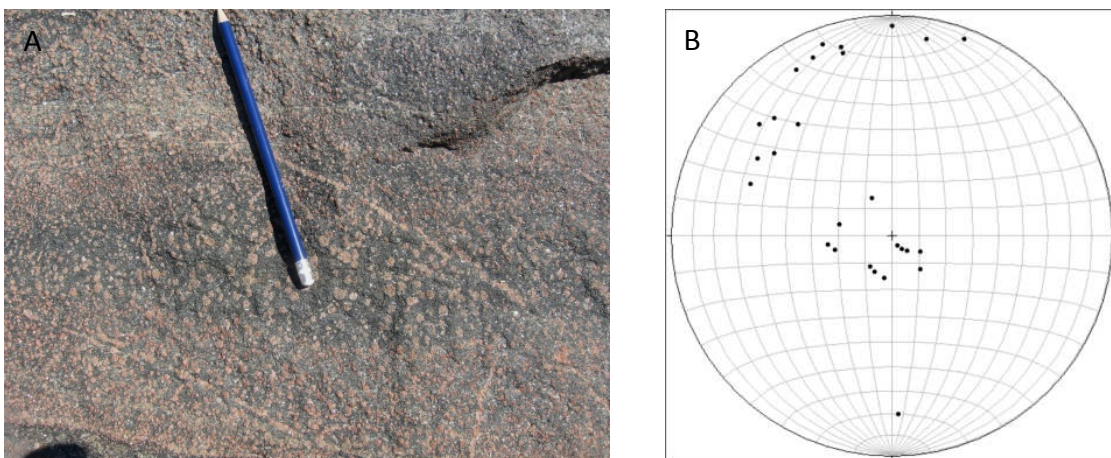


Fig. 4.11: (A) High angle Grt-bearing veins comprised within Amp and Grt layers of the amphibole-eclogite, crosscutting the banding; (B) Grt-bearing veins orientation with a sub-horizontal maximum and a second set of veins with high dipping angle (>50°) mainly dipping to NWN.

In zoisite-eclogite Grt-bearing veins have a lateral continuity of up to 2m with garnet up to 2cm wide. Moreover here, unlike in amphibole-eclogite in zoisite-eclogite, not all the Grt trails have been transposed

parallel to D2 axial planes, but some of them crosscut the S2 foliation. Only one group of orientation disposed at high angle with the S1 or S2 foliation is recorded.

4.3.4 D2 deformation stage

D2 is a geometrically coherent fold system evidenced by 1m to 10m folds (Fig. 4.12A), with similar shape class 3 of Ramsay (1983) and wavelengths of 2 to 10m. The development of a new axial plane S2 foliation is locally associated to this fold system in all lithologic types, except for the Atg-serpentinite in which the main foliation could be synchronous with the D1 or the D2 stage. D2 folds deform the contact between Ivazio Complex intrusives and their country rocks of the EMC.

In amphibolite-eclogite the development of a fine-grained mm-spaced S2 foliation is localized in 10 to 20m-thick bands (Fig. 4.12B), where a large amount of omphacite almost totally replaces a pre-existing blue-green amphibole found as relict and where the syn-D1 bands are thinned and almost completely transposed to 1-2cm thick layers. In poorly-foliated amphibole-eclogite the main effect of syn-D2 transformations is the development of poorly to randomly oriented medium- to coarse-grained omphacite crystals.

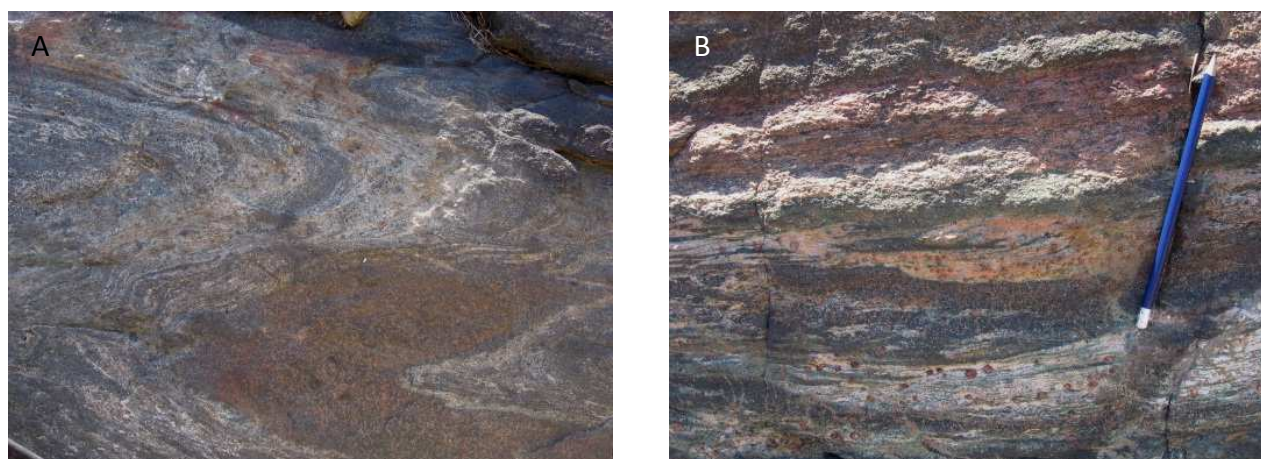


Fig. 4.12: (A) similar-shaped syn-D2 fold marked by a 10-cm-thick layer of amphibole-eclogite comprised within aosite-eclogite; (B) amphibole- and zoisite-eclogite cm-thick alternations generated by the formation of S2 mylonitic foliation.

In zoisite-eclogite and zoisite- and quartz-eclogite lithologic types, S2 is a cm-spaced foliation marked by medium-grained omphacite, blue-amphibole, white mica and zoisite SPO. In syn-D2 low strain domains coarse-grained Omp and Grt crystals, up to 5cm wide, develop. Locally S2 may have mylonitic character with mm-spacing and very small grain size: here S2 envelops Omp and Grt coarse-grained prophyroclasts. In zoisite-eclogite S2 foliation always wraps around Lws pseudomorphs.

In amphibole-epidote-bearing eclogite, mm-spaced S2 foliation defined by the orientation of fine-grained blue-amphibole and epidote with lesser amounts of omphacite and white mica, locally occurs. In non-foliated D2 volumes, medium-grained randomly oriented omphacite crystals occur.

In metapyroxenite, a cm-spaced discontinuous foliation is marked by fine-grained diopside, tremolite and Mg-chlorite, and wraps around them, but coarse-grained randomly oriented omphacite develops in poorly deformed syn-D2 domains.

The orientation of D2 axial planes and S2 foliation is sub-oriental, due to their exposure in the field within sub-horizontal limb of D5 folding systems; the dispersion of D2 axes highlights the non-cylindrical shape of D2 folds (Fig. 4.13).

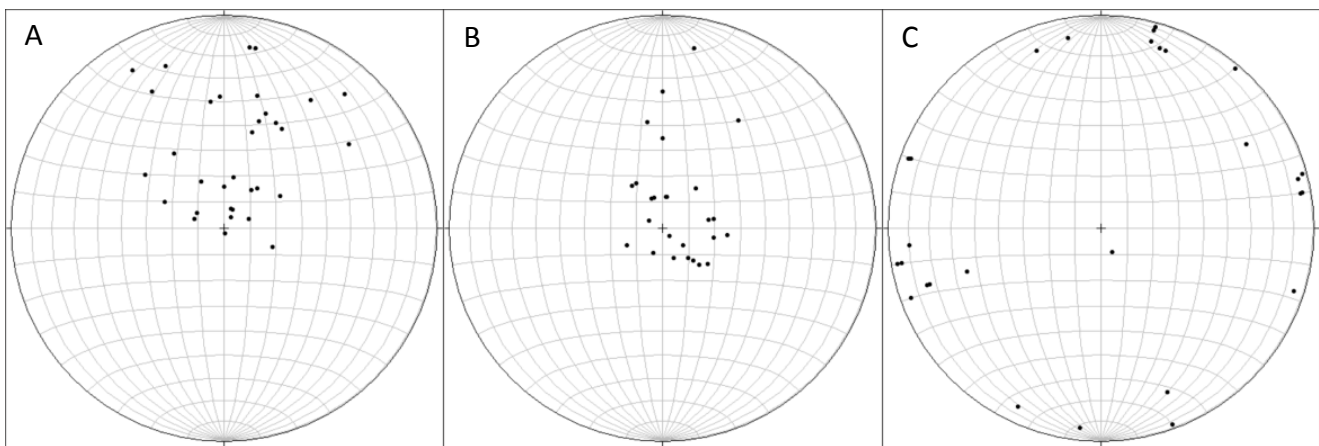


Fig. 4.13: Orientations of S2 foliation (A) and D2 axial planes (B) is principally sub-horizontal, with lesser evident influence of the D5 folding; (C) D2 axes are mostly sub-horizontal, not displaying a concentration, due to the non-cylindrical shape of D2 folds.

4.3.5 Omp-bearing veins

Omp-bearing veins are rare, they occur only in zoisite-eclogite and in amphibole-eclogite, as 1- to 10-cm-thick fractures filled by omphacite, quartz, phengite and glaucophane (Fig. 4.14A). Their lateral continuity is 10m maximum. A multistage mechanism of dilation is suggested by a complex growth of omphacite and sometimes glaucophane. In the embedding rocks omphacite overgrows mineral assemblages of the enclosing rocks at the margins of the vein. These veins always crosscut the S1 and S2 foliations. In one case boudinaged segments of a 10-cm-thick Omp-bearing vein could be followed on the sides of a D3 fold limb. Most of the times these veins are reoriented by D3 folds (Fig. 4.14B).

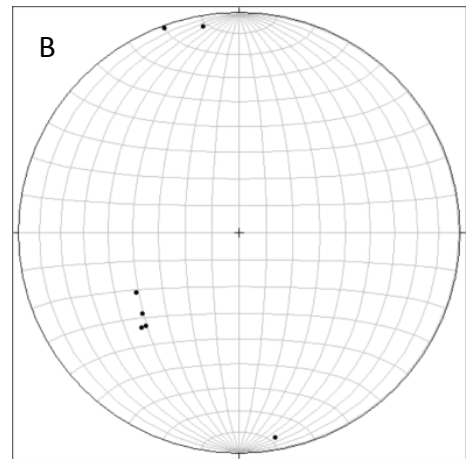


Fig. 4.14: (A) 10-cm-thick Omp-bearing vein filled by coarse-grained Omp and Ph, occurring within a zoisite-eclogite; (B) Omp-bearing veins orientation with a maxima dipping 50° to 70°N, the data scattering is coherent with D3 folding.

4.3.6 D3 deformation stage

D3 is a close to open fold system with m to 10-m wavelength, occurring in all lithologic types. It is associated to fine-grained dynamic recrystallization of blue amphibole, zoisite and white mica substituting syn-D1 and syn-

D2 minerals. D3 folds are class 2 of Ramsay (1983), have sub-vertical axial planes striking N/S. D3 axial traces orientations is not modified by D5, because they are almost orthogonal to their axes and axial planes. In fact D3 mainly strike toward S/SSE with a zero to vertical dipping angle inferred by D5 folding (Figs. 4.15).

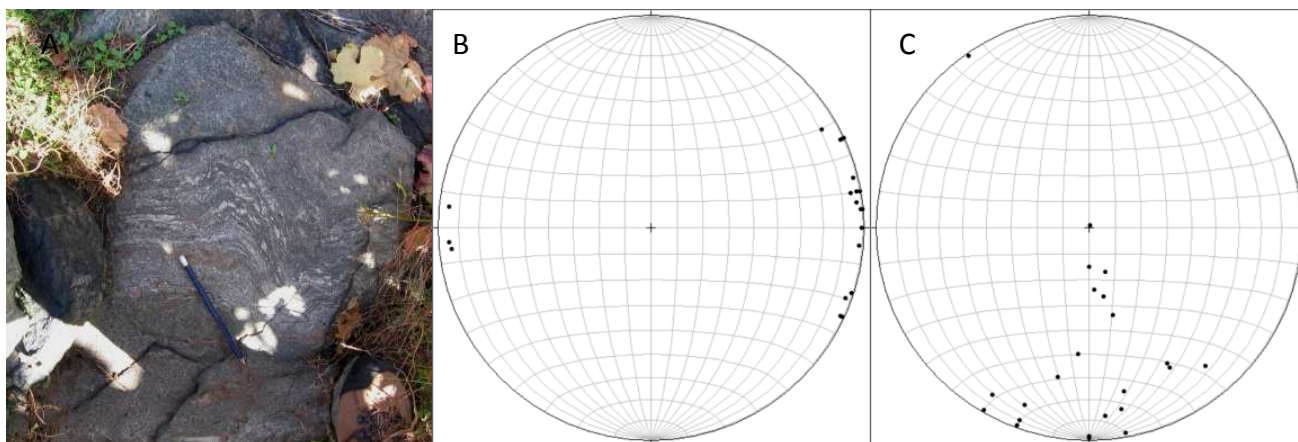


Fig. N. 4.15: (A) syn-D3 hinge zone with well develop crenulation of S2 foliation in zoisite-eclogite; (B) the orientation of D3 axial planes in sub-vertical, mainly striking N-S; (C) D3 axes are mainly striking toward S/SSE variable inclination angle influenced by D5 folding event.

4.3.7 D4 deformation stage, Gln- and Zo-bearing veins

A set of sub-horizontal m-thick shear zones formed during D4 deformation stage, occurs within amphibole-eclogite (Fig. 4.16B). Here, fine-grained mylonites are characterized by a new S4 mm-thick foliation where abundant glaucophane with minor epidote and white mica crystallize (Fig. 4.16A).

Gln-bearing veins occur in all lithologic types, with the exception of Atg-serpentinite. These veins have a lateral continuity of 10 to 20m and are further evidenced by the growth of fine-grained Gln halos in the country rocks. At times they also have a dilation of up to 2cm, with syntactical filling of medium- to fine-grained glaucophane, white mica and zoisite of the fracture generating the vein (Fig. 4.16C). The group of up to 20m long Gln-bearing veins dipping NWN with an inclination of about 30° represents the principal set; the dip angle may be increased or decreased by D5 (Fig. 4.16D). Shorter Gln-bearing veins depart from the main set, generally at high angle with it, but no preferred orientation is recognizable.

Rare Zo-bearing veins almost parallel to the Gln-bearing veins occur in amphibole- and zoisite-eclogite (Fig. 4.16F); they are fractures, up to 1cm wide, filled by fine-grained syntactical growth of zoisite or clinozoisite (Fig. 4.16E), and have a lateral continuity of maximum 2m.

No geometrical evidence of relative time relation between D4 shear zones, Gln and Zo-bearing veins has been detected. They have been grouped together due to their relationships with the previous and successive deformation stages: crosscutting D3 structure and bended by D5 fold system.

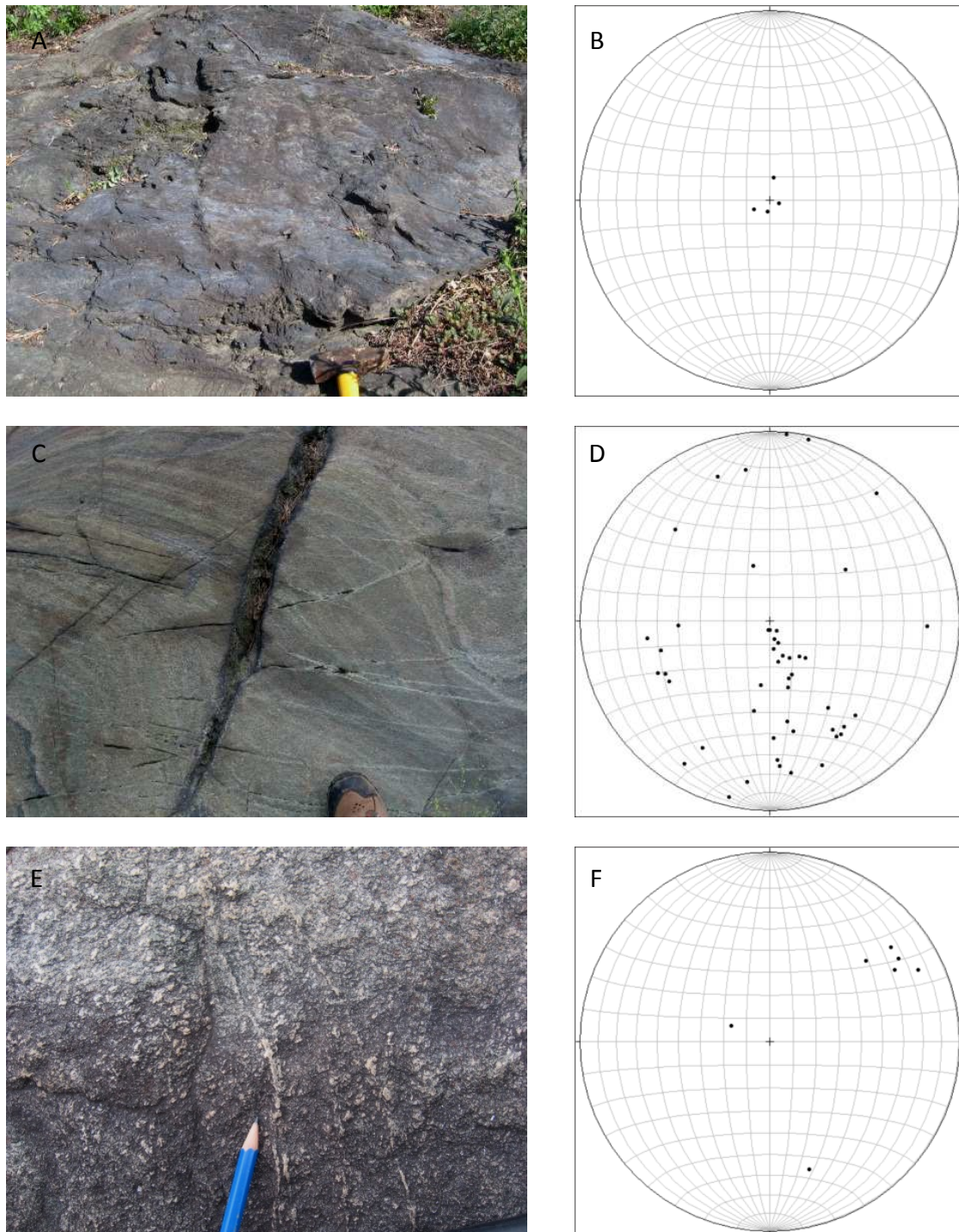


Fig. 4.16: (A) 2m-thick Gln-bearing shear zone in amphibole-eclogite; (B) sub-horizontal orientation of S4 foliation; (C) 10-cm-thick Gln-bearing vein within amphibole-epidote-bearing eclogite, with thinner Gln-bearing veins departing from the thicker one; (D) Gln-bearing veins disposition with a maxima of orientation dipping NWN with an inclination of about 30°; (E) mm-thick Zo-bearing veins in zoisite-eclogite; (F) Zo-bearing veins are mainly dipping 50° to the SW.

4.3.8 D5 deformation stage

The D5 fold system is the most important geometrical feature, and it influences the orientation and relationships of the other structural elements. It consists of 10m wide gentle to close folds (Fig. 4.17A), class 1B of Ramsay (1983) occurring in all the lithologic types of the Ivozio Complex and within the surrounding EMC.

No new mineral assemblages associated to D5 structures is observed in the poorly deformed domains, but coronitic replacement occurs, with the development of fine-grained albite, chlorite, green amphibole, white mica and epidote on the previous minerals, especially substituting omphacites and garnets. D5 axial planes dip NEN with angles between 20 and 50°, and have sub-horizontal axes oriented at about 80°N (Fig. 4.17B and 4.17C).

D5 is associated to cm- to m-thick shear zones where the mm-thick S5 foliation marked by fine-grained chlorite, green amphibole, albite, white mica and epidote occurs in all lithologic types. Metre-length fractures up to 1cm wide filled by fine-grained epidote, albite or chlorite are associated to these shear zones (Fig. 4.18A). The disposition of syn-D5 planes is bimodal, with sub-horizontal shear planes and sub-vertical m-length fractures striking NW-SE (Fig. 4.18B).

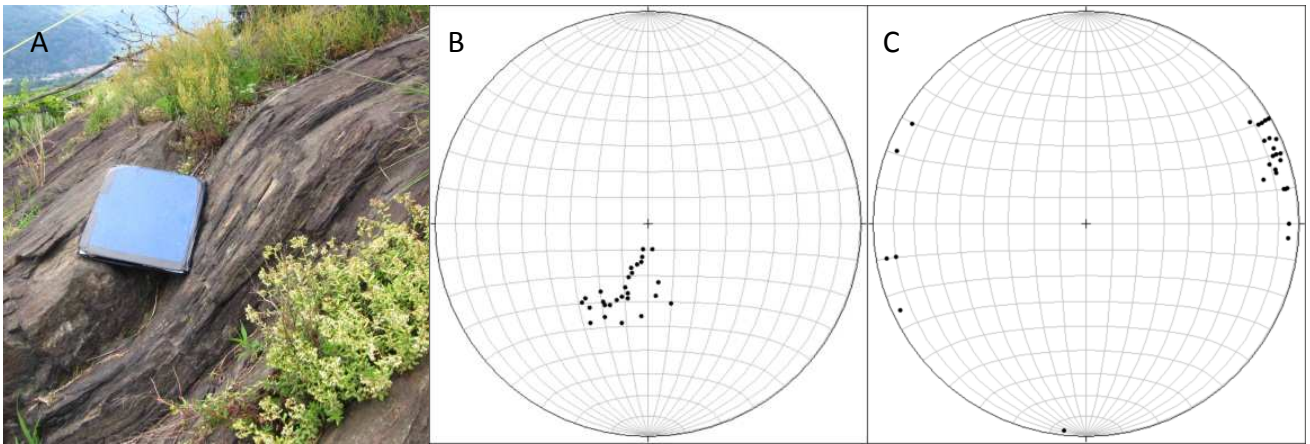


Fig. 4.17: (A) 50-cm wavelength syn-D5 gentle folding in amphibole-eclogite; (B) syn-D5 axial plane are mainly disposed with a NEN dipping and an inclination angle comprised between 20 and 50°; (C) syn-D5 axes are sub-horizontal and mainly dipping towards 80°N.

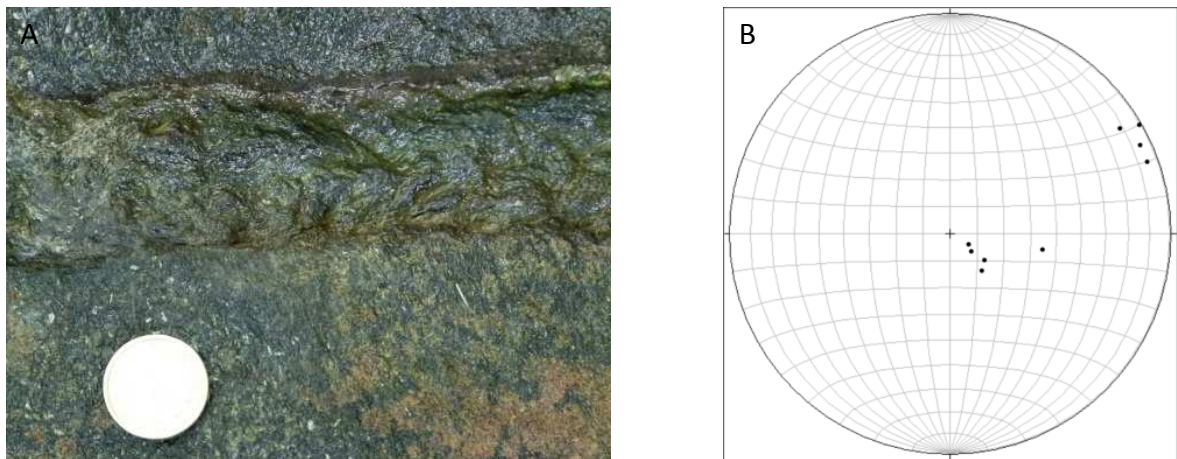


Fig. 4.18: (A) 3cm-thick syn-D5 shear zone marked by fine-grained Chl in amphibole-epidote-bearing eclogite; (B) disposition of syn-D5 have two maxima, with sub-horizontal and sub-vertical syn-D5 structural elements striking NW-SE.

4.4 Microscales structural analysis of the Ivazio Complex

A number of 108 thin sections have been cut on samples collected in the mapped area. The analysis at the optical microscope aimed at the detailed petrographic characterization of each structural element recognized in the field and at the reconstruction of parageneses marking successive fabrics within all lithologic types, for an appropriate evaluation of the metamorphic evolution of the Ivozio metagabbroic Complex. The results of this analysis are summarized in Table 4.2.

4.4.1 Pre-D1 microstructure and mineral association evolution of pre-D1 veins

The only possible textural relic of pre-D1 age within the lithologic types of the Ivozio Complex, occurs in amphibole-bearing eclogite, in the form of 2 to 5mm-sized square-shaped phengite + blue-green amphibole aggregates rimmed by medium-grained garnet crystals. Such aggregates could represent pseudomorphic replacements of igneous amphibole (Fig. 4.19A).

Mineral relicts of pre-D1 age are almost totally represented by relicts of amphiboles and garnets retained within veins crosscutting the pre-Alpine igneous banding and belonging to the Ep-bearing and Amp- and Wm-bearing veins. More in detail:

- a) Qz-bearing veins are composed by medium- to fine-grained Qz (95%) with a size < 1mm, possibly Alpine, of magnetite and rutile. Medium-grain quartz has granoblastic polygonal texture, acquired after D2 deformation. A grain-size reduction is observed during the following D4 to D5 deformation stages with the obliteration of the granoblastic texture related to syn-D5 oriented recrystallization. In the veins Grt, Omp, Ph and Gln crystals of syn-D1 to syn-D2 age can develop parallel to the S1 or S2 fabric respectively; Omp and Gln crystals may present a composite complex zonation (Fig. 4.19B).
- b) Ep-bearing veins are composed of epidote (80%), garnet (10%) and chlorite (10%) with minor white mica. They contain coarse-grained ruby-red garnets wrapped by S1. Epidote crystals within these veins have a polyphase evolution: epidote cores (diameter < 1mm) are included within syn-D1 medium grained clinozoisite, both crosscut by coarse-grained randomly oriented clinozoisite, probably developed during D2. Finally, a new generation of epidote rims all the previous epidote and clinozoisite crystals. Garnets crystals are inclusions free.
Fine- to very fine-grained colorless Mg-chlorite fills the interstices between epidote and clinozoisite crystals, but Mg-chlorite crystals, up to 2mm in size, coexist with syn-D2 clinozoisite (Fig. 4.19C) and are partially replaced by thin Mg-chlorite, probably developed during D3. Fine-grained pale green Fe-chlorite partially overgrows garnets along fractures. Rare fine-grained white mica crystals crosscut syn-D1 mineral association.
- c) Amp- and Wm-bearing veins are composed of amphibole (70%), white mica (20%) and Mg-chlorite (10%) with rutile and magnetite as accessories. Most of the amphibole crystals are coarse-grained green/dark-green amphibole, of up to 5cm long. Pre-D2 cores are rimmed by syn-D2 medium- to fine grained blue-green amphibole (Fig 4.19D). Very fine-grained white mica is included within pre-D2 amphibole cores, whereas fine- to medium-grained white mica and Mg-chlorite crystals enclose the amphibole cores coexisting with syn-D2 amphibole. Very fine-grained Mg-chlorite and white mica form by the grain size reduction of previous crystals of amphibole and white mica during D5.

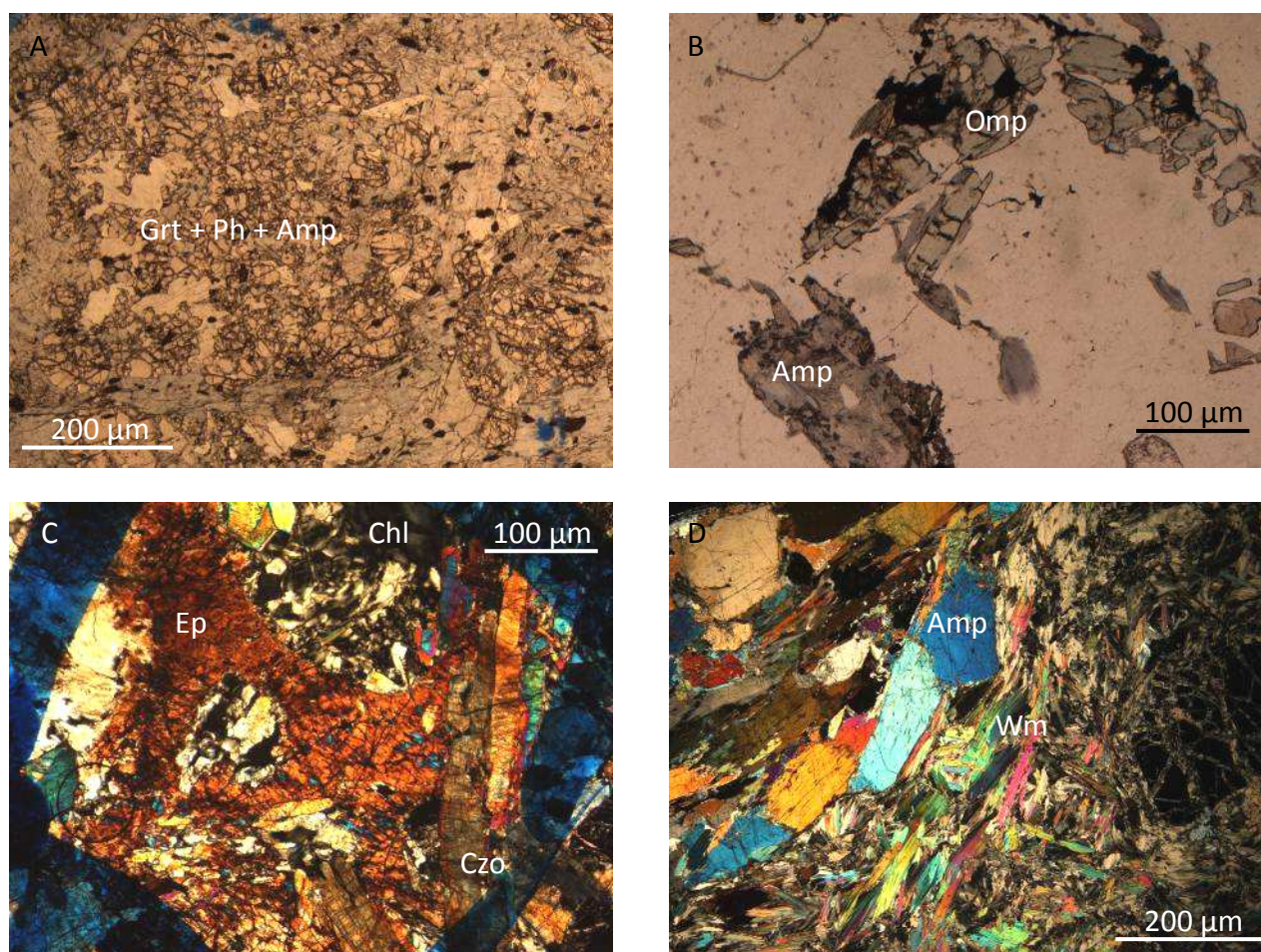


Fig. 4.19: (A) square-shaped Ph + Amp aggregates rimmed by medium-grained Grt crystals; they may derive from corona-type replacement of previous igneous Amp in amphibole-bearing eclogite (plane polarized light); (B) Omp and Amp syn-D1 and syn-D2 crystals growing in Qz-bearing vein, Amp crystals have a composite zonation marked by color variations (plane polarized light); (C) Ep-bearing vein in amphibole-epidote-bearing eclogite constituted by fine-grained Ep and Mg-Chl overgrown by coarse-grained Czo crystals (crossed polars); (D) coarse-grained Amp and Wm crystals recrystallized during Alpine deformation close to the contact with zoisite-bearing eclogite (crossed polars).

4.4.2 Amphibole-bearing eclogite microstructure

The Alpine mineral associations in amphibole-bearing eclogites are the same within the three different layers occurring at Ivozio, differing simply in the modal quantities of mineral phases appearing throughout the stages of the deformation sequence D1 to D5. The average composition of each of the amphibole-bearing eclogite layers is, respectively (see 4.2.1.3.1):

- amphibole rich layer: blue or blue-green Amp (50%), Grt (25%), Omp (20%) and Wm (5%), with Zo, Rt, Mt, Qz, Ab and Chl as accessories in Amp layers.
- garnet rich layer: Grt (60%), blue-green Amp (20%) and Omp (20%), with Zo, Wm, Rt, Mt, Qz, Ab and Chl as accessories in Grt layers.
- omphacite rich layer: Omp (50%), Amp (25%), Ph (20%) and Grt (5%), with Zo, Wm, Rt, Mt, Qz, Ab and Chl as accessories in Omp layers.

D1 mineral assemblage relicts are very poorly preserved, and only consist of rare blue-green amphibole porphyroclasts (Fig. 4.20A), of syn-D1 garnet reddish cores and their inclusions of blue-green Amp, Ep, Mt and

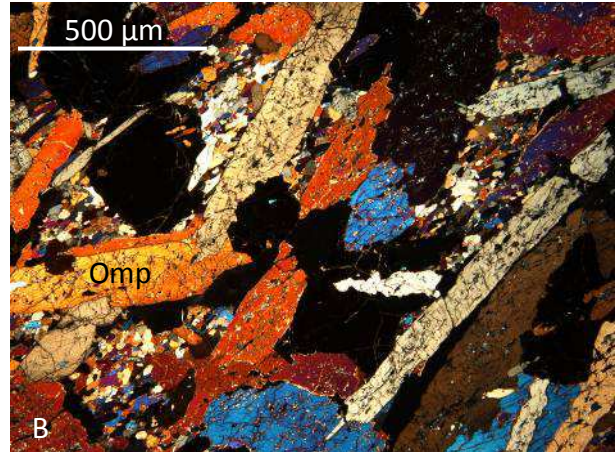
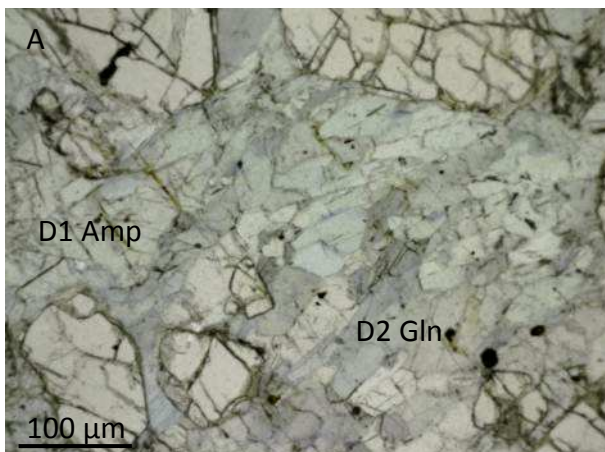
Rt. In large syn-D2 Omp crystals inclusion of syn-D1 blue-green Amp and Wm survive the D2 mineral reorganization, which causes the recrystallization of almost all the syn-D1 Amp and Wm (Fig. 4.20B).

In high strain D2 domains the mm-thick S2 foliation is principally marked by fine-grained omphacite, phengite, zoisite and glaucophane SPO (Fig. 4.20C). Where S2 foliation is pervasive, no relics of blue-green Amp are found. On the other hand, in low strain D2 domains pinkish garnet develops as new, atoll-shaped or idioblastic, fine-grained crystals and is found as rims around D1 Grt cores. A new generation of Gln develops, rimming or replacing the syn-D1 blue-green amphibole; randomly oriented medium- to coarse-grained omphacite and phengite develops. Locally, in both low- and high- strain domains, the growth of omphacite crystals is continuous, progressing after D2 deformation with development of coarse-grained, up to 5cm long omphacite crystals overgrowing syn-D2 fine-grained SPO omphacite and randomly oriented unzoned omphacite (Fig. 4.20D).

Syn-D3 recrystallization of previous amphiboles, phengite and zoisite is observed at their rims.

Only one m-thick D4 shear zone occurs within amphibole-bearing eclogite. Here a mm-thick S4 foliation marked by fine grained glaucophane and phengite occurs (Fig. 4.20F). Shear planes involve 10-cm-thick lens-shaped volumes with the progressive replacement of omphacite and garnet by amphibole, producing the change of the eclogite into a phengite-bearing glaucophane schist (Fig. 4.20E). Boudinaged amphibole-bearing eclogite tension gashes filled by medium-grained syntactical growth of clinozoisite, glaucophane and titanite develop.

D5 is characterized by corona reactions, with the development of fine-grained Ab, Chl, green Amp, Wm and Ep pseudomorphic on previous Omp, Amp, Wm, Zo and Grt. Among D5 shear planes and related fractures, a large amount, up to 40% in modal volume, of fine-grained Chl, Ab, Wm and Ep develops.



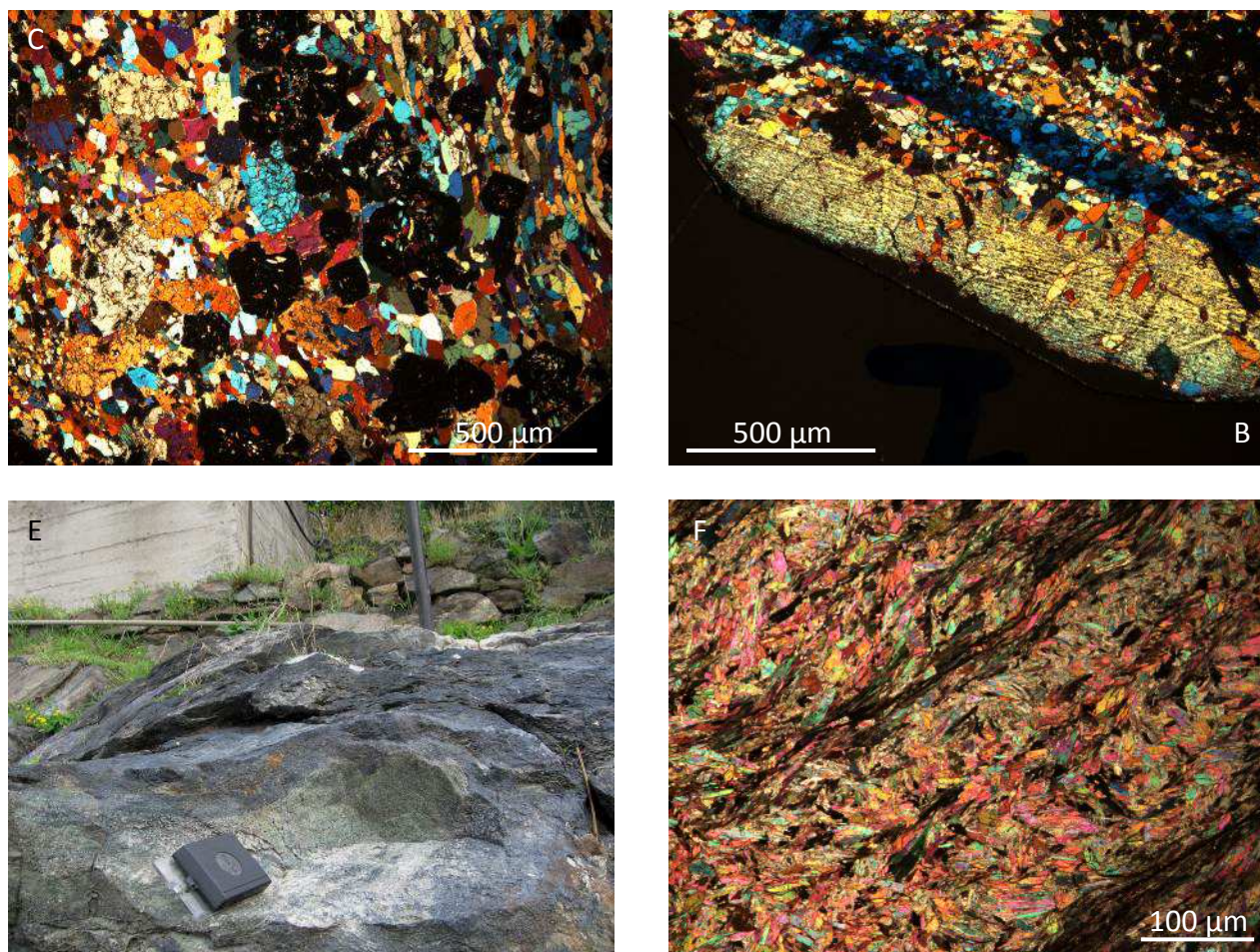


Fig. 4.20: (A) syn-D2 Gln rimming sub-grains of syn-D1 blue-green Amp in Amp layer of the amphibole-bearing eclogite (plane polarized light); (B) syn-D2 coarse-grained Omp crystals with numerous inclusion of the syn-D1 Amp and interstitial fine grained Gln, in an Amp layer of the amphibole-bearing eclogite (crossed polars); (C) Amp layer of the amphibole-bearing eclogite with S2 marked by Gln, with syn-D1 Grt preserving syn-D1 Amp with continuous syn-D2 rims; (D) amphibole-bearing eclogite with mm-thick S2 foliation mainly marked by fine-grained Omp, with coarse-grained Omp partially substituting the fine grained crystals (crossed polars); (E) 10-cm-thick S4 shear zones with abundant amphibole growth in the interposed amphibole-bearing eclogite lens-shaped volume; (F) mm-thick S4 foliation almost totally composed by Gln with minor Wm locally transposed into parallelism with thin S5 shear planes with associated grain size reduction (crossed polars).

4.4.3 Zoisite-bearing eclogite microstructure

The average composition of zoisite-bearing eclogite is Zo (35%), blue Amp (20%), Wm (both Ph and Pg 15%), Grt (10%), Omp (10%) and Qz (10%), with Rt, Ab and Chl as accessories.

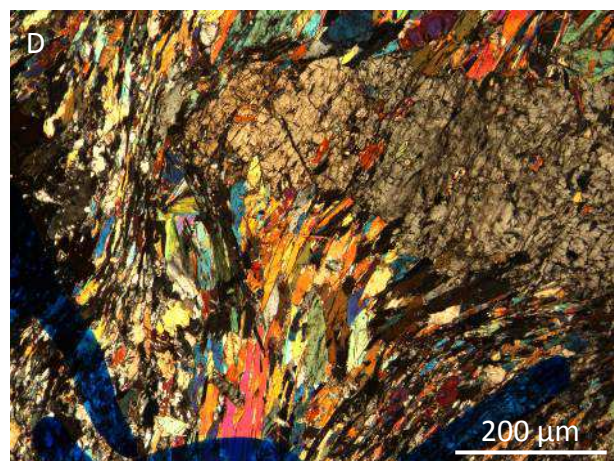
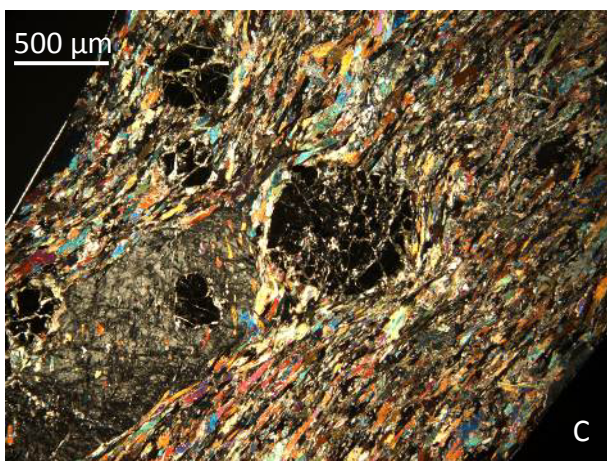
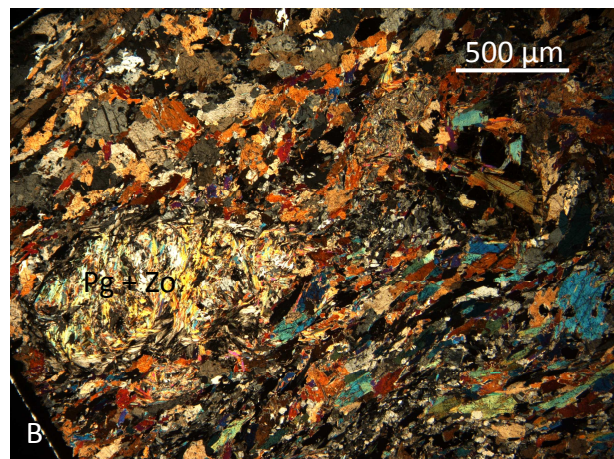
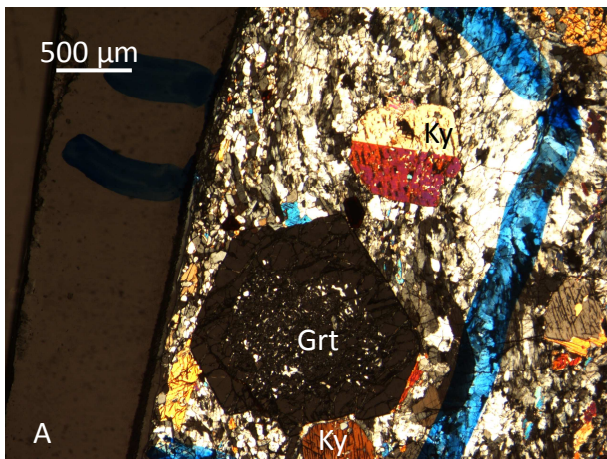
Medium- to fine-grained crystals marking the S1 foliation are blue-green Amp, Zo and Ph SPO, mainly transposed into the S2 foliation; other syn-D1 minerals are reddish Grt cores preserving syn-D1 relict inclusions of Rt, blue-green Amp, Zo and Ph.

In this lithologic type most of the lawsonite textural relicts of the Ivazio Complex and have the following characters: pseudomorphs after lawsonite are parallel to the S1 foliation; lawsonite pseudomorphed by kyanite crystals with inclusions of Qz and Zo, are mainly enveloped by S2 foliation, but some of them are not involved and enclose an internal foliation marked by Zo and Qz trails parallel to the S2 foliation (Fig. 4.21A); most of the kyanites are partially pseudomorphosed by paragonite and zoisite, locally with syn-D2 SPO (Fig. 4.21B).

The S2 foliation has mylonitic character, with a mm-thick foliation associated to grain size reduction, marked by fine-grained Zo, Ph, Pg, Gln and Omp SPO, totally obliterating S1. In syn-D2 low strain domains a diffused coarse-grain growth of Omp, Ph and Grt with no preferred orientation develops. Due to the penetration of mylonitic S2 foliation throughout the zoisite-bearing eclogite volume, the relation of S2 foliation and the syn-D2 large grain blastesis is not always the same: in some cases Omp and Grt are wrapped by the S2 foliation (Fig. 4.21C), in others they are superposed upon the S2 foliation (Fig. 4.21D); unzoned Omp and Grt crystals with snowball microstructure form in zoisite-bearing eclogite. In all these cases no appreciable optical differences in the Omp and Grt crystals are observed, suggesting that they all have the same composition.

During D3 S2 Amp, Ph and Zo rims recrystallize (Fig. 4.21E) and concurrently formation of paragonite + zoisite rims between Ky crystals may attain complete replacement of Ky.

During D5 only pseudomorphic reactions occur, with development of fine-grained Ab, Chl, green Amp, Wm and Ep. Locally cm scale shear zones associated to D5 folds form within zoisite-bearing eclogite, generating mm-thick layers constituted by Chl and Wm (Fig. 4.21F). Among D5 shear zones up to 50% modal volume of fine-grained Chl, Ab, Wm and Ep develops, in association to shear planes and related fractures.



(B)

(C)

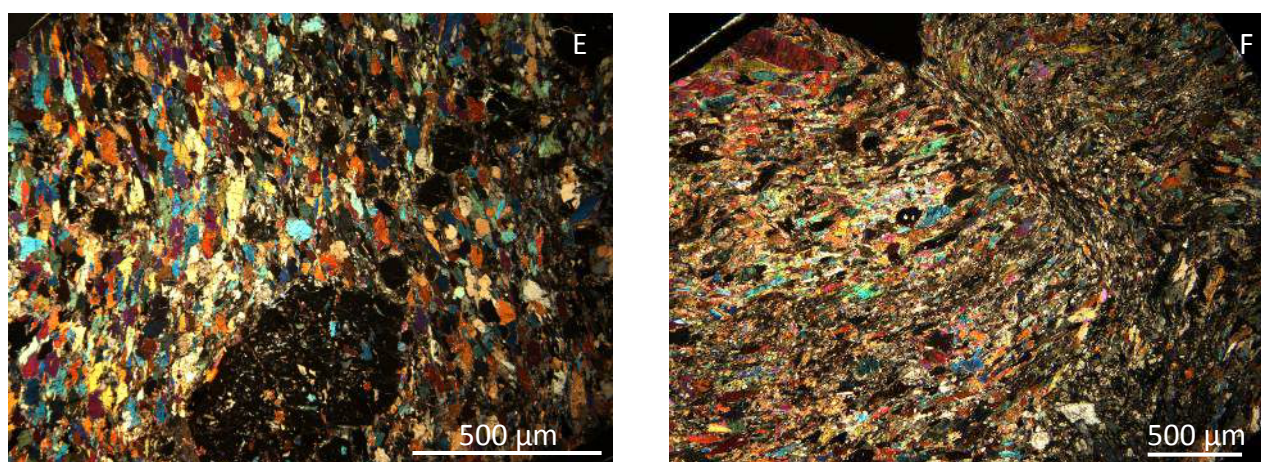


Fig. 4.21: (A) Lws pseudomorphs composed by a core of Ky including fine crystals of Zo and Qz, rimmed by medium grained Pg crystals (plane polarized light); (B) complete replacement of Ky by Pg + Zo aggregate defining syn-D2 crenulated fabric (crossed polars); (C) Grt and Omp coarse-grained crystals enveloped by mm-thick S2 foliation marked by Ph, Zo, Gln and Omp, with an internal foliation of coarse-grained crystals gradually oriented parallel to the external S2 foliation (crossed polars); (D) coarse-grained Omp crystal with an internal foliation almost parallel to the external S2 foliation marked by fine-grained Ph, Zo, Gln and Omp (crossed polars); (E) S2 foliation deformed during D3 event with partial recrystallization of Zo, Ph and Gln boundaries (crossed polars); (F) a very fine-grained mm-thick S5 shear plane marked by Chl and Wm develops in partial transposition of the S2 foliation in zoisite-bearing eclogite (crossed polars).

4.4.4 Amphibole-epidote-bearing eclogite microstructure

The Alpine mineral associations in amphibole-epidote-bearing eclogite evolves similarly within the two different layers (amphibole- and epidote-rich, respectively), the only difference is the modal quantity of mineral phases during time. The average composition of the amphibole-epidote-bearing eclogite layers is:

- Dark-green Amp (75%), Grt (10%), Omp (10%) and Wm (5%), with Ep, Rt, Mt, Qz, Ab and Chl as accessories in dark-green Amp layers.
- Ep (65%), dark-green Amp (25%) and Chl (10%), with Omp, Grt, Wm, Rt, Mt, Qz and Ab as accessories in Ep layers.

D1 mineral assemblage relicts consist of very poorly preserved blue-green Amp and Ep porphyroclasts, as in amphibole eclogite. Pseudomorphs after lawsonite are not observed in this lithologic type.

In syn-D2 low strain domains a diffuse medium-grain crystallization of Omp and Wm with no preferred orientation develops. In mm-thick S2 domains (Fig. 4.22A), the foliation is marked by fine- to medium-grained blue-green Amp, Omp, Wm, Ep and Chl; locally syn-D2 pinkish poikiloblastic coarse-grained Grt develops abundantly, up to 30% of the rock volume.

During D5 only partial substitution of dark-green Amp, Wm, Ep and Chl rims by fine-grained Ab, Chl, Act, Wm and Ep is observed (Fig. 4.22B). Syn-D5 shear zones are particularly well developed within this lithologic type, forming up to 2m thick shear zones marked by up to 90% in modal volume of fine-grained Chl, Ab, Wm and Ep, defining the mm-thick S5 foliation.

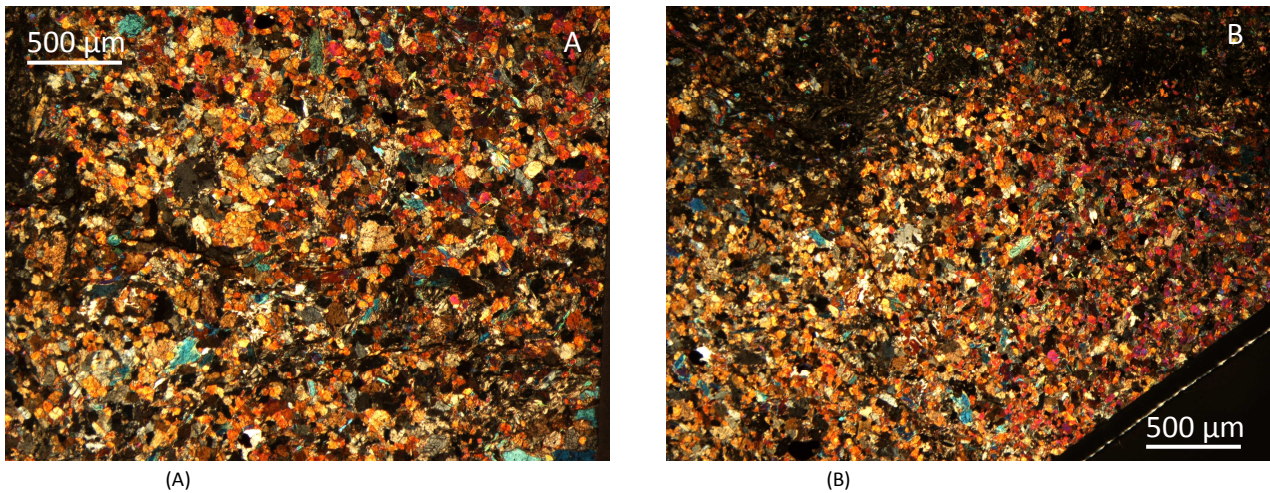


Fig. 4.22: (A) S2 foliation marked by fine-grained Amp and Ep (crossed polars); (B) mm-thick Chl-rich layer within Ep layer of amphibole-epidote-bearing eclogite evidencing a D5 fold (crossed polars).

4.4.5 Quartz-rich eclogite microstructure

The average composition of this eclogite type is Zo (30%), Qz (30%), Omp (25%) and Ph (15%), with Amp, Grt, Chl, Ep, Rt, Ttn and Ab as accessories.

A cm-space discontinuous S1 foliation is marked by medium-grained Zo, Ph and blue-Amp SPO and by lens-shaped Qz domains. Locally, where S1 is poorly developed or absent, the syn-D1 mineral assemblage is recognizable as pseudomorphic replacements of the igneous minerals: calcic plagioclase and primary amphibole are mainly replaced by zoisite and blue amphibole respectively.

During D2 a cm-spaced foliation marked by medium-grained Zo, Ph and Omp SPO develops. In syn-D2 low strain domains coarse-grained up to 5cm wide, Omp, Ph and Grt with no preferred orientation develop (Fig. 4.23A). As in the zoisite-bearing eclogite also in the quartz-rich eclogite the migration of the strain front during D2 may cause enveloping of large syn-D2 crystals within the S2 foliation (Fig. 4.23B).

During D3 recrystallization of D2 Amp, Ph and Zo occurs.

During D5 large porphyroclasts are pseudomorphosed by fine-grained Ab, Chl, green Amp, Wm and Ep aggregates, especially omphacite which is often boudinaged, and the necks of fractures are filled by Ab, Chl and Act. D5 shear zones are concentrated in mm-thick planes within the quartz-rich eclogite, mainly developing fine-grained recrystallization of Qz and Wm, with minor of Chl, Ab and Ep.

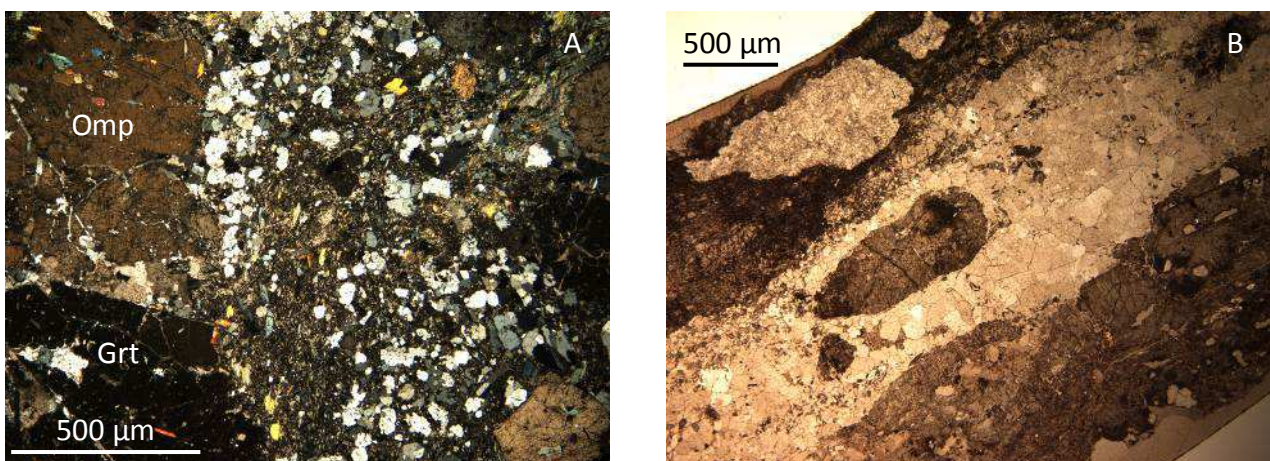


Fig. 4.23: (A) large Omp and Grt crystals in contact with Qz-rich domain composed by fine-grained Qz, Zo and Ph aggregates (crossed polars); (B) lens-shaped Qz domain and Omp crystals parallelized to the S2 foliation (plane polarized light).

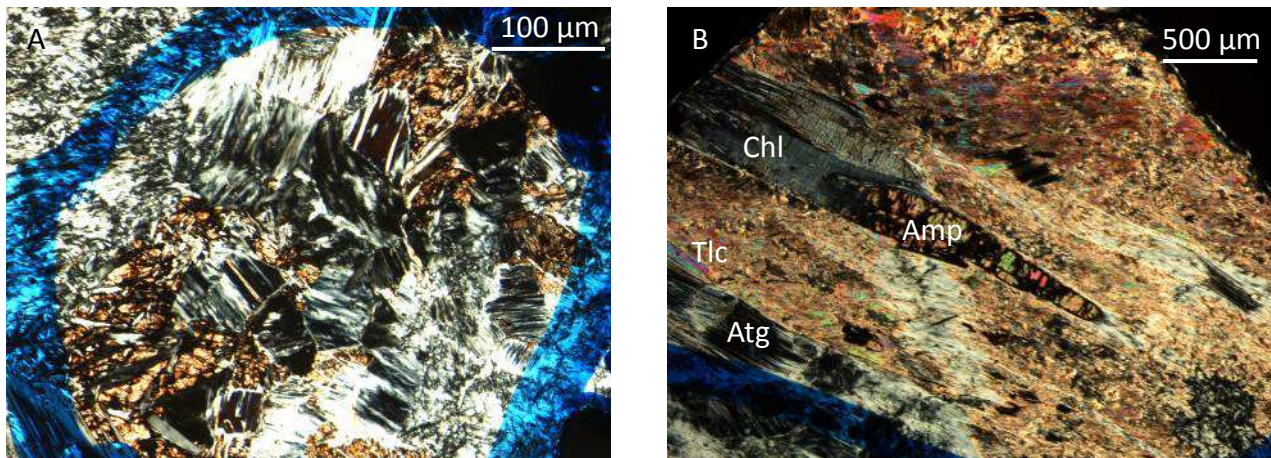
4.4.6 Ultramafic rocks microstructure

The average composition of Atg-serpentinites is Atg (60%), Ctl (20%), Ank (10%), Mg-Chl (5%) and Mt (5%), with Tr, Di and Wm as accessories.

As noted before, the absence of field continuity of planar fabrics in the other lithologic-types does not permit to link physically the Atg-serpentinite fabrics with those observed elsewhere; confidence was given in these cases on petrogenetic correlations. 1- to -10 mm-thick layers of tremolite, Di and Chl or Atg, Mt and ankerite are locally recognizable as relicts in the main mm-thick foliated fabric marked by fine-grained antigorite, Mg-Chl, Tr and Wm in Atg-serpentinite (Fig. 4.24B). Fractures filled by fibrous chrysotile, medium-grained Mg-Chl and Tr occur at high angle with the main foliation. Hexagonal-shaped textural relicts, replaced by Atg, are probably related to igneous or metamorphic Ol (Fig. 4.24A).

The average composition of metapyroxenites is Di (50%), Tr (25%), Omp (10%), Mg-Chl (10%), Ph/Phl (5%), with Zo, Mt, Chr and Spl as accessories.

Syn-D1 relicts are represented by medium- to coarse-grained Di and Tr pale cores (Fig. 4.24C) enveloped in the S2 foliation marked by fine- to medium-grained Di, Tr, Ph, Phl and Mg-Chl SPO, with pale green tremolite rimming the pre-existing amphiboles; medium- to coarse-grained randomly oriented omphacite crystals developed in thinner metapyroxenite layers (Fig. 4.24D); they are rimmed by fine-grained phengite and phlogopite crystals. D5 shear zones are concentrated in mm-thick planes in metapyroxenite, mainly developing very fine-grained formation of Fe-Chl and Ab.



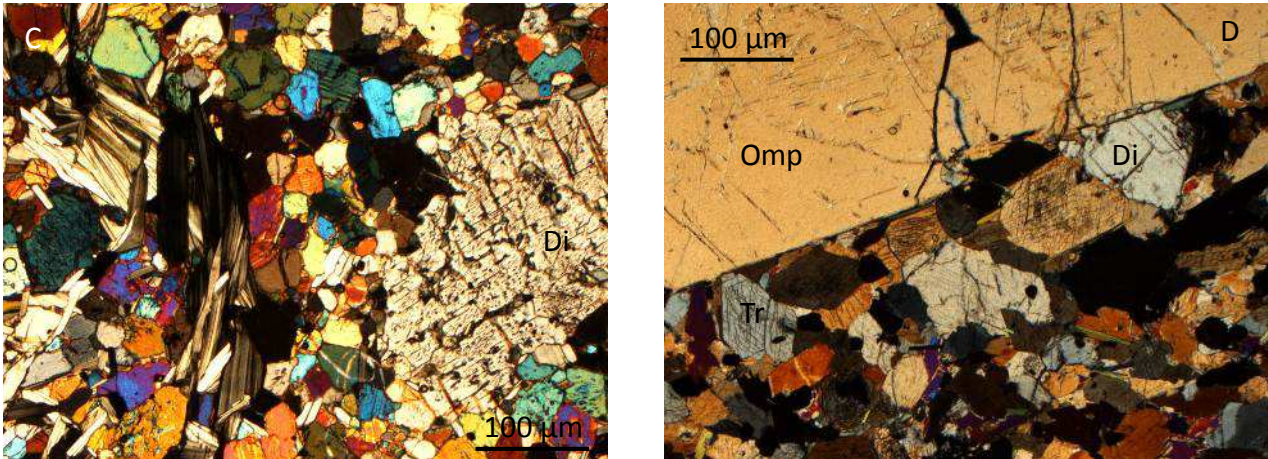


Fig. 4.24: (A) hexagonal-shaped textural relicts, composed by fine-grained Atg suggest the presence of Ol in Atg-serpentinite (crossed polars); (B) mm-thick main foliation of Atg-serpentinite marked by medium- to fine-grained Atg, Tr, Wm and Mg-Chl (crossed polars); (C) Di relic with numerous inclusion of very fine-grained Ilm crystals, rimmed by fine-grained Di + Tr granoblastic aggregates in metapyroxenite (crossed polars); (D) coarse-grained Omp crystal rimming a medium- to fine-grained Tr, Di, Ph and Phl aggregate in metapyroxenite (crossed polars).

4.4.7 Chlorite-amphibolite microstructure

The average composition of chlorite-amphibolite is gren amphibole (55%), Chl (20%), Ep (10%), Wm (10%) and Omp (5%), with Ksp, Qtz and Ab as accessories.

Syn-D1 relicts are represented by pale-green amphibole cores, with exsolutions of Wm along the cleavage planes of amphibole (Fig. 4.25A). Most of the chlorite-amphibolite D1 minerals recrystallize parallel to the new cm-spaced S2 foliation (Fig. 4.25B), marked by Amp, Chl, Omp, Ep and Wm SPO.

During D5 only corona type reactions occur in poorly deformed domains with partial recrystallization and grain size reduction of Act, Wm, Ep and Chl boundaries. Along D5 shear planes and related fractures large amounts, up to 40% in volume, of fine-grained Fe-Chl, Ab, Wm and Ep can develop. Locally medium-grained K-feldspar occurs in fractures.

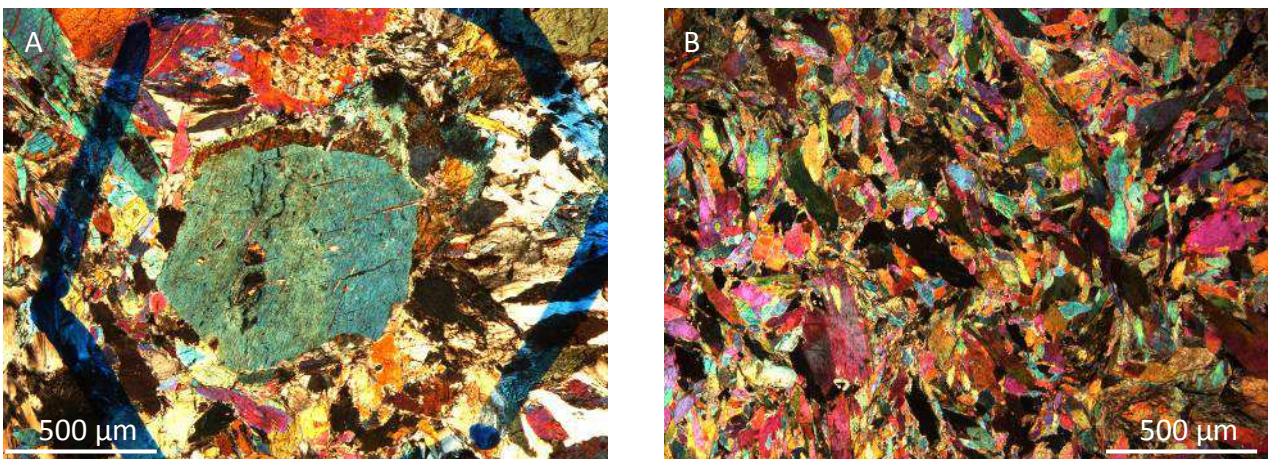


Fig. 4.25: (A) coarse-grained Amp core with Wm inclusions rimmed by syn-D2 Amp (crossed polars); (B) mm-thick S2 foliation mainly marked by medium- to fine-grained Amp with minor Wm and Chl fine-grained crystals (crossed polars).

4.4.8 Grt-, Omp-, Gln- and Zo-bearing veins microstructure

Grt-bearing veins are composed by pinkish garnet forming fine- to coarse-grained idiomorphic poikiloblastic crystals (Fig. 4.26A). In veins within amphibole-rich layers of the amphibole-bearing eclogite, garnets have skeletal textures and are rimmed by syn-D2 Grt. Grt-bearing veins crosscutting S2 foliation are formed by aggregates of fine-grained idioblastic Grt.

Omphacite-bearing veins have average composition of Omp (50%), Ph (20%), Qtz (20%) and Gln (10%); Omp and Gln have a composite complex zonation, probably due to a compositional change of the fluid phase during their crystallization (Fig. 4.26B). During D3 and D5 fine-grained recrystallization of phengite and quartz occur.

Gln-bearing veins have average composition of Gln (80%), Wm (15%) and Zo (5%). Gln and Ep rims around Amp and Zo, respectively (Fig. 4.26C), and Wm grain size reduction occur during D5 deformation stage (Fig. 4.26D).

Zo-bearing veins are composed of idioblastic fine-grained zoisite or Czo, locally rimmed by syn-D5 epidote.

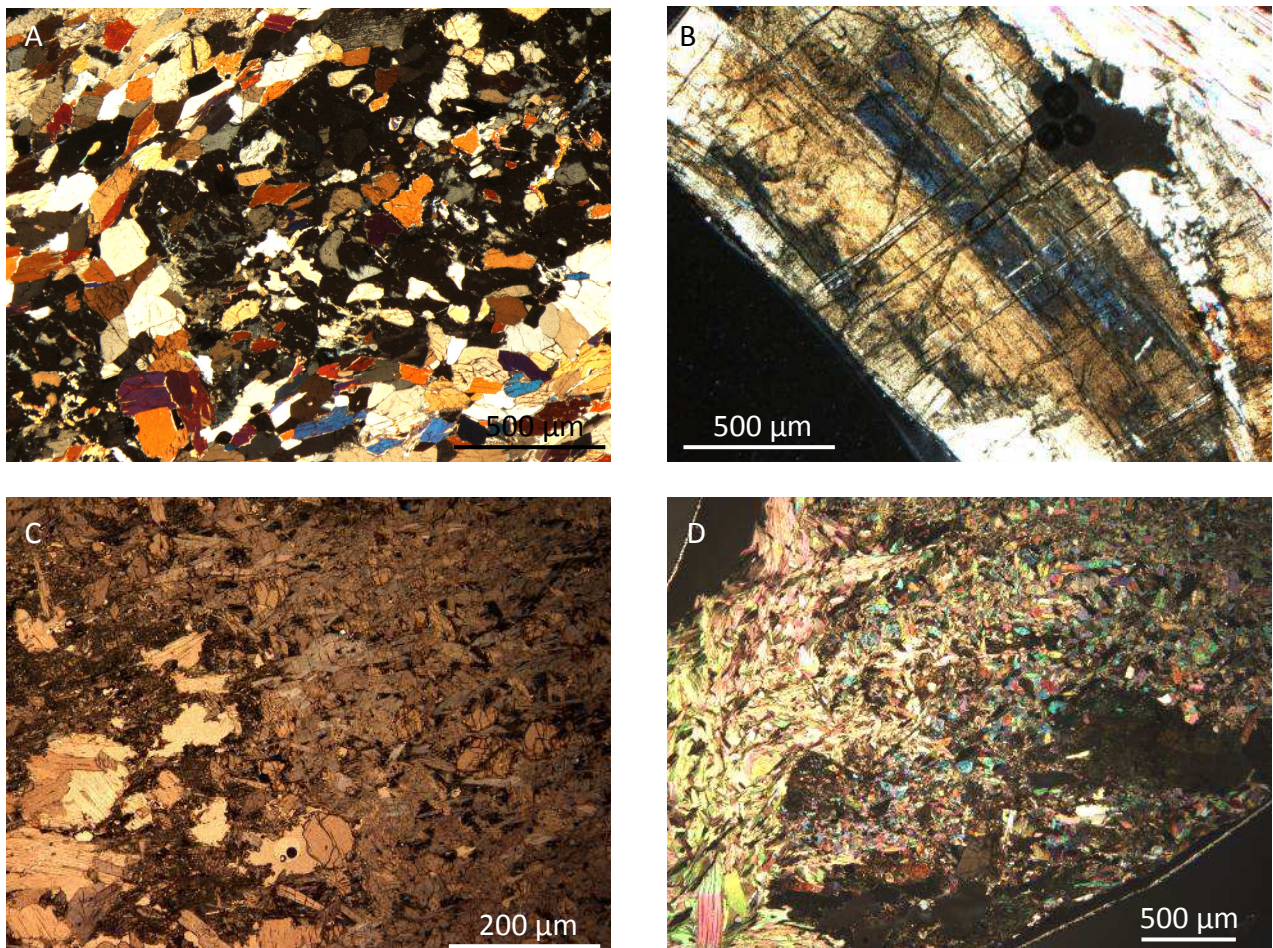


Fig. 4.26: (A) coarse-grained skeletal Grt crystals in Amp of the amphibole-bearing eclogite (crossed polars); (B) coarse grained Omp with composite complex zonation marked by different crystal planes orientation (crossed polars); (C) amphibolized rim/margin of a Gln bearing vein in amphibole-bearing eclogite (plane polarized light); (D) Gln-bearing vein boundary and inner filling of coarse-grained Ph deformed and recrystallized in S5 shear planes (crossed polars).

4.5 Fabric evolution vs reaction progress

In the Ivozio Complex relationships between degree of planar fabric evolution and progress of metamorphic reactions could not be evaluated with a good confidence for the evolution comprising D1 and D2 stages due to the absence of pre-Alpine mineral relicts and to the widespread eclogite-facies mineral growth within all lithotypes during D2.

During the successive deformation stages the degree of metamorphic transformation (evaluated as the % in volume of syn-tectonic minerals) proportionally increases with the increase in degree of fabric evolution. During D3 only LD and MD domains occur and the volume occupied by new minerals rises up to 20% in the crenulated portions of fold hinges. HD domains developing only during D4 and D5 as shear zones are characterised by widespread mineral transformations, up to 90% in volume, both under blueschist and greenschist facies conditions. In LD and MD syn-D5 domains coronitic pseudomorphic partial substitution never exceed 10%, with some exception for Grt crystals that are locally widely replaced by Chl aggregates in MD domains.

4.6 Mineral chemistry of the Ivozio Complex assemblages

4.6.1 Samples selection and analytical technique

A selection of 31 thin sections including the most representative mineral assemblages and microstructural textures, of samples from all the lithotypes, pre- and post-D1 veins of the Ivozio Complex, have been carbon coated for electron microprobe analysis. The JEOL 8200 Super Probe of the Earth Science Department "A. Desio", equipped with WDS X-ray spectrometer system (detectable wavelength 0.087 to 9.3 nm) with hairpin type tungsten filament has been used with 15 kV accelerating voltage and 15 nA beam current.

The analysed samples comprise: nine thin sections for each amphibole- and zoisite- eclogite; four metapyroxenite samples; three amphibole-epidote-bearing eclogite samples; three pre-D1 veins samples; one from each vein type and finally one sample of quartz-rich eclogite; Atg-serpentinite and chlorite-amphibolite each.

The detection of variations in mineral composition have been performed selecting grains occupying microstructural sites of known relative age in the meso- and micro-structural deformation history to ensure the quality of metamorphic evolution reconstruction, especially considering mineral phases that have a wide stability field as amphibole, clinopyroxene, garnet, white mica, epidote and chlorite.

A selection of most representative analysis growing during deformation stages is provided at the end of this chapter (Tabs. 4.1 – 4.11).

4.6.2 Amphibole group

In amphiboles (Tabs. 4.1-4.3), as already evidenced by the large colour variations, a wide compositional range is observed (Figs. 4.27): Fe-Mg-Amp, gedrite (Ged) and anthophyllite (Ath); Ca-Mg-Amp, tremolite (Tr); Na-Mg-Amp, eckermannite (Eck), richterite (Rct) and glaucophane (Gln); Ca-Mg-Fe Amp, actinolite (Act), barrosite (Brs) and winchite (Wnc); Ma-Ca-Mg-Fe-Amp, pargasite (Prg). Ranges of amphibole compositions are controlled by bulk chemistry of rocks in which they are found and variations in composition between grains occupying different microstructural sites are not so significant. Nonetheless, considering each lithotype, compositional trends in amphiboles, related to different microstructures and described in detail in the

following, suggesting a metamorphic evolution marked by an increase in T and P from D1 to D2 stages and a P-T retrograde evolution from D2 to D5 stages.

Cores of porphyroclastic amphiboles are defined by the presence of large amounts of very fine inclusions of Ttn, and are widespread in all lithologic types, representing relics of pre-Alpine Ti-rich Amphibole, probably hornblende (Fig. 4.28A and Fig. 4.28B).

In chlorite-amphibolite pre-D2 Ath cores, with white mica inclusions parallel to cleavages, have two rims (Fig. 4.28C and 4.28D): the first one is syn-D2 Na-rich Amp, the second one syn-D5 Act (Figs. 4.27C and 4.27B). White mica associated to the Ath cores has less phengitic component than the Na-rich Amp.

In amphibole-bearing eclogite amphibole inclusions in syn-D1 garnet and syn-D2 omphacite are edenitic and actinolitic hornblende. Those included in syn-D2 Omp may have a rim of syn-D2 Rct (Figs. 4.27B and 4.29A). Locally the syn-D2 zonation of Amp included in Omp shows a composite oscillatory zonation of the Fe content, changing from Fe = 0.6 a.p.f.u., in Ed, to Fe = 1.6 a.p.f.u., in Na-Amp. During D3 Amp ranges between Na-Amp and Ed, with higher Fe- and Ca-content and lower Mg- and Al-content than syn-D2 Amp (Figs. 4.27N and 4.29B). As stated before the D4 deformation stage is observed only in amphibole-bearing eclogite, and related to the development of mm-thick S4 foliation marked by Mg-rich Na-Amp and phengitic white mica; amphibole and white mica are very similar in composition to those of the Gln-bearing veins.

In amphibole-epidote-bearing eclogite some relict cores of edenitic hornblende occur within S2 foliation, which in turn is marked by syn-D2 Prg, with very-thin rims of post-D2 Ed (Figs. 4.27B). This latter is mainly characterized by higher iron content than pre-D2 Amp.

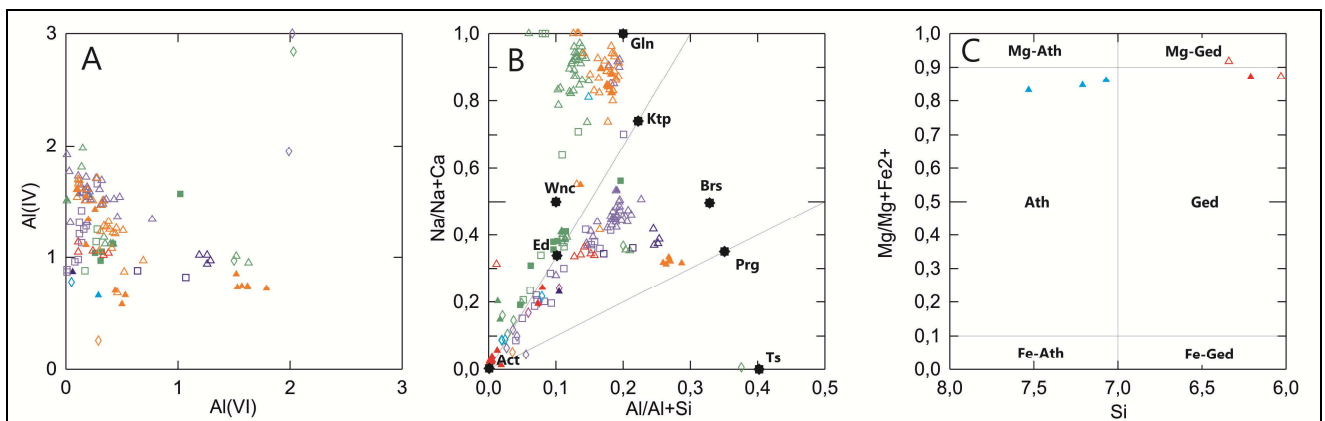


Fig. 4.27: Al(VI) vs Al(IV) diagram (A) and classificative diagrams of Ca-Na (B) and Fe-Mg (C) amphiboles from lithologic types of Ivazio Complex; in diagram B the stars locate end-member composition (Act = actinolite; Brs = barrosite; Ed = edenite; Gln = glaucophane; Ktp = katophorite; Prg = pargasite; Ts = tschermakite; Wnc = winchite). Different colors identify rock types and symbols deformation stages: in red ultramafic rocks; in green amphibole-bearing eclogite; in dark blue amphibole-epidote-bearing eclogite; in violet zoisite-bearing eclogite; in light-blue chlorite-amphibolite; in orange pre-D1 veins; D1 = full triangle for; pre-D1 = full triangle for pre-D1 bearing veins; pre-D2 = full triangle for ultramafic rocks (in Fe-Mg amphiboles from Atg-serpentinites the full triangle is syn-Atg foliation Amp and open triangle represents post-Atg foliation); D2 = open triangle; D3 = open box; D4 = full box; D5 = open diamond.

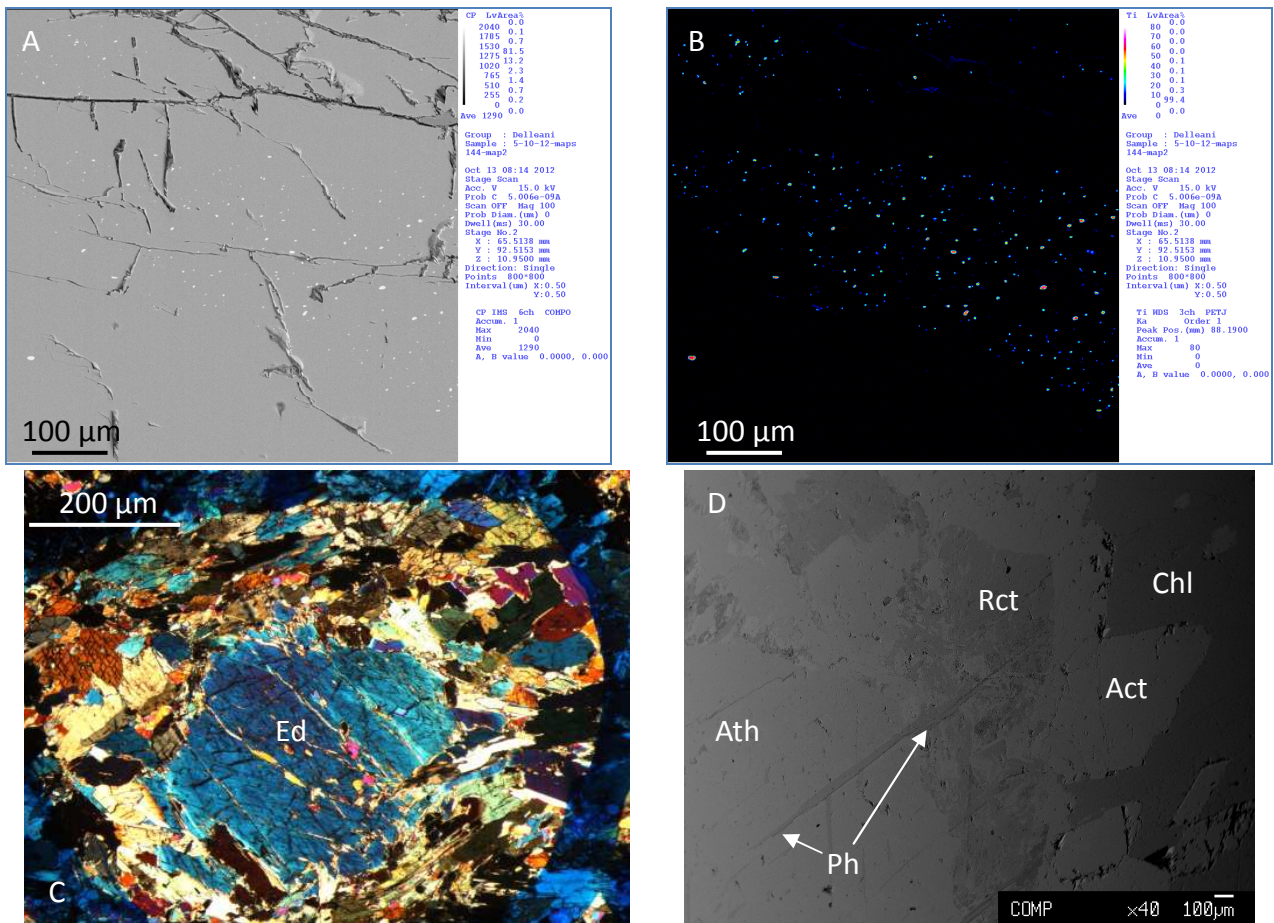


Fig. 4.28: (A/B) compositional mapping of Amp syn-D1 in amphibole-bearing eclogite, Amp core in which the innermost part of the crystals is evidenced by the Ttn very fine-grained inclusions: BSE image (A) and Ti content map (B); (C) porphyroclastic Ed core relict in amphibole-epidote-bearing eclogite wrapped by S2 foliation (D) Syn-D1 Ath core including with the mica and rimmed by Na-Amp and syn-D5 Act (BSE image).

In zoisite-bearing eclogite amphiboles are Ed and Act forming from D1 to D5 stages, only during syn-D2 some Na-rich Amp develops. Edenitic hornblende associated with titanite, epidote and carbonate (Cc) crystals develops in tension gashes during D5. Ed or Act occurrence is related to the local abundance of Al in the system and they present a retrograde depletion of Na and increasing of Ca from D2 stage to D5 stage.

In quartz-rich eclogite, only syn-D5 actinolitic hornblende was analyzed and shows: Al = 0.5-0.9; Fe = 1.1-0.6; Mg = 3.8-4.1; Ca = 1.7-1.8; Na = 0.4-0.5.

Ultramafic rocks present different Amp types. In Atg-serpentinite the Amp associated to the main mm-thick Atg foliation is Mg-rich Ged, rimmed by Si-richer Ged (Fig. 4.27C); in clinopyroxenite amphiboles are Tr or Act and develop during D1, D2 and D5 deformation stages, but no significant compositional variation could be observed. In the clinopyroxenite with abundant phengite and phlogopite, the amphiboles have higher Na content than pyroxenite poor in phengite and phlogopite. In the first type edenitic hornblende develops during D2 (Na = 0.81 to 0.85 a.p.f.u.) is observed from syn-D1 to syn-D2 grains, suggesting a pressure increase.

In pre-D1 stage veins Amp crystals were analyzed only within Qz- and Amp- and white mica-bearing veins: in Amp- and white mica-bearing veins Prg pre-D1 cores are rimmed by syn-D2 Wnc (Fig. 4.29.B); in Qz-bearing veins Na-Ca amphibole cores, constituted by Prg or Na-Amp (Fig. 4.27B), are rimmed by a composite zonation of Na-Amp, defined by the alternance of Rbk, Gln and Fe-Gln (Fig. 4.29C). The Na-Ca amphibole cores can be related to D1 or pre-D1, and the composite zonation occurs during D2. As a matter of fact, the idioblastic shape of late Gln marks S2 foliation within Qz-bearing veins. In Amp- and white mica-bearing veins, Prg cores,

with large amounts of chlorite along cleavage planes, are rimmed by pre-D2 Ed with high Na content (Fig. 4.29D).

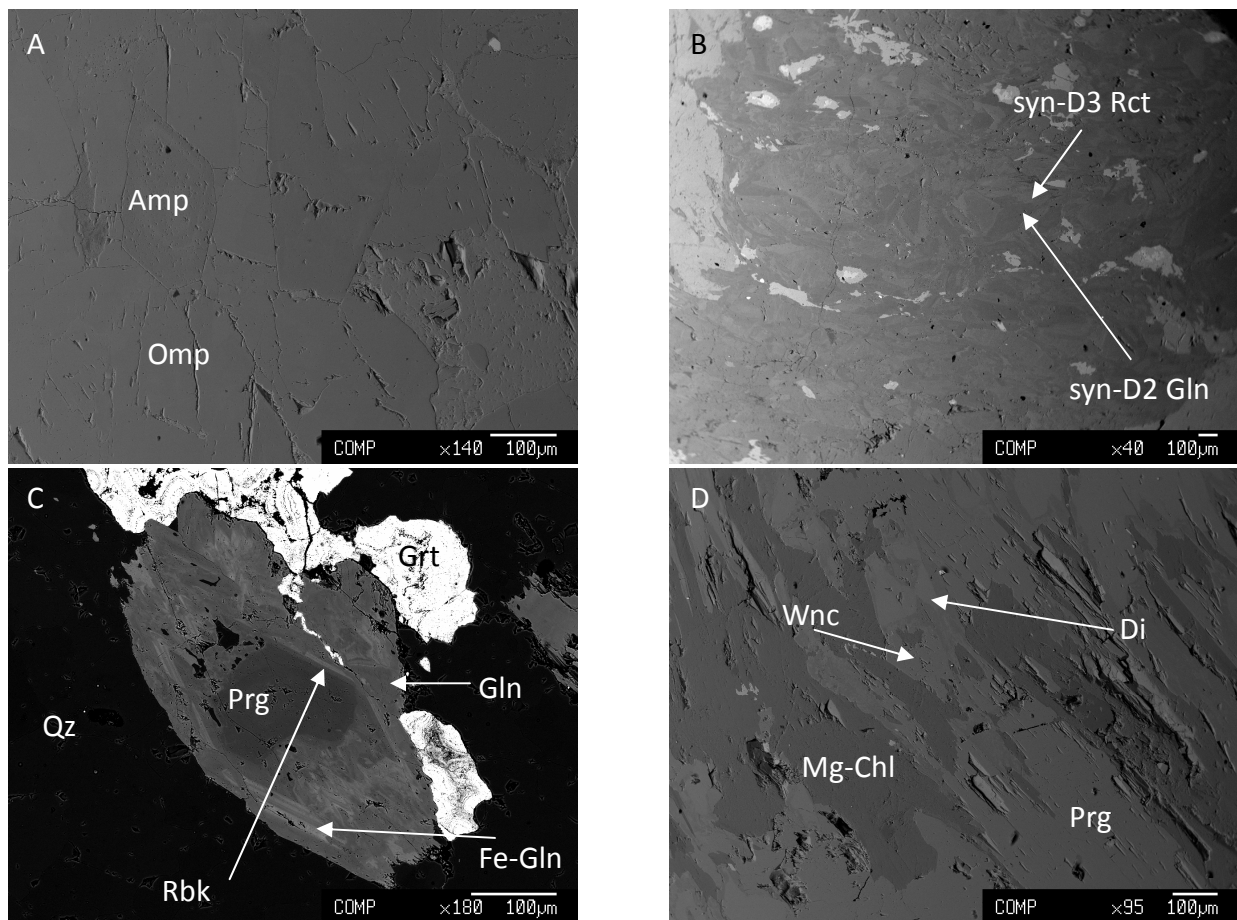


Fig. 4.29: (A) Syn-D2 coarse-grained Omp including zoned Amp crystals in amphibole-bearing eclogite (BSE image); (B) fine-grained syn-D3 Amp recrystallization of syn-D2 Na-rich Amp in amphibole-bearing eclogite (BSE image); (C) composite rim zoning of Gln, Fe-Gln and Rbk involving Prg core, in Qz-bearing vein comprised within amphibole-bearing eclogite (BSE image); (D) coarse-grained Prg cores with inclusion of Mg-Chl parallel to cleavages rimmed by Ed in Amp- and white mica-bearing vein comprised within zoisite-bearing eclogite (BSE image).

4.6.3 Clinopyroxene group

Clinopyroxenes (Tabs. 4.4 and 4.5) are mainly represented by omphacite with a Jd from 20% to 60% and small quantities of AcM component in eclogites, whereas Di-richer Cpx are detected in metapyroxenites and Amp and white mica-bearing veins. The compositional variation is principally influenced by the relative age of crystal formation: they are richer in sodium when syn-D2 and then have a retrograde zonation with post-D3 Q-rich Cpx (Fig. 4.30A) according to Morimoto (1988).

In amphibole-bearing eclogite clinopyroxenes are Omp, with Jd content from 40 to 50% and they crystallized during D2. Q-richer Cpx forms during the successive D3 and D5 stages, suggesting a retrograde zonation.

In amphibole-epidote-bearing eclogite Jd content in Cpx never exceeds 20% of Jd within S2 but in post-D3 stage rims of AcM-rich Cpx are common.

In zoisite-bearing eclogite the average composition of large centimetric post-S2 omphacite crystals and of small syn-S2 omphacite have Jd content of about 45%; rarely some large omphacites overgrowing S2 have a minimum Jd content of 40%. The absence of chemical composition changes are interpreted as due to the continuous formation of Omp during a stage of progressive deformation with localized strain gradient in

different volumes of the rock during D2. In Omp-bearing veins occurring within zoisite-bearing eclogite, clinopyroxenes have cores with 48% Jd without Acm, rimmed by a Jd-poor Cpx with Acm up to 15%.

The Cpx richer in Jd occurs in quartz-rich eclogite, where syn-D2 Omp has Jd up to 60% (Fig. 4.30A).

In both zoisite-bearing and quartz-rich eclogite in post-D3 stage an almost pure Di forms thin rims on the previous Cpx.

In the pyroxenite with no or scarce Ph and Phl, Cpx is an almost pure Di with no chemical variations related to the crystallization during D1 or D2. In rocks with Ph and Phl, the two Cpx occur: the higher Na content characterizing this type of pyroxenite show up to 25% in Jd.

In Ep- and in Amp- and white mica-bearing veins cores of Di-rich Cpx are rimmed by syn-D2 Omp with 40% Jd (Figs. 4.30A and 4.30B).

In Qz-bearing veins omphacites have cores with about 45% Jd and show a composite zonation evidenced by the Acm content: rims are composed by alternances of Cpx with up to 15% Acm, similar to the cores, and Cpx with no Acm and 45% Jd (Figs. 4.30A, 4.30C and 4.30D).

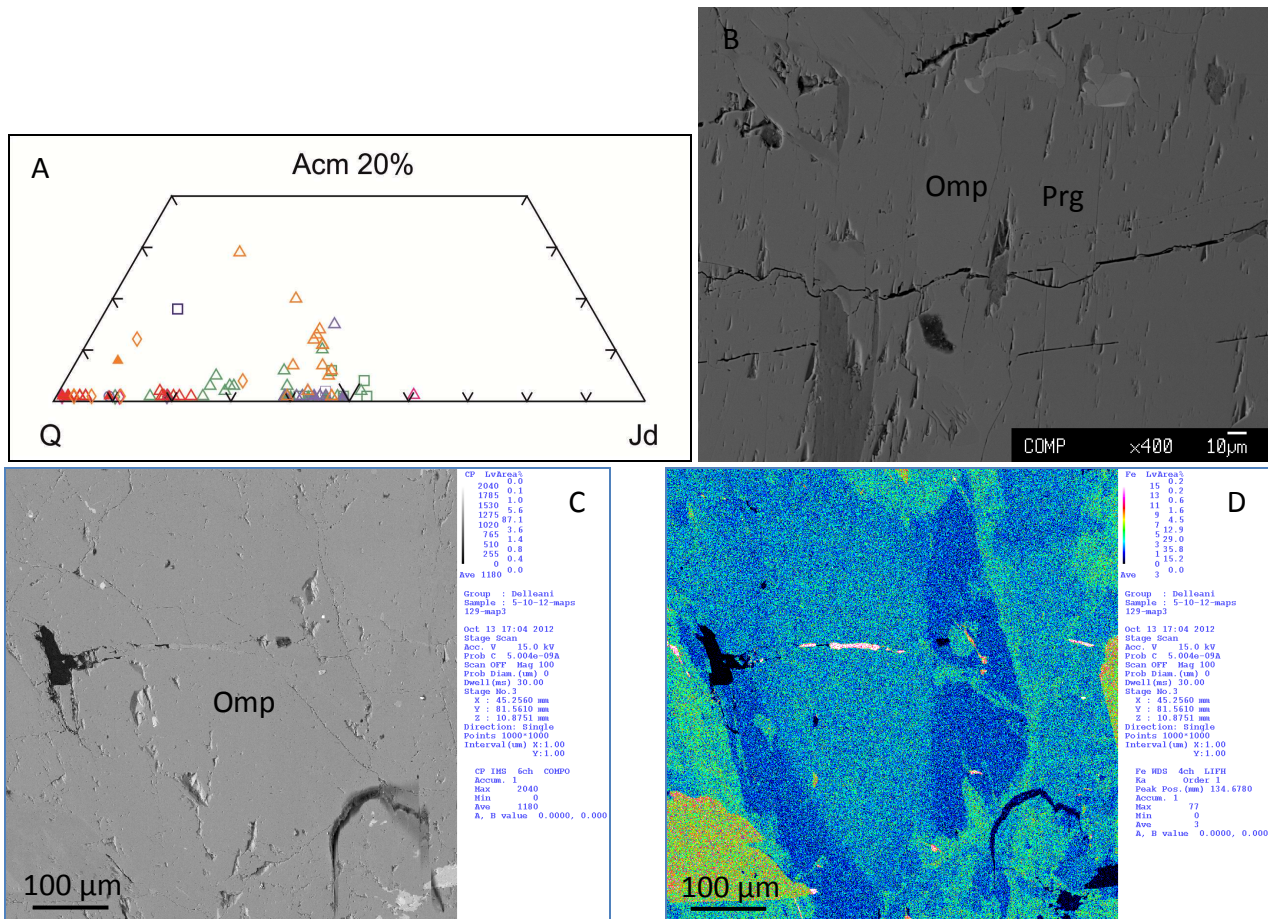


Fig. 4.30: (A) Clinopyroxene compositions (Morimoto, 1988) from lithologic types of Ivozio Complex. Different colors identify rock types and symbols deformation stages: in red ultramafic rocks; in green amphibole-bearing eclogite; in dark blue amphibole-epidote-bearing eclogite; in violet zoisite-bearing eclogite; in pink quartz-rich eclogite; in orange pre-D1 veins; pre-D2 = full triangle; D2 = open triangle; D3 = open box; post-D3 = open diamond. (B) Syn-D2 Omp relicts occurring within pre-D1 bearing veins; (C/D) coarse-grained Omp with poorly defined zoning in the BSE image (C) is zoned, as shown in the Fe concentration compositional map (D).

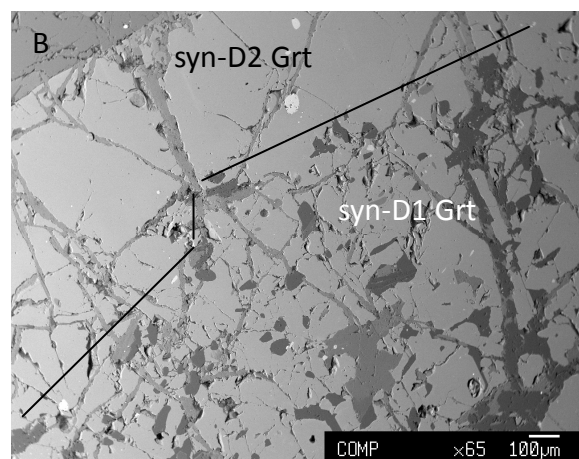
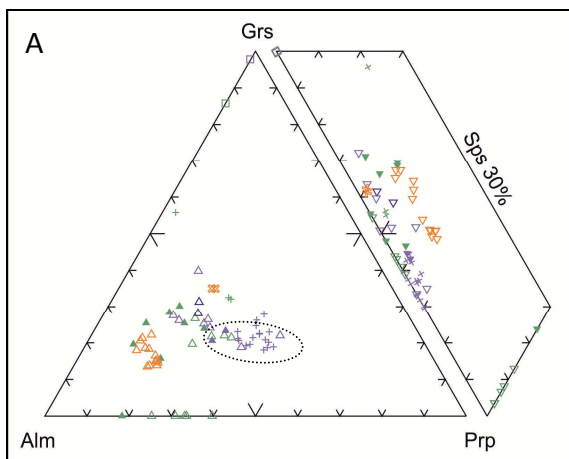
4.6.4 Garnet group

Garnets (Tab. 4.6) have large compositional variations ranging from almost pure Grs to non-calcic Grt, with a variation in Fe-Mg ratio. These differences are mostly due to the lithologic type where garnets are found, similarly to what already described for amphiboles, with minor compositional differences related to the deformative stage of formation (Fig. 4.31A).

In amphibole-bearing eclogite Grt generally has a D1-D2 zonation (Figs. 4.31A and 4.31B) marked by enrichment in Prp and decrease in Sps and Alm end-members, probably due to the increase in P and T conditions. Grt from mylonitic S2 foliated amphibole-bearing eclogite are Grs-free, probably due to the synchronous growth of large amount of Omp adsorbing all the Ca available in the system. Grt occurring in Grt-bearing veins has composition very similar to the syn-D2 crystals of Omp-bearing layers (Figs. 4.31A and 4.31C); locally these crystals have micro-fractures filled by Grt with composition of 35% Alm, 5% Prp, 50% Grs and 10% Sps (Fig. 4.31D).

In amphibole-epidote-bearing eclogite only poikiloblastic syn-D2 Grt occurs, with average composition of 45% Alm, 30% Prp, 25% Grs and >5% Sps (Fig. 4.31A).

In zoisite-bearing eclogite garnets from medium-grained tectonic to mylonitic S2 foliated rocks have a compositional zoning from Alm-rich syn-D1 cores, with 45% Alm, 35% Prp, 20% Grs and >5% Sps, to Prp-rich syn-D2 rims, with 35% Alm, 45% Prp and 15% Grs (violet full and open triangles plotting in the dashed elliptical field in Fig. 4.31A), however in fine-grained syn-D2 mylonitic textures garnets have composition poorer in Prp (50%Alm, 25% Prp, 25% Grs and < 5% Sps). Garnets occurring in Grt-bearing veins have cores with 40% Alm, 35% Prp, 20% Grs and >5% Sps rimmed by syn-D2 Grt with 70% Alm, 15% Prp, 15% Grs and > 5% Sps (Figs. 4.31C and 4.31D). Locally, in post-D3 micro-fractures in Grt crystals, thin filling of almost pure Grs occurs.



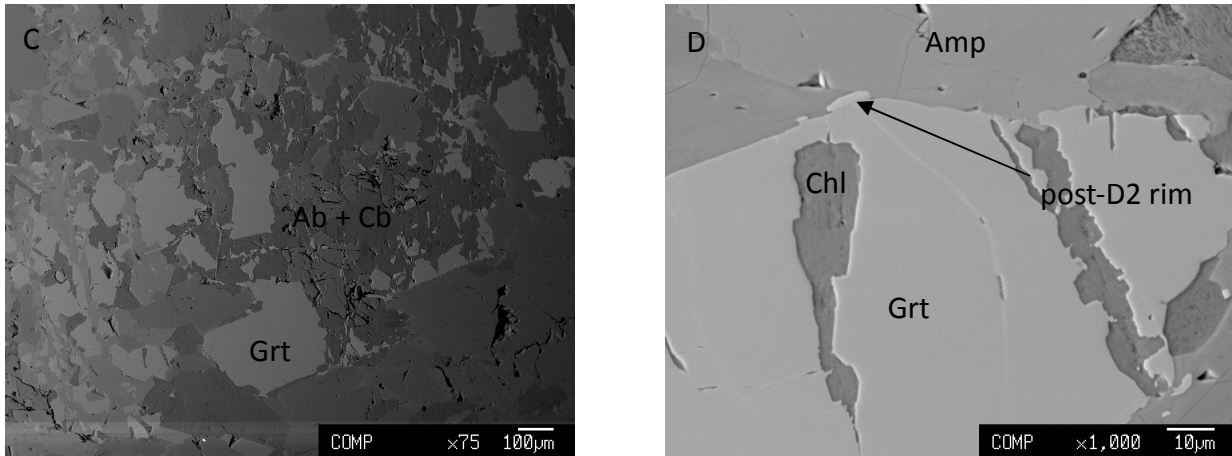


Fig. 4.31: (A) compositional range of garnets from lithologic types of Ivozio Complex. Different colors identify rock types and symbols deformation stages: in green amphibole-bearing eclogite; in dark blue amphibole-epidote-bearing eclogite; in violet zoisite-bearing eclogite; in yellow pre-D1 veins; D1 = full triangle; D2 = open triangle; D5= full box; (B) syn-D1 Grt with numerous inclusions of Amp, Qz and Rt rimmed by syn-D2 Grt (inclusion-free) in amphibole-bearing eclogite (BSE image). C and R indicates syn-D1 and syn-D2 Grt represented as full and open green triangles in the diagram of Fig. (A); (C) skeletal- Grt in Grt-vein of an amphibole-bearing eclogite: Grt is partially substituted by Ab and Cb aggregate (BSE image); (D) enlargement of Fig. (C) evidencing the thin bright rim of post-D2 Grt (BSE image).

In Ep-bearing veins coarse-grained Grt crystals have homogeneous composition, with 42% Alm, 22% Prp, 35% Grs and >2% Sps. The absence of D1 and D2 zonation could be due to diffusion during wide replacement by Chl, substituting syn-D1 and syn-D2 rims.

In Qz-bearing veins Grt included in Amp cores, with 64% Alm, 12% Prp, 20% Grs and 5% Sps, are rimmed by syn-D2 Grt with 62% Alm, 18% Prp, 15% Grs and 5% Sps.

4.6.5 White mica group

White mica (Tabs. 4.7 and 4.8) varies in composition between paragonite and phengite in zoisite- and in quartz-rich eclogite, whereas margarite occurs exclusively in zoisite-bearing eclogite. In the other rocks only one type of white mica occurs, with variable phengitic content (see details in the continuation) due to the metamorphic condition of syn-deformative crystallization and indicating an increase in P passing from D1 to D2 and a decrease in P from D2 to D6 (Fig. 4.32). However, unlike in Amp and Grt, poor data on syn-D1 white mica are available, due to the almost complete re-equilibration of Wm during D2 stage and to the scarcity of white mica inclusions in syn-D1 minerals. Some pre-D2 cores of white mica with $\text{Si}^{4+} = 3.27$ a.p.f.u. locally occur in coarse-grained grains of the Omp-rich layer in the amphibole-bearing eclogite, but they are not clearly related to the syn-D1 stage (Fig. 4.33A).

In chlorite-amphibolite white mica associated to the syn-D1 Amp cores has lesser phengitic component than that associated to the syn-D2 Na-rich Amp.

In amphibole-bearing eclogite syn-D1 white mica is only found as relict cores in Omp layers; it is a phengitic mica with Si^{4+} content of about 3.30 a.p.f.u., whereas the rims and white mica aligned in S2 have a higher, up to 3.42 a.p.f.u., Si^{4+} content. Also white micas marking S4 and filling the Gln-bearing veins have $\text{Si}^{4+} = 3.4$ a.p.f.u..

In zoisite-bearing eclogite and quartz-rich eclogite white mica shows the same chemical evolution recorded during D2 (Fig. 4.33B) and D5 stages; syn-D1 grains are lacking. Grains parallel to S2 foliation always are both phengite and paragonite, with Ph containing $\text{Si}^{4+} > 3.45$ a.p.f.u.. The retrograde evolution of Ph is clearly evidenced by a Si^{4+} decrease in syn-D5 Ph. The compositions of Mrg and Pg occurring in Lws pseudomorphs of

the zoisite-bearing eclogite are discussed separately. Omp-bearing veins contain Ph cores with $\text{Si}^{4+} = 3.4$ a.p.f.u., rimmed by syn-D3 Ph with $\text{Si}^{4+} = 3.32$ a.p.f.u..

In pyroxenite syn-D2 white mica is Ph, with $\text{Si} = 3.45$ a.p.f.u.; thin segregation of Pg along (001) planes occurs. Pg has $K \leq 0.05$ a.p.f.u., whereas Pg content in Ph is about 0.07. Pg formation starts during late-D2 and dynamically recrystallize during D3 crenulation.

White mica in Qz-bearing veins underlines S2 foliation, and has the same value of silica as the syn-D2 Ph of the zoisite-bearing and of the quartz-rich eclogite (3.57 a.p.f.u.) as expected for Qz normative rocks.

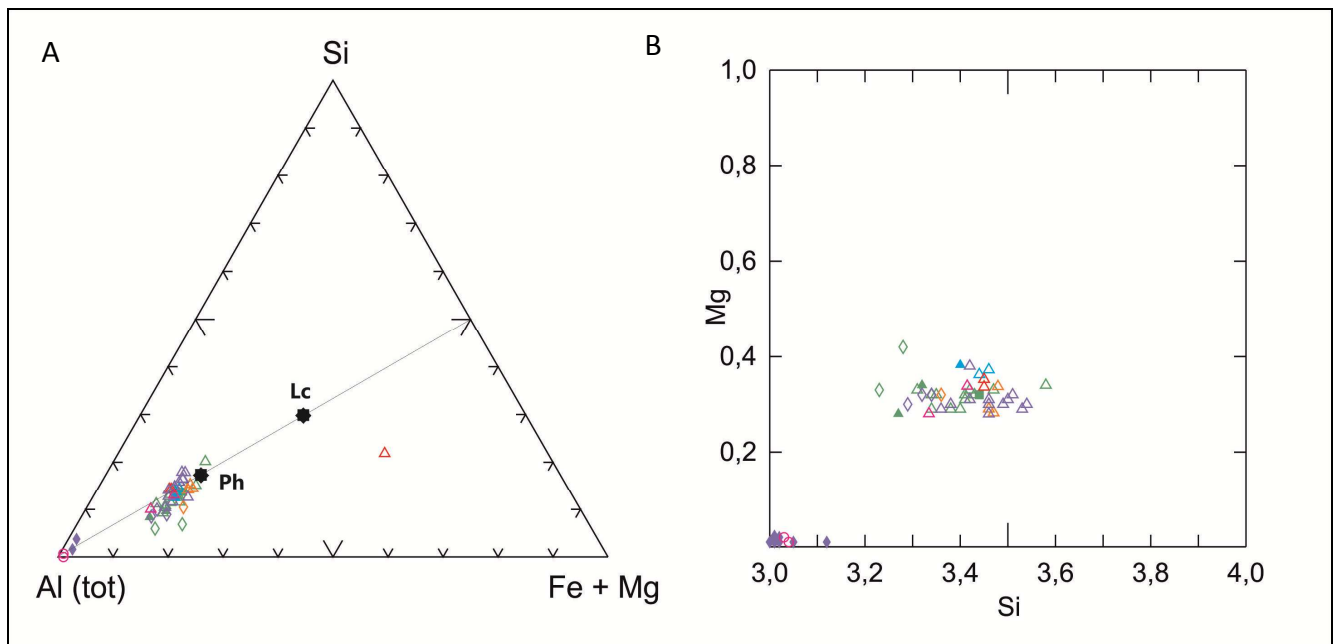


Fig. 4.32: Compositional range of white micas from lithologic types of Ivozio Complex displayed in the ternary diagram (A) of Massonne & Schreyer (1987) and in the Si/Mg (in a.p.f.u.) plot (B). Stars locate end-member composition (Ph = phengite; Lc = leucite). Different colors identify rock types and symbols deformation stages: in green amphibole-bearing eclogite; in violet zoisite-bearing eclogite; in pink quartz-rich eclogite; in light-blue chlorite-amphibolite; in orange pre-D1 veins; D1 Ph = full triangle; pre-D2 Ph = full triangle (in chlorite-amphibolite); D2 Ph = open triangle; D4 Ph = full box; D2 Pg = open diamond; D3 Pg = open circle.

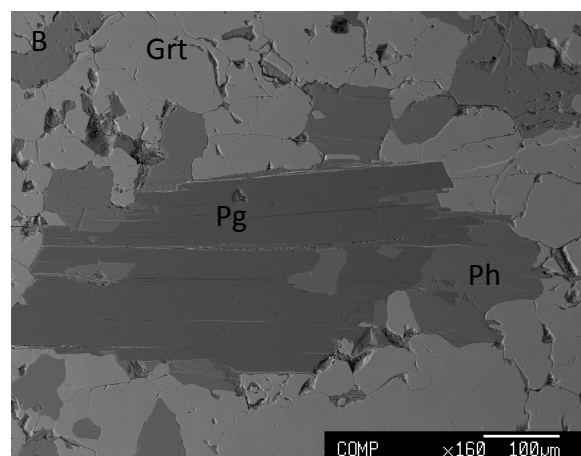
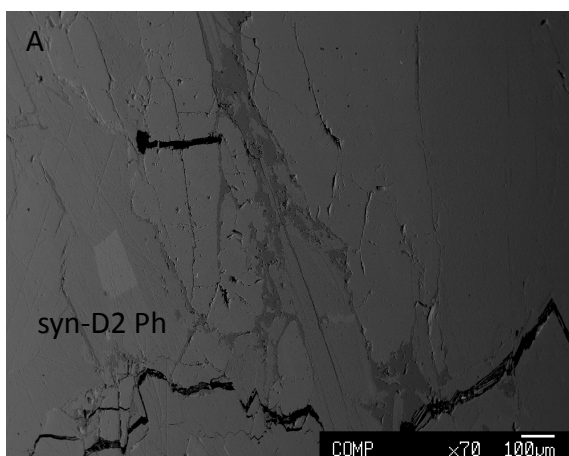


Fig. 4.33: (A) pre-D2 core of Wm rimmed by darker syn-D2 Ph in Omp layer of amphibole-bearing eclogite (BSE image); (B) syn-D2 Pg and Ph aggregate enclosed within syn-D2 Grt aggregate in zoisite-bearing eclogite (BSE image).

4.6.6 Epidote group

Epidote (Tab. 4.9) may have a wide range of Fe content linked to both the different stage of crystallization, and therefore microstructure in which it is observed, and the lithologic type considered.

Ep chemical evolution in zoisite- and quartz, in zoisite- and in amphibole-bearing eclogite is represented by a syn-D1 or syn-D2 pure Zo core rimmed by syn-D3 Czo, with the final growth of syn-D5 Ep (Fig. 4.34A). On the other hand, in amphibole-epidote-bearing eclogite (Fig. 4.34B), Ep-bearing and in Amp- and Wm-bearing veins the initial composition of syn-D1 Ep cores have $Fe \geq 0.4$ a.p.f.u., and are enriched in Fe during the successive deformation stages.

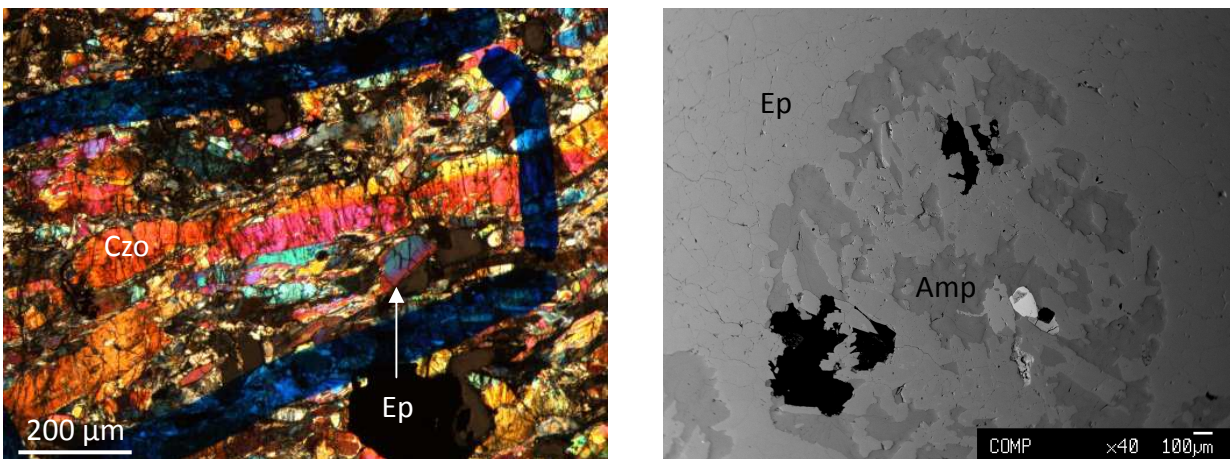
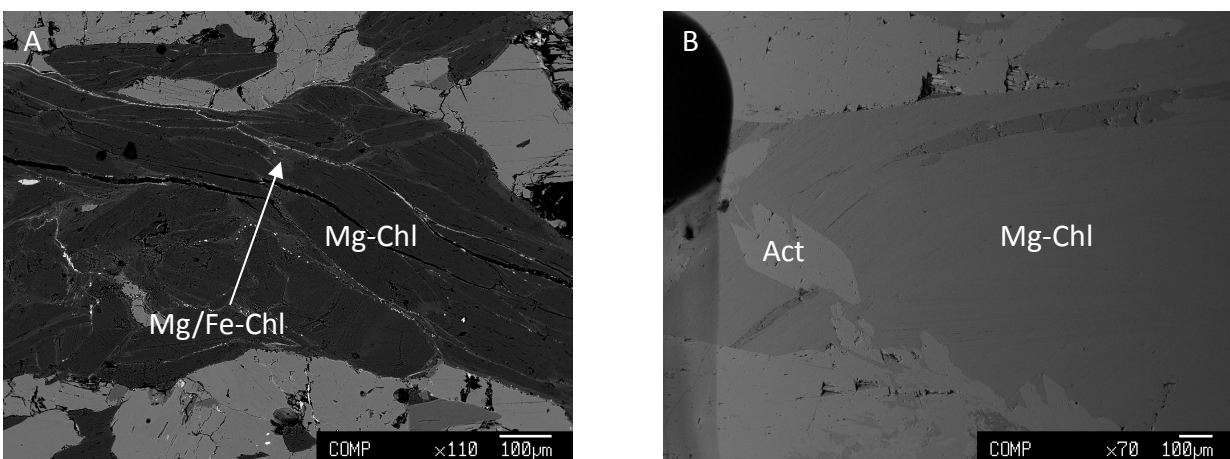


Fig. 4.34: (A) S2 SPO Czo rimmed by syn-D5 Ep in zoisite-bearing eclogite (crossed polars); (B) Ep and Ed fine-grained aggregate in amphibole-epidote-bearing eclogite (BSE image).

4.6.7 Chlorite group

Variations in Mg/Fe ratio of Chl are mainly related to the growth timing with respect to deformation stage. As a matter of fact, Mg-Chl marking the S2 foliation is widespread in all lithologic type, and it is commonly rimmed by Fe-Chl formed during D5 stage (Fig. 4.35A). The Mg/Fe ratio is generally comprised between 2.0 and 3.0 in most of lithologic types (Tab. 4.10, Fig. 4.35B), except for the ultramafic rocks in which the ratio is generally >3.0 and ≤ 7.0 , with $Fe = 0.4$ a.p.f.u. and $Mg = 2.8$ a.p.f.u.. Aggregates representing possible Ol textural relics are composed by Cr-rich Chl and Atg (Fig. 4.35C and 4.35D).



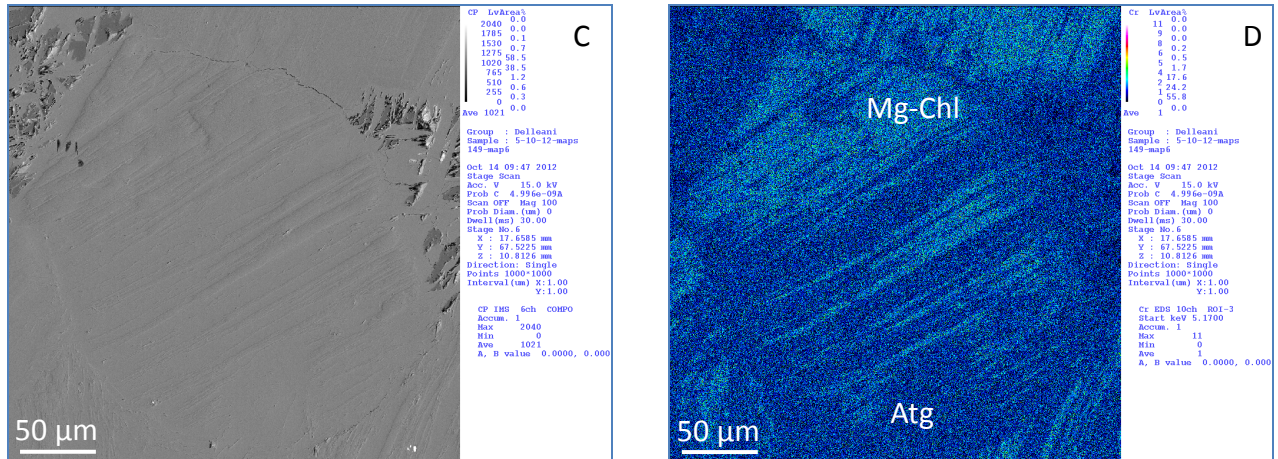


Fig. 4.35: (A) Syn-D2 Mg-Chl aggregate rimmed by lighter Fe-rich syn-D6 Chl in clinopyroxenite (BSE image); (B) Syn-D2 Mg-Chl crystals crosscut by idioblastic syn-D5 Act, with Ab filling parallel to the Chl cleavage in chlorite-amphibolite (BSE image); (C/D) Ol-bearing hexagonal textural relict substituted by Atg + Mg-Chl, (C) BSE image, in which Chl have a high Cr content as evidenced by the compositional map in (D).

4.6.8 Serpentine, carbonate, phlogopite and talc group

These minerals occur only in ultramafic rocks. Srp, Tlc and Cb are observed in Atg-serpentinite and Phl occurs only in clinopyroxenite (Tab. 4.11).

Atg and Tlc form poorly to non-zoned Mg-rich crystals with SPO parallel to the main foliation (Fig. 4.36A), crosscut by Mg-rich Ctl. Cb associated to the main Atg foliation of serpentinite are Mgs rich-Cb, with little Fe component, of about 0.1 a.p.f.u..

Phl crystals show a compositional zoning evidenced by cores with a high Ni content of 0.41 a.p.f.u., but without any large variation in the major elements (Fig. 4.36B).

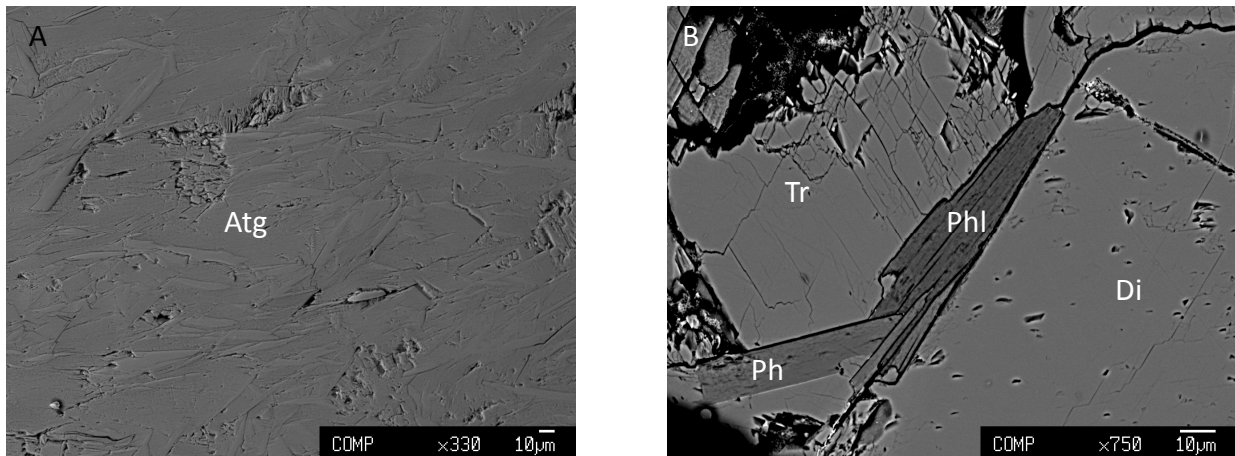


Fig. 4.36: (A) Atg aggregate marking the main foliation in serpentinite (BSE image), variation of lightening are cue to surface inequality; (B) Ph and Phl rimming syn-D2 Tr and Di (BSE image).

4.6.9 Lawsonite textural relicts

Square-shaped pseudomorphs after Lws occurring in zoisite-bearing eclogite have been analyzed. They are wrapped by S2 foliation and have a core of Ky with very fine inclusions of almost pure Zo, Qz and sodium-calcic Amp. Mrg forms in substitution of Ky crystals along microfractures. The composition of Mrg has a higher Ca

content in the portion adjacent to the Ky than far from it (Fig. 4.37A); far from the Ky margin a more Na-rich Mrg + Crn develop. Finally a syn-D2/D3 Pg corona develops around the previous structure (Fig. 4.37B).

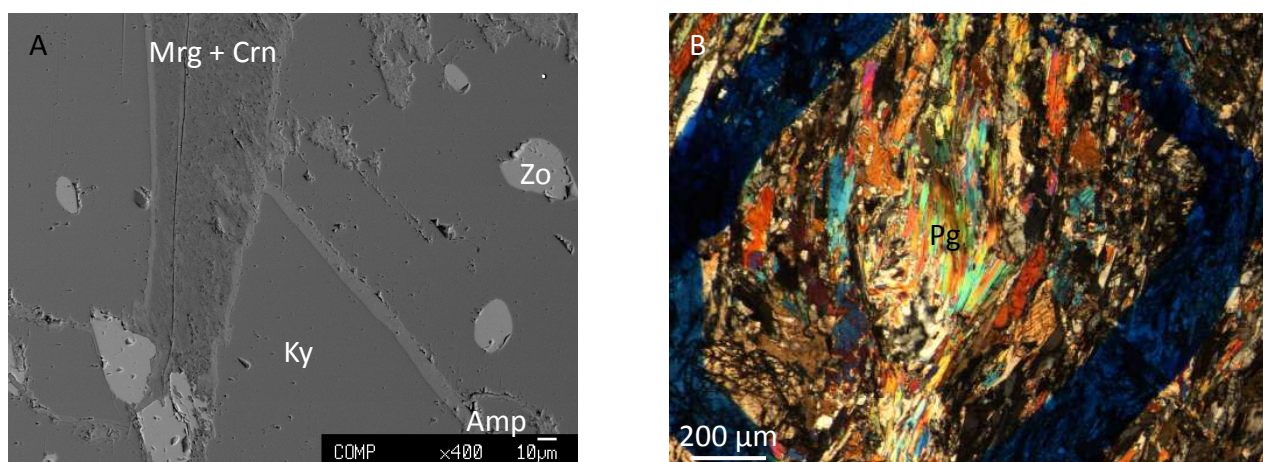


Fig. 4.37: (A) Ky constituting the core portion of a Lws textural relic including Zo and Amp, with Mrg formation among fracture planes and cleavages (BSE image); (B) Syn-D2/D3 complete substitution of Lws textural relic by Pg aggregate in zoisite-bearing eclogite (crossed polars).

	Chlorite-amphibolite			Amphibole-bearing eclogite								Qz-rich eclogite	
	Ath	Rct	Ed	Ed	Act	Rct	Gln	Gln	Gln	Act	Ed	Ed	
Stage	pre-D2	D2	D5	incl. D1 Grt	incl. D1- Cpx	incl. D1- Cpx	D2	D3	D4	D5	D5	D5	
Sample	174	173	175	55	50	52	256	324	293	234	97	99	
SiO ₂	51.92	58.45	57.01	55.38	47.39	56.99	58.10	57.18	55.01	54.26	54.96	54.55	
TiO ₂	0.16	0.04	0.06	0.15	0.14	0.10	0.04	0.02	0.06	0.00	0.09	0.07	
Al ₂ O ₃	5.36	10.49	2.74	8.99	8.74	11.31	11.77	12.12	11.86	1.51	2.93	5.43	
Cr ₂ O ₃	0.10	0.12	0.06	0.08	0.00	0.04	0.03	0.12	0.04	0.00	0.08	0.00	
FeO	5.54	7.19	6.85	3.53	5.39	10.32	11.64	12.62	8.54	15.28	8.41	4.71	
MnO	0.04	0.14	0.20	0.01	0.03	0.04	0.04	0.16	0.03	0.22	0.28	0.03	
MgO	19.19	13.35	18.65	9.29	13.41	9.81	9.37	8.11	10.81	13.55	17.26	18.28	
CaO	11.07	2.63	10.79	15.41	8.45	1.71	1.85	0.86	0.36	12.07	11.35	10.69	
Na ₂ O	0.26	0.02	0.07	5.88	3.20	6.64	6.60	7.29	7.55	0.65	1.26	1.86	
K ₂ O	1.95	6.24	1.48	0.00	0.38	0.04	0.05	0.03	0.04	0.05	0.07	0.10	
Si	8.36	7.71	8.40	7.99	7.73	8.01	7.88	7.88	8.00	7.86	8.28	8.13	
Ti	0.00	0.02	0.01	0.02	0.02	0.01	0.00	0.00	0.01	0.00	0.01	0.01	
Al	1.77	0.94	0.48	1.53	1.68	1.97	1.88	2.09	2.08	0.28	0.52	0.95	
Fe ³⁺	0.00	0.00	0.00	0.00	0.00	0.00	0.07	0.00	0.00	0.00	0.00	0.00	
Fe ²⁺	0.86	0.69	0.84	0.43	0.74	1.27	1.25	1.54	1.06	1.98	1.06	0.59	
Mn ²⁺	0.02	0.01	0.03	0.00	0.00	0.01	0.01	0.02	0.00	0.03	0.04	0.00	
Mg	2.85	4.25	4.10	2.00	3.26	2.16	1.90	1.77	2.40	3.12	3.88	4.06	
Ca	0.40	1.76	1.70	2.38	1.48	0.27	0.27	0.14	0.06	2.00	1.83	1.71	
Na	0.17	0.56	0.42	1.65	1.01	1.90	1.74	2.07	2.18	0.20	0.37	0.54	
K	0.01	0.01	0.01	0.00	0.08	0.01	0.01	0.01	0.01	0.01	0.01	0.02	

Tab. 4.1: Representative analyses of amphiboles from chlorite-amphibolite, amphibole-bearing eclogite and Qz-rich eclogite (incl. = included within).

Name	Zoisite-bearing eclogite						Ultramafic rocks				Amp- and Wm-bearing vein	
	Wnc	Ed	Ed	Ed	Ed	Ed	Ged	Tr	Tr	Tr	Prg	Ed
Stage	pre-D2	incl. Ky	D2	D3	D5 t.gash	D5	S-Atg	pre-D2	D2	D5	pre-D2	D2
Sample	335	409	157	152	193	68	491	35	44	54	371	385
SiO2	53.28	51.81	52.07	50.57	54.45	56.02	56.10	57.96	57.77	59.05	44.47	56.26
TiO2	0.12	0.21	0.13	0.09	0.08	0.02	0.04	0.00	0.00	0.00	0.30	0.04
Al2O3	10.43	11.39	8.55	9.92	5.09	1.78	0.57	0.26	0.11	0.17	13.53	9.48
Cr2O3	0.00	0.01	0.23	0.00	0.03	0.13	0.00	0.19	0.07	0.09	0.00	0.07
FeO	6.93	5.24	6.06	5.56	7.94	8.22	4.84	3.67	4.05	3.99	7.73	3.44
MnO	0.11	0.04	0.09	0.04	0.07	0.27	0.06	0.05	0.09	0.05	0.08	0.07
MgO	14.28	15.72	15.48	14.78	17.44	16.16	30.44	22.06	21.82	22.25	15.24	9.23
CaO	8.16	8.38	8.31	8.15	10.96	12.20	0.04	12.69	12.98	12.87	11.94	15.44
Na2O	3.75	3.63	3.61	3.70	0.13	0.89	0.01	0.29	0.19	0.17	2.99	6.06
K2O	0.17	0.22	0.13	0.20	2.04	0.03	0.02	0.06	0.00	0.04	1.08	0.00
Si	7.82	7.57	8.00	7.69	7.64	8.07	6.34	8.02	8.03	8.07	6.43	8.00
Ti	0.01	0.02	0.00	0.01	0.01	0.00	0.00	0.00	0.00	0.00	0.03	0.00
Al	1.80	1.96	1.44	1.78	0.84	0.32	0.08	0.05	0.02	0.03	2.31	1.59
Fe3+	0.00	0.00	0.00	0.00	0.00	0.00	0.00	0.00	0.00	0.00	0.03	0.00
Fe2+	0.85	0.64	0.53	0.71	0.93	1.06	0.44	0.45	0.50	0.49	0.91	0.41
Mn2+	0.01	0.01	0.01	0.01	0.01	0.04	0.00	0.01	0.01	0.01	0.01	0.01
Mg	3.12	3.42	1.98	3.35	3.64	3.70	5.12	4.84	4.81	4.82	3.29	1.96
Ca	1.28	1.31	2.37	1.33	1.65	2.01	0.00	2.00	2.06	2.01	1.85	2.35
Na	1.06	1.03	1.65	1.09	0.04	0.27	0.00	0.08	0.05	0.05	0.84	1.67
K	0.03	0.04	0.00	0.04	0.37	0.05	0.00	0.01	0.00	0.01	0.20	0.00

Tab. 4.2: Representative analyses of amphiboles from zoisite-bearing eclogite, ultramafic rocks and Amp- and Wm-bearing vein (t.gash = tension gash).

Name	Qz-bearing vein				
	Prg	Wnc	Gln	Fe-Gln	Rbk
Stage	pre-D2	pre-D2	D2	D2	D2
Sample	42	43	44	45	84
SiO2	53.27	53.35	54.51	51.73	50.76
TiO2	0.12	0.16	0.08	0.14	0.21
Al2O3	7.15	6.85	10.51	9.47	8.00
Cr2O3	0.00	0.04	0.03	0.07	0.00
FeO	11.08	11.41	14.33	20.38	24.71
MnO	0.10	0.15	0.12	0.09	0.20
MgO	14.42	13.75	8.56	5.49	4.72
CaO	6.45	6.92	2.43	2.10	2.42
Na2O	4.34	3.96	6.54	6.18	6.48
K2O	0.37	0.28	0.04	0.09	0.15
Si	7.48	7.56	7.72	7.61	7.48
Ti	0.01	0.02	0.01	0.02	0.02
Al	1.18	1.14	1.75	1.64	1.39
Fe3+	0.65	0.46	0.25	0.65	0.96
Fe2+	0.65	0.89	1.45	1.85	2.08
Mn2+	0.01	0.02	0.01	0.01	0.03
Mg	3.02	2.91	1.81	1.20	1.04
Ca	0.97	1.05	0.37	0.33	0.38
Na	1.18	1.09	1.79	1.76	1.85
K	0.07	0.05	0.01	0.02	0.03

Tab. 4.3: Representative analyses of amphiboles from Qz-bearing vein .

Mineral	Amphibole-bearing eclogite								Amphibole-epidote eclogite		Zoisite-bearing eclogite				
	Omp	Omp	Omp	Omp	Omp	Omp	Di	Di	Di	Omp	Omp	Omp	Di		
	D2	D2	D2	D2	D2	D3	post-D3	D2	post-D3	pre-D2	S2	post-D2	post-D3		
Sample	129	133	134		52	51	60	358		505	506	150	338	403	404
K2O	0.00	0.00	0.00	0.00	0.00	0.00	0.38	0.01	0.01	0.61	0.00	0.00	0.01	0.00	
CaO	0.00	0.00	0.01	13.63	13.37	9.63	22.97	20.13	10.25	13.31	13.82	13.98	22.98		
TiO2	0.08	0.10	0.07	0.05	0.12	0.17	0.00	0.10	0.26	0.07	0.07	0.02	0.18		
Cr2O3	0.06	0.12	0.08	0.01	0.08	0.04	0.03	0.01	0.00	0.00	0.03	0.00	0.08		
MnO	0.02	0.03	0.00	0.03	0.00	0.05	0.15	0.02	0.10	0.00	0.00	0.02	0.02		
FeOt	4.39	4.36	4.43	4.04	3.18	6.83	4.64	4.31	11.07	2.48	2.50	2.61	4.15		
Na2O	4.59	4.32	4.55	5.68	5.77	3.18	1.43	2.74	3.44	5.99	6.37	6.36	1.22		
SiO2	56.71	56.43	56.48	53.27	51.74	50.95	55.33	53.67	45.64	54.00	56.15	55.87	54.16		
Al2O3	7.74	7.75	7.44	8.23	8.30	9.02	1.91	5.13	12.04	11.06	11.57	11.42	3.34		
MgO	9.97	10.54	10.38	8.49	8.26	14.47	13.69	12.21	13.12	8.80	8.73	8.78	13.52		
Si	2.43	2.41	2.42	2.04	2.03	1.92	2.02	1.98	1.70	2.00	2.00	2.00	1.99		
Al.IV	0.00	0.00	0.00	0.00	0.00	0.08	0.00	0.02	0.30	0.00	0.00	0.00	0.01		
Al.VI	0.39	0.39	0.38	0.37	0.38	0.32	0.08	0.20	0.23	0.48	0.49	0.48	0.13		
Ti	0.00	0.00	0.00	0.00	0.00	0.00	0.00	0.00	0.01	0.00	0.00	0.00	0.00		
Cr	0.00	0.00	0.00	0.00	0.00	0.00	0.00	0.00	0.00	0.00	0.00	0.00	0.00		
Fe3+	0.00	0.00	0.00	0.00	0.00	0.00	0.00	0.01	0.33	0.00	0.00	0.00	0.00		
Fe2+	0.16	0.16	0.16	0.13	0.10	0.22	0.14	0.12	0.01	0.08	0.07	0.08	0.13		
Mg	0.64	0.67	0.66	0.48	0.48	0.81	0.75	0.67	0.73	0.49	0.46	0.47	0.74		
Mn	0.00	0.00	0.00	0.00	0.00	0.00	0.00	0.00	0.00	0.00	0.00	0.00	0.00		
Ca	0.00	0.00	0.00	0.56	0.56	0.39	0.90	0.80	0.41	0.53	0.53	0.54	0.90		
Na	0.38	0.36	0.38	0.42	0.44	0.23	0.10	0.20	0.25	0.43	0.44	0.44	0.09		
K	0.00	0.00	0.00	0.00	0.00	0.02	0.00	0.00	0.03	0.00	0.00	0.00	0.00		
En%	40.57	42.46	41.90	24.00	23.78	40.73	37.36	33.54	36.00	24.56	23.54	23.57	37.44		
Fs%	10.08	9.93	10.04	6.46	5.14	10.88	7.34	6.15	0.75	3.88	3.78	3.96	6.48		
Q	0.51	0.54	0.52	0.58	0.57	0.75	0.90	0.80	0.70	0.56	0.55	0.55	0.91		
Jd	0.49	0.46	0.48	0.42	0.43	0.25	0.10	0.19	0.12	0.44	0.45	0.45	0.09		
Ae	0.01	0.01	0.01	0.01	0.01	0.01	0.01	0.01	0.18	0.01	0.01	0.01	0.01		

Tab. 4.4: Representative analyses of pyroxenes from amphibole-bearing eclogite, amphibole-epidote-bearing eclogite and zoisite bearing eclogite.

Mineral	Quartz-rich eclogite		Metapyroxenite			Amp- and Wm-vein		Ep- and Grt-vein		Qz-bearing vein		
	Omp	Di	Di	Di	Di	Di	Omp	Omp	Di	Omp	Omp	Omp
	D2	post-D3	D1	S2	ricri D2	in-Amp	D2	D2	post-D3	D2	D2	D2
Sample	92	93	11	219	78	366	377	516	517	51	85	86
K2O	0.00	0.00	0.01	0.00	0.01	0.00	0.00	0.00	0.00	0.12	0.02	0.00
CaO	0.00	11.53	23.88	24.71	24.76	24.50	14.78	13.99	21.63	2.58	12.26	12.38
TiO2	0.11	0.03	0.04	0.03	0.00	0.05	0.10	0.04	0.12	0.13	0.15	0.03
Cr2O3	0.00	0.00	0.09	0.15	0.00	0.08	0.00	0.03	0.00	0.00	0.00	0.00
MnO	0.04	0.23	0.14	0.07	0.10	0.15	0.08	0.19	0.00	0.20	0.13	0.13
FeOt	2.72	7.78	2.63	2.12	1.57	3.80	3.25	6.08	5.02	18.79	7.17	6.51
Na2O	6.25	1.49	0.32	0.17	0.13	0.49	6.48	6.28	1.94	6.61	7.31	7.21
SiO2	57.20	54.91	55.45	54.52	55.68	54.71	56.65	54.89	52.46	53.02	55.42	56.44
Al2O3	11.17	3.36	0.26	0.07	0.04	0.89	10.27	8.85	3.67	10.46	8.99	9.28
MgO	8.74	17.46	16.96	17.06	17.46	15.45	9.08	8.27	13.72	6.55	7.66	7.49
Si	2.34	2.06	2.02	2.00	2.03	2.00	2.00	1.99	1.93	1.99	2.00	2.03
Al.IV	0.00	0.00	0.00	0.00	0.00	0.00	0.00	0.01	0.07	0.01	0.00	0.00
Al.VI	0.54	0.15	0.01	0.00	0.00	0.04	0.42	0.37	0.09	0.45	0.38	0.39
Ti	0.00	0.00	0.00	0.00	0.00	0.00	0.00	0.00	0.00	0.00	0.00	0.00
Cr	0.00	0.00	0.00	0.00	0.00	0.00	0.00	0.00	0.00	0.00	0.00	0.00
Fe3+	0.00	0.00	0.00	0.00	0.00	0.00	0.02	0.07	0.10	0.05	0.13	0.05
Fe2+	0.09	0.24	0.08	0.07	0.05	0.12	0.08	0.11	0.05	0.54	0.09	0.14
Mg	0.53	0.97	0.92	0.93	0.95	0.84	0.48	0.45	0.75	0.37	0.41	0.40
Mn	0.00	0.01	0.00	0.00	0.00	0.00	0.00	0.01	0.00	0.01	0.00	0.00
Ca	0.00	0.46	0.93	0.97	0.97	0.96	0.56	0.54	0.85	0.10	0.47	0.48
Na	0.50	0.11	0.02	0.01	0.01	0.03	0.44	0.44	0.14	0.48	0.51	0.50
K	0.00	0.00	0.00	0.00	0.00	0.00	0.00	0.00	0.00	0.01	0.00	0.00
En%	32.07	50.63	46.42	46.73	47.77	42.20	23.83	22.41	37.29	18.31	20.52	19.76
Fs%	5.68	13.04	4.26	3.36	2.56	6.05	3.90	5.91	2.53	27.46	4.62	7.20
Q	0.39	0.89	0.98	0.99	0.99	0.97	0.56	0.56	0.86	0.51	0.49	0.50
Jd	0.61	0.11	0.02	0.01	0.01	0.03	0.42	0.37	0.07	0.44	0.38	0.44
Ae	0.01	0.01	0.01	0.01	0.01	0.01	0.02	0.07	0.08	0.05	0.13	0.06

Tab. 4.5: Representative analyses of pyroxenes from quartz-rich eclogite, metapyroxenite, Amp- and Wm- bearing vein, Ep- and Grt- vein and Qz-bearing vein.

Mineral	Amphibole-bearing eclogite		Amp-Ep-bearing eclogite	Zoisite-bearing eclogite			Grt veins				Ep- and Grt vein	Qz- vein
	Grt	Grt	Grt	Grt	Grt	Grt	Grt	Grt	Grt	Grt	Grt	Grt
Stage	D1	D2	D2	D1	D2	D3	pre-D2	post-D2 core	post-D2 rim	post-D3	pre-D2	D2
No.	241	240	503	398	397	161	344	437	435	143	511	88
SiO ₂	38.74	38.18	39.42	39.00	40.10	14.86	40.47	35.31	34.81	18.50	39.89	37.82
TiO ₂	0.03	0.02	0.20	0.10	0.01	0.02	0.00	0.05	0.00	0.01	0.06	0.01
Cr ₂ O ₃	0.04	0.00	0.00	0.02	0.00	0.02	0.03	0.05	0.02	0.03	0.00	0.00
Al ₂ O ₃	23.00	22.27	22.56	23.14	23.30	10.34	22.73	20.41	20.50	18.63	22.86	21.37
FeO	23.98	24.75	22.58	23.21	20.84	0.45	18.74	15.24	13.50	0.26	19.81	29.58
MnO	0.39	2.97	1.67	0.78	0.39	0.04	1.02	0.77	0.24	0.02	0.58	2.17
MgO	5.89	3.80	5.72	7.66	9.90	4.16	7.43	7.00	8.69	0.01	6.07	3.06
CaO	9.80	9.74	9.88	7.45	6.94	1.45	11.80	5.62	5.19	7.74	12.86	7.08
K ₂ O	0.00	0.00	0.00	0.01	0.00	0.01	0.00	0.00	0.00	0.00	0.02	0.01
Na ₂ O	0.03	0.02	0.04	0.04	0.04	0.00	0.00	0.02	0.06	0.02	0.06	0.08
Total	101.90	101.76	102.07	101.40	101.52	31.36	102.22	84.47	83.01	45.23	102.21	101.19
Si	2.93	2.94	2.99	2.95	2.98	3.17	3.01	3.10	3.07	2.83	2.99	2.97
Ti	0.00	0.00	0.01	0.01	0.00	0.00	0.00	0.00	0.00	0.00	0.00	0.00
Al	2.05	2.02	2.01	2.06	2.04	2.60	1.99	2.11	2.13	3.35	2.02	1.98
Cr	0.00	0.00	0.00	0.00	0.00	0.00	0.00	0.00	0.00	0.00	0.00	0.00
Fe ₂	1.52	1.60	1.43	1.47	1.30	0.08	1.17	1.12	1.01	0.03	1.24	1.94
Mn	0.03	0.19	0.11	0.05	0.02	0.01	0.06	0.06	0.02	0.00	0.04	0.14
Mg	0.67	0.44	0.65	0.86	1.10	1.33	0.82	0.92	1.15	0.00	0.68	0.36
Ca	0.80	0.80	0.80	0.60	0.55	0.33	0.94	0.53	0.49	1.27	1.03	0.60
Na	0.00	0.00	0.01	0.01	0.01	0.00	0.00	0.00	0.01	0.01	0.01	0.01
K	0.00	0.00	0.00	0.00	0.00	0.00	0.00	0.00	0.00	0.00	0.00	0.00
Alm	50.98	52.65	47.91	49.17	43.61	4.61	38.92	42.69	37.88	2.50	41.54	63.88
Py	22.33	14.41	21.64	28.93	36.94	75.95	27.51	34.96	43.47	0.01	22.69	11.78
Grs	26.69	26.54	26.86	20.22	18.61	19.01	31.41	20.17	18.66	97.41	34.55	19.59
Spss	0.01	6.40	3.59	0.01	0.83	0.01	2.14	2.18	0.01	0.01	1.22	4.75

Tab. 4.6: Representative analyses of garnets from Ivozio Complex rocks.

Stage	Chlorite-amphibolite			Amphibole-bearing eclogite				Amphibole-epidote bearing eclogite			
	D1	D2	D5	pre-D2	in	Omp	D2	S4	D2	D2	D5
Sample	172	176	178	538	228	54	303	156	66	84	
Mineral	Ph	Ph	Ph	Ph	Ph	Ph	Ph	Pg	Ph	Ph	
SiO ₂	51.10	54.43	53.27	48.64	51.66	50.11	52.89	46.95	50.30	49.06	
TiO ₂	0.08	0.09	0.15	0.55	0.54	0.50	0.10	0.05	0.27	0.11	
Cr ₂ O ₃	0.05	0.09	0.08	0.05	0.02	0.00	0.01	0.19	0.20	0.27	
Al ₂ O ₃	27.97	29.19	27.97	30.18	29.74	26.81	27.83	40.01	26.52	27.96	
FeO	1.48	1.43	1.43	1.56	1.78	1.51	2.80	0.27	1.55	2.03	
MnO	0.02	0.03	0.02	0.00	0.00	0.00	0.01	0.00	0.02	0.05	
MgO	3.79	3.83	3.82	2.75	3.35	3.17	3.33	0.15	2.90	3.62	
CaO	0.01	0.01	0.02	0.01	0.00	0.01	0.02	0.43	0.05	0.05	
K ₂ O	10.17	9.43	9.22	8.42	9.16	8.90	10.18	0.62	8.84	8.95	
Na ₂ O	0.34	0.36	0.35	1.12	0.72	0.63	0.41	5.96	0.64	0.33	
Total	95.01	98.88	96.33	93.28	96.96	91.64	97.57	94.64	91.29	92.43	
Si	3.40	3.44	3.46	3.27	3.35	3.43	3.44	3.00	3.46	3.34	
Ti	0.00	0.00	0.01	0.03	0.03	0.03	0.00	0.00	0.01	0.01	
Al	2.19	2.17	2.14	2.39	2.27	2.16	2.13	3.02	2.15	2.33	
Al VI	1.59	1.62	1.60	1.67	1.62	1.59	1.57	2.02	1.60	1.67	
Cr	0.00	0.00	0.00	0.00	0.00	0.00	0.00	0.01	0.01	0.01	
Fe ₂	0.08	0.08	0.08	0.09	0.10	0.09	0.15	0.01	0.09	0.12	
Mn	0.00	0.00	0.00	0.00	0.00	0.00	0.00	0.00	0.00	0.00	
Mg	0.38	0.36	0.37	0.28	0.32	0.32	0.32	0.01	0.30	0.38	
Ca	0.00	0.00	0.00	0.00	0.00	0.00	0.00	0.03	0.00	0.00	
Na	0.04	0.04	0.04	0.15	0.09	0.08	0.05	0.74	0.09	0.04	
K	0.86	0.76	0.76	0.72	0.76	0.78	0.84	0.05	0.77	0.80	

Tab. 4.7: Representative analyses of white micas from chlorite-amphibolite, amphibole-bearing eclogite and amphibole-epidot bearing eclogite.

	Omp-vein	Zoisite-bearing eclogite					Metapyroxenite		Qz-bearing veins
Stage	D2	D2	D2	D3	on Ky	D5	D2	post-D2	D2
Sample	167	156	95	396	410	115	99	95	114
Mineral	Ph	Pg	Ph	Pg	Mrg	Ph	Ph	Pg	Ph
SiO2	50.50	46.95	52.52	49.04	31.48	51.65	53.64	58.86	53.52
TiO2	0.36	0.05	0.21	0.14	0.00	0.02	0.01	0.02	0.40
Cr2O3	0.06	0.19	0.08	0.01	0.05	0.04	0.18	0.00	0.02
Al2O3	28.13	40.01	28.46	40.91	51.14	31.10	28.87	12.05	26.91
FeO	2.39	0.27	2.03	0.29	0.58	1.36	1.16	5.44	2.86
MnO	0.00	0.00	0.01	0.01	0.04	0.00	0.03	0.01	0.00
MgO	3.01	0.15	3.44	0.18	0.10	3.00	3.57	12.74	3.51
CaO	0.00	0.43	0.02	0.49	10.23	0.00	0.11	1.73	0.06
K2O	9.03	0.62	9.02	0.62	0.03	9.37	8.93	0.02	9.24
Na2O	0.67	5.96	0.44	6.58	1.94	0.28	0.49	6.99	0.40
Total	94.16	94.64	96.24	98.27	95.59	96.82	97.73	98.08	96.98
Si	3.38	3.00	3.42	3.02	2.07	3.34	3.45	3.78	3.48
Ti	0.02	0.00	0.01	0.01	0.00	0.00	0.00	0.00	0.02
Al	2.22	3.02	2.19	2.97	3.97	2.37	2.19	0.92	2.06
Al VI	1.60	2.02	1.61	2.00	2.05	1.71	1.63	0.70	1.54
Cr	0.00	0.01	0.00	0.00	0.00	0.00	0.01	0.00	0.00
Fe2	0.13	0.01	0.11	0.01	0.03	0.07	0.06	0.29	0.16
Mn	0.00	0.00	0.00	0.00	0.00	0.00	0.00	0.00	0.00
Mg	0.30	0.01	0.33	0.02	0.01	0.29	0.34	1.22	0.34
Ca	0.00	0.03	0.00	0.03	0.72	0.00	0.01	0.12	0.00
Na	0.09	0.74	0.06	0.79	0.25	0.04	0.06	0.87	0.05
K	0.77	0.05	0.75	0.05	0.00	0.77	0.73	0.00	0.77

Tab. 4.8: Representative analyses of white micas from Omp-bearing vein, zoisite-bearing eclogite, metapyroxenite and qz-bearing vein.

	Amphibole-bearing eclogite				Amp-Ep-bearing eclogite		Zoisite-bearing eclogite				Quartz-rich eclogite		Amp- and Wm-	Ep- and Grt-vein	
Stage	D2	Zo-vein	D4	D5	D1	D2	incl. Ky	D2	D3	D5	D2	D5	D5	D2	D5
Analysis	57	265	317	247	68	69	408	159	463	168	105	107	376	512	513
Mineral	Zo	Ep	Czo	Ep	Ep	Ep	Zo	Zo	Czo	Ep	Zo	Czo	Ep	Ep	Ep
SiO2	39.63	38.29	38.93	38.25	39.24	37.42	40.12	38.88	33.84	36.93	39.55	37.46	36.71	37.74	37.92
TiO2	0.03	0.10	0.08	0.07	0.10	0.10	0.00	0.04	0.08	0.13	0.09	0.00	0.13	0.17	0.11
Cr2O3	0.10	0.00	0.02	0.03	0.00	0.00	0.02	0.03	0.08	0.00	0.02	0.01	0.00	0.00	0.00
Al2O3	29.73	24.91	26.68	24.73	27.31	26.35	33.02	32.23	24.54	26.38	32.34	26.13	24.91	24.30	24.19
FeO	2.80	11.29	9.20	11.18	8.08	7.11	1.29	1.51	3.42	7.42	2.21	7.42	7.79	11.76	11.75
MnO	0.02	0.54	0.13	0.50	0.10	0.02	0.02	0.04	0.06	0.06	0.03	0.19	0.15	0.42	0.43
MgO	0.10	0.01	0.04	0.05	0.14	0.51	0.01	0.05	0.12	0.16	0.00	0.12	0.75	0.03	0.02
CaO	24.12	21.92	23.30	21.48	23.13	21.09	24.07	23.36	17.08	19.79	24.49	21.99	20.54	22.69	22.67
K2O	0.01	0.00	0.00	0.00	0.00	0.00	0.00	0.00	0.00	0.02	0.01	0.00	0.01	0.01	0.02
Na2O	0.00	0.00	0.00	0.01	0.03	0.01	0.00	0.02	0.00	0.00	0.01	0.00	0.04	0.01	0.03
Si	3.09	3.10	3.08	3.12	3.09	3.10	3.03	3.01	3.19	3.11	3.00	3.10	3.11	3.08	3.09
Ti	0.00	0.01	0.00	0.00	0.01	0.01	0.00	0.00	0.01	0.01	0.01	0.00	0.01	0.01	0.01
Al	2.73	2.38	2.49	2.38	2.53	2.57	2.94	2.94	2.73	2.62	2.90	2.55	2.49	2.34	2.32
Cr	0.01	0.00	0.00	0.00	0.00	0.00	0.00	0.00	0.01	0.00	0.00	0.00	0.00	0.00	0.00
Fe2	0.18	0.77	0.61	0.76	0.53	0.49	0.08	0.10	0.27	0.52	0.14	0.51	0.55	0.80	0.80
Mn	0.00	0.04	0.01	0.03	0.01	0.00	0.00	0.00	0.00	0.00	0.00	0.01	0.01	0.03	0.03
Mg	0.01	0.00	0.00	0.01	0.02	0.06	0.00	0.01	0.02	0.02	0.00	0.01	0.10	0.00	0.00
Ca	2.01	1.90	1.97	1.88	1.95	1.87	1.95	1.94	1.72	1.79	1.99	1.95	1.87	1.98	1.98
Na	0.00	0.00	0.00	0.00	0.00	0.00	0.00	0.00	0.00	0.00	0.00	0.00	0.01	0.00	0.00
K	0.00	0.00	0.00	0.00	0.00	0.00	0.00	0.00	0.00	0.00	0.00	0.00	0.00	0.00	0.00

Tab. 4.9: Representative analyses of epidotes from Ivozio Complex rocks (incl. = included within)..

Mineral	Chlorite-amphibolite	Amphibole-bearing eclogite		Amphibole-epidote bearing eclogite		Zoisite-bearing eclogite		Qz-rich eclogite	Ultramafic rocks		Ep- and Grt vein		Qz-bearing vein
	Chl	Chl	Chl	Chl	Chl	Chl	Chl	Chl	Chl	Chl	Chl	Chl	Chl
Sample	181	354	537	499	526	332	402	94	478	3	370	515	104
Stage	D2	D2	D5	D2	D5	D5	D6	D5	D2	D5	D5	D5	D6
SiO2	29.36	29.44	28.94	28.62	27.32	28.90	26.73	29.09	33.13	23.17	28.82	26.80	24.67
TiO2	0.00	0.07	0.05	0.00	0.03	0.03	0.07	0.01	0.06	0.04	0.02	0.01	0.00
Cr2O3	0.08	0.02	0.00	0.04	0.09	0.04	0.00	0.04	2.57	0.47	0.07	0.00	0.00
Al2O3	20.81	21.34	19.29	21.02	18.38	21.31	21.01	20.61	12.31	12.33	21.00	20.78	18.97
FeO	13.38	8.32	19.72	12.94	20.80	13.02	22.44	15.11	6.96	12.38	12.89	20.46	30.85
MnO	0.21	0.00	0.34	0.14	0.38	0.06	0.27	0.25	0.03	0.05	0.18	0.39	0.36
MgO	24.31	26.89	19.55	23.63	16.70	23.80	16.60	21.99	30.60	17.72	23.55	19.18	11.08
CaO	0.02	0.08	0.05	0.02	0.00	0.13	0.12	0.08	0.02	0.52	0.06	0.01	0.04
K2O	0.01	0.08	0.06	0.01	0.01	0.00	0.01	0.01	0.02	0.02	0.00	0.02	0.01
Na2O	0.01	0.00	0.00	0.00	0.02	0.03	0.04	0.05	0.01	0.04	0.01	0.04	0.05
Total	88.19	86.24	88.00	86.42	83.73	87.32	87.29	87.25	0.00	0.05	86.61	87.69	86.05
Si	1.91	1.91	1.96	1.90	1.96	1.90	1.85	1.93	2.17	2.04	1.91	1.83	1.83
Ti	0.00	0.00	0.00	0.00	0.00	0.00	0.00	0.00	0.00	0.00	0.00	0.00	0.00
Al	1.60	1.63	1.54	1.64	1.56	1.65	1.72	1.61	0.95	1.28	1.64	1.68	1.66
Cr	0.00	0.00	0.00	0.00	0.01	0.00	0.00	0.00	0.13	0.03	0.00	0.00	0.00
Fe2	0.73	0.45	1.11	0.72	1.25	0.71	1.30	0.84	0.38	0.91	0.71	1.17	1.92
Mn	0.01	0.00	0.02	0.01	0.02	0.00	0.02	0.01	0.00	0.00	0.01	0.02	0.02
Mg	2.36	2.60	1.97	2.34	1.79	2.33	1.72	2.18	2.98	2.32	2.32	1.96	1.23
Ca	0.00	0.01	0.00	0.00	0.00	0.01	0.01	0.01	0.00	0.05	0.00	0.00	0.00
Na	0.00	0.00	0.00	0.00	0.00	0.00	0.01	0.01	0.00	0.01	0.00	0.01	0.01
K	0.00	0.01	0.01	0.00	0.00	0.00	0.00	0.00	0.00	0.00	0.00	0.00	0.00

Tab. 4.10: Representative analyses of chlorites from Ivazio Complex rocks.

Stage	Ultramafic rocks							
	S-Atg	S-Atg	S-Atg	post S-Atg	S-Atg		D2	pre-D2
Sample	473	474	475	477	484	Sample	101	102
Mineral	Mgs	Atg	Atg	Ctl	Tlc	Mineral	Phl	Phl
SiO2	0.03	43.07	42.49	62.96	62.96	SiO2	54.19	52.05
TiO2	0.00	0.08	0.03	0.00	0.02	TiO2	0.00	0.06
Cr2O3	0.00	0.22	0.40	0.07	0.00	Cr2O3	0.30	0.28
Al2O3	0.00	1.92	2.38	0.06	0.04	Al2O3	29.71	28.45
FeO	6.32	8.27	8.23	2.26	2.57	FeO	1.11	1.24
MnO	0.31	0.05	0.11	0.00	0.00	MnO	0.03	0.02
MgO	42.81	33.30	32.67	28.45	27.69	MgO	3.58	3.08
CaO	0.53	0.00	0.00	0.04	0.03	CaO	0.03	0.07
K2O	0.00	0.00	0.00	0.00	0.01	K2O	9.32	8.40
Na2O	0.00	0.00	0.00	0.03	0.01	Na2O	0.49	0.69
NiO	0.00	0.00	0.00	0.00	0.00	NiO	0.85	3.96
S2O3	0.00	0.00	0.00	0.00	0.00	S2O3	0.00	0.00
Total	50.00	86.91	86.31	93.87	93.33	Total	99.61	98.29
Si	0.00	2.06	2.05	2.59	4.09	Si	3.41	3.37
Ti	0.00	0.01	0.00	0.00	0.00	Ti	0.00	0.01
Al	0.00	0.22	0.27	0.01	0.00	Al	2.20	2.17
Cr	0.00	0.02	0.03	0.00	0.00	Cr	0.03	0.03
Fe2	0.11	0.66	0.66	0.16	0.14	Fe2	0.12	0.13
Mn	0.01	0.00	0.01	0.00	0.00	Mn	0.00	0.00
Mg	1.37	2.37	2.35	1.74	2.68	Mg	0.67	0.60
Ca	0.01	0.00	0.00	0.00	0.00	Ca	0.00	0.01
Na	0.00	0.00	0.00	0.00	0.00	Na	0.12	0.17
K	0.00	0.00	0.00	0.00	0.00	K	0.75	0.69
						Ni	0.09	0.41

Tab. 4.11: Representative analyses of magnesite, antigorite, chrysotile, talc and phlogopites from Ivazio Complex rocks.

4.7 Thermodynamic modeling

4.7.1 Database, chemical systems selection and bulk composition

Phase equilibria calculation was undertaken using the software THERMOCALC (Powell et al., 1998, with recent upgrade, tc335i) and the internally consistent thermodynamic dataset ds55 (Holland and Powell, 1998; upgrade tc-ds55.txt from Nov. 2003).

The activity-composition models of the solid solutions used in the NCKFMASH system are: amphibole from Diener *et al.* (2007); clinopyroxene from Green *et al.* (2007); orthopyroxene from Powell and Holland, (1999); chlorite from Holland *et al.* (1998); garnet from White *et al.* (2007); plagioclase from Holland and Powell (2003); talc and spinel from Holland and Powell (1998); biotite from White *et al.* (2007); muscovite and paragonite from Coggon and Holland (2002). The other phases are pure end-members: lawsonite, quartz, zoisite, antigorite and kyanite. The modeling was undertaken with H₂O in excess and no O (Fe₂O₃).

PT pseudo-sections are presented for three chosen rock compositions (Figs. 4.38-4.40): metapyroxenite; amphibole-bearing eclogite; zoisite-bearing eclogite.

Rock composition in oxide weight % was determined through whole rock analysis on homogeneous samples. An XRF dispersive spectrometer "Philips X'Unique" from the Earth Sciences Department "A. Desio" of Milano University was employed. It has a Rhodium (Rh) tube and operates under vacuum conditions at a temperature of 30°C.

Large samples (up to 30x30x30cm) were picked with portable saw with a diamond blade, considered the coarse-grained and multiple layers of the analyzed rocks.

4.7.2 Isochemical diagrams (pseudo-sections)

Molar % of oxides used for the calculation are summarized in the following table:

Lithologic type	SiO ₂	Al ₂ O ₃	CaO	MgO	FeO	K ₂ O	Na ₂ O
Metapyroxenite	49.94	4.15	10.03	26.44	7.62	0.40	1.42
Amphibole-bearing eclogite	56.48	5.68	12.56	9.59	14.73	0.11	0.85
Zoisite-bearing eclogite	59.80	14.14	13.26	5.91	5.55	0.25	1.07

4.7.2.1 Metapyroxenite

The analyzed and modeled sample is a phengite and phlogopite bearing metapyroxenite. It is a 10-cm-thick layer comprised within zoisite-bearing eclogites, as already described, and it is characterized by the presence of randomly oriented green omphacite crystals and by the occurrence of phengite and phlogopite as major components.

In this rock type the main fabric is S₂ marked by diopside, tremolite, phengite, phlogopite and Mg-chlorite. S₂ wraps around diopside and tremolite porphyroclasts (probably syn-D₁). Other syn-D₁ minerals may be micas and Mg-chlorite. Electron microprobe analysis allowed identifying the presence of paragonite associated to phengite crystals after phengite (along its cleavages planes). These are related to post-D₂ deformation stages. These late minerals are very small and found only within phengite, therefore they have not been subtracted from the used composition.

The PT pseudosection in the NCFMASH system considers ten mineral phases (*chlorite, talc, garnet, muscovite, biotite, amphibole, zoisite, diopside, omphacite* and *lawsonite*), and excess water (Fig. 4.38). In the grid the name Amp is used to cover the compositional range of calculated Ca- (Tremolite) and Ca-Na (Edenite) amphiboles, as observed in the sample. Czo is the epidote-group mineral we consider, as observed in the rocks (zoisite was never observed nor analyzed). The fluid in the model system is considered to be pure H₂O.

The calculated field representing the observed D2 mineral association is the trivariant Amp, Di, Mu, Bi, Chl field at 1.1-2.3 GPa and 500-590°C. However, also the Amp, Di, Mu, Bi, Chl, Grt field at 1.5-2.5 GPa and 540-590°C could represent the D2 assemblage, considered that the modeled amount of Grt in this field never exceed 2% in volume, and such a small amount could be difficult to detect in the rock unless several thin sections were made. A fact that corroborate this possibility is that the calculated clinopyroxene composition in the garnet bearing field is very similar to that measured in our sample, with X_{Jd} 15 to 20%, whereas the clinopyroxene composition calculated in the Grt-free field (x_{Jd} < 10%) is very different to that observed in the rock. Of course such it is not possible to exclude that such difference is due to an error in the calculation of the equilibrium volume, but preliminary calculations made using different bulk rock composition point us to the above hypothesis.

The combination of X_{Jd} isopleths of Di and X_{Fe} isopleths of chlorite in the Grt-bearing field suggests PT estimates for the D2 assemblage of 2.9-2.35 GPa and 560-580°C that are in good agreement with what observed in the other lithologies.

Plagioclase growth during the D5 stage in pseudomorphs and along fractures and shear planes is calculated to have happened at P < 0.8 GPa and T comprised between 380 and 520°C.

For this composition no univariant reactions are calculated and only two divariant fields are observed, with the presence of talc above the Qz-Coe transition. The maximum variance is 7 and it is observed in the HT-LP field where the amphibole - biotite association is stable. The syn-D1 assemblage could be represented by the amphibole, chlorite, biotite, muscovite, diopside field between 1.0-2.2 GPa and 490-580°C or, alternatively, by the biotite free field comprised between 1.9-2.3 GPa and 510-540°C, since at lower temperature omphacite should coexist with diopside and no syn-D1 Na-rich Cpx relicts have been detected.

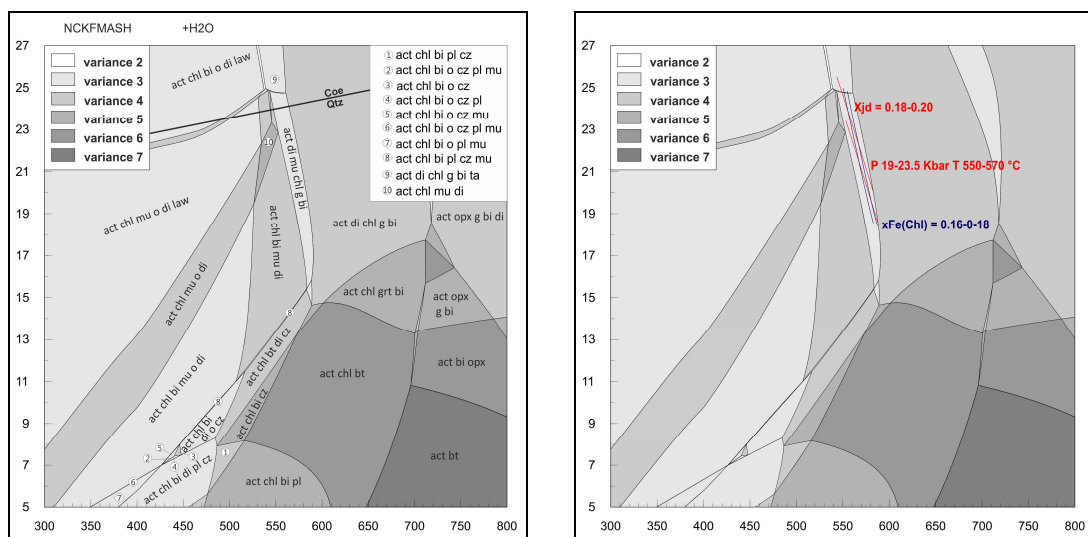


Fig. 4.38: P-T pseudosection calculated using the metaproxenite composition: SiO₂ = 49.94; Al₂O₃ = 4.15; CaO = 10.03; MgO = 26.44; FeO = 7.62; K₂O = 0.40; Na₂O = 1.42 (in moles%), in NCFMASH system using THERMOCALC. H₂O is in excess. On the right calculated isopleths for x_{Jd} and x_{Fe} of the syn-D2 Chl-Cpx association are shown in red and blue respectively. Mineral abbreviations: o = omphacite; g = garnet; ta = talc; q = quartz; law = lawsonite; gl = glaucophane; chl = chlorite; mu = muscovite; act = actinolite (= CaNa-Amp); di = diopside; cz = clinozoisite. Pressure is in Kbar and temperature in °C, as in the output produced with "drawpd115".

4.7.2.2 Amphibole-bearing eclogite

To obtain a representative sample for amphibole-bearing eclogite, two sets of 5/9-cm thick Amp- and Grt-layers were milled and mixed. Omp-layers were instead excluded due to their rarity with respect to the other two layers, that constitute almost the whole volume of this rock type. Moreover, selected samples are from volumes of the amphibole-eclogite with scarce or absent syn-D2 fabrics.

The Amp- and Grt-layers are mostly composed of fine-grained amphibole and garnet, with scarce (< 10%) coarse-grained omphacite and phengite. The main mesoscopic feature is the S1 compositional banding defined by modal variation of amphibole and garnet, whereas the main S2 foliation is marked by amphibole, phengite and zoisite SPO.

The PT projection in the NCKFMASH system considers eleven mineral phases (chlorite, talc, garnet, muscovite, biotite, amphibole, zoisite, diopside, omphacite, lawsonite and quartz), and excess water (Fig. 4.39).

In the pseudosection (Fig. 4.39) the field glaucophane, garnet, diopside, muscovite and quartz comprised between 1.7-2.7 GPa and 510-670°C represent the stability field of D1, D2 and D3 mineral association. The D4 deformation and mineral assemblages occur only in this rocks and its mineral assemblages occur in the field glaucophane, diopside, muscovite/phengite, quartz and zoisite at $P < 1.4$ and $T < 500^\circ\text{C}$.

In this pseudosection the exhumation path is strictly bonded by the complete absence of biotite and the occurrence of amphibole in the D4 field.

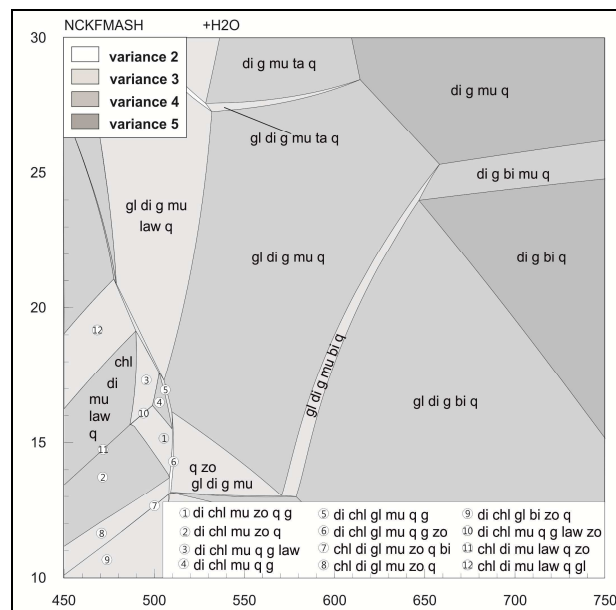


Fig. 4.39: P-T pseudosection calculated using the eclogite composition: $\text{SiO}_2 = 56.48$; $\text{Al}_2\text{O}_3 = 5.68$; $\text{CaO} = 12.56$; $\text{MgO} = 9.59$; $\text{FeO} = 14.73$; $\text{K}_2\text{O} = 0.11$; $\text{Na}_2\text{O} = 0.85$ (in moles%), in NCKFMASH system using THERMOCALC. H₂O is in excess. Mineral abbreviations: o = omphacite; g = garnet; ta = talc; ky = kyanite; q = quartz; law = lawsonite; gl = glaucophane; chl = chlorite; mu = muscovite; di = diopside. Pressure is in Kbar and temperature in °C, as in the output produced with "drawpd115".

4.7.2.3 Zoisite-bearing eclogite

A medium-grained zoisite-bearing eclogite with S2 cm-spaced foliation has been analyzed to determine the composition to be used in the modelling. The foliation is defined by zoisite, omphacite, phengite, paragonite and amphibole SPO, by garnet trails and lens-shaped quartz domains. In zoisite-bearing eclogites, the S1 foliation occurs in relicts within S2 and is marked by zoisite, amphibole and phengite SPO, Grt trails and lens-shaped Qz domains.

The PT projection in the NCKFMASH system considers twelve mineral phases (chlorite, talc, garnet, muscovite, biotite, amphibole, zoisite, diopside, omphacite, lawsonite, kyanite and quartz), and excess water (Fig. 4.40).

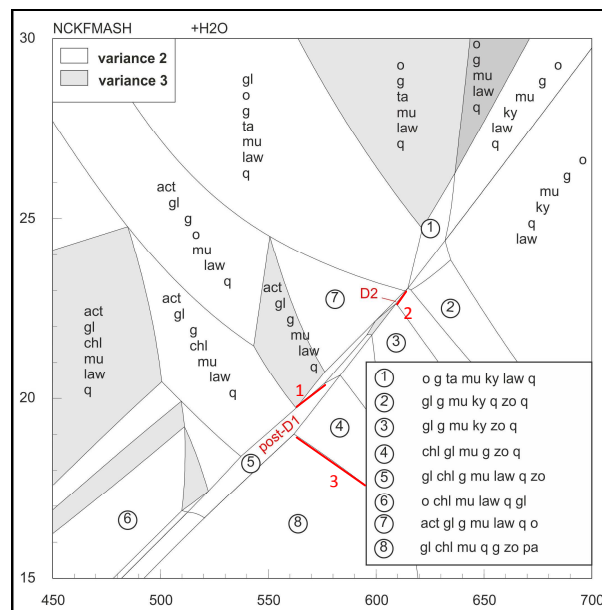
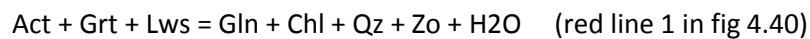
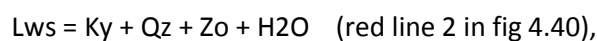


Fig. 4.40: P-T pseudosection calculated using the eclogite composition: SiO₂ = 59.80; Al₂O₃ = 14.14; CaO = 13.26; MgO = 5.91; FeO = 5.55; K₂O = 0.25; Na₂O = 1.07 (in moles%), in NCKFMASH system using THERMOCALC. H₂O is in excess. Mineral abbreviations: o = omphacite; g = garnet; ta = talc; ky = kyanite; q = quartz; law = lawsonite; gl = glaucophane; chl = chlorite; pa = paragonite; mu = muscovite; act = actinolite (= CaNa-Amp). Pressure is in Kbar and temperature in °C, as in the output produced with "drawpd115".

The stability of syn-D1 mineral association is calculated in the field Nr. 5 (Gln, Chl, Ph, Lws, Qz and Zo) and can be estimated at P = 1.7-2.05 GPa and T = 510-590°C. A first reaction:

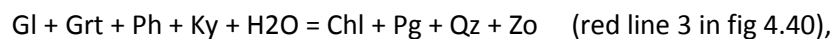


of lawsonite breakdown occurs until the complete consumption of Act (= CaNa-Amp): moving to the D2 stage conditions at P = 2.2-2.3 GPa and T = 600-620°C a second reaction:



completely consumes the lawsonite.

D3 assemblage occurs in the field at P < 1.9 GPa and T < 600°C. It is constrained by the reaction:



that produces partial replacement of kyanite by paragonite and zoisite-dominated aggregates.

Chapter 5

Discussion and conclusions on the Ivozio tectono-metamorphic evolution

Petro-structural mapping revealed that the Ivozio complex is composed of different layers reflecting an igneous bedding, that had been probably reworked structurally and mineralogically during pre-Alpine times.

Microstructural and petrographic analysis led to infer that:

- 1) Amphibole eclogite derived from a cumulitic gabbro whit layers originally more rich in Al and Ca alternating to layers more rich in Si, as suggested by the variations in Grt modal amount; zoisite-eclogite probably corresponds to original leucogabbro layers.
- 2) Metapyroxenite comes from cumulitic layers of Cpx and Ol, as indicated by the occurrence of Chr ($\leq 5\%$) in all these rocks: these layers are characterized by a very low Al-content (<7 wt% in Al_2O_3 in Ph- and Phl-bearing metapyroxenite, as detected with XRF).
- 3) In amphibole- epidote-eclogite layers constituted by Ep + Chl (modal amount of 70-80%) and Amp (modal amount of 20-30%) occur, with thickness of about 10 cm. They are interpreted as original layers characterized by high Ol and Cpx modal amounts.
- 4) Atg-serpentinite layers can be the metamorphic products of both original mantle enclaves or of dunitic cumulus layers.
- 5) Ti- and K-rich amphibole should correspond to pre-Alpine igneous or metamorphic assemblages in chlorite-amphibolite, as suggested by the occurrence of white mica and titanite inclusions in the core of pre-D2 Fe-Mg amphibole.

The detailed petro-structural mapping (performed at 1:10 to 1:50 scale) led to identify five groups of syn-metamorphic superposed structures (D1-D5), consisting of fold systems, foliation sets, shear zones, veins and fracture zones, as synthesized in Tab. 5.1. With respect to previous works (Zucali et al., 2004; Zucali & Spalla 2011), an improvement of the definition of the sequence of superposed structures has been made, and consequently a refinement of the deformation-metamorphism relationships has been proposed (Tab. 5.2); Two more groups of structures have been recognized with respect to the sequence proposed by Zucali and Spalla (2011), in which D3 syn-eclogitic folding was missing. The recognition of this group of folds allowed a better separation of the previous stages indicated as D2a and D2b and to consider D2b stage as

the equivalent of D4 stage of the new deformation sequence inferred in this work. As a consequence D3 of previous authors correspond to D5 of this work.

Deformation	Metamorphism	P/T mineral marker in	P/T mineral marker out	Veining
preD1	Blueschist facies (?)	Grt		Amp- and Wm, Ep and Qz veins
D1: folds and foliations	Eclogite facies			
post-D1		Lws (early) and Ky (late)	Lws (late)	Grt-bearing veins (A), transposed during D2
D2: folds, foliations and localized shear zones		Omp (early) and Pg (late)	Ky (late)	Grt-bearing veins (B)
post-D2				Grt-bearing veins (B) and Omp-bearing veins
D3: folds			Omp	
D4: shear zones and tension gashes	Blueschist facies		Grt	Gln- and Zo-bearing veins
D5: folds, shear zones and fractures	Greenschist facies			

Tab. 5.1: Synthesis table of metamorphism, mineral markers appearance/disappearance and veining during the evolution of deformation in the Ivozio Complex.

	pre-D1	D1	post-D1	D2	D3	D4	D5
Amp- and Wm-bearing vein	/	Prg, Wm and Di (pre-D2)	/	Wnc, Ph and Mg-Chl	/	/	Wm, Ab, Ep, Fe-Chl and Ed
Ep-bearing vein	Grt, Ep and Mg-Chl (pre-D2)	Czo	/	Czo and Mg-Chl	/	/	Wm, Ab, Ep, Fe-Chl and Ed
Qz-bearing vein	/	Qz and Wnc/Prg (pre-D2)	/	Qz, Omp, Gln/Fe-Gln/Rbk/Rct/Eck, Grt, Zo and Ph	Qz, Na-Amp/Ed, Ph, Pg and Czo	/	Wm, Ab, Ep, Fe-Chl and Ed
Chlorite-amphibolite	/	Ath and Wm (pre-D2)	/	Na-Amp, Ph and Mg-Chl	/	/	Wm, Ab, Ep, Fe-Chl and Ed
Amphibole-bearing eclogite	/	Ed, Grt, Wm and Zo	Lws / Ky (late)	Na-Amp, Zo, Grt, Omp, Ky(early), Ph and Pg /late)	Qz, Na-Amp/Ed, Ph, Pg and Czo	Gln, Ph, Mg-Chl, Di and Czo	Wm, Ab, Ep, Fe-Chl and Ed
Amphibole-epidote bearing eclogite	/	Ed, Ep, Mg-Chl and Wm (pre-D2)	/	Prg, Wm, Mg-Chl, Grt, Di and Czo	/	/	Wm, Ab, Ep, Fe-Chl and Ed
Zoisite-bearing eclogite	/	Qz, Zo, Ed/Act, Wm and Grt	Lws / Ky (late)	Qz, Omp, Na-Ca Amp, Grt, Zo, Ky (early), Pg(late) and Ph	Qz, Ca-Na Amp/Ed, Ph, Pg and Czo	/	Wm, Ab, Ep, Fe-Chl and Ed
Quartz-rich eclogite	/	Qz, Zo, Amp, Wm and Grt	/	Qz, Omp, Amp, Grt, Zo, Ph and Pg (late)	Qz, Amp, Ph, Pg and Czo	/	Wm, Ab, Ep, Fe-Chl and Ed
Antigorite serpentinite	/	Ol (pre-D2)	/	Atg, Ged, Mg-Chl and Cb(Atg foliation)	/	/	Ctl, Mg-Chl and Cb
Metapyroxenite	/	Di, Tr/Act and Mg-Chl (pre-D2)	/	Di, Tr/Act/Ed, Mg-Chl, Phl and Ph	/	/	Wm, Ab, Ep, Fe-Chl, Ed/Act
Grt-bearing vein	/	/	/	Grt	/	/	Wm, Ab, Ep, Fe-Chl and Amp
Omp-bearing vein	/	/	/	/	Ph	/	Wm, Ab, Ep, Fe-Chl and Amp
Gln-bearing vein	/	/	/	/	/	/	Wm, Ab, Ep, Fe-Chl and Amp
Zo-bearing vein	/	/	/	/	/	/	Wm, Ab, Ep, Fe-Chl and Amp

Tab. 5.2: Mineral assemblages marking successive fabric elements in different lithologic type and veins of Ivazio Complex. Amp names are specified only for analyzed rocks.

The block-diagram of Fig. 5.1 depicts the 3D structural setting resulting from overprinting of the three groups of structures. From Tabs. 5.2 and 5.1 it is possible to deduce that D1 structures developed at the limit between blueschist and eclogite facies conditions, D2 under eclogite facies conditions, contemporaneous with the growth of the PT-peak assemblages, D3 at the transition eclogite-blueschist facies, D4 under blueschist facies, and D5 under greenschist facies conditions.

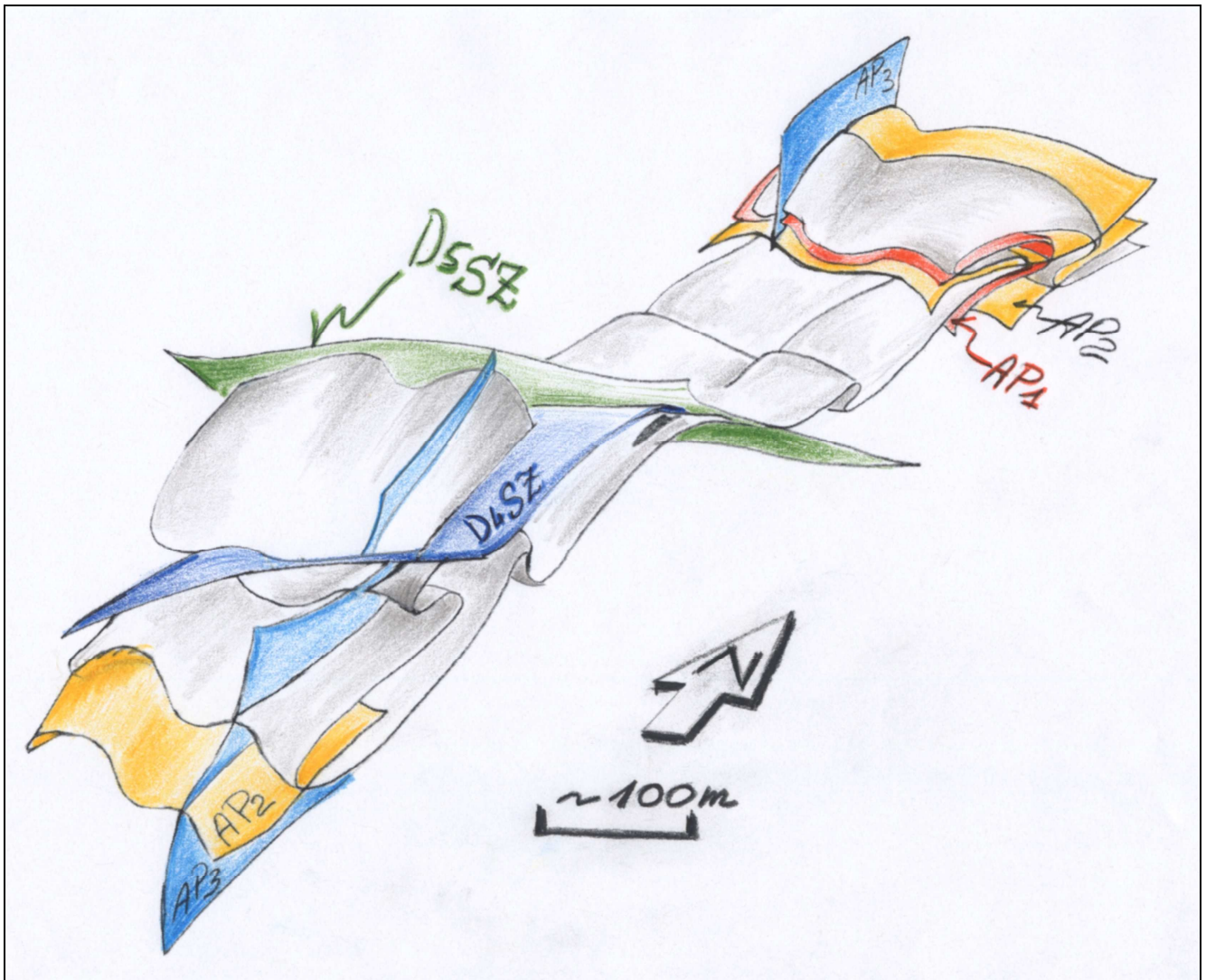


Fig. 5.1: Block diagram of the structural setting resulting from overprinting of D1, D2, D3 and D5 folding and from D4 and D5 shear zones.

Different generations of veins have been detected from pre-D1 to syn-D4. The age of Pre-D1 veins can be interpreted as pre-Alpine or Alpine: in this second case they should have developed during the PT prograde path before D1 deformation stage. Composition of Amp filling these veins lies outside the trend defined by prograde and retrograde Alpine amphiboles, suggesting that they may have formed during the pre-Alpine evolution. Di inclusions in these Amp are rimmed by Omp and/or by edenite. Quartz-veins are filled by a mineral association compatible with the prograde metamorphic evolution, characterizing the transition from D1 to D2 stage. They probably developed in presence of aqueous fluids responsible for a local variation of the bulk composition, originating Wnc/Brs cores rimmed by Gln and/or FeGln and/or Eck and/or Rbk as a function of Fe oxidation degree consequent to variations in H_2O activity.

Alpine veins from post-D1 to syn-D4 consist of four types: Grt-bearing, Omp-bearing, Gln-bearing and Zo-bearing veins. Structural analysis and petrologic modeling related the formation of these veins to the sequence of deformation stages and the modeled de-hydration reactions of Lws. Grt-veins develop in two successive steps of the structural evolution: a first set cuts across S1 and was deformed during D2 (Grt-bearing veins A in tab. 5.1); a second set cuts across S2 (Grt-bearing veins B in tab. 5.1). Post-D1 Grt-veins were generated together with Lws-dehydration reactions, initially by $Lws + Ca-Na\ Amp + Grt = Gln + Chl + Qz + Zo + H_2O$, occurring post-D1, and successively by $Lws = Ky + Qz + H_2O$, beginning after D1 and during early D2 stages, as suggested by Ky microstructural relationships. The complete disappearance of Lws, associated with the production of aqueous fluids and with Ky, Zo, Qz assemblages is accomplished between

post-D1 and the early stages of D2. At that stage, production of fluids facilitated also the development of large Omp crystals (centimeter size) in the country rocks. Grt veins and Omp porphyroblasts were deformed during successive stages of D2 progressive deformation as indicated by the homogeneous compositions of Omp blasts, in spite of their randomly oriented, parallel to S2 or internally deformed microstructural occurrences. The second set of Grt-bearing veins and Omp-bearing veins cut across S2 and are folded during D3.

Gl- and Zo-bearing veins are contemporaneous with the development of D4 shear zones as supported, in addition to kinematic indications of mineral growth, by the composition of filling minerals that is homogeneous with those of grains marking the S4 foliation. Fluids associated with this veining stage, and with the wide hydration of D4 shear zones, could have been injected from the gabbro country rocks, because no de-hydration reactions are observed at this step of the metamorphic evolution in the lithologic types of the Ivazio gabbroic complex.

Pressure and temperature conditions, characterizing successive deformation stages have been determined by three pseudo-sections on metapyroxenite, zoisite-eclogite and amphibole-eclogite, to infer the PTdt evolution of Fig. 5.2. The comparison between modeled and natural syn-tectonic assemblages, taking into account their compositional variations (isopleths), indicate that D1 occurred at $T < 510^{\circ}\text{C}$ and $P < 1.7$ GPa. A successive re-equilibration stage has been estimated for the post-D1 assemblage Gln, Chl, Ph, Lws, Qz, Grt and Zo at $T = 510^{\circ}\text{-}590^{\circ}\text{C}$ and $P = 1.7\text{-}2.05$ GPa. Successively D2 structures developed at $T = 600^{\circ}\text{-}620^{\circ}\text{C}$ and $P = 2.2\text{-}2.3$ GPa, D3 at $T = 520^{\circ}\text{-}600^{\circ}\text{C}$ and $P = 1.4\text{-}1.9$ GPa; D4 at $T < 500^{\circ}\text{C}$ and $P < 1.4$ GPa, and D5 at $T = 380^{\circ}\text{-}520^{\circ}\text{C}$ and $P < 0.8$ GPa.

Peak conditions reached on D2 times are accomplished after a P and T prograde path, during the post-D1 evolution (in the Lws-stability field), characterized by a P/T ratio typical of cold subduction zones (Cloos, 1993). This P/T ratio persists up to the PT-peak conditions achieved at the beginning of D2. The subsequent P-retrograde evolution shows the transitions of successive re-equilibration stages towards higher P/T ratios, up to D5 stage, where PT conditions are comprised between those of warm subduction zones and of plate interiors, according to Cloos (1993). This indicates, as in the previous case of Mt. Mucrone, that only the last exhumation stage occurred under PT conditions compatible with continental collision.

This PT prograde and retrograde path is in good agreement with that inferred by Zucali & Spalla (2011), but indicated more details in terms of structural history, as already discussed. Mechanical and chemical re-equilibrations recorded under eclogite-facies conditions occurred at 65 ± 3 Ma according to U/Pb determinations on Zrn of Montestrutto metapelites (Rubatto et al., 1999), which are part of the Ivazio complex country rocks.

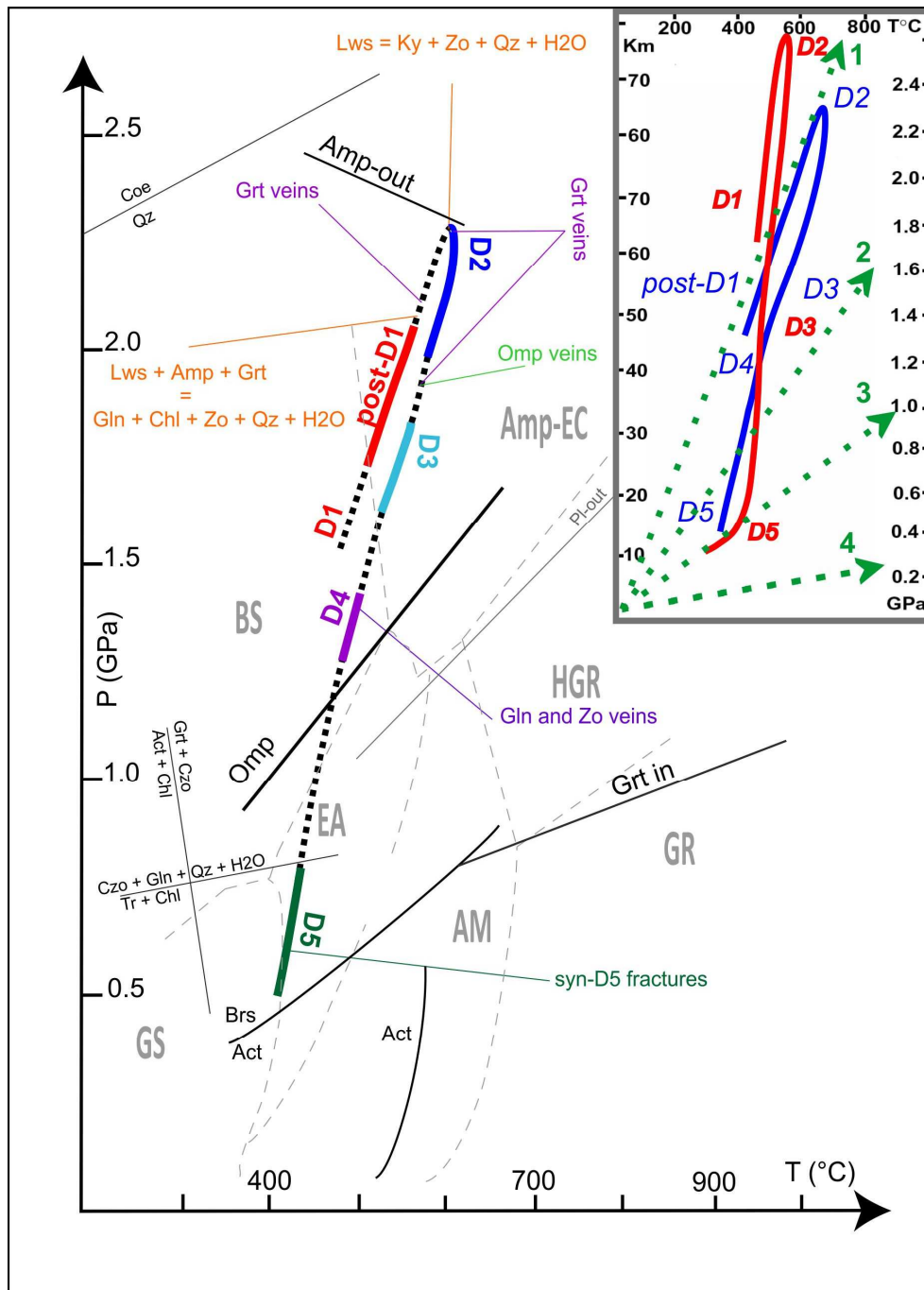


Fig. 5.2: PT paths inferred for the Ivazio Complex: black dashed line is the PT path; colored lines represent the development of stages mineral assemblages; GS = greenschist; EA = epidote-amphibolite; BS = blueschist; AM = amphibolite; Amp-EC = amphibole-bearing eclogite; HGR = high pressure granulite; GR = granulite. Brs/Act transition (Ernst, 1979); Act/Hbl transition (Moody et al., 1983); Amp-in and Amp-out (Poli & Schmidt, 1995); Pi-out and Grt-in (Liu et al., 1996). In the inset the inferred PTdt path (blue) is compared with that of Delleani et al. (2013), shown in red. Green dashed lines are geotherms: 1) "cold" subduction zones, 2) "warm" subduction zones, 3) normal gradient of old plate interior, 4) near spreading ridge or volcanic arc (Cloos, 1993).

Chapter 6

Conclusions

The aim of this work was the comparison of the structural and metamorphic evolution of two portions of the Sesia-Lanzo Zone, which is the most renowned Austroalpine nappe, because it represents the widest portion of continental crust subducted and exhumed during Alpine convergence, under a very low thermal regime. It is a matter of fact that Sesia-Lanzo Zone is one of the rare portions of subducted continental crust, together with Dabie (China), Calabrian and Turkish basement units (Li et al., 2004; Piccarreta, 1981; Okay and Whitney, 2010), containing Lws-bearing assemblages that are, on the contrary, commonly diffused within the oceanic lithosphere subducted under extremely depressed thermal gradients. This peculiar metamorphic evolution has driven towards the interpretation of a geodynamic scenario such as a burial-exhumation cycle accomplished in a regime of active oceanic subduction (e.g., Spalla et al., 1996; Zucali et al., 2004). Different P-T and P-T-d-t evolutions, inferred within the different complexes of SLZ led to the recent interpretation that this “Alpine nappe” results by the accretion of different crustal slices, tectonically eroded, subducted and exhumed in a hydrated mantle wedge, prior to the Oligocene continental collision (Meda et al., 2010; Roda et al., 2012). Such evolutions at low T/P ratio facilitate the preservation of relics of a pre-Alpine history, making the memory of Sesia-Lanzo rocks particularly rich, because of the strong deformation and metamorphic transformations partitioning that generally occurs under LT conditions.

For this reason, in the in the two selected areas, characterised by pre-Alpine protoliths with markedly different bulk compositions, investigations to unravel accurately the tectono-metamorphic evolutions, have been approached with multiscale structural analysis, associated with detection of changes in chemical compositions of minerals supporting successive fabrics. The results on interactions between mechanical and chemical re-equilibrations, during these two subduction-related polyphase evolutions, are discussed in the partial conclusions on the Mt. Mucrone and Ivozio area in Chapt. 3 and 5, respectively.

The resulting quality PTdt paths, summarised in Tab. 6.1, point out that these two portions of the same tectonic complex (the Eclogitic Micaschists Complex of SLZ), underwent different tectono-metamorphic evolutions. In particular the PTdt path recorded by the Mt. Mucrone metagranitoids and their country rocks (see Chapt. 3 for a detailed discussion of conclusive remarks) underwent a multi-stage structural and metamorphic re-equilibration during Alpine times in which D2 structures formed at peak conditions of $T = 530^{\circ}\text{C} \pm 50^{\circ}\text{C}$ and $P = 2.5 \pm 0.2 \text{ GPa}$, after a prograde path accomplished during D1, under blueschist facies conditions. The eclogite facies structural history took place between 90 and 66 Ma (Cenki-Tok et al., 2011). The retrograde path is marked by a transition to $T = 470^{\circ} - 560^{\circ}\text{C}$ and $P = 1.4 \pm 0.4 \text{ GPa}$ during D3, up to a final re-equilibration under greenschist facies conditions up to $P \leq 0.4 \text{ GPa}$ and $T \leq 400^{\circ} \text{C}$ (D5 stage). This structural and metamorphic evolution predates the Tertiary magmatic activity (as discussed in Chapt. 3),

indicating that these rocks have been exhumed to greenschist facies conditions before 30 Ma (e.g. Zanoni et al., 2010).

	Monte Mucrone	Ivozio
Intrusive age	Granitoid intrusion at 290 Ma	Gabbro emplacement at 355
pre-D1	preserved igneous textures and mineral relicts igneous (Bt, Aln and Kfs) and metamorphic (Grt)	preserved igneous layering and cumulitic structures; pre-Alpine mineral relicts igneous and/or metamorphic (Ol and Amp?)
D1	430°-530°C 1.6-2.2 GPa at the transition between blueschist and eclogite facies conditions	<510°C <1.7 GPa blueschist facies conditions
post-D1	/	510°-590° C 1.7-2.05 GPa eclogite facies conditions
D2	480°-580°C 2.3-2.7 GPa under eclogite facies conditions	600°-620°C 2.0-2.3 GPa eclogite facies conditions
D3	470°-570° 1.0-1.8 GPa at the transition between blueschist and eclogite facies conditions	520°-600°C 1.4-1.9 GPa at the the transition between eclogite and blueschist facies conditions
D4	greenschists facies conditions	< 500°C <1.4 GPa blueschist facies conditions
D5	<400°C <0.4 GPa greenschist facies conditions	380°-520°C <0.8 GPa greenschist facies conditions

Tab. 6.1: Summary table of pre-Alpine relicts and Alpine deformation stages for Mt. Mucrone and Ivozio rocks.

Also the PTdt path recorded by the Ivozio metagabbros underwent a multi-stage structural and metamorphic re-equilibration during Alpine times (see Chapt. 5 for a detailed discussion of conclusive remarks) in which D1 occurred at $T < 510^{\circ}\text{C}$ and $P < 1.7\text{ GPa}$, followed by the successive post-D1 re-equilibration assemblage at $T = 510^{\circ}\text{C}$ - 590°C and $P = 1.7\text{--}2.05\text{ GPa}$. Subsequently D2 structures developed under peak conditions at $T = 600^{\circ}\text{C}$ - 620°C and $P = 2.2\text{--}2.3\text{ GPa}$. During early exhumation D3 structures developed at $T < 600^{\circ}\text{C}$ and $P < 1.9\text{ GPa}$, up to the final syn-D5 re-equilibration at $T = 380^{\circ}\text{C}$ - 520°C and $P < 0.8\text{ GPa}$.

Eclogite-facies conditions structural and metamorphic evolution occurred at $65 \pm 3\text{ Ma}$ (Rubatto et al., 1999).

Different ages for PT peak conditions, together with significantly different P/T ratios between the two burial and early exhumation paths account for the interpretation that these two portions of the Eclogitic Micaschists Complex are different tectono-metamorphic units. They could have coupled during the final stages of exhumation, between blueschist and greenschist facies conditions. A further refinement of petrological and age data for the final portions of the PT trajectories can shed light on this aspect, together with a structural field survey to identify a main syn-metamorphic tectonic contacts between the two areas. To conclude, in both cases PT prograde trajectories an climax conditions are characterised by a P–T ratio compatible with that of cold subduction zones (Cloos, 1993), indicating that this part of the structural and metamorphic history has been recorded in a scenario of active subduction of a cold and old oceanic plate. The main part of the exhumation is still accomplished under a subduction-related P/T ratio, whereas last exhumation stages took place under a thermal state comprised between those corresponding to warm

subduction zones and plate interior (Cloos, 1993), suggesting that this is the part of the PTdt paths recorded in a collisional setting.

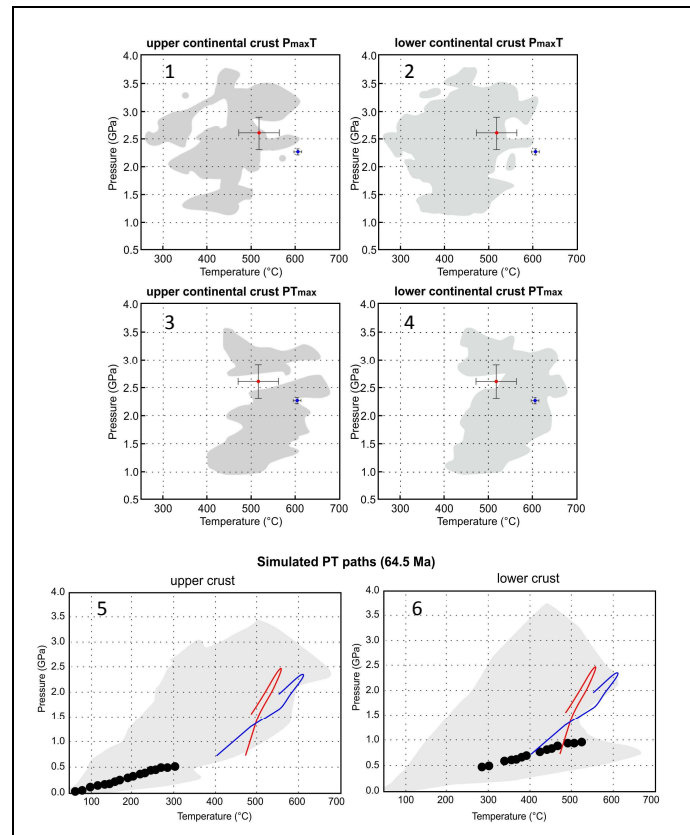


Fig. 6.1: Comparison with simulated data of Roda (2011) $P_{\max}T$ (T at maximum P) for of slices ablated from upper (1-3) and lower (2-4) continental crust and PT paths of the estimated PT conditions inferred for the Ivazio Complex rocks (blue dots and lines) and Mt. Mucrone rocks (red dots and lines).

Finally in figure 6.1 estimated climax PT conditions are compared with the field in which the predicted P_{\max} and T_{\max} conditions of the crustal markers that were subducted during the numerical simulation of the Alpine subduction process are plotting (Roda, 2011; Roda et al., 2012). The values plotting in the shaded field are referred to the peak conditions recorded by the markers before the last exhumation cycle, after 65 Ma from the beginning of the subduction. The inferred PTdt paths are compared with the PT fields in which the simulated PT-trajectories, of the ablated continental markers during a 64.5 Ma of active subduction, are accomplished. The very good fitting of the natural PTdt paths with the model predictions reinforce the interpretation envisaging the accretion of thin crustal slices, tectonically sampled by the upper plate (both from the lower and the upper crust) of an ocean-continent subduction system, in the dynamic mantle wedge developed above the subduction zone, before continental collision.

Acknowledgements: D. Castelli and is thanked for stimulating discussions and helpful suggestions. A. Risplendente provided the technical support at the Dipartimento di Scienze della Terra "A. Desio", where the analytical work with the EPMA has been performed. E. Ferraris provided the technical support at the Dipartimento di Scienze della Terra "A. Desio", where the XRF analysis has been performed.

References

- AGARD, P., YAMATO, P., JOLIVET, L. AND BUROV, E. (2009). Exhumation of oceanic blueschists and eclogites in subduction zones timing and mechanisms. *EarthScience Reviews.*, 92, 53-79.
- ARGAND, E. (1911). Les nappes de recouvrement des Alpes Pennines et leurs prologements structuraux. *Matériaux pour la Carte Géologique de la Suisse*, n.s. 31, 1-26.
- BABIST, J., HANDY, M.R., KONRAD-SCHMOLKE, M. AND HAMMERSCHMIDT, K. (2006). Precollisional, multistage exhumation of subducted continental crust: The Sesia Zone, western Alps. *Tectonics*, 25, TC6008, doi:10.1029/2005TC001927.
- BALLÈVRE, M., KIENAST, J.R. AND VUICHARD, J.P. (1986). La "nappe de la Dent-Blanche" (Alpes Occidentales): deux unités austroalpines indépendantes. *Eclogae Geol. Helvetiae*, 79,57-74.
- BELL, T.H. AND RUBENACH, M.J. (1983). Sequential porphyroblast growth and crenulation cleavage development during progressive deformation. *Tectonophysics*, 92: 171-194.
- BERNARDELLI, P., CASTELLI, D. AND ROSSETTI, P. (2000). Tourmaline-rich ore-bearing hydrothermal system of lower Valle del Cervo (western Alps, Italy): field relationships and petrology. *Schweiz. Mineral. Petrogr. Mitt.*, 80, 257-277.
- BIGI, G., CASTELLARIN, A., COLI, M., DAL PIAZ, G.V., SARTORI, R., SCANDONE, P. AND VAI, G.B. (1990). Structural Model of Italy, sheets 1-2. In: *Progetto Finalizzato Geodinamica del C.N.R.* S.E.L.C.A., Florence.
- BIGI, G., COLOMBO, A., DEL MORO, A., GREGNANIN, A., MACERA, P. AND TUNESI, A. (1994). The Oligocene Valle Cervo Pluton: an example of shoshonitic magmatism in the Western Italian Alps. *Mem. Soc. Geol. It.*, 46, 409-421.
- BUATIER, M. AND LARDEAUX, J.M. (1987). Intracrystalline deformation of omphacite and garnet under high-pressure and low-temperature conditions - example from the Sesia-Lanzo Zone (Western Alps). *Comptes Rendus Academie des Sciences (Series II)*, 305(9): 797-800.

- BUATIER, M. AND LARDEAUX, J.M. (1987). Intracrystalline deformation of omphacite and garnet under high-pressure and low-temperature conditions - example from the Sesia-Lanzo Zone (Western Alps). *Comptes Rendus Academie des Sciences (Series II)*, 305(9): 797-800.
- BUSSY, F., VENTURINI, C., HUNZIKER, J. AND MARTINOTTI, G. (1998). U-Pb ages of magmatic rocks of the Western Austroalpine Dent Blanche-Sesia Unit. *Schweizerische Mineralogische und Petrographische Mitteilungen*, 78: 163-168.
- BUCHER, K. AND FREY, M. (2002). *Petrogenesis of metamorphic rocks*. 7th ed. Springer-Verlag, Berlin.
- CALLEGARI, E., CIGOLINI, C., MEDEOT, O. AND D'ANTONIO, M. (2004). Petrogenesis of calc-alkaline and shoshonitic post-collisional Oligocene volcanics of the cover series of the Sesia Zone, western Italian Alps. *Geodinamica Acta*, 17, 1-29.
- CALLEGARI, E., COMPAGNONI, R., DAL PIAZ, G.V., FRISATTO, V., GOSSO, G. AND LOMBARDO, B. (1976). Nuovi affioramenti di metagranitoidi nella zona Sesia-Lanzo. *Rendiconti della Società Italiana di Mineralogia e Petrologia*, 32: 97-111.
- CALLEGARI, E. AND VITERBO, C. (1966). I granati delle eclogiti comprese nella "formazione dei micascisti" della Zona Sesia-Lanzo. *Rend. Soc. It. Min. Petr.*, 22, 3-26.
- CANEPA, A., CASTELLETTO, M., CESARE, B., MARTIN, S. AND ZAGGIA, L. (1990) – The Austroalpine Mont Mary nappes (Italian Western Alps). *Mem. Sc. Geol.*, 42, 1-17
- CARON, J.M. AND SALIOT, P. (1969). Nouveaux gisements de lawsonite et de jadeite dans les Alpes franco-italiennes. (New occurrences of lawsonite and jadeite in the French-Italian Alps). *Comptes Rendus Hebdomadaires des Seances de l'Academie des Sciences. Serie D Sciences Naturelles* 268 (26), 3153-3156
- CASSINIS, R. (2006). Reviewing pre-TRANSALP DSS models. *Tectonophysics*, 414, 79-86.
- CASTELLI, D. (1987). Il metamorfismo alpino delle rocce carbonatiche della Zona Sesia-Lanzo (Alpi occidentali). PhD Thesis, Univ. Torino, 141 p.
- CASTELLI, D. (1991). Eclogitic metamorphism in carbonate rocks: the example of impure marbles from the Sesia-Lanzo Zone, Italian Western Alps. *J. metam. Geol.*, 9, 61-77.
- CASTELLI, D., COMPAGNONI, R. AND NIETO, J.M. (1994). High pressure metamorphism in the continental crust: eclogites and eclogitized metagranitoids and paraschists of the Monte Mucone area, Sesia Zone. In: Compagnoni R., Messiga B. AND Castelli D. Eds., *High pressure metamorphism in the Western Alps. Guide-book to the B1 field excursion of the 16th General IMA Meeting, Pisa, Sept. 4-9, 1994*, 107-116.

- CASTELLI, D. AND RUBATTO, D. (2002). Stability of Al and F-rich titanite in metacarbonate: petrologic and isotopic constraints from a polymetamorphic eclogitic marble of the internal Sesia Zone (Western Alps). *Contributions to Mineralogy and Petrology*, 142: 627-639.
- CENKI-TOK, B. OLIOT, E., RUBATTO, D., BERGER, A., ENGI, M., JANOTS, E., THOMSEN, T.B., MANZOTTI, P., REGIS, D., SPANDLER, C., ROBYR, M. AND GONCALVES, P. (2011). Preservation of Permian allanite within an Alpine eclogite facies shear zone at Mt Mucrone, Italy: Mechanical and chemical behavior of allanite during mylonitization. *Lithos*, 125: 40-50.
- CETINKAPLAN, M., CANDAN, O., OBERHANSLI, R., BOUSQUET, R., (2008). Pressure-temperature evolution of lawsonite eclogite in Sivrihisar; Tavsanli Zone, Turkey. *Lithos* 104, 12-32.
- CIMMINO, F. AND MESSIGA, B. (1979). I calcescisti del Gruppo di Voltri (Liguria occidentale): le variazioni composizionali delle miche bianche in rapporto all'evoluzione tettonico-metamorfica alpina. *Ofioliti*, 4(3): 269-294.
- CLOOS, M. (1982). Flow melanges: Numerical modeling and geologic constraints on their origin in the Franciscan subduction complex, California. *Geol. Soc. Am. Bull.* 93, 330-345.
- CLOOS, M. (1993). Lithospheric buoyancy and collisional orogenesis: subduction of oceanic plateaus, continental margins, island arcs, spreading ridges and seamounts. *Geological Society of America Bulletin*, 105: 715-737.
- COGGON, R. AND HOLLAND, T.J.B., (2002). Mixing properties of phengitic micas and revised garnet-phengite thermobarometers. *Journal of Metamorphic Geology*, 20, 683-696.
- COMPAGNONI, R. (1977). The Sesia-Lanzo Zone: high-pressure low-temperature metamorphism in the Austroalpine continental margin. *Rend. Soc. It. Min. Petr.*, 23, 335-374.
- COMPAGNONI, R. AND MAFFEO, B. (1973). Jadeite-bearing metagranites l.s. and related rocks in the Mount Mucrone area (Sesia-Lanzo Zone, Western Italian Alps). *Schweiz. Mineral. Petrogr. Mitt.*, 53, 355-378.
- COMPAGNONI, R., DAL PIAZ, G.V., HUNZIKER, J.C., GOSSO, G., LOMBARDO, B. AND WILLIAMS, P.F. (1977). The Sesia-Lanzo zone, a slice of continental crust with Alpine high-pressure - low-temperature assemblages in the Western Italian Alps. *Rend. Soc. It. Min. Petr.*, 33, 281-334.
- CONNORS, K.A. AND LISTER, G.S. (1995). Polyphase deformation in the western Mount Isa Inlier, Australia; episodic or continuous deformation? *Journal of Structural Geology*, 17(3): 305-328.
- DAL PIAZ, G.V. (1999). The Austroalpine-Piedmont nappe stack and the puzzle of Alpine Tethys. *Memorie di Scienze Geologiche*, Padova, 51: 155-176.
- DAL PIAZ, G.V. (2001). History of tectonic interpretations of the Alps. *J. of Geodyn.*, 32, 99-114.

- DAL PIAZ, G.V. HUNZIKER, J.C. AND MARTINOTTI, G. (1972). La Zona Sesia-Lanzo e l'evoluzione tettonico-metamorfica delle Alpi Nordoccidentali interne. Mem. Soc. Geol. It., 11, 433-460.
- DAL PIAZ, G.V., HUNZIKER, J.C. AND STERN, W.B. (1978). The Sesia-Lanzo Zone, a slice of subducted continental crust? US Geological Survey, Open File Report, 83-86.
- DAL PIAZ, G.V., LOMBARDO, B. AND GOSSO, G. (1983). Metamorphic evolution of the Mt Emilius klippe, Dent Blanche nappe, Western Alps. Am. J. Sci., 283A, 438-458
- DESMONS, J. AND GHENT, E.D. (1977). Chemistry zonation and distribution coefficients of elements in eclogitic minerals from the eastern Sesia unit, Italian Western Alps. Schweiz. Mineral. Petrogr. Mitt., 57, 397-411.
- DESMONS, J. AND O'NEIL, J.R. (1978). Oxygen and hydrogen isotope compositions of eclogites and associated rocks from the eastern Sesia Zone (Western Alps, Italy). Contrib. Mineral. Petrol., 67, 79-85.
- DUCHÊNE, S., BLICHERT-TOFT, L., LUIS, B., TÉLOUK, P., LARDEAUX, J.M. AND ALBARÈDE, F. (1997) – The Lu-Hf dating of garnets and the ages of the Alpine high-pressure metamorphism. Nature, 387, 586-589.
- DE SITTER, L.U. AND DE SITTER-KOOMANS (1949). Geology of the Bergamask Alps, Lombardia, Italy. Leidse Geologische Mededelingen. 14, 1-257.
- DELLEANI, F., CASTELLI, D., SPALLA, M.I. AND GOSSO, G. (2010). The record of subduction-related deformation in the Mt. Mucrone metagranitoids (Sesia-Lanzo Zone, Western Alps). Rendiconti online Società Geologica Italiana, 10: 46-49.
- DELLEANI, F., SPALLA, M.I., CASTELLI, D. AND GOSSO, G. (submitted). A new petrostructural map of Monte Mucrone metagranitoids (Sesia-Lanzo Zone, Western Alps). J. of Maps.
- DI PAOLA, S. AND SPALLA, M.I. (2000). Contrasting tectonic records in pre-Alpine metabasites of the Southern Alps (Lake Como, Italy). Journal of Geodynamics, 30: 167-189.
- DIENER, J.F.A., POWELL, R., WHITE, R.W. AND HOLLAND, T.J.B. (2007) A new thermo-dynamic model for clino- and orthoamphiboles in Na₂O-CaO-FeO-MgO-Al₂O₃-SiO₂-H₂O-O. Journal of Metamorphic Geology, 25, 631-656.
- DIEHL, E.A., MASSON, R. AND STUTZ, A.H. (1952). Contributo alla conoscenza del ricoprimento Dent Blanche. Mem.Ist.Geol.Min.Univ.Padova, 17, 5-52.
- DIELLA, V., SPALLA, M.I. AND TUNESI, A. (1992) – Contrasting thermomechanical evolutions in the South-alpine metamorphic basement of the Orobic Alps (Central Alps, Italy). Journ. of Metamorphic Geology, 10, 203-219.

- DOGLIONI, C. AND BOSELLINI, A. (1987) – Eoalpine and Mesoalpine tectonics in the Southern Alps. *Geol. Rund.*, 76, 735-754.
- DROOP, G.T.R., LOMBARDO, B. AND POGNANTE, U. (1990). Formation and distribution of eclogite facies rocks in the Alps. In: Carswell D.A. Ed., *Eclogite Facies Rocks*, Blackie, Glasgow, 225-259.
- ELLIS, D.J. AND GREEN, D.H. (1979). An experimental study of the effects of Ca upon garnet-clinopyroxene Fe Mg exchange equilibria. *Contrib. Mineral. Petrol.*, 71, 13-22.
- ERNST, W.G. (1979). Coexisting sodic and calcic amphiboles from high pressure metamorphic belts and the stability of barroisitic amphibole. *Mineralogical Magazine*, 43: 269-278.
- ERNST, W.G. AND LIOU, J.G. (2008). High- and ultrahigh-pressure metamorphism: Past results and future prospects. *American Mineralogist*, 93: 1771-1786.
- FRANCHI, S. (1900). Sopra alcuni giacimenti di rocce giadeitiche nelle Alpi Occidentali e nell'Appennino ligure. *Boll. R. Com. Geol. It.*, 31, 119-158.
- FREY, M., HUNZIKER, J.C., BOCQUET, J., DAL PIAZ, G.V., JAGER, E. AND NIGGLI, E. (1974). Alpine metamorphism of the Alps. A review. *Schweiz. Mineral. Petrogr. Mitt.*, 54, 247-290.
- FRÜH-GREEN, G.L. (1994). Interdependence of deformation, fluid infiltration and reaction progress recorded in eclogitic metagranitoids (Sesia Zone, Western Alps). *J. metam. Geol.*, 12, 327-343.
- FRY, N. AND BARNICOAT, A.C. (1987). The tectonic implications of high-pressure metamorphism in the Western Alps. *J. Geol. Soc. London*, 44, 653-659.
- GAZZOLA, D., GOSSO, G., PULCRANO, E. AND SPALLA, M.I. (2000). Eo-Alpine HP metamorphism in the Permian intrusives from the steep belt of the central Alps (Languard-Campo nappe and Tonale Series). *Geodinamica Acta*, 13: 149-167.
- GHENT, E.D., TINKHAM, D. AND MARR, R., (2009). Lawsonite eclogites from Pinchi Lake area, British Columbia: new P-T estimates and interpretation. *Lithos* 109, 248-253.
- GIL IBARGUCHI, J. I., MENDIA, M. AND GIRARGEAU, J. (1991). High-pressure metamorphism within the northwestern Iberian Massif. In: Gil Ibarguchi, J. I. Ed., *Betic Cordilleras-Iberian Massif. Field Guide. 2nd Eclogite Field Conference*, Granada, Malaga, La Coruña, Sept. 4-10, 1991, p. II±1±II-62. International Eclogite Conference Co-ordinating Committee, Granada.
- GOSSO, G. (1977). Metamorphic evolution and fold history in the eclogite micaschists of the upper Gressoney valley (Sesia-Lanzo zone, Western Alps). *Rendiconti della Società Italiana di Mineralogia e Petrologia*, 33: 389-407.

GREEN, ECR, HOLLAND, TJB AND POWELL, R (2007) An order-disorder model for omphacitic pyroxenes in the system jadeite-diopside-hedenbergite-acmite, with applications to eclogite rocks. *American Mineralogist*, 92, 1181-1189.

HANDY, M.R. AND ZINGG, A. (1991) The tectonic and rheological evolution of an attenuated cross section of the continental crust; Ivrea crustal section, southern Alps, northwestern Italy and southern Switzerland. *Geol. Soc. of Am. Bulletin*, 103, 236-253.

HANDY, M.R. AND OBERHÄNSLI, R. (2004) Metamorphic structure of the Alps; explanatory notes to the map 1:100000. *Mitt. der Oester. Mineral. Gesellschaft Print.*, 149, 201-226.

HANDY, M.R., BABIST, J., WAGNER, C., ROSEMBERG, C. AND KONRAD, M. (2005). Decoupling and its relation to strain partitioning in continental lithosphere: insight from the Periadriatic fault system (European Alps). *Geol. Soc. London Spec. Publications*, 243, 249-276.

HANDY, M. R., SCHMID, S. M., BOUSQUET, R., KISSLING, E. AND BERNOULLI, D. (2010). Reconciling plate tectonic reconstructions of Alpine Tethys with the geological-geophysical record of spreading and subduction in the Alps. *EarthScience Reviews.*, 102, 121-158.

HIRAJIMA, T., WALLIS, S. R., ZHAI, M. AND YE, K. (1993). Eclogitized metagranitoid from the Su-Lu ultra-high pressure province, eastern China. *Proceedings of the Japan Academy*, 69, (Series B), 249-254.

HOBBS, B.E., MEANS, W.D. AND WILLIAMS, P.F. (1976). *An outline of structural geology*. Wiley, New York, 571 pp.

HOBBS, B.E., ORD, A., SPALLA, M.I., GOSSO, G. AND ZUCALI, M. (2010). The interaction of deformation and metamorphic reactions. *Geological Society of London Special Publication*, 332: 189-222.

HOLLAND, T.J.B. AND POWELL, R. (1998). An internally-consistent thermodynamic data set for phases of petrological interest. *Journal of Metamorphic Geology*, 16: 309-343.

HOLLAND, TJB, BAKER, JM AND POWELL, R (1998) Mixing properties and activity-composition relationships of chlorites in the system MgO-FeO-Al₂O₃-SiO₂-H₂O. *European Journal of Mineralogy*, 10, 395-406.

HOLLAND, TJB AND POWELL, R (2003) Activity-composition relations for phases in petrological calculations: an asymmetric multicomponent formulation. *Contributions to Mineralogy and Petrology*, 145, 492-501.

HUNZIKER, J.C. (1974). Rb-Sr and K-Ar age determinations and the Alpine tectonic history of the Western Alps. *Mem. Ist. Geol. Mineral. Univ. Padova*, 31, 54 p.

- HUNZIKER, J.C., DESMONS, J. AND HURFORD, A.J. (1992). Thirty-two years of geochronological work in the Central and Western Alps: a review on seven maps. *Mém. Géol.*, Lausanne, 13, 1-59.
- HY C. (1984). Métamorphisme polyphasé et évolution tectonique dans la croûte continentale éclogitisée: les séries granitiques et pélitiques du Monte Mucrone (Zone Sesia-Lanzo, Alpes italiennes). Thèse 3ème cycle, Univ. Paris VI, 198 p.
- JOHNSON, S.E. AND VERNON, R.H. (1995). Inferring the timing of porphyroblast growth in the absence of continuity between inclusion trails and matrix foliations: can it reliably done? *Journal of Structural Geology*, 17(8): 1203-1206.
- KONRAD-SCHMOLKE, M., BABIST, J., HANDY, M.R. AND O'BRIEN, P.J. (2006). The Physico-Chemical Properties of a Subducted Slab from Garnet Zonation Patterns (Sesia Zone, Western Alps). *J. Petrol.*, 47, 2123-2148.
- KOONS, P.O. (1982). An investigation of experimental and natural high-pressure assemblages from Sesia Zone, Western Alps, Italy. PhD Thesis, ETH Zürich, 261 p.
- KOONS, P.O., RUBIE, D.C. AND FRÜH-GREEN, G. (1987). The effects of disequilibrium and deformation on the mineralogical evolution of quartz-diorite during metamorphism in the eclogite facies. *J. Petrol.*, 28, 679-700.
- KROGH RAVNA, E. (2000). The garnet-clinopyroxene Fe^{2+} -Mg geothermometer: an updated calibration. *Journal of Metamorphic Geology*, 18(2): 211-219.
- INGER, S., RAMSBOTHAM, W.R., CLIFF, R.A. AND REX, D.C. (1996) Metamorphic evolution of the Sesia Lanzo Zone, Western Alps: time constraints from multi-system geochronology. *Contrib. Mineral. Petrol.*, 126, 152-168.
- LAIRD, J. AND ALBEE, A.L. (1981). Pressure, temperature and time indicators in mafic schists: their application to reconstructing the polymetamorphic history of Vermont. *American Journal of Science*, 281: 127-175.
- LARDEAUX, J.M. (1981). Evolution tectono-metamorphique de la zone nord du Massif de Sesia-Lanzo (Alpes occidentales): un exemple d'éclogitisation de croûte continentale. PhD Thesis, Université Paris VI, 226 pp.
- LARDEAUX, J.M, GOSSO G., KIENAST, J.R. AND LOMBARDO, B. (1982). Relations entre le métamorphisme et la déformation dans la zone Sésia-Lanzo (Alpes Occidentales) et le problème de l'éclogitisation de la croûte continentale. *Bull. Soc. géol. France*, 24, 793-800.

- LARDEAUX, J.M., GOSSO, G., KIENAST, J.R. AND LOMBARDO, B. (1983). Chemical variations in phengitic micas of successive foliations within the Eclogitic Micaschists complex, Sesia-Lanzo zone (Italy, Western Alps). *Bulletin de Minéralogie*, 106: 673-689.
- LARDEAUX, J.M. AND SPALLA, M.I. (1991). From granulites to eclogites in the Sesia zone (Italian Western Alps): a record of the opening and closure of the Piedmont ocean. *Journal of Metamorphic Geology*, 9: 35-59.
- LI, X.-P., ZHENG, Y.-F., WU, Y.-B., CHEN, F., GONG, B. AND LI, Y.-L. (2004). Low-T eclogite in the Dabie terrane of China: petrological and isotopic constraints on fluid activity and radiometric dating. *Contributions to Mineralogy and Petrology* 148, 443-470.
- LIU, J., BOHLEN, S.R. AND ERNST, W.G. (1996). Stability of hydrous phases in subducting oceanic crust. *Earth and Planetary Science Letters*, 143: 161-171.
- MAFFEO, B. (1970). Studio petrografico dell'ammasso granitico del Monte Mucrone (Zona Sesia-Lanzo) e dei suoi rapporti con i "micaschisti eclogitici". Diploma Thesis, Univ. Torino, 117 p.
- MANZOTTI, P., RUBATTO, D., DARLING, J., ZUCALI, M., CENKI-TOK, B. AND ENGI, M. (2012). From Permo-Triassic lithospheric thinning to Jurassic rifting at the Adriatic margin; petrological and geochronological record in Valtournenche (Western Italian Alps). *Lithos Oslo.*, 146-147, 276-292.
- MAROTTA, A.M. AND SPALLA, M.I. (2007). Permian-Triassic high thermal regime in the Alps: result of Late Variscan collapse or continental rifting? Validation by numerical modeling. *Tectonics*, 26: TC4016, doi:10.1029/2006TC002047
- MAROTTA, A.M., SPALLA, M.I. AND GOSSO, G. (2009). Upper and lower crustal evolution during lithospheric extension: numerical modelling and natural footprints from the European Alps. *Geological Society of London Special Publication*, 321: 33-72.
- MARTINOTTI, G. (1970). Studio petrografico delle eclogiti della zona del Lago Mucrone (Zona Sesia-Lanzo) e dei loro rapporti con i "micaschisti eclogitici" incassanti. Diploma Thesis, Univ. Torino, 135 p.
- MASSONNE, H.J. AND SCHREYER, W. (1987). Phengite geobarometry based on the limiting assemblage with k-feldspar, phlogopite and quartz. *Contributions to Mineralogy and Petrology*, 96: 212-224.
- MEDA, M., MAROTTA, A.M. AND SPALLA, M.I. (2010). The role of mantle hydration into continental crust recycling in the wedge region. *Geological Society of London Special Publication*, 332: 149-172.

MOODY, J.B., MEYER, D. AND JENKINS, J.E. (1983). Experimental characterization of the greenschist-amphibolite boundary in mafic system. *American Journal of Science*, 283: 48-92.

MORIMOTO, N. (1988). Nomenclature of pyroxenes. *Mineralogical Magazine*, 52: 535-550.

MORTEN, L. (1993). Italian eclogites and related rocks, including Field Guide Book of the 4th Int. Ecl. Conf., Calabria (Italy), Sept 1993. *Accad. Naz. Sci., Roma, Scritti e Documenti XII*, 275 p.

MUTTONI, G., KENT, D. V., GARZANTI, E., BRACK, P., ABRAHAMSEN, N. AND GAETANI, M. (2003). Early Permian Pangea "B" to Late Permian Pangea "A". *Earth and Planetary Science Letters.*, 215, 379-394.

NIETO, J.M. AND COMPAGNONI, R. (1994). Metamorphism versus deformation in the eclogitized granitoids of the Monte Mucrone area, Sesia-Lanzo Zone, Italian Western Alps. 16th IMA Meet., Pisa, 4-8 Sept., 1994. Abs. Vol.

OBERHÄNSLI, R., HUNZIKER, J.C., MARTINOTTI, G. AND STERN, W.B. (1985). Geochemistry, geochronology and petrology of Monte Mucrone: an example of Eo-Alpine eclogitization of Permian Granitoids in the Sesia-Lanzo zone, Western Alps, Italy. *Chem. Geol.*, 52, 165-184.

OKAY, A.I. (2002). Jadeite-chloritoid-glaucophane-lawsonite schists from northwest Turkey: unusually high P/T ratios in continental crust. *Journal of Metamorphic Geology* 20, 757-768.

OKAY, A.I. AND WHITNEY, D.L., (2010). Blueschists, ophiolites, and suture zones in northwest Turkey. Guide-book to the pre-Conference Field Excursion of the GSA meeting: "Tectonic Crossroads: Evolving Orogens of Eurasia-Africa-Arabia 4-8 October 2010 Ankara, Turkey". 54

PAQUETTE, J.L., CHOPIN, C. AND PEUCAT, J.J. (1989). U-Pb zircon, Rb-Sr and Sm-Nd geochronology of high- to very-high-pressure meta-acidic rocks from the Western Alps. *Contrib. Mineral. Petrol.*, 101, 280-289.

PARK, R.G. (1969). Structural correlations in metamorphic belts. *Tectonophysics*, 7(4): 323-338.

PASSCHIER, C.W., MYERS, J.S. AND KRÖNER, A. (1990). Field geology of high-grade gneiss terrains. Springer Verlag, Berlin, 150 pp.

PASSCHIER, C.W. AND TROUW, R.A.J. (2005). *Microtectonics*, Second Edition. Springer, 366 pp.

PASSCHIER, C. W., URAI, J. L., VAN LOON, J. AND WILLIAMS, P. F. (1981). Structural geology of the central Sesia Lanzo Zone. *Geologie en Mijnbouw* 60, 497-507.

PENNACCHIONI, G. AND GUERMANI, A. (1993). The mylonites of the Austroalpine Dent Blanche nappe along the northwestern side of the Valpelline valley (italian western Alps). *Mem. Sci. Geol.*, 45, 37-55.

- PICCARRETA, G., 1981. Deep-rooted overthrusting and blueschistic metamorphism in compressive continental margins. An example from Calabria (Southern Italy). *Geological Magazine* 118, 539-544.
- PLYUSNINA, L.P. (1982). Geothermometry and geobarometry of plagioclase-hornblende bearing assemblages. *Contributions to Mineralogy and Petrology*, 80: 140-146.
- POGNANTE, U. (1989a). Lawsonite, blueschist and eclogite formation in the southern Sesia Zone (Western Alps, Italy). *European Journal of Mineralogy*, 1: 89-104.
- POGNANTE, U. (1989b). Tectonic implications of lawsonite formation in the Sesia zone (Western Alps). *Tectonophys.*, 162: 219-227.
- POGNANTE, U. (1991). Petrological constraints on the eclogite- and blueschist-facies metamorphism and P-T-t paths in the Western Alps. *J. metam. Geol.*, 9, 5-17.
- POGNANTE, U., TALARICO, F., RASTELLI, N. AND FERRATI, N. (1987). High-pressure metamorphism in the nappes of the Valle dell'Orco traverse (Western Alps collisional belt). *J. metam. Geol.*, 5, 397-414.
- POLI, S. (1993). The amphibolite-eclogite transformation: an experimental study on basalt. *American Journal of Science*, 293: 1061-1107.
- POLI, S. AND SCHMIDT, M.W. (1995). H₂O transport and release in subduction zones: experimental constraints on basaltic and andesitic system. *Journal of Geophysical Research*, 100(B11): 22299 - 22314.
- POLINO, R., DAL PIAZ, G.V. AND GOSSO, G. (1990). Tectonic erosion at the Adria margin and accretionary processes for the Cretaceous orogeny of the Alps. *Mém. Soc. géol. France*, 156, 345-367.
- POWELL, R. AND HOLLAND, T.J.B. (1994). Optimal geothermometry and geobarometry. *American Mineralogist*, 79: 120-133.
- POWELL, R., AND HOLLAND, T.J.B., 1999. Relating formulations of the thermodynamics of mineral solid solutions: activity modelling of pyroxenes, amphiboles and micas. *American Mineralogist*, 84, 1-14.
- RAMSAY, J.G., 1967. *Folding and Fracturing of Rocks*. McGraw-Hill, New York, 568 pp.
- REBAY, G. AND MESSIGA, B. (2007). Prograde metamorphic evolution and development of chloritoid-bearing eclogitic assemblages in subcontinental metagabbro (Sesia-Lanzo Zone, Italy). *Lithos*, 98: 275-291.

- REBAY, G. AND SPALLA, M.I. (2001). Emplacement at granulite facies conditions of the Sesia-Lanzo metagabbros: an early record of Permian rifting? *Lithos*, 58: 85-104.
- ROBERT, C., JAVORY, M. AND KIENAST, J.-R. (1985). Coefficients de distribution et mesures isotopiques $^{18}\text{O}/^{16}\text{O}$: comparaisons thermométriques et barométriques sur quelques écloïtes et micaschistes de la zone Sesia-Lanzo (alpes italiennes). *Bull. Minéral.*, 108, 699-711.
- RODA, M. (2011). Integration of natural data within a numerical model for the geodynamic reconstruction of an inner portion of the Alps. PhD Thesis, Univ. di Milano, 184 pp.
- RODA, M., MAROTTA, A.M. AND SPALLA, M.I. (2010). Numerical simulations of an ocean/continent convergent system: influence of subduction geometry and mantle wedge hydration on crustal recycling. *Geochemistry Geophysics Geosystems* 11.
- RODA, M. AND ZUCALI, M. (2008). Meso and microstructural evolution of the Mont Morion metaintrusive complex (Dent-Blanche Nappe, Austroalpine Domain, Valpelline, western Italian Alps). *Boll. Soc. Geol. It.*, 127, 105-123.
- RODA, M. AND ZUCALI, M. (2011). Tectono-metamorphic map of the Mont Morion Permian metaintrusives (Mont Morion - Mount Collon - Matterhorn Complex, Dent Blanche Unit), Valpelline -Western Italian Alps. *Journal of Maps*, 2011: 519-535.
- RODA, M., SPALLA, M.I. AND MAROTTA, A.M. (2012). Integration of natural data within a numerical model of ablative subduction: a possible interpretation for the Alpine dynamics of the Austroalpine crust. *Journal of Metamorphic Geology*, 30: 973-996.
- ROMER, R.L., SCHÄRER, U. AND STECK, A. (1996). Alpine and pre-Alpine magmatism in the root-zone of the western Central Alps. *Contrib. Mineral. Petrol.*, 123, 138-158
- ROSSETTI, P., AGANGI, A., CASTELLI, D., PADOAN, M. AND RUFFINI, R. (2002) – Magmatic versus hydrothermal activity in the roof zone of the Valle del Cervo pluton (Italian Western Alps). 81st Congr. Soc. Geol. It. Cinematiche collisionali: tra esumazione e sedimentazione, Torino, 10-12 settembre, Abstr. Vol., 154-155.
- ROSSI, G., SMITH, D.C., UNGARETTI, L. AND DOMENEGHETTI, M.C. (1983). Crystal chemistry and cation ordering in the system diopside-jadeite: a detailed study by crystal structure refinement. *Contrib. Mineral. Petrol.*, 83, 247-258.
- ROBERT, C., JAVORY, M. AND KIENAST, J.-R. (1985). Coefficients de distribution et mesures isotopiques $^{18}\text{O}/^{16}\text{O}$: comparaisons thermométriques et barométriques sur quelques écloïtes et micaschistes de la zone Sesia-Lanzo (alpes italiennes). *Bull. Minéral.*, 108, 699-711.

- RUBATTO, D., GEBAUER, D. AND COMPAGNONI, R. (1999). Dating of eclogite facies zircons: The age of Alpine metamorphism in the Sesia-Lanzo Zone (Western Alps). *Earth Planet. Sci. Lett.*, 167, 141-158.
- RUBIE, D.C. (1990). Role of kinetics in the formation and preservation of eclogites. In: Carswell D.A. Ed., *Eclogite facies rocks*, Blackie, Glasgow, 111-140.
- SALVI, F., SPALLA, M.I., ZUCALI, M. AND GOSSO, G. (2010). Three-dimensional evaluation of fabric evolution and metamorphic reaction progress in polycyclic and polymetamorphic terrains: a case from the Central Italian Alps. *Geological Society of London Special Publication*, 332: 173-187.
- SCHALTEGGER, U. AND BRACK, P. (2007). Crustal-scale magmatic systems during intracontinental strike-slip tectonics; U, Pb and Hf isotopic constraints from Permian magmatic rocks of the southern Alps. *Continental extension Geologische Rundschau = International Journal of Earth Sciences* 1999., 96, 1131-1151.
- SCHMIDT, M.W. (1993). Phase relations and compositions in tonalite as a function of pressure: an experimental study at 650°C. *American Journal of Science*, 293: 1011-1060.
- SPALLA, M.I. (1983). *Struttura e petrografia delle successioni del margine esterno della zona Sesia-Lanzo al contatto con la Falda Piemontese tra il lago di Monastero e il Ponte Cusard (Valli di Lanzo)*. Unpublished Tesi di Laurea, Università di Torino, 181 pp.
- SPALLA, M.I. (1993). Microstructural control on the P-T path construction in the metapelites from the Austroalpine crust (Texel Gruppe, Eastern Alps). *Schweizerische Mineralogische und Petrographische Mitteilungen*, 73: 259-275.
- SPALLA, M.I., DE MARIA, L., GOSSO, G., MILETTO, M. AND POGNANTE, U. (1983). Deformazione e metamorfismo della Zona Sesia - Lanzo meridionale al contatto con la falda piemontese e con il massiccio di Lanzo, Alpi occidentali. *Memorie della Società Geologica Italiana*, 26: 499-514.
- SPALLA, M. I., LARDEAUX, J. M., DAL PIAZ, G. V., GOSSO, G. AND MESSIGA, B. (1996). Tectonic significance of alpine eclogites. *J. Geodynamics* 21, 257-285.
- SPALLA, M.I., LARDEAUX, J.M., DAL PIAZ, G.V. AND GOSSO, G. (1991). *Metamorphisme et tectonique a la marge externe de la zone Sesia-Lanzo (Alpes occidentales)*. *Memorie di Scienze Geologiche*, Padova, 43: 361-369.
- SPALLA, M.I. AND MAROTTA, A.M. (2007). P-T evolutions vs numerical modelling: a key to unravel the Paleozoic to early-Mesozoic tectonic evolution of the Alpine area. *Per. Miner.*

- SPALLA, M.I., SILETTO, G.B., DI PAOLA, S. AND GOSSO, G. (2000). The role of structural and metamorphic memory in the distinction of tectono-metamorphic units: the basement of the Como Lake in the Southern Alps. *Journal of Geodynamics*, 30: 191-204.
- SPALLA, M.I., ZANONI, D., WILLIAMS, P. AND GOSSO, G. (2011). Deciphering cryptic P-T-d-t histories in the western Thor-Odin dome, Monashee Mountains, Canadian Cordillera: A key to unravelling pre-Cordilleran tectonic signatures. *Journal of Structural Geology*, 33: 399-421.
- SPALLA, M.I. AND ZUCALI, M. (2004). Deformation vs. metamorphic re-equilibration heterogeneities in polymetamorphic rocks: a key to infer quality P-T-d-t path. *Periodico di Mineralogia*, 73(2): 249-257.
- SPALLA, M.I., ZUCALI, M., DI PAOLA, S. AND GOSSO, G. (2005). A critical assessment of the tectono-thermal memory of rocks and definition of tectono-metamorphic units: evidence from fabric and degree of metamorphic transformations. *Geological Society of London Special Publication*, 243: 227-247 pp.
- SPALLA, M. I. AND ZULBATI, F. (2003). Structural and Petrographic map of the Southern Sesia-Lanzo Zone (Monte Soglio - Rocca Canavese, Western Alps, Italy). *Mem. Sci. Geol., Padova* 55, 119-127.
- STÄMPFLI, G. M. AND HOCHARD, C. (2009). Ancient orogens and modern analogues. *Geol. Soc. Special Publications*. 327; Pages: 89-111. 2009.
- STAEHLE, V., FRENZEL, G., HESS, J. C., SAUPE, F., SCHMIDT, S. T. AND SCHNEIDER, W. (2001). Permian metabasalt and Triassic alkaline dykes in the northern Ivrea Zone; clues to the post-Variscan geodynamic evolution of the Southern Alps. *Schw. Min. Petr. Mitt. = Bull. Sui. Min. Petr.*, 81, 1-21.
- STOCKHERT, B. AND GERYA, T.V. (2005). Pre-collisional high pressure metamorphism and nappe tectonics at active continental margins: a numerical simulation. *Terra Nova* 17, 102-110.
- STAUB, R. (1917). Ueber Faziesverteilung und Orogenese in den Suedoestlichen Schweizeralpen. *Beitr. Geol. Karte. Schweiz.*, 46, 165-198.
- THÖNI, M. (2006). Dating eclogite-facies metamorphism in the Eastern Alps - approaches, results, interpretations: a review. - *Mineral. Petrol.*, 88, 123-148.
- THOUVENOT, F., PAUL, A., SENECHAL, G., HIRN, A. AND NICOLICH, R. (1990). ECORS-CROP wide-angle reflection seismics; constraints on deep interfaces beneath the Alps. *Memoires de la Societe Geologique de France Nouvelle Serie*. 156; Pages: 97-106; 1990.

- TSUJIMORI, T., SISSON, V.B., LIOU, J.G., HARLOW, G.E. AND SORENSEN, S.S. (2006). Very-lowtemperature record of the subduction process: a review of worldwide lawsonite eclogites. *Lithos* 92, 609-624.
- TROPPER, P. AND ESSENE, E.J. (2002). Thermobarometry in eclogites with multiple stages of mineral growth: an example from the Sesia-Lanzo Zone (Western Alps, Italy). *Schweiz. Miner. Petrogr. Mitt.*, 82, 487-514.
- TURNER, F.J. AND WEISS, L.E. (1963). Structural analysis of metamorphic tectonites. MacGraw-Hill, New York, 545 pp.
- UNGARETTI, L., LOMBARDO, B., DOMENEGHETTI, C. AND ROSSI, G. (1983). Crystal-chemical evolution of amphiboles from eclogitized rocks of the Sesia-Lanzo Zone, Italian Western Alps. *Bull. Minéral.*, 106, 645-672.
- VAN ROERMUND, H., LISTER, G.S. AND WILLIAMS, P.F. (1979). Progressive development of quartz fabrics in a shear zone from Monte Mucrone, Sesia-Lanzo Zone, Italian Alps. *J. Struct. Geol.*, 1, 43-52.
- VANNUCCHI, P. (2001). Monitoring paleo-fluid pressure through vein microstructures. *J. of Geodyn.*, 32, 567-581.
- VENTURELLI, G., THORPE, R.S., DAL PIAZ, G.V., DEL MORO, A. AND POTTS, P.J. (1984). Petrogenesis of calc-alkaline, shoshonitic and associated ultrapotassic Oligocene volcanic rocks from the Northwestern Alps, Italy. *Contrib. Mineral. Petrol.*, 86, 209-220.
- VENTURINI, G. (1995). Geology, geochemistry and geochronology of the inner central Sesia Zone (Western Alps, Italy). *Memoires de Geologie, Lausanne*, 25, 148 p..
- VENTURINI, G., MARTINOTTI, G. AND HUNZIKER, J.C. (1991). The protoliths of the "Eclogitic Micaschists" in the lower Aosta Valley (Sesia-Lanzo Zone, Western Alps). *Mem. Sci. Geol., Padova*, 43, 347-359.
- VENTURINI, G., MARTINOTTI, G., ARMANDO, G., BARBERO, M. AND HUNZIKER, J.C. (1994). The central Sesia-Lanzo Zone (Western Italian Alps): new field observations and lithostratigraphic subdivisions. *Schweiz. Mineral. Petrogr. Mitt.*, 74, 115-125.
- VERNON, R.H. (2004). A practical guide to rock microstructure. Cambridge Univ. press, 594 pp.
- VITERBO, C. AND BLACKBURN, C. (1968). The eclogitic rocks of the "eclogitic micaschist formation", Sesia-Lanzo Zone (western Alps, Italy). *Mem. Ist. Geol. Mineral. Univ. Padova*, 27, 1-45.

WALLIS, S. R., ISHIWATARI A., HIRAJIMA, T., YE, K., GUO, J., NAKAMURA, D., KATO, T., WHITE, RW, POWELL, R AND HOLLAND, TJB (2007) Progress relating to calculation of partial melting equilibria for metapelites. *Journal of Metamorphic Geology*, 25, 511-527.

WHITNEY, D.L. AND EVANS, B.W. (2010). Abbreviations for names of rock-forming minerals. *American Mineralogist*, 95: 185-187.

WILLIAMS, P.F. (1985). Multiply deformed terrains - problems of correlation. *Journal of Structural Geology*, 7(3/4): 269-280.

WU, C.M., WANG, X.S., YANG, C.H., GENG, Y.S. AND LIU, F.L. (2002). Empirical garnet-muscovite geothermometry in metapelites. *Lithos*, 62: 1-13.

ZANONI, D. (2010). Structural and petrographic analysis at the north-eastern margin of the Oligocene Traversella pluton (Internal Western Alps, Italy). *Italian Journal of Geosciences*, 129(1): 51-68.

ZANONI, D., BADO, L. AND SPALLA, M.I. (2008). Structural analysis of the Northeastern margin of the Tertiary intrusive stock of Biella (Western Alps, Italy). *Bollettino della Società Geologica Italiana*, 127(1): 125-140.

ZANONI, D., SPALLA, M.I. AND GOSSO, G. (2010). Structure and PT estimates across late-collisional plutons: constraints on the exhumation of Western Alpine continental HP units. *International Geology Review*, 52: 1244-1267.

ZHAI, M., ENAMI, M., CONG, B. AND BANNO, S. (1997). Occurrence and field relationships of ultrahigh-pressure metagranitoid and coesite eclogite in the Su-Lu terrane, eastern China. *Journal of the Geological Society, London*, 154, 45-54.

ZINGG, A. AND HUNZIKER, J.C. (1990) – The age of movements along the Insubric Line West of Locarno (northern Italy and southern Switzerland). *Eclogae geol. Helv.*, 83, 629-644.

ZUCALI, M. (2002). Foliation map of the "Eclogitic Micaschists Complex" (M. Mucrone-M.Mars-Mombarone, Sesia-Lanzo Zone, Italy). *Memorie di Scienze Geologiche, Padova*, 54: 87-100.

ZUCALI, M., CHATEIGNER, D., DUGNANI, M., LUTTEROTTI, L. AND OULADDIAF, B. (2002a). Quantitative texture analysis of naturally deformed hornblendite under eclogite facies conditions (Sesia-Lanzo Zone, Western Alps): comparison between x-ray and neutron diffraction analysis. *Geological Society of London Special Publication*, 200: 239-253.

ZUCALI, M. AND SPALLA, M.I. (2011). Prograde lawsonite during the flow of continental crust in the Alpine subduction: Strain vs. metamorphism partitioning, a field-analysis approach to infer

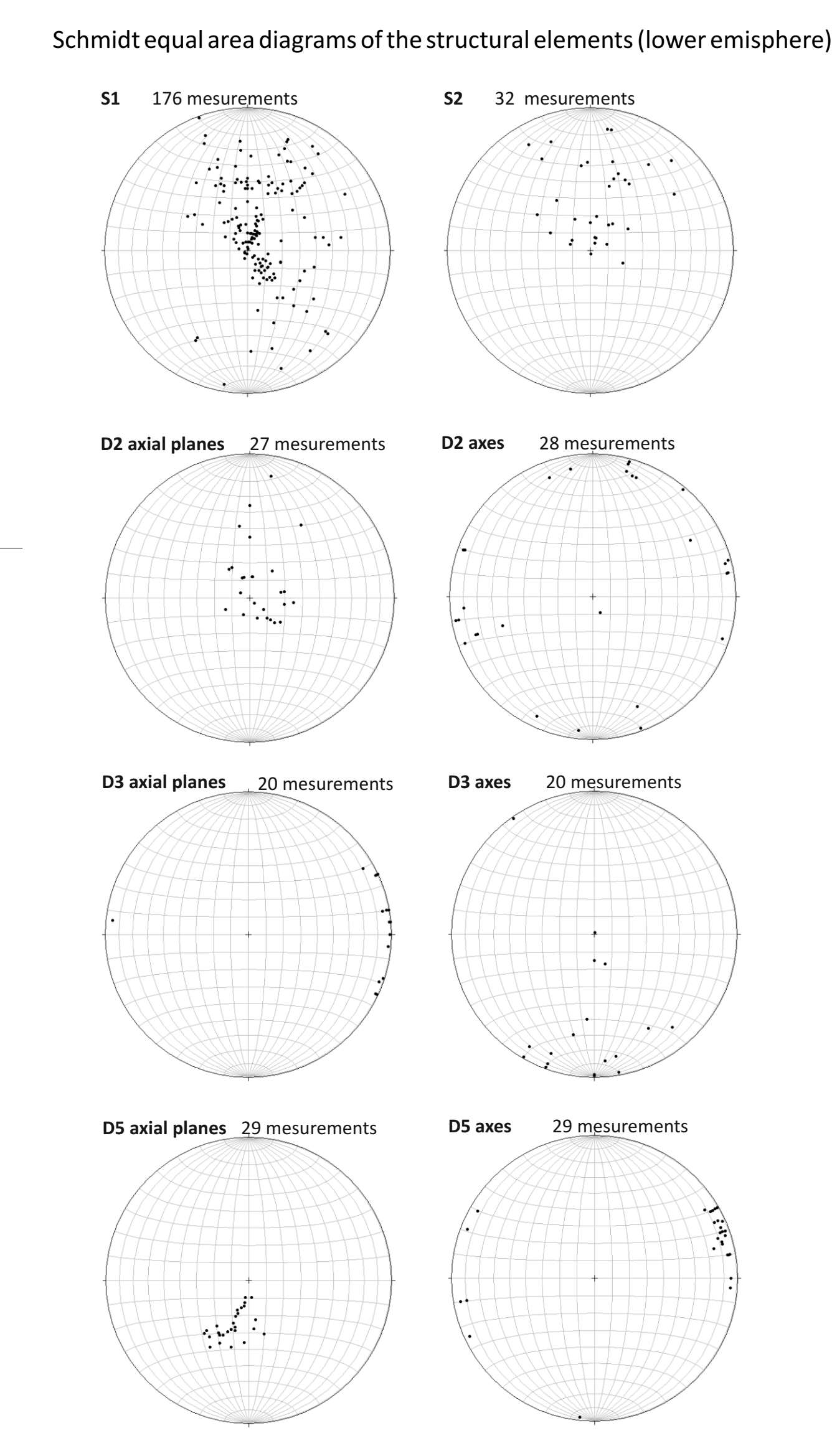
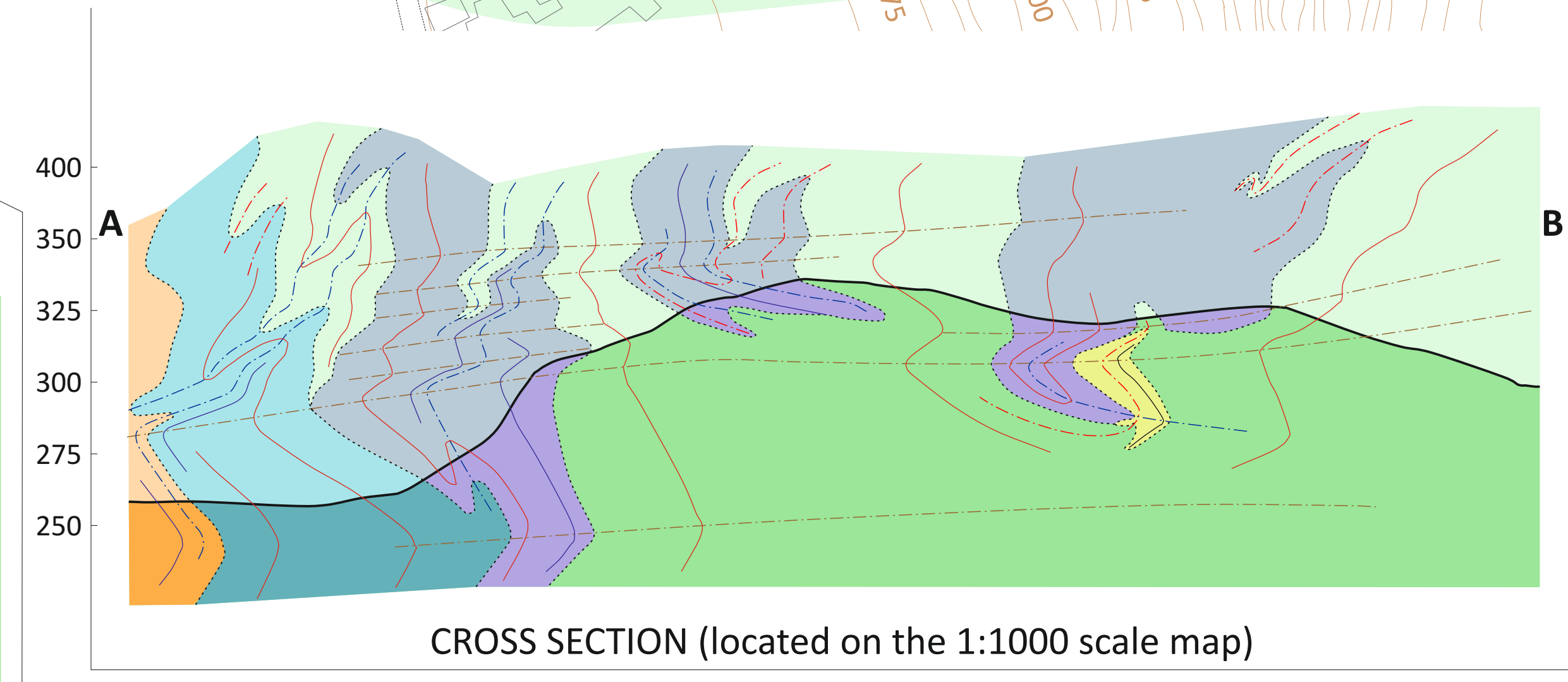
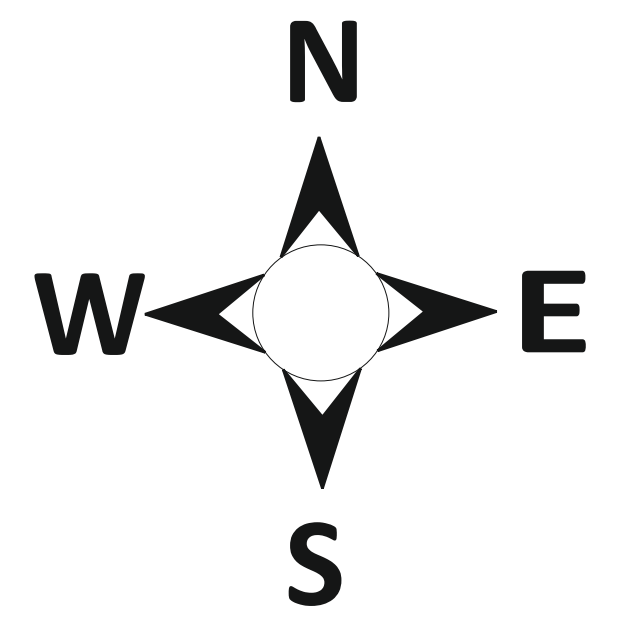
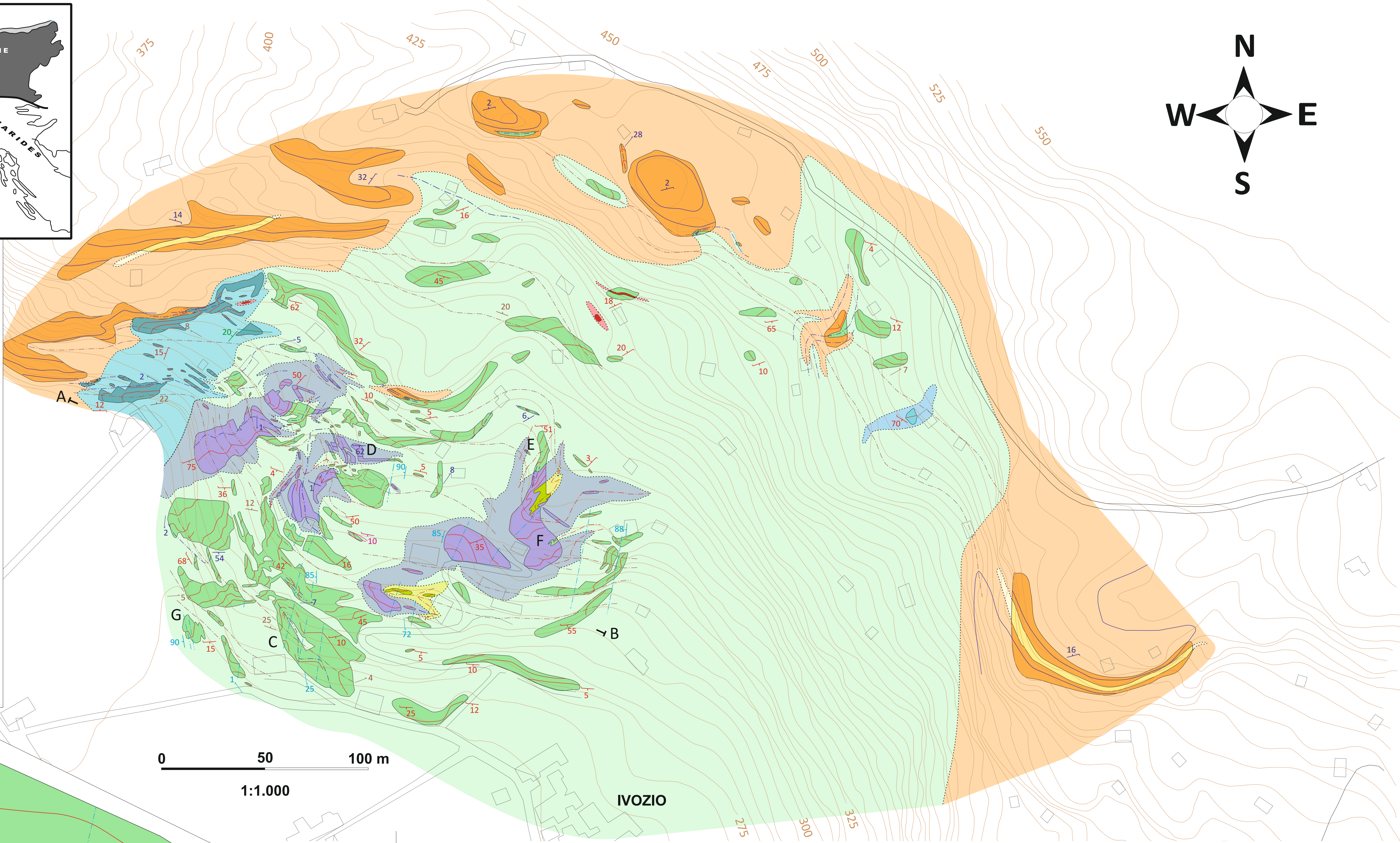
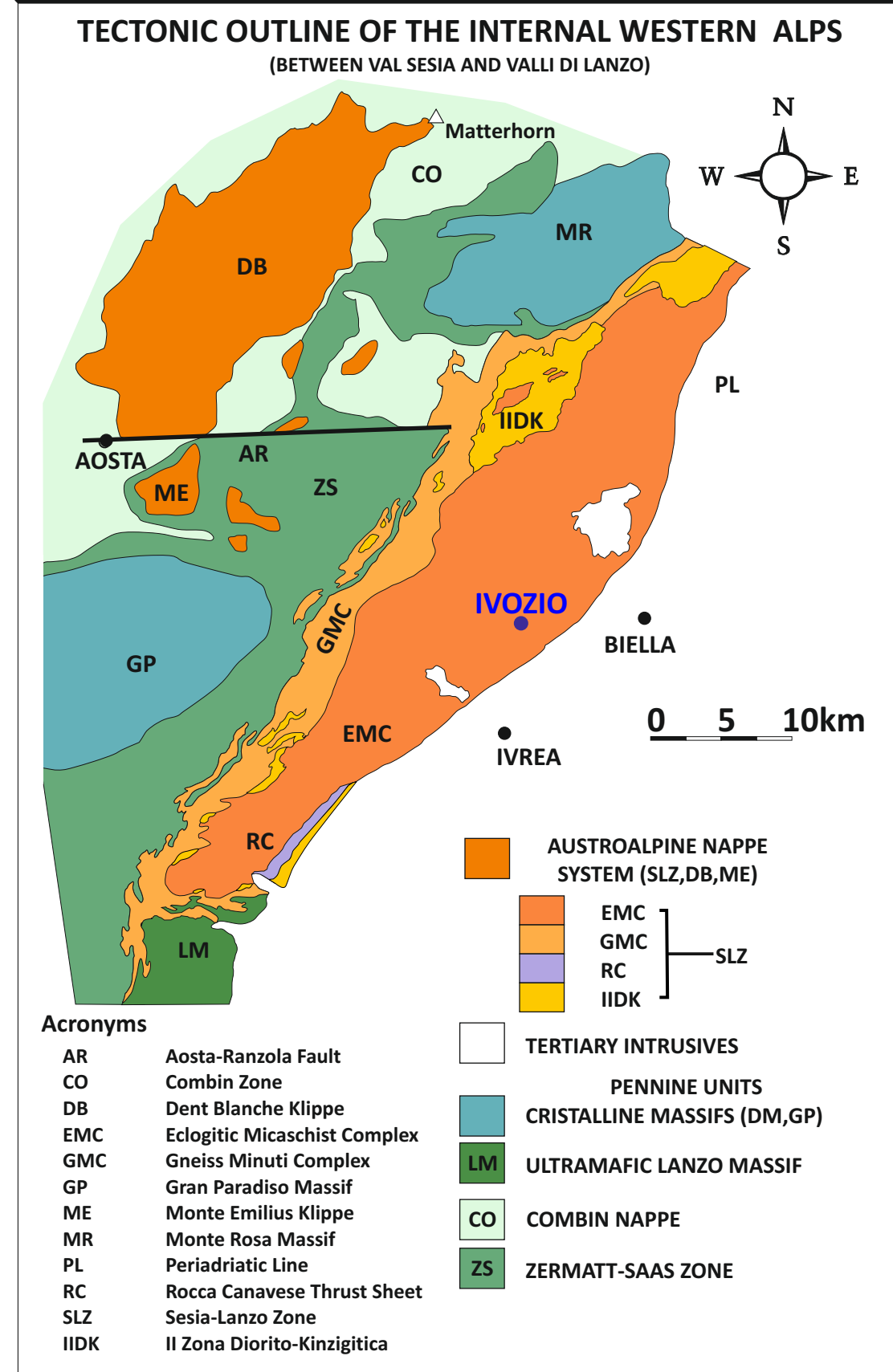
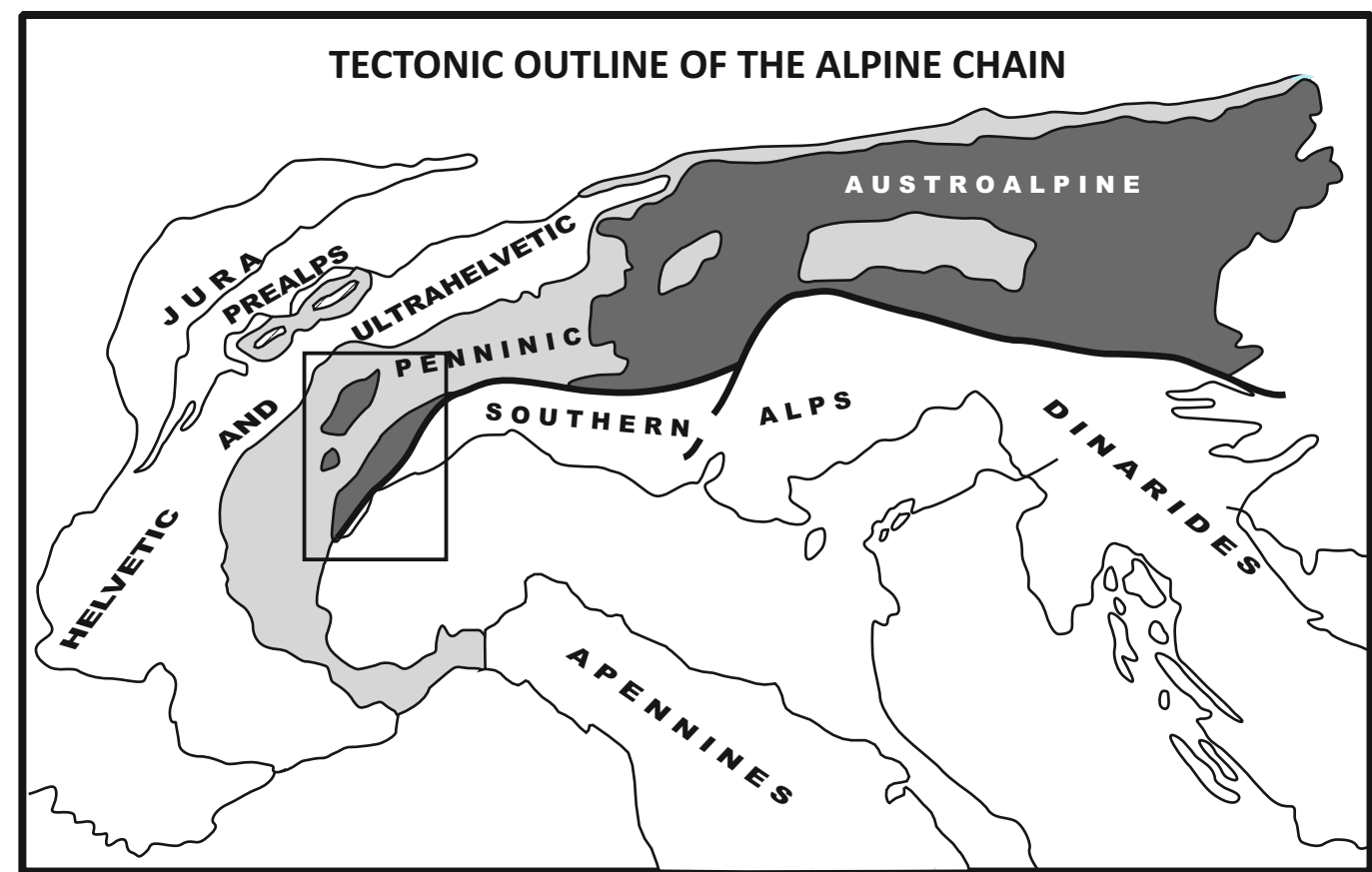
tectonometamorphic evolutions (Sesia-Lanzo Zone, Western Italian Alps). *Journal of Structural Geology*, 33: 381-398.

ZUCALI, M., SPALLA, M.I. AND GOSSO, G. (2002b). Fabric evolution and reaction rate as correlation tool: the example of the Eclogitic Micaschists complex in the Sesia-Lanzo Zone (Monte Mucrone – Monte Mars, Western Alps Italy). *Schweizerische Mineralogische und Petrographische Mitteilungen*, 82: 429-454.

ZUCALI, M., SPALLA, M. I., GOSSO, G., RACCHETTI, S. AND ZULBATI, F. (2004). Prograde LWS-KY transition during the Alpine continental crust subduction of the Sesia-Lanzo Zone: the Ivazio Complex. *J. Virt. Expl.*, 16, paper 4.

ZULAUF, J., ZULAUF, G., KRAUS, R., GUTIÉRREZ-ALONSO, G. AND ZANELLA, F. (2011). The origin of tablet boudinage: Results from experiments using power –law rock analogs. *Tectonophysics*, 510, 327-336.

Petro-structural map of the Ivozio metagabbroic Complex (Sesia-Lanzo Zone, Western Alps).



Ivovio Metagabbroic Complex

- Amphibole-bearing eclogite: medium- to fine-grained blue-green Amp and Grt eclogites with minor Omp, Wm (Ph or Pg) and Zo, mainly showing a massive up to 10-cm-spaced S1 foliation, marked by Grt trails and alternating Amp-rich/poor layers
- Zoisite-bearing eclogite: medium- to coarse-grained Zo, Wm, Omp and Lws eclogites with minor blue or blue-green Amp, Grt and Wm, mainly showing a 10-cm to cm-spaced S1 foliation marked by Zo, Wm and Amp shape preferred orientation (SPO). Minor volumes have S2 mm-spaced foliation marked Omp, Wm and Zo wrapping around Lws square-shaped porphyroblasts.
- Amphibole-epidote-bearing eclogite: medium- to coarse-grained blue-green Amp, Ep and Grt eclogites with minor Wm and Omp, mainly showing cm- to mm-spaced S1 foliation marked by blue-green Amp, Ep and Wm, overgrown by randomly oriented coarse-grained Omp.
- Quartz-rich eclogite: coarse-grained Zo, Omp and Qz eclogites with minor Wm and blue Amp, mainly showing a discontinuous 10-cm-spaced S1 foliation marked by Wm, Zo and Amp.
- Ultramafic rocks: medium- to fine-grained metaclinopyroxenites and Ol-bearing Atg-serpentinites with minor Tr and Chl. Metaclinopyroxenites showing a 10-cm-spaced S2 foliation marked by Chl, Tr and Di. Atg-serpentinites showing a mm-spaced foliation marked by Atg, Tr and Chl.
- Chlorite-amphibolite: medium- to fine-grained blue-green Amp and Chl amphibolites with minor Omp, Ep and Wm, mainly showing a cm-spaced S1 foliation marked by Amp, Chl, Ep and Wm SPO.

Eclogitic Micaschist Complex

- Fine-grained Qz, Wm, Grt, Gln and Omp micaschists, with a dominant mm spaced S2 foliation marked by Wm, Gln and Omp SPO, transposing a previous S1 mm-spaced foliation.
- Medium- to coarse-grained Jd, Wm and Qtz metagranitoids, mainly showing a spaced discontinuous foliation, marked by Wm SPO and Qz elongated domains involving Jd porphyroblasts.

Veins

- Grt-bearing veins
- Omp-bearing veins
- Gln-bearing veins
- Zo-bearing veins

LEGEND OF THE MAP AND ENLARGEMENTS

Metamorphic foliations and axial plane trajectories

- S1 foliation defined by blue-Amp, Wm, Zo/Ep and Grt trails.
- S2 foliation defined by blue-Amp, Omp, Wm, Zo/Ep and Grt.
- S4 mylonitic foliation with Gln, Ep and Wm.
- S6 mylonitic foliation with Chl, Act, Ab, Wm and Ep.
- D1AP: axial plane trajectory to D1 fold systems.
- D2AP: axial plane trajectory to D2 fold systems.
- D3AP: axial plane trajectory to D4 fold systems.
- D5AP: axial plane trajectory to D6 fold systems.

12 12 12 12 Fold axes attitude (D1, D2, D3 and D5)

12 12 12 Axial plane attitude (D2, D3 and D5)

12 12 12 12 Foliation attitude (S1, S2, S4 and S5)

